Fabrication of Polyvinylidene fluoride membranes using gamma-valerolactone as an alternative green solvent

Osamudiamen P. Eweka

Department of Chemical and Process Engineering
University of Strathclyde

A thesis submitted to the Department of Chemical and Process Engineering University of Strathclyde in fulfilment of the requirement for the degree of Doctor of Philosophy

August 20

Declaration of Authenticity and Author's rights

This thesis is the result of the author's original research. It has been composed by the author and has not been previously submitted for examination for an award of a degree.

Signed:

Date:

ABSTRACT

Polyvinylidene fluoride (PVDF) membranes were synthesised using the nonsolvent phase inversion method (NIPS) to design tailored separation films suitable for different membrane processes. Based on the green chemistry principles "*safer solvents and auxiliaries*" and "*use of renewable feedstocks*", this study proposes the possibility of using an alternative green solvent - gamma-valerolactone - as a solution for a more sustainable production of PVDF membranes. Gamma-valerolactone (GVL), a bio-derived green and non-toxic solvent with eco-friendlier properties, was used as an alternative solvent to replace the commonly used, toxic and problematic, petroleum-derived solvent N-methyl-2-pyrrolidone (NMP).

Preliminary studies examined the thermodynamic/kinetic behaviour of the PVDF, gamma-valerolactone and water ternary system using a developed "polymer dissolution in a vial" (PDV) method. Results obtained from cloud points analysis and literature studies were decisive in determining the location of the demixing boundary curve and suitable casting compositions. Furthermore, comparative analysis at different temperatures of the PVDF/GVL/water system reveals the location and transient nature of the demixing boundary/miscibility gap due to the effect of temperature and time. Finally, the proposed PDV method was validated with the known PVDF/DMSO/water ternary system, with experimental results demonstrating reasonable agreement with results published in the literature.

PVDF membranes fabricated using PVDF/GVL binary solutions were compared to PVDF membranes fabricated using PVDF/NMP binary solutions (direct solvent swap), with the membranes prepared using GVL exhibiting significantly different membrane structures and permeation performance (low gas and no pure water permeation) when compared with the membranes prepared using the traditional NMP. The possibility of regulating the PVDF dope using GVL as a solvent to obtain improved membrane properties was further investigated. Different polymer dope/casting solutions based on different concentrations of PVDF, cosolvent (DMSO), polymer additive polyvinylpyrrolidone (PVP), as well as preparation/operating temperatures were prepared to investigate their effect on the morphology and properties of the fabricated PVDF membranes.

The membranes fabricated with different PVDF concentrations, different solution preparation temperatures, and different casting temperatures all demonstrated a very thin film, with a unique membrane structure of large thick, dense top layer and globular/spongy substructure. The prepared membranes' morphology demonstrated that the PVDF/GVL system exhibits a delayed demixing phenomenon, leading to the typically widely recognised observed dense/spongy membrane structures. Additionally, the examined ranges of solution

preparation temperature (Tdissol) and casting temperature (Tcast), showed a correlation between the membrane morphology and the experimental ternary PVDF system phase diagram. The analysis of the results shows that the location of the demixing boundary differs significantly for the PVDF/GVL/water system for conditions at different solution preparation temperatures (Tdissol). In contrast, by varying the examined Tcast parameters, the location of the demixing boundary showed very little or no shift change. PVDF membranes prepared with lower PVDF concentrations or by employing lower temperatures (Tdissol and Tcast), showed high gas permeation fluxes and no pure water permeation, making them unsuitable for ultrafiltration membrane processes, contrary to the ones obtained using the traditional solvent NMP.

PVDF membranes prepared by adding either a non-toxic cosolvent (DMSO) or a polymer additive (PVP) resulted in a modification of the morphology and improved PVDF membrane performance properties. The PVDF membranes produced as a result of combining GVL with different concentrations of a DMSO as cosolvent or by adding PVP (acting as a pore former) to the polymer dope, displayed promising results and is a good development in the fabrication of PVDF membrane using more sustainable materials. The formation of finger-like, macrovoid and spongy membrane sub-structures resulted in improved membrane properties in terms of porosity, membrane thickness, wettability, gas and water performance. Furthermore, the assessment and analysis of the fabricated PVDF membranes indicate that the concentration of these additives (cosolvent or pore former) played a significant role in the membrane formation process.

Finally, a holistic view of the performance of all fabricated PVDF membranes provides a suitability indicator to identify membranes that can be used in different membrane processes such as membrane contactors, membrane distillation and gas-liquid separation applications. Nevertheless, as suggested in the section “Recommendations for Future Work”, a better understanding of the thermodynamic and kinetic behaviour of the PVDF systems containing additives should be addressed to improve further. Overall, this study highlights that it is possible to fabricate PVDF membranes with specific characteristics using the bio derived and more environmentally friendly solvent gamma-valerolactone, and that these membranes can be tailored to perform similarly to membranes produced using traditional polar aprotic solvents.

Acknowledgement

I would like to first express my immense gratitude to my primary supervisor Dr. Vitor Magueijo for his patience, unbounded enthusiasm, guidance, criticism and, above all, support and encouragement throughout the course of the PhD project.

I am very grateful to Dr Paul Edward at the University of Strathclyde, Siti Elida and her colleagues at the Advanced membrane technology research centre (AMTEC) for allowing me to use their equipment. In addition, I thank the technical staff in the chemical and process engineering laboratory, who were very helpful with providing technical assistance and receiving deliveries. I also thank my fellow PhD colleagues, member of staff and all my friends (who are too many to name) for making these research years an enjoyable experience. Many thanks to the Really Small Science Team and the Faculty of Engineering for the outreach programmes and opportunity to be an ambassador.

Finally, I give all thanks to God almighty for the grace and strength to complete this project. In addition, my immense gratitude goes to my parents, siblings, grandmother, aunties and family; without their financial support, constant encouragement, patience and understanding, this project work would not have been possible.

Table of Content

List of Tables

List of Figures

List of Acronyms

NMP	*N*-methyl pyrrolidinone
DMSO	Dimethyl sulfoxide
GVL	Gamma valerolactone
PVDF	Poly (vinylidene fluoride)
PVP	Polyvinylpyrrolidone
NIPS	Nonsolvent induced phase separation
PDV	Polymer dissolution in vial method
Tcast/Tcoag	Casting preparation temperature
Tdissol	Solution preparation temperature (temperature of dissolved polymer)
AFM	Atomic force microscopy
SEM	Scanning electron microscopy
FTIR-ATR	Fourier-transform infrared spectroscopy with attenuated total reflection

List of symbols

δ_i	Solubility parameter of component *i*
θ	Contact angle
ε	Porosity
J	Flux
K	Temperature in Kevin
$℃$	Temperature in Kevin
ρ_L	Density of wetting liquid
ρ_P	Density of polymer
W_w	Wet membrane
W_d	Dry membrane
X_C	Degree of crystallinity
T_m	Melting temperature
Δ_{H_m}	The melting enthalpy of material
$\Delta_{H_{100}}$	Pure crystallinity of polymer
D_{A-B}	Liquid mutual diffusivity of the component
D_m	Harmonic mean value
R_a	Interaction distance
R_o	Radius of a Hansen solubility parameter sphere

Chapter 1

1.1 Introduction

Membrane application is a growing technology widely used in industrial operations within the fine chemical, food, water and biopharmaceutical industries [1]. The main attributes exploited in designing polymeric membranes for separation processes include low operating cost, simplicity of operation, separation performed under mild conditions, the flexibility of material film in contrast to conventional separation techniques, increased separation efficiency and promising technology applications that can be employed in process intensification. As a result, the technology offers potential separation alternatives that have several benefits over traditional separation methods (such as adsorption, distillation, evaporation, recrystallisation and extraction).

Membrane technology is usually considered an environmentally friendly option for separation processes and is associated with increased energy efficiencies and reduced environmental footprints [2]. The significant advances are due to improved membrane materials with better mechanical, selectivity, permeability, thermal and chemical properties. Furthermore, membrane technology keeps experiencing substantial demand from various industries. A recent study in 2022 projects a CAGR of 12.2% of the membrane market, which is expected to reach 62.4 billion USD by 2030 due to the growing population and scarcity of clean drinking water [3].

However, the same environmental benefits cannot be said about the membrane fabrication processes since the majority of traditional polar aprotic solvents used to fabricate polymer membranes, such as *N, N*-dimethyl acetamide (DMAc), dimethylformamide (DMF), *N*-Methyl-2-pyrrolidone (NMP) and tetrahydrofuran (THF) are derived from petroleum sources. They have poor environmental, health and safety credentials [4]. Thus, the fabrication process is hardly green due to toxic solvents and contaminated water that affect the ecosystem and human health. It has been estimated that over 50 billion litres of polluted water are generated annually by membrane manufacturing industries [5], are classified as highly harmful due to their toxicity and account for over 95% of generated waste during membrane fabrication.

The urgent push for sustainable production of polymeric membranes has increased interest in technologies adopting renewable and non-toxic solvents to implement zero emissions of the greenhouse effect by 2050. Hence, stringent environmental regulations drive initiatives are proposed to replace or use less toxic solvents with environmentally friendly alternatives for sustainable membrane technology. The challenge is identifying a suitable green or non-toxic solvent that does not compete with food applications. Selected should be

miscible in water and can dissolve conventional polymers to enhance the growth of the membrane technology market. Additionally, the choice of green, non-toxic solvent for membrane fabrication meets green chemistry principles that aim to eliminate or reduce the use of hazardous substances in chemical processes, which are considered concerning for environmental and human health [6]. The ability to explore new possibilities in material design is made possible by substituting harmful petroleum-derived organic solvents with less hazardous solvents represents a valuable tool.

The thesis employs a solvent screening strategy developed by the in-house research group [7]. Analyses of the study exclude harmful chemicals and highlight non-toxic dipolar aprotic green solvents that can be used to replace toxic solvents and promote sustainable material innovation and the production of polymeric membranes. Several other studies have relied on different strategies that focused on identifying toxic free solvent materials [8,9]. The presented study explores the use of *gamma-valerolactone* (GVL) as a relatively low-cost solvent that satisfies the legislative demands for the sustainability of membrane preparation. GVL is a colourless bio-based renewable dipolar aprotic solvent derived from biomass that consists of a five-carbon cyclic ester with five atoms (four carbons and one oxygen) in the ring (*gamma*-lactone) [10,11]. In addition, the physicochemical properties of the GVL, such as its low toxicity, low vapour pressure, high flash point, low melting point, and high boiling point [11], allow this solvent to be considered a desirable and sustainable replacement for traditional aprotic dipolar solvents (DMAc, DMF, NMP) [12] used in membrane fabrication. GVL has been industrially used in chemical synthesis as an additive for fuel, flavour, and perfume production [13,14]. Furthermore, several recently reported studies have proposed using GVL to prepare polysulfone, cellulose acetate, and polyethersulfone membranes [15,16,17].

The fabrication of membrane using cellulose acetate (CA), polyacrylonitrile (PAN), Polybenzimidazole (PBI), polyethersulfone (PES), polyimide (PI), polypropylene (PP), and Polyvinylidene fluoride (PVDF) [18,19] for hydrophobic or hydrophilic microporous membranes have been the subject of numerous studies and use as commercial polymer materials.

Polyvinylidene fluoride (PVDF), a semi-crystalline [20] and widely used organic polymer with excellent thermal stability, mechanical strength, hydrophobicity, chemical resistance [21,22,23] and availability, has found broad employment in the process industries. Its remarkable physicochemical properties, the combination of processability as a ubiquitous material, and its capacity to dissolve in various organic solvents have been used to satisfy specific manufacturing needs, including membrane separation processes like microfiltration, ultrafiltration, nanofiltration, membrane distillation, and pervaporation [24,25,26,27,28].

Furthermore, the PVDF market, with a growing CAGR of 6.3%, is projected to reach US$958.2 by 2027, [29] indicating an emerging market prospect for PVDF membranes.

Most polymeric membranes are prepared by immersion precipitation, consisting of phase separation in a homogenous polymer solution that is achieved by the effect of an external medium, most likely via a nonsolvent (NIPS) or temperature (TIPS) [30,31,32]. The nonsolvent induced phase separation (NIPS) is widely used commercially and in pilot lab scale fabrication despite the complex process due to understanding the effect and selection of several process parameters, including the choice of nonsolvent, casting thickness, temperature, and polymer solution concentration. Hence, the presented study in the thesis will focus on synthesising PVDF membranes using green, non-toxic materials that can be used for membrane processes and applications. The effect of different process parameters is examined in the preparation and characterisation of PVDF membranes using non-toxic components. Therefore, the study aims to promote a sustainable strategy and demonstrate using a bio-based green solvent as the primary solvent for membrane fabrication.

1.2 Research Objective

This research aims to synthesise PVDF membranes by employing an eco-compatible process involving non-toxic/green solvents in the production stage. The scope of study merges two research areas: material science, which requires selecting sustainable materials, and process engineering, which involves designing the membranes using the NIPS approach. The presented study will examine the thermodynamic behaviour of the polymer system (PVDF/GVL) and assess the viability of replacing a toxic solvent, NMP, with a green bio-based solvent (GVL) to synthesise PVDF membranes via the NIPS approach. The idea is to understand the PVDF system's behaviour and mechanism influencing the membrane formation during the NIPS process since understanding the polymer solution phase behaviour is essential not only from a scientific standpoint but also from a production aspect of the polymeric membrane.

The specific objectives thesis will focus on the following:

1. The study aims to examine the equilibrium thermodynamic behaviour of the PVDF system (PVDF, GVL, water) by proposing an economically advantageous forward approach that saves materials and allows for sample preservation while conducting analysis.

2. Explore the sustainable synthesis of PVDF membrane using a bio-based green solvent GVL to replace a common toxic solvent NMP via the NIPS process. The choice of NMP is based on

the similarities of physiochemical properties and chemical structure to GVL. The study will compare both sets of membranes and evaluate their properties and performance.

3. Explore the effect of different selected process parameters to design tailored PVDF membranes using GVL via the NIPS method under controlled conditions. In addition, the cast films prepared are characterised and presented.

1.3 Thesis Outline

The overview of the thesis is composed of eight (8) chapters as summarised as follows:

Chapter 1 introduces the thesis with an overview of membrane technology, its application, market prospects and the identification of sustainable biobased solvents proposed as an alternative to replacing conventional toxic solvents in the fabrication of PVDF membrane. In addition, the objective of the thesis is summarised.

Chapter 2 presents critical literature that covers membrane processes, membrane preparation techniques, and descriptions of the physical properties of the proposed bio-based solvent and membrane materials used in the thesis. Reported studies are presented in which toxic and non-toxic solvents have been used to dissolve PVDF to fabricate polymeric membranes that will meet several specific membrane process applications. Furthermore, fundamental studies regarding the thermodynamic and kinetic analysis relating to the fabrication phase of polymeric membranes are highlighted and discussed.

Chapter 3 describes the methodology used to prepare the PVDF membrane using the NIPS method. Experimental procedures for membrane fabrication and characterisation methods for analysing fabricated PVDF membranes are presented.

Chapter 4 investigates the thermodynamic behaviour of the ternary polymer/solvent/nonsolvent system and the kinetics of the membrane formation process. Preliminary studies related to the physical and chemical properties of the solvent, theoretical solubility parameters and experimental solubility analysis of the PVDF system are examined. In addition, the effect of temperature and time on the PVDF system was investigated, and the results were discussed.

Chapter 5 demonstrates the sustainable synthesising of PVDF flat sheet membranes using GVL solvent to replace traditional toxic solvents via nonsolvent-induced phase separation (NIPS). Characterising the membrane morphology and properties was used to investigate the potential new solvent as replacements by comparing them with membranes obtained using a common non-toxic solvent NMP. Further study was introduced to examine the influence of the polymer concentration using the bio-based solvent GVL as an alternative

new solvent. Finally, the designed membranes are characterised, and correlated properties are discussed.

Chapter 6 investigates the effect of the temperature of the dissolved polymer and the casting temperature as process variables in designing PVDF membranes via the NIPS process. The fabricated PVDF membranes are assessed by examining the morphological structure and performance of the cast films, with results presented and discussed.

Chapter 7 examines the effect of using a solvent blend by adding a non-toxic cosolvent to the polymer dope to modify the membrane structure and obtain PVDF membranes with improved pure water permeation performance. The theoretical study examines the solubility of the solvent blends consisting of bio-based green solvent GVL and a non-toxic cosolvent, DMSO, to determine suitably mixed solvent concentrations that can synthesise PVDF membrane via the NIPS method. The designed PVDF membrane's morphology, porosity, wettability behaviour, and performance were presented, and the results were discussed.

Chapter 8 describes the fabrication of PVDF membranes using a polymeric additive polyvinylpyrrolidone (PVP) blend with PVDF/GVL to fabricate by the nonsolvent induced phase separation (NIPS) process. The goal is to physically modify the surface of synthesised PVDF membranes and investigate the synergistic effect in controlling the membrane structure. Tailored membranes are manufactured, characterisation of the membrane structure, wettability and performance properties are examined, and possible correlations between resulting membrane characteristics are discussed.

Chapter 9 summarises the work presented, and general conclusions are drawn from the study investigated in chapters 4 to 8. Furthermore, recommendations are highlighted that can be implemented.

1.4 Reference

[1] Strathmann, H., Giorno, L., & Drioli, E. (2011). *Introduction to membrane science and technology* (Vol. 544). Weinheim: Wiley-VCH.

[2] Sutherland, K. (Ed.). (2003). Profile of the International Membrane Industry-Market Prospects to 2008. Elsevier.

[3] Global Membrane Separation Technology Market Size, Share & Trends Analysis Report by Technology (Microfiltration, Ultrafiltration, Nanofiltration, Reverse Osmosis), by Application, by Region, and Segment Forecasts, 2022-2030. [https://www.researchandmarkets.com/reports/5644930/global-membrane-separation-technology-market?] Accessed June, 2022.

[4] Smallwood, I. (2012). *Handbook of organic solvent properties*. Butterworth-Heinemann.

[5] Razali, M., Kim, J. F., Attfield, M., Budd, P. M., Drioli, E., Lee, Y. M., & Szekely, G. (2015). Sustainable wastewater treatment and recycling in membrane manufacturing. *Green Chemistry*, *17*(12), 5196-5205.

[6] Anastas, P., & Eghbali, N. (2010). Green chemistry: principles and practice. *Chemical Society Reviews*, *39*(1), 301-312.

[7] Magueijo et al. University of Strathclyde chemical Day poster, 2016.

[8] Clarke, C. J., Tu, W. C., Levers, O., Brohl, A., & Hallett, J. P. (2018). Green and sustainable solvents in chemical processes. *Chemical Reviews*, *118*(2), 747-800.

[9] Zhenova, A. (2020). Challenges in the development of new green solvents for polymer dissolution. *Polymer International*, *69*(10), 895-901.

[10] Ismalaj, E., Strappaveccia, G., Ballerini, E., Elisei, F., Piermatti, O., Gelman, D., & Vaccaro, L. (2014). γ-Valerolactone as a renewable dipolar aprotic solvent deriving from biomass degradation for the Hiyama reaction. *ACS Sustainable Chemistry & Engineering*, *2*(10), 2461-2464.

[11] Horváth, I. T., Mehdi, H., Fábos, V., Boda, L., & Mika, L. T. (2008). γ-Valerolactone—a sustainable liquid for energy and carbon-based chemicals. *Green Chemistry*, *10*(2), 238-242.

[12] Wypych, G. (Ed.). (2019). Handbook of Solvents, Volume 2: Volume 2: Use, Health, and Environment. Elsevier.

[13] Bond, J. Q., Alonso, D. M., Wang, D., West, R. M., & Dumesic, J. A. (2010). Integrated catalytic conversion of γ-valerolactone to liquid alkenes for transportation fuels. *Science*, *327*(5969), 1110-1114.

[14] Savage, N. (2011). Fuel options: the ideal biofuel. *Nature*, *474*(7352), S9-S11.

[15] Zou, D., Nunes, S. P., Vankelecom, I. F., Figoli, A., & Lee, Y. M. (2021). Recent advances in polymer membranes employing non-toxic solvents and materials. *Green Chemistry*.

[16] Dong, X., Al-Jumaily, A., & Escobar, I. C. (2018). Investigation of the use of a bio-derived solvent for non-solvent-induced phase separation (NIPS) fabrication of polysulfone membranes. *Membranes*, *8*(2), 23.

[17] Rasool, M. A., & Vankelecom, I. F. J. (2019). Use of γ-valerolactone and glycerol derivatives as bio-based renewable solvents for membrane preparation. *Green Chemistry*, *21*(5), 1054-1064.

[18] Vandezande, P., Gevers, L. E., & Vankelecom, I. F. (2008). Solvent resistant nanofiltration: separating on a molecular level. *Chemical Society Reviews*, *37*(2), 365-405.

[19] Padaki, M., Murali, R. S., Abdullah, M. S., Misdan, N., Moslehyani, A., Kassim, M. A., ... & Ismail, A. F. (2015). Membrane technology enhancement in oil–water separation. A review. *Desalination*, *357*, 197-207.

[20] Cui, Z., Drioli, E., & Lee, Y. M. (2014). Recent progress in fluoropolymers for membranes. *Progress in Polymer Science*, *39*(1), 164-198.

[21] Yeow, M. L., Liu, Y. T., & Li, K. (2004). Morphological study of poly (vinylidene fluoride) asymmetric membranes: effects of the solvent, additive, and dope temperature. *Journal of Applied Polymer Science*, *92*(3), 1782-1789.

[22] Curcio, E., & Drioli, E. (2005). Membrane distillation and related operations—a review. *Separation and Purification Reviews*, *34*(1), 35-86.

[23] Tan, X., & Rodrigue, D. (2019). A review on porous polymeric membrane preparation. Part I: production techniques with polysulfone and poly (vinylidene fluoride). *Polymers*, *11*(7), 1160.

[24] Kuo, C. Y., Lin, H. N., Tsai, H. A., Wang, D. M., & Lai, J. Y. (2008). Fabrication of a high hydrophobic PVDF membrane via nonsolvent induced phase separation. *Desalination*, *233*(1-3), 40-47.

[25] Sukitpaneenit, P., & Chung, T. S. (2021). Molecular elucidation of morphology and mechanical properties of PVDF hollow fiber membranes from aspects of phase inversion, crystallization, and rheology. In *Hollow Fiber Membranes* (pp. 333-360). Elsevier.

[26] Kang, G. D., & Cao, Y. M. (2014). Application and modification of poly (vinylidene fluoride)(PVDF) membranes–a review. *Journal of membrane science*, *463*, 145-165.

[27] Fontananova, E., Bahattab, M. A., Aljlil, S. A., Alowairdy, M., Rinaldi, G., Vuono, D., ... & Di Profio, G. (2015). From hydrophobic to hydrophilic poly vinylidene fluoride (PVDF) membranes by gaining new insight into material's properties. *RSC Advances*, *5*(69), 56219-56231.

[28] Ji, J., Liu, F., Hashim, N. A., Abed, M. M., & Li, K. (2015). Poly (vinylidene fluoride)(PVDF) membranes for fluid separation. *Reactive and Functional Polymers*, *86*, 134-153.

[29] Market Intelligence Data, h., 2021. *Polyvinylidene Fluoride (PVDF) Market - Growth, Trends, And Forecast (2020 - 2025) | Market Intelligence Data*. [online] Marketintelligencedata.com. Available at: <https://www.marketintelligencedata.com/reports/82901/polyvinylidene-fluoride-pvdf-market-growth-trends-and-forecast-2020-2025> [Accessed 8 September 2021].

[30] Liu, F., Hashim, N. A., Liu, Y., Abed, M. M., & Li, K. (2011). Progress in the production and modification of PVDF membranes. *Journal of membrane science*, *375*(1-2), 1-27.

[31] Rajabzadeh, S., Maruyama, T., Sotani, T., & Matsuyama, H. (2008). Preparation of PVDF hollow fiber membrane from a ternary polymer/solvent/nonsolvent system via thermally induced phase separation (TIPS) method. *Separation and Purification Technology*, *63*(2), 415-423.

[32] Su, Y., Chen, C., Li, Y., & Li, J. (2007). PVDF membrane formation via thermally induced phase separation. *Journal of Macromolecular Science Part A: Pure and Applied Chemistry*, *44*(1), 99-104.

CHAPTER 2
LITERATURE REVIEW

2.1 Membrane Process

Membranes are selective barriers between two phases used for separation processes [1,2]. Its technology currently shows a steady reduction in the cost of manufacturing and installation compared to over 60 years earlier, when membranes were limited to laboratory-scale application due to their high cost per unit area [3]. Membrane technology plays a fundamental role in separation processes such as microfiltration (MF); ultrafiltration (UF); nanofiltration (NF); reverse osmosis (RO); membrane distillation (MD); pervaporation (PV) [4,5] e.t.c. These processes are mainly used for water treatment and purification. The membrane processes highlighted in Table 2-1 are widely recognised for their numerous advantages, which include the low energy consumption required, the mild operating conditions summarised in figure 2.1, and their relatively small footprint compared to other separation methods[6,7].

Table 2-1: Common Polymers used to prepare separation membranes and their respective membranes properties [8,9]

Membrane processes	Polymers Used	Typical membrane properties	Applications
Reverse Osmosis	Cellulose acetate (CA); polybenzimidazole (PBI); polyamide (PA).	High membrane resistance; very small pore sizes <0.1 nm; are hydrophilic; pressure-driven within (10 -100) bar.	Water desalination.
Nanofiltration	Polyimides (PI); polysulfone (PSf); polyphenols (PPs) polyvinylidene fluoride (PVDF); Poly-ether-ether-ketone (PEEK).	It has a thin dense top layer and porous sublayer; pore size of 0.1 - 1 nm; excellent thermal stability; membrane process is pressure driven with a 5 - 40 bar range.	They are used in the separation of organic molecules and multivalent salts.
Ultrafiltration	Polysulfone (PSF); polyacrylonitrile (PAN); polyvinyl butyral (PVB); polyether sulfone (PES);	Asymmetric structure with a dense top layer; pore size is 1 nm-100nm; operates	Fractionation of molecular mixtures.

	polyvinylidene fluoride (PVDF).	with a pressure range between 1 -10 bar.	
Microfiltration	Polyethersulfone (PES); polyvinylidene fluoride (PVDF); polypropylene (PP); poly (tetra-fluoro-ethylene) (PTFE); Polyethylene (PE); Polyetheretherketone (PEEK).	It has a thin, porous skin layer with pore size distribution >0.1 µm; operates with a pressure range between 0.05- 5 bar.	Water purification; wastewater treatment.
Membrane distillation	Poly (tetra-fluoro-ethylene) (PTFE); polyvinylidene fluoride (PVDF).	Symmetric or asymmetric structure; porous; It has no macro voids and a pore size distribution between 0.2-0.3 µm. They are primarily hydrophobic, and their operation is a temperature gradient process.	Gas/water purification
Pervaporation /vapour permeation	Poly(vinyl alcohol) (PVA); polyimide (PI), cellulose acetate (CA); polydimethylsiloxane (PDMS)	Nonporous membrane; the process is pressure driven, has a dense top layer, is stable in organic solvents & has a narrow pore size distribution.	Separation of azeotropic mixtures and recovery of organic vapours from the air.
Gas separation	Polydimethylsiloxane (PDMS); cellulose acetate (CA); polyimide (PI); polysulfone (PSf); polyvinylacetate (PVAc)	Porous/nonporous membrane with no macro voids; possesses an elastomeric/glassy top layer and has a narrow pore size of ≤ 0.1 µm.	They are used for Co_2 capture and separation of gasses.

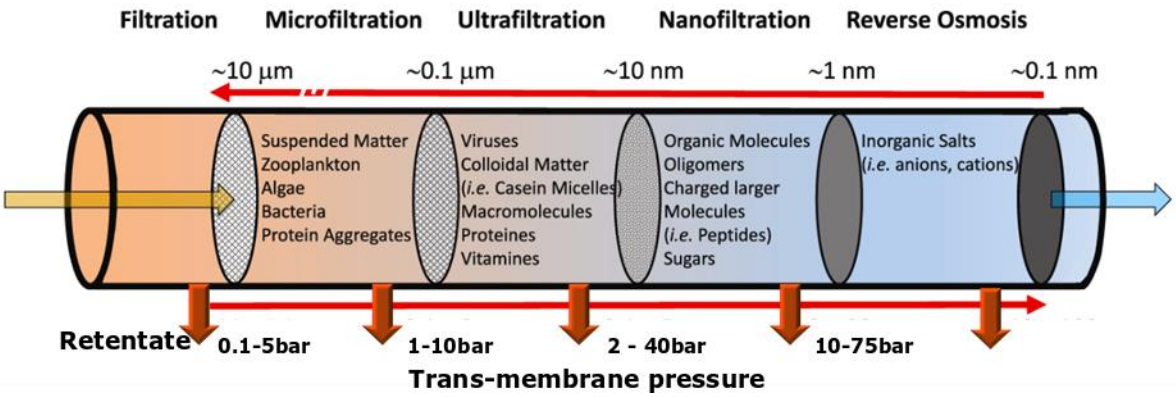

Figure 2.1: Pressure driven membrane processes for materials separation (water treatment)

2.2 Membrane Fabrication Methods and Material selection.

Many techniques are developed to prepare polymeric membranes for separation processes, such as phase inversion, track etching, sintering, dip coating, interfacial polymerisation, and stretching, all of which depend on the choice of polymer and the desired membrane structure/morphology [9]. Commercial polymeric membranes are commonly fabricated by the phase inversion method, which Loeb and Sourirajan first developed to separate water from saline solution [10]. The method is described as a demixing process that occurs when a homogenous polymer solution in a liquid state changes to a solid state due to several factors that induce incompatibility in the polymer solution, such as the removal/loss of solvent causing phase separation [11]. The resulting phenomenon produces two inter dispersed liquid phase regions: a polymer-rich phase that forms the membrane matrix after precipitation and a polymer-lean phase that forms the membrane pores. The phase inversion method can be accomplished by different techniques such as solvent evaporation-induced phase separation (EIPS), nonsolvent-induced phase separation (NIPS), thermally induced phase separation (TIPS) and vapour-induced phase separation (VIPS).

The solvent evaporation induced phase separation (EIPS) is a method achieved by obtaining a homogenous one-phase polymer/solvent/nonsolvent solution and controlling the evaporation (temperature) [12]. EIPS is based on the mass transfer principle, with the selected solvent having higher volatility than the nonsolvent. EIPS method is also known as the dry casting and is used in fabricating asymmetric poly (ether ketone) membranes by varying the solvent-nonsolvent compositions for applications in gas separation [13]. Therefore, the EIPS allows for good reproducibility. However, it can be challenging to identify desirable nonsolvents and solvents based on the EIPS technique.

Thermally induced phase separation (TIPS) is based on the principle of heat transfer. Polymeric membranes are fabricated from a homogeneous polymer solution consisting of

solvent and polymer prepared at a high temperature and cast onto a support under convective conditions to achieve the desired membrane film shape and cool down. [14,15]. Typically, the TIPS method employs crystalline and thermoplastic polymers to fabricate microporous membranes, which allows for easy control and reproducibility of membranes [16,17]. However, the drawback is the high temperature required to achieve miscibility with polymer, the high cost of energy required and the need to control different parameters such as cooling rate, composition and temperature that influences the phase separation process[18].

The vapour induced phase separation (VIPS) has been described as a slow process used to produce symmetric porous membranes [19]. The technique involves casting a homogenous polymer solution under controlled humidity and exposing the film to air. As a result, a mass transfer of the nonsolvent vapour occurs, thereby inducing phase separation with solvent vaporising and a solid film is obtained [20]. The technique allows uniform vapour diffusion into the cast film under controlled relative humidity, temperature and air exposure to design membranes of unique morphologies [21,22]. The VIPS technique has been applied to produce PVDF membranes for membrane distillation, develop drug delivery and self-cleaning super hydrophobic membranes [23]. The advantage of the VIPS is the ability to control the mass exchange and obtain different structural morphologies. However, the conversion process of nonsolvent into vapour to diffuse into the cast film and induce phase separation requires the use of high energy.

The nonsolvent-induced phase separation (NIPS) method is a process used to prepare polymeric membranes by utilising a mixture of a polymer and a suitable solvent/nonsolvent to obtain a homogenous solution. The polymer solution (dope) can be cast on support as flat sheet film or spun as hollow fibers. The cast polymer solution is transformed by the precipitation of the polymer in a nonsolvent coagulation bath. The transformation occurs through the immersion of the cast liquid film in the nonsolvent coagulation bath, which results in an interplay between the solvent in the cast film and the nonsolvent. The process disturbs the stability of the polymer solution, and the cast liquid film is transformed into a solid (typically, an asymmetric polymeric membrane).

Many review papers have provided an overview describing the membrane formation mechanism via the non-induced phase separation (NIPS) [24,8] and their suitable downstream industrial separation applications. However, several drawbacks that limit the NIPS method are the consideration of controlling too many operational parameters that influence the thermodynamic and kinetic properties of the polymer solution during the preparation process. Secondly, achieving an even distribution during the phase separation process is

difficult, resulting in the asymmetric formation of membrane material. Furthermore, the method generates a substantial amount of solvent contaminated waste water[25].

Among all these phase inversion techniques highlighted, the NIPS is the most widely used method due to its simplicity and reproducibility in preparing fluoropolymer membranes [22,27]. Another benefit of adopting the NIPS method is the ability to control specific parameters, which enables the implementation of a systematic and practical fabrication strategy for designing membranes [26]. Furthermore, it is commercially attractive, can be readily scaled up and allows for synthesising different membrane morphology. However, the limitation is that too many operational parameters must be controlled to obtain desired membrane material. Despite the drawbacks, the aforementioned benefits provide an appeal to why it has been selected and used for membrane fabrication in the thesis.

2.2.1 Membrane material Selection for NIPS technique

The backbone material for the membrane generally depends on its application, with the two main common categories of membrane materials divided into organic (polymeric) and inorganic material (ceramics/metallic) [1]. The inorganic membranes are more robust regarding mechanical strength, are reluctant to swell in organic solvents, offer high stability at high temperatures, and are desirable to withstand higher pressures without compacting during operational use [**27**]. Their main drawbacks are their rigidity and high cost, which makes them more brittle and difficult to scale up [**28**]. On the other hand, polymeric materials tend to be flexible, possess good mechanical stability, offer a selective transfer of components, are relatively cheaper and are mainly used for applications which require enhanced separation properties. Polymeric membrane downside is their limited resistance to organic solvents and inability to withstand extreme temperatures [**29**].

Nevertheless, polymers, usually synthetic, are traditionally used for commercial membrane production, with several reported sustainable polymers [**30**,**31**] such as polylactic acid (PLA), bamboo fibers [**32**], a blend of lignin with cellulose [**33**], and chitosan [**34**,**35**] also considered as potential materials for fabrication of membranes. This study will focus on the prevalent semi-crystalline polyvinylidene fluoride (PVDF) with a repeated unit of $–(CH_2CF_2)_n$- and widely used commercial polymeric membrane material for different membrane processes due to its physical and chemical properties. Additionally, the choice of polymer enables it to compete favourably in terms of polymer properties with other polymeric materials for membrane separation. Typically, reported studies [11,**36**,**37**] have pointed to the potential solvent's ability to dissolve the polymer and the formation mechanism during preparation. Several non-toxic, mostly polar aprotic, and renewable solvents from bio-

derived processes have been identified and investigated for PVDF membrane fabrication using the phase inversion technique. Table 2-2 highlights the preparation methods, membrane geometry, and potential applications of PVDF membranes reported.

Table 2-2: PVDF membranes produced via the phase inversion method using water as nonsolvent

Type of Polymer	Solvent	Preparation Technique	Membrane geometry	Membrane Application processes	Ref.
PVDF	triethyl phosphate (TEP)	NIPS	Flat sheet	Membrane distillation	[38]
PVDF	N N-dimethylformamide (DMF), N-dimethylacetamide (DMAc), N, 1-methyl-2-pyrrolidone (NMP), and triethyl phosphate (TEP)	NIPS	Flat sheet	Microfiltration (MF)	[39]
PVDF	trimethyl phosphate (TMP); *N-N* dimethylformamide (DMF); triethyl phosphate & hexamethylphosphoramide (HMPA)	NIPS	Flat sheet	Ultrafiltration	[37]
PVDF	*N-N* dimethylacetamide (DMAc), DMF, TEP and dimethyl sulfoxide (DMSO)	NIPS	Flat sheet	Microfiltration (MF)	[36]
PVDF	triethyl phosphate (TEP)	NIPS	Flat sheet	Microfiltration (MF)	[40]
PVDF	triethyl phosphate (TEP), DMSO	NIPS	Flat sheet	Wastewater treatment	[41]

Type of Polymer	Solvent	Preparation Technique	Membrane geometry	Membrane Application processes	Ref.
PVDF	triethyl phosphate (TEP)	VIPS-NIPS	Flat sheet	Ultrafiltration (UF)	[42]
PVDF	Rhodiasolv PolarClean	N-TIPS	hollow fiber	Microfiltration (MF)	[43]
PVDF	methyl-5-dimethylamino -2-methyl-5-xopentanoate (PolarClean®)	TIPS	Hollow fibre	Membrane distillation	[44]
PVDF	γ-butyrolactone	TIPS	Hollow fibre	microfiltration	[45]
PVDF	Glycerol triacetate (triacetin)	TIPS	Hollow fibre	microfiltration (MF) and ultrafiltration (UF)	[46,47]
PVDF	Tamisolve® NxG	NIPS	Flat sheet	Nanofiltration (NF)	[48]
PVDF	Tamisolve® NxG	VIPS-NIPS	Flat sheet	membrane distillation (MD), crystallisation	[49,50]
PVDF	Cyrene®	VIPS-NIPS	Flat sheet	microfiltration (MF) and ultrafiltration (UF)	[51]
PVDF	Dimethyl isosorbide (DMI)	VIPS-NIPS	Flat sheet	microfiltration (MF) and ultrafiltration (UF)	[52]

The solubility of polymers plays a vital role in membrane fabrication, and the choice of solvent is very relevant because it influences certain factors such as membrane mechanical properties, structure, interfacial characteristics and separation performance. The solubility of membrane components depends primarily on the affinity of selected materials especially using the phase inversion method to synthesise membranes [**53**]. The solubility parameter is the most commonly used approach to predict the association of selected materials in many practical applications due to the general availability of values for many solvents and other solutes. The solubility parameter concept, developed by Scatchard and then improved by Hildebrand [**54**], is based on cohesive energy density. The total solubility parameter, δ was defined as the square root of the cohesive energy per volume and expressed in equation (6).

$$\delta = \left(\frac{\Delta E_v}{V}\right)^{1/2} \qquad (6)$$

Where ΔE_v is the energy of vaporisation and V, the molar volume, Hildebrand stated that the solvation is most reliable when the solubility parameter values of the solvent and solute are close or equal. Hence, providing a qualitative indication of the solvency behaviour of specific polymer-solvent systems. However, the Hildebrand parameters have severe limitations, such as the inability to account for specific interactions between non-polar compounds without hydrogen bonding or, in some cases, the failure to provide accurate values due to the presence of polar components. Therefore, Hansen solubility parameters (HSP) were subsequently proposed [55]. The HSP measures the total energy, expressed in equation (7) as the contribution sum of the three interactions based on the numerical values attributed to the component structural group. The HSP was based on the assumption that it was possible to divide the cohesive energy into three parts corresponding to the atomic dispersion, molecular dipolar and hydrogen bonding interactions, with all three combinations providing a more precise value[56].

$$\delta = \sqrt{\delta_d^2 + \delta_p^2 + \delta_h^2} \qquad (7)$$

Where the dispersion forces are δ_d, δ_P is the polar interaction, and δ_h represents hydrogen bonding. The contribution of the three interactions was measured for many solvent systems, and the HSP used a geometric mean approximation to estimate the interactions between two pure solvents. The results indicated that “like components dissolve like” and have been validated by comparing experimental data to those determined using the geometric mean for systems investigated. The solute solubility parameter is determined by measuring the

solubility of a specific concentration of a group of solvents. A plot of the solvent parameters values in three-dimensional space was carried out, and a sphere was fitted for the solute corresponding to the measured data. The radius of the HSP sphere gives a parameter for the solute R_o. The solubility of the solute (polymer) and solvent can be estimated by calculating the distance (R_a) between any solvent parameter and the solute in the Hansen space. The distance R_a is expressed in equation (8), a small value of the distance between solvent and polymer indicates that the solvent can dissolve the polymer. However, if the distance value is relatively large, this would suggest that the solvent is poorly compatible and may not likely dissolve the polymer.

$$R_a = \sqrt{4(\delta_{d1} - \delta_{d2})^2 + (\delta_{p1} - \delta_{p2})^2 + (\delta_{h1} - \delta_{h2})^2} \qquad (8)$$

δ_d represents the dispersion force, δ_p is the polar interaction and δ_h is the hydrogen bonding component of the Hansen solubility parameter. Subscripts 1 and 2 indicate the polymer and solvent, respectively. A relative energy difference (RED) is a valuable parameter to determine which solvents can dissolve a polymer. It is defined as a ratio of the distance between the polymer and solvent parameters in Hansen space (Ra) and the radius of the HSP sphere (Ro) for the polymer, which is expressed mathematically in equation (9). Presented in figure (2.2) is a HSP sphere to depict solvents that are good for the polymer and those referred to as poor solvents. A point in the three-dimensional structure characterises each solvent, and a close component in the geometrical plot was used to interpret the solubility between the components.

The Hansen model can also be illustrated in a two-dimensional (2D) plot using only two of the three parameters [57]. Typically the parameters δ_p (polar interaction) and δ_h (hydrogen bonding). The model introduces the solubility sphere of the polymer as a circle in the 2D system located at the point ($\delta_{h,P}$, $\delta_{P,P}$) with the Hansen solubility parameters, and the radius of the circle is represented as R_o. The HSP values also represent the solvent, and the axes denote the two solubility components ($\delta_{h,S}$, $\delta_{P,S}$). Hence, like the 3D analysis, solvents closer to the located polymer point in the sphere will dissolve the polymer and are classified as good solvents. However, solvents far from the sphere or outside are more likely to be categorised as poor or nonsolvent because they cannot dissolve the polymer. (See appendix for 2D solubility plot of different solvents used for membrane fabrication).

$$RED = \frac{R_a}{R_o} \qquad (9)$$

Values of $\frac{Ra}{R_o} < 1$ indicates a high likelihood of the solvent dissolving the polymer, and this is represented by the black dots in figure (2.2), while progressively poor solvents would have $\frac{Ra}{R_o} > 1$ and lie outside the sphere [58]. For conditions when $\frac{Ra}{R_o} = 0$, such a value indicates the likelihood of the solvent swelling the polymer.

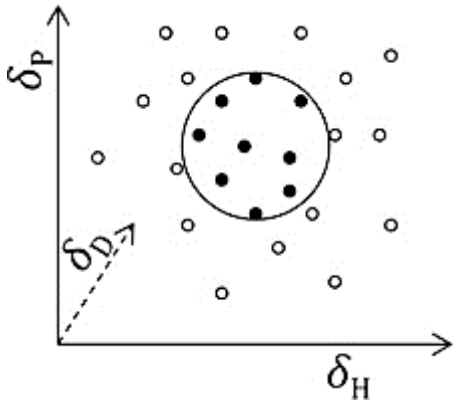

Figure 2.2: 3D illustration of the HSP sphere – The dots in the plot are solvents plotted based on their solubility parameters, and the black identifies the solvents that dissolve the solute [59].

The drawback of using the Hansen solubility parameters is the inconsistent values derived due to the different ways the HSP can be determined, such as using the Hoftyzer Van Krevelen method [60]. However, despite these drawbacks, the relative benefit and ease at which the solubility parameter can be estimated outweigh its limitations. In addition, the Hansen theory, based on the "like dissolves like" principle, is easy to understand and interpret. Finally, the readily available literature data for many popular polymers and solvents are perhaps the most crucial. Osmotic pressure [54], equilibrium swelling measurement values [61], turbidimetric titration [62], matrix assisted laser desorption ionisation [63], intrinsic viscosity [64], and the Flory Huggins interaction parameter method, which is based on lattice theory [65], are some additional strategies to evaluate the solubility interaction parameters that include direct and indirect techniques.

The group contribution method (GPC) can also be used to evaluate the polymer solubility parameter without relying on experimental data. It assumes that the liquid mixture does not consist of molecules but functional groups. The UNIversal quasichemical Functional group Activity Coefficients (UNIFAC) [66] and analytical solutions of groups (ASOG) [67] are two widely used models that employ the liquid vapour equilibrium (VLE) data to fit the group interaction parameters [68]. Most GPC models are highly computationally complicated and

expensive to implement. However, it makes fewer assumptions and is a powerful tool. The in-house research study used the HSP method and a quantum chemical-based COSMO-RS approach to predict an efficient green alternative solvent that can replace the traditional toxic solvent currently used in producing membranes. In addition, a comparison of properties such as boiling point, water solubility, polymer-solvent solubility, molar volume, acute toxicity index, molecular weight and examining a set of eco-friendly and toxic solvents previously investigated in a review of the technical and scientific research studies of the environmental, health and safety (EHS) profile of preferably biobased solvents were considered as a strategy in the choice of the sustainable/non-toxic solvent used for this research study described in section 2.2.2 [69,70,71].

2.2.2 Solvent selection

The use of solvents details a considerable aspect of the environmental performance of processes in the membrane industry as well as the impact on health, cost and safety issues. Generally, Solvents act as heat sinks and temperature regulators, enabling selective extractions, enhancing mass transfer and making separations possible [72]. Hence exploration of green solvents based on their ecological importance is thus necessary to minimise the environmental impact of solvents in membrane production. Furthermore, solvent selection tools do not always necessitate individuals to calculate or compare some numerical ranking scheme. Instead, a straightforward methodology can be implemented to oversee its selection process.

Environmental impacts, health and safety issues in the membrane and chemical industry are related to highly toxic polar aprotic solvents with tremendous utility, given their ability to solubilise many chemicals [73]. The membrane preparation involves dissolving the polymer (PVDF) in a polar aprotic low molecular weight solvent. These commonly used solvents have been classified as substances of very high concern (SVHC), with some even having limited authorisation use as directed by the regulatory authorities Registration, Evaluation, Authorisation and Restriction of Chemicals (REACH). These regulatory bodies propose restrictions for chemicals that have the potential to cause harm, under which EU member states must comply [74]. However, seeking a replacement or substitute for these conventional toxic solvents is difficult. Exploiting the concept of green chemistry to reduce or eliminate hazardous solvents used during membrane fabrication is a method considered in solvent selection. Its sustainable options rely on its availability [75]. Most of the preferred solvents used in membrane preparation tend to have high boing points and low molecular weight and are miscible with the nonsolvent and polymer. Thus, the challenge in determining

which solution is suitable was to conduct an initial guide study by considering the solvent properties of some non-toxic, bio-based and green solvents. Rhodiasolv® Polarclean, methyl lactate, γ-valerolactone, DMSO and ionic liquids have been proposed as sustainable candidates to replace traditional toxic solvents.

2.2.2.1 Rhodiasolv® Polarclean

Methyl-5-(-(dimethylamino)-2-methyl-5-ox-opentanoate) with the trade name Rhodiasolv PolarClean is a water-soluble, eco-friendly, and biodegradable polar green solvent. PolarClan (figure 2.3) is a commercialised green solvent by Solvay novecare that is produced from the valorisation of 2-methylglutaronitrile, a byproduct of the synthesis of nylon 6,6 [76]. The solvent is inexpensive, has a low molecular weight, non-toxic, recyclable, non-volatile, and has a high boiling point (280°C). In addition, the low vapour pressure, low acute toxicity with no evidence of genotoxicity, carcinogenicity or mutagenicity and similar solubility parameters to conventional solvents like NMP, DMAc and DMF make it a promising alternative solvent in replacing traditional common hazardous polar aprotic solvents used in membrane fabrication.

PolarClean, a green solvent, has been identified and proposed to fabricate microporous PVDF membranes via NIPS and TIPS methods [43,44]. Despite PVDF and polarclean not being soluble at room temperature, the thermodynamic properties of a semi-crystalline polymer and the solvent were examined to understand the phenomenon between the competitive behaviour of NIPS and TIPS during membrane preparation. The effect of several factors such as polymer concentration, membrane performance and mechanical properties have been investigated for polymeric membranes prepared using polarclaen [77], with the result indicating a dense top layer with small or no pores formed. Pore additives components were considered to induce surface pores for membrane process application.

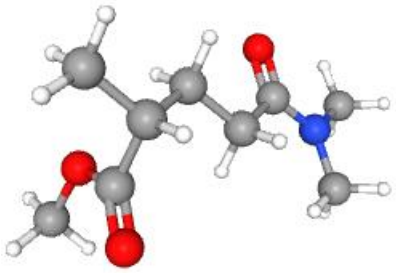

Figure 2.3: Schematic diagram showing the chemical structure of methyl-5-(-(dimethylamino) -2-methyl-5-ox-opentanoate)

2.2.2.2 Methyl lactate

Methyl lactate (figure 2.4) is water miscible, biodegradable and an attractive solvent that shows characteristics for membrane preparation via phase inversion [78]. Moreover, the solvent possesses benignant qualities and is used to prepare flat sheet Cellulose acetate (CA) and Cellulose triacetate (CTA) membranes for water treatment [6]. However, methyl lactate is not easy to use. It is still quite expensive compared to conventional solvents and does not dissolve in various polymers.

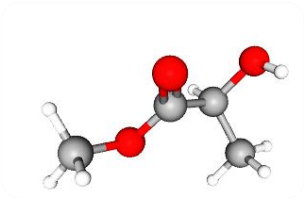

Figure 2.4: Schematic diagram showing the chemical structure of Methyl lactate

2.2.2.3 Dimethyl sulfoxide (DMSO)

Dimethyl sulfoxide (figure 2.5) is a water-miscible, benign and non-toxic polar solvent that can dissolve several polymers, including polysulfone (PSf), polyvinylidene fluoride (PVDF), to prepare membrane for ultrafiltration, microfiltration, membrane distillation and nanofiltration process [79]. The solvent is derived from lignin, a natural aromatic compound that exists as a sufficient polymer and forms a structural integrity tissue material for plants. DMSO has been widely used as a blended solvent (cosolvent) or enhancer in preparing PVDF membranes with high pure water flux, excellent mechanical properties and antifouling capabilities. The thermodynamic and kinetic properties were also studied to understand the interaction with the polymer system to fabricate PVDF membranes [80]. However, despite the broad use of DMSO for different industrial and biological applications, its hygroscopic adverse effects can lead to hazardous environmental conditions if used as mixtures with other substances. However, if the focus of solvent choice is primarily based on the principles of Green Chemistry and its intrinsic toxicity for human health, DMSO would seem like a suitable replacement for hazardous solvents for membrane fabrication.

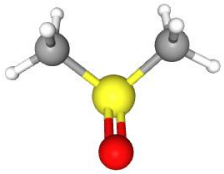

Figure 2.5: Schematic diagram showing the chemical structure of DMSO

2.2.2.4 γ-valerolactone (GVL)

γ-valerolactone (figure 2.6), a polar aprotic solvent, is an environmentally friendly bio-developed solvent that consists of a five-carbon cyclic ester with five atoms (four carbons and one oxygen) in the ring (γ-lactone) [81,82]. GVL synthesis begins by fractionating lignocellulosic biomass into hemicellulose, cellulose and lignin. The primary intermediates produced products when starting from cellulose are glucose, hydroxymethylfurfural (HMF), formic acid and levulinic acid (LA). Several reaction pathways and conversion methods exist, and the latter (levulinic acid) is characterised by hydrogenation to produce hydroxyvaleric acid, which spontaneously condensates to γ-valerolactone [83]. A second pathway is the dehydration of levulinic acid to angelica lactone, which is then hydrogenated to γ-valerolactone or the esterification of levulinic acid, followed by hydrogenation and transesterification over an RU-based catalyst to produce γ-valerolactone [84,85]. The productions step of γ-valerolactone, which is produced in smaller quantities than ionic liquid or some solvents like tetrahydrofuran, has been identified to be a colourless water soluble liquid stable at standard temperature conditions, biodegradable and has no reported health hazard [86,87]. The application of GVL can be found in the production of sustainable chemical fuels, used as starting materials for synthesising biologically active pharmaceutical, agricultural compounds and as a valuable substance for biomass-derived chemicals, perfumes and sustainable products [81, 88]. The solvent has a low molecular weight, is inexpensive, has a high capacity to absorb energy, can reduce environmental impact and carbon footprint, occurs naturally in fruits, has a sweet smell, and is used as a food additive [89,90]. In addition, GVL is miscible in water and has been observed to form no azeotrope in a hybrid system, which indicates that the solvent can be easily separated from the aqueous solution [87].

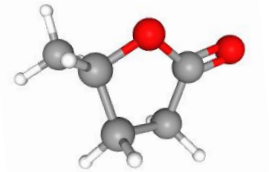

Figure 2.6: Schematic diagram showing the chemical structure of GVL

The growing attention to GVL developed from its similarity with the traditionally used organic solvent NMP. The use of pure GVL or cosolvent via phase inversion techniques for fabricating polymeric membranes such as cellulose acetate (CA), cellulose triacetate (CTA) and polysulfone membranes has been reported. However, the characteristics of synthesised membranes are limited, and little information about their performance has been noted [91].

2.2.2.5 Ionic liquids

Ionic liquid (IL) is a non-polluting odourless, recyclable, thermally and chemically stable organic salt widely used for organic synthesis, extraction and catalysis applications [92]. IL are fluids consisting of organic cations and inorganic or organic anions and possess excellent and unique properties such as low melting point, negligible vapour pressure, low flammability, peculiar phase behaviour and high thermal stability. Ionic liquids have been proposed as green solvents. They have shown promising applications in preparing polymeric membranes via the phase inversion technique. It also applies to the production of cellulose acetate using 1-butyl-3-methylimidazolium thiocyanate ([BMIM]SCN) as the solvent to produce hollow fibre and flat sheet membrane [93,94] exhibiting a relatively dense top layer with free macrovoid porous material structure. Polymeric materials using a blend of ionic liquid and organic solvent have been prepared and examined to improve the characteristics and performance of PVDF membranes, despite PVDF not being readily soluble in most ionic liquids at room temperature [95,96]. Studies [97,98] shows that the outstanding properties of IL make them an alternative replacement for conventional toxic organic solvent and appeal to the sustainable development of polymeric membrane [99,100]. However, the slow biodegradability of these ionic liquids, their environmental impact, cost, and the awareness that not all ionic liquids are green raises several arguments regarding their suitability as green solvents [101].

The presented study employed an in-house research group methodology for solvent substitution and formulation of a green dope solution. The proposed framework strategy suggests identifying problematic and green membrane production solvents and selecting green solvents with comparable Hansen solubility parameters based on the minimisation of modified solubility difference [70].

The specified toxic solvents are recognised as harmful solvents mainly derived from petroleum products and adversely impact the environment, human health, and living organisms. In contrast, green solvents are described as environmentally friendly solvents derived from sustainable agricultural and biomass sources. In addition, they are non-toxic to the environment and human health. Green solvents that meet the solubility criteria with a confidence level of 95% from initially identified solvents are then evaluated by considering the physical properties process of the green solvent, such as boiling point, molar volume, water miscibility, viscosity, density and surface tension. The physical properties are examined because it influences the exchange rate during the membrane fabrication process via phase inversion. At this stage, green solvents that meet both solubility and process criteria are further evaluated by using the Conductor-like Screening model for real solvents (COSMO-RS)

and segment activity coefficient (COSMO-SAC) and minimising the difference [102,103] to obtain a weighted sum of sigma profiles of the selected solvents. Based on the described strategy above, the biobased green solvent gamma valerolactone (GVL) with similar physicochemical properties with N-methyl-2-pyrrolidone (NMP) was considered a replacement solvent and selected as a suitable alternative to produce PVDF membranes in this thesis. The other reason GVL was chosen was that there was no published study or results for fabricating PVDF membrane using the non-toxic biobased solvent as a standalone or blended solvent. Further studies are presented in subsequent chapters to investigate the use of Dimethyl sulfoxide (DMSO) as a non-toxic solvent and employed as a blend, is discussed in the thesis. The choice of nonsolvent was selected from an environmental viewpoint considering its availability, low cost and miscibility with selected polar aprotic solvents.

2.3 Membrane formation mechanism

The principle behind all the phase inversion methods is based on either mass or heat transfer to induce phase separation in the fabrication process of the polymeric membranes. The NIPS methodology, which was chosen for this study, was based on the versatility and popularity in preparing commercial membranes, is further investigated by examining the thermodynamic behaviour of the polymer system using a ternary phase diagram[104]. Both theoretical and experimental studies have been proposed and used to examine the thermodynamics of a ternary polymer system, determine the location of the binodal curve in the ternary diagram and predict the morphology of the membranes. The polymer system demixing boundary is relevant mainly when a novel PVDF/GVL/water system is considered to fabricate membranes because it aids in characterising the phase behaviour of the mixture. Furthermore, it provides a qualitative guide for the specific polymeric membrane formation, which includes suitable compositions of the polymer dope and predicting the membrane morphology.

The Flory-Huggins theory, a theoretical, computational approach, is convenient and provides a valuable framework by employing the lattice model to describe the thermodynamics of the polymer system [105]. The technique was based on Gibbs's free energy of mixing (ΔG_m) per unit volume for the single and multicomponent system presented in equation (1) involves the gas constant (R), absolute temperature (T), the molar volume ratio of the solvent and the total volume of the binary mixture (m_i), volume fraction (ϕ_i), mole fraction (n_i) and the binary interaction parameters $\left({X_{ij}}^{FH}\right)$ between the components in the polymer solution.

$$\frac{\Delta G_m}{RT} = \sum m_i n_i \,.\left(\sum \frac{\phi_i}{m_i} \ln \phi_i + \sum {X_{ij}}^{FH} \phi_i \phi_j\right) \quad (1)$$

The chemical potential $\Delta\mu$ of component i is used to determine the free enthalpy when two components are mixed and mathematically expressed as the partial differential of equation (1) at constant pressure, temperature and number of moles of other components.

$$\frac{\Delta\mu_i}{RT} = \left(\frac{\partial \Delta G_m}{\partial n_i}\right)_{P,T,n_{j...}} \quad (2)$$

Thus, for a given condition for a liquid-liquid equilibrium; $\Delta\mu_i{}^R = \Delta\mu_i{}^P \quad i = 1,2,3 \quad (3)$

Where $\Delta\mu_i$ superscripts R and P refer to rich and lean polymer phases, respectively. A quantitative description based on Flory-Huggin's theory to describe the relationship between the behaviour of the ternary phase diagram and membrane formation in a phase inversion process was also proposed by Altena *et al.* [106]. The study was based on a least square numerical calculation method and suggested that varying the interaction parameter between the solvent and the nonsolvent while keeping the other interaction parameters (polymer with solvent and nonsolvent) constantly plays a critical role in the formation of the membrane structure. The Gibbs free energy mixing was given in equation (4) as:

$$\frac{\Delta G_m}{RT} = n_1 \mathrm{In}\phi_1 + n_2 \mathrm{In}\phi_2 + n_3 \mathrm{In}\phi_3 + g_{12}(u_2) n_1 \phi_2 + X_{13}(\phi_3) n_1 \phi_3 + X_{23}(\phi_3) n_2 \phi_3 \quad (4)$$

R and T refer to gas constant and absolute temperature, respectively. Subscripts refer to nonsolvent (1), solvent (2) and polymer (3). ϕ_i & n_i are the volume fraction and number of moles of component (i *=1, 2, 3*), respectively, while X_{13} denotes the nonsolvent-polymer interaction parameter, X_{23}- the solvent-polymer interaction parameter and g_{12} is the nonsolvent–solvent interaction parameter, assumed as a function quantity u_2 given as:

$$u_2 = \frac{\phi_2}{\phi_1 + \phi_2} \quad (5)$$

From equation (4), an iterative process by making a few assumptions considering the components' molar volume is used to obtain the chemical potential equations for the components in the polymer solution. The conditions of liquid-liquid equilibrium are satisfied mathematically using equation (3). The binary interaction parameters are either obtained from literature studies or experiments. The conditions for liquid-liquid equilibrium and a set of chemical potential equations are defined from equation (4) to determine the composition of each component equation. A numerical procedure that minimises an objective function of the chemical potentials with no penalty function is established to predict the miscibility gap. Results can be compared to experimentally obtained values from cloud point data. The interaction parameter of solvent/nonsolvent (g_{12}) depends on solvent concentration because the nonsolvent and solvent exchange influences the formation of membrane

structure via the NIPS. In contrast, other parameters, polymer/solvent and polymer/nonsolvent, are constant. The (g_{12}) parameter is determined from the excess Gibbs free energy data [1] mathematically expressed in equation (6)

$$g_{12} = \frac{1}{x_1\phi_2}\left[x_1 \mathrm{In}\left(\frac{x_1}{\phi_1}\right) + x_2 \mathrm{In}\left(\frac{x_2}{\phi_2}\right) + \frac{G^E}{RT}\right] \qquad (6)$$

The relationship between G^E and ΔG_m is mathematically expressed in equation (7)

$$G^E = \Delta G_m - RT(x_1 Lnx_1 + x_2 Lnx_2) \quad (7)$$

G^E can be determined from the activity coefficient data or calculated by experimental liquid-vapour equilibrium data [107]. The theory was further extended to consider binary interaction parameter that quantifies the enthalpy interactions between the polymer system components [108]. The study suggested a penalty objective function that minimises the chemical potential of the components in the polymer solution and the concentration-dependent binary interaction parameter to control the phase behaviour. The outcome revealed that shifting the binodal curve might offer a way to theoretically evaluate the thermodynamic properties of the polymer system and predict the membrane formation process.

The Flory-Huggins method provides valuable results that have shown good agreement with cloud-point measurement for various polymer systems used to synthesise polymeric membranes. However, the application of the theory needs to be carefully studied. The assumption that only the binary interactions of the polymer system need to be considered and the ternary interactions negligible could be misleading. However, most ternary solutions employed for membrane fabrication seem enough to consider only the binary interactions. It has been pointed out that some polymer systems require the inclusion of ternary interactions [109,110]. Applying the Flory-Huggins theory to systems with macroscopic concentration gradients is challenging, and it seems to only apply to homogeneous polymer solutions.
Further drawbacks regarding the Flory Huggins theory include complex computations, assumptions of negligible polymer polydispersity [111], and mathematical modification to binodal and spinodal analysis to achieve acceptable results, which could sometimes make the process unrealistic. In addition, the solvent proposed in this thesis is relatively new, with minimal reported data regarding vapour-liquid equilibrium data.

A phase diagram is a convenient tool to describe the phase transformation behaviour of a homogeneous ternary polymer mixture employed for membrane fabrication. However, understanding the polymer solution precipitation path is complex since thermodynamic and kinetic factors significantly impact the process. The ternary phase diagram represents the

mixture of polymer, solvent and nonsolvent. It provides information regarding the thermodynamic behaviour by a composition path of the phase separation during the membrane formation [112]. Furthermore, an equilibrium phase diagram can predict thermodynamically favourable phase transitions. Several phase separation phenomena in polymer solutions have been reported [113,114], including liquid-liquid phase separation crystallisation and gelation. Figure 2.7 shows the possible thermodynamic paths for the polymer/solvent/water system in its most basic form at isothermal conditions.

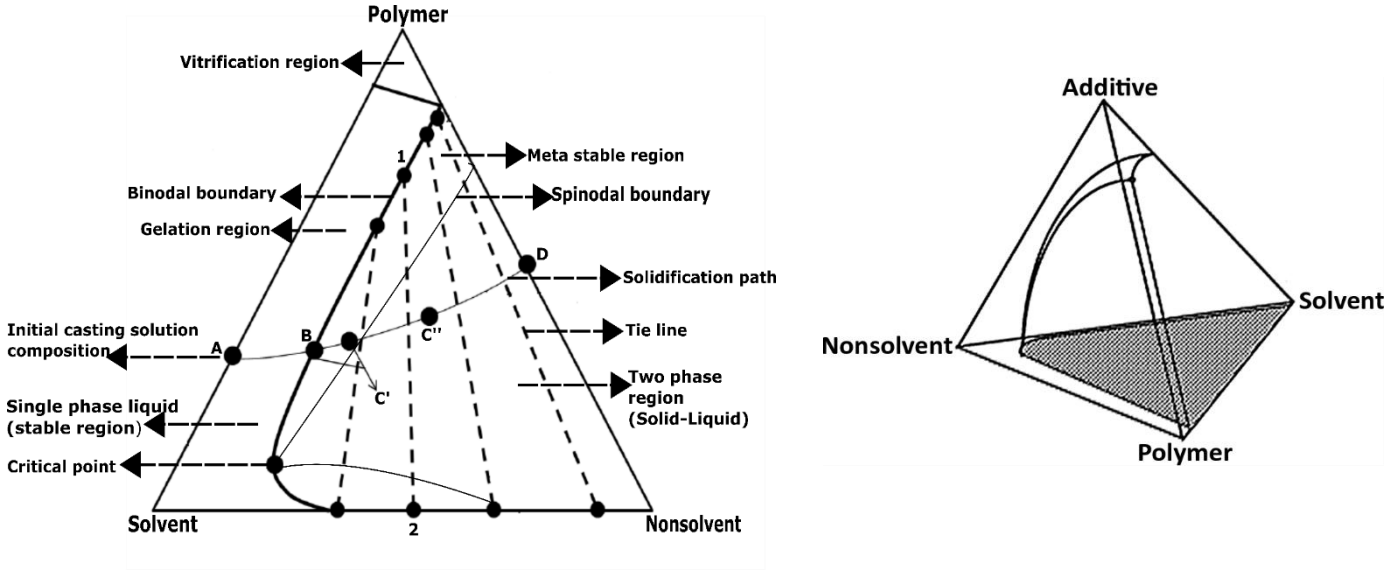

(a) (b)

Figure 2.7: (a)-Schematic representation of the ternary and (b)-quaternary phase diagram adapted from *[115]*

In the ternary diagram, each corner of the triangle represents a pure component, points along the triangle represent the mixture of two corresponding components and points inside the triangle represents the mixture of all three components. The essential elements of the ternary phase diagram consist of a binodal and spinodal boundary, tie lines, critical point, gelation and vitrification region. These identified precipitation paths and regions describe the compositional changes and state of the polymer mixture during the membrane formation process.

Typically, the starting point of the phase inversion process is a thermodynamically stable solution that is subject to demixing. The binodal boundary defines the polymer system's liquid-liquid (L-L) demixing phase or cloud point curve. The ternary diagram is divided into a homogenous region, a metastable region and an unstable region due to external parameters such as adding a sufficient amount of nonsolvent or varying the temperature. At isothermal conditions, the polymer mixture's composition separates into two liquid phases when the binodal composition is reached. Thus, a polymer mixture

transforms into a thermodynamic metastable or unstable state, forming two coexisting phases that differ in composition. The transformation of the polymer mixture, namely: rich and lean polymer phases, are in thermodynamic equilibrium with each other and are connected via tie lines [116]. The region is thus referred to as the miscibility gap. Enclosed within it is the spinodal region, representing an area for the unstable polymer mixture that develops due to instability. The critical point indicates an actual location in the definition of the metastable and unstable regions and is the point where the binodal and spinodal curves meet [117]. The critical point is usually located at the limit of the two-phase region. Therefore, nucleation of the polymer lean phase tends to occur when polymer dope enters the metastable miscibility gap at compositions above the critical point.

Furthermore, the polymer mixture may exhibit processes like crystallisation, gelation or vitrification at increased polymer concentration, limiting the polymer's lean phase growth [115]. Polymer mixture with high viscosity tends to exhibit activities leading to precipitation path proceeding to this region. However, their behaviour is poorly understood or well defined. In contrast, if the precipitation route passes below the critical point, phase separation due to the nucleation of the polymer-rich phase would proceed. What's more intriguing is that accurate experimental techniques and reliable theoretical models are not readily available or understood.

The complexity increases when a cosolvent or polymeric additive is added to the polymer mixtures, causing the ternary system to transform into a quaternary system. Hence, analysing such a system in a pseudo-ternary diagram is usually easier. The additive is considered one component with the polymer or solvent, represented by a tetrahedron in the phase diagram. Furthermore, the identified precipitation paths are locations where various separation mechanisms occur, allowing for the prediction of morphologies. Therefore, it is relevant to understand the compositional alterations that occur when the polymer mixture and nonsolvent are in contact with the evolution of time and the location it enters the two-phase region.

The ternary phase diagram of the phase separation process relating to the polymer system that undergoes crystallisation is considered since PVDF is a semi-crystalline polymer. Figure 2.8 (A) shows a phase diagram for semi-crystalline polymers that highlights the crystallisation curve and the various phase separation mechanism, which happens during the membrane fabrication before equilibrium is reached and is demarcated into regions ($\mathbf{I}-\mathbf{V}$). $\mathbf{I}$ represents a stable single-phase region of the polymer system solution with all phases in equilibrium. $\mathbf{II}$ denotes the liquid-liquid demixing phase region that begins to take place when the binodal is reached due to the addition of the nonsolvent, and $\mathbf{III}$ is the solid-liquid demixing

region that occurs due to micro crystallites being formed from the solution, leading to gelation. The process happens due to crystallisation at temperatures below the melting point of the polymer system, which results in the polymer solution moving directly from the homogenous liquid state to the gel state without passing the liquid-liquid demixing region. Ⅳ is an unstable thermodynamic region with a two-phase equilibrium system comprising rich and lean polymer phases. The demixing mechanism comprises a liquid and solid-liquid phase transition in equilibrium that signifies overlaps between Ⅱ and Ⅲ. Ⅴ is an unstable region that denotes the equilibrium of the initiated polymer crystallites and the polymer lean phase. As a result, the homogenous polymer solution becomes unstable, and phase separates. The crystallisation of this polymer occurs at a slow rate, and more often than not, the membrane formation process occurs very fast, which might leave the final membrane exhibiting low crystallinity. The associated membrane mechanism that describes the formation process is based on the fabrication process's thermodynamics and kinetics aspect.

Figure 2.8-(b) depicts a composition path to understand the formation mechanism that takes place via the NIPS method. A set of entry points into the miscibility region was used to explain the membrane mechanism and structure formation. Hence, certain membrane structure is obtained depending on which composition path occurs during the membrane formation. The compositional path **"B"** shows that a highly viscous polymer solution can form due to the polymer concentration or solvent used. The composition **"B"** path does not enter the miscibility gap due to a solution-gel transition process. When nonsolvent is introduced into the polymer system, and its inflow is slower than its outflow, or when the temperature is lowered, the polymer molecules can form ordered agglomerates or become entangled, which causes mixtures to solidify by crystallisation or gelation [[120],[118]]. Membranes obtained following this path usually have a compact and dense structure. The compositional path **"C"** demonstrates that the binodal is reached above the critical point and moves into the metastable region within the miscibility gap, causing liquid-liquid demixing to be in play and leading to nucleation and growth of the polymer lean phase until equilibrium is achieved [[119]]. Membranes obtained tend to have a cellular structure with a porous sublayer formed due to coalescing action. Spinodal decomposition occurs as the compositional path **"D"** moves into the thermodynamically unstable area.

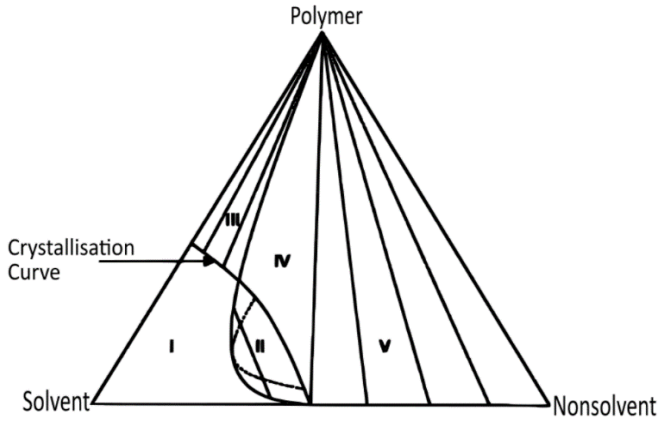

(A)

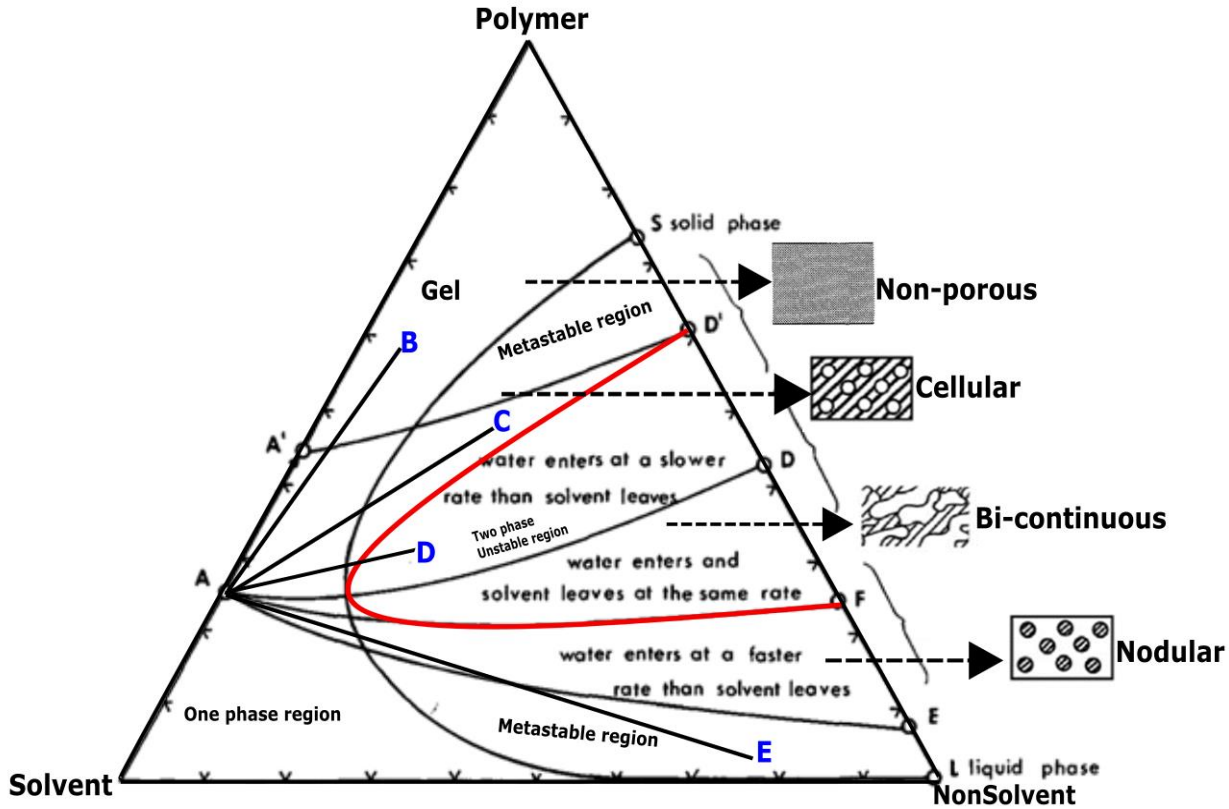

(b)

Figure 2.8: Schematic representation of the ternary phase diagram (A) semi-crystalline polymer and (b) Directional path that occurs during membrane forming process adapted from [120]

The absence of nucleation formation results in a fast solidification of the polymer-rich phase, forming the membrane. Therefore, an instantaneous demixing caused by the induced phase separation makes the solution unstable regardless of infinitesimally concentration fluctuations, which may form a bicontinuous membrane structure [121].

The ternary polymer solution's composition path **"E"** crosses the binodal boundary below the critical point and enters the metastable miscibility gap. As a result, liquid-liquid demixing associated with nucleation and growth of the polymer-rich phase occurs within the polymer-lean phase matrix. Theoretically, the polymer lean regions constitute the continuous phase, and the polymer-rich phase consists of the nuclei dispersed in the solvent. Typically, varying the temperature or composition of the polymer/solvent/nonsolvent system alters the phase inversion's thermodynamic characteristics. Hence, modifying either transfer phenomena (heat or mass transfer) can lead to phase separation. The use of a mass transfer model was proposed to understand the formation of the membrane based on the NIPS method [122]. A ternary phase diagram was used to predict how the mass transfer affects the film formation through the interaction of the polymer solution with a nonsolvent. The reported study proposed a diffusional mass exchange model rather than a nucleation and growth mechanism. However, suppose the polymer-rich phase grows large enough and sticks to each other before solidification. In that case, a compact membrane structure is obtained differently, resulting in a highly porous membrane structure that could be defective and limit industrial application [123].

The model showed that the diffusion exchange results in unstable formations in the polymer solution depending on the location of the binodal and spinodal curves. Further improvement of the model for diffusion-controlled formation was proposed in studies [124,125,126,127]using a set of general diffusion equations and boundary conditions. The diffusion exchange of the solvent into the coagulation bath (J_2) and the nonsolvent into the cast film (J_1) at a given time (t) for membrane formation is presented in figure (2.9).

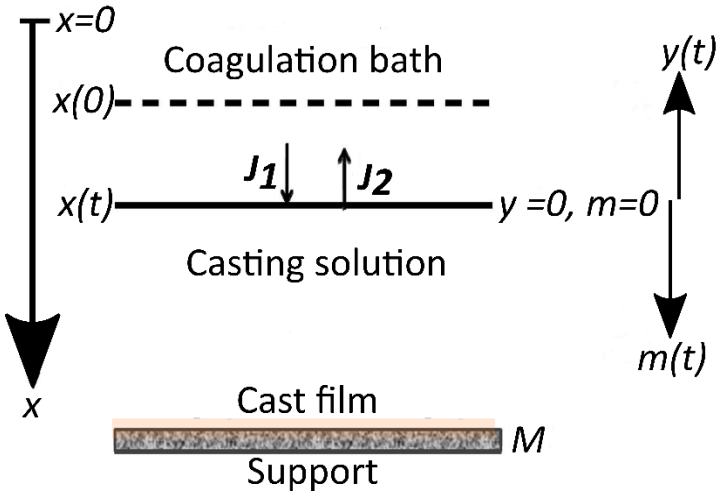

Figure 2.9: Exchange between the solvent and nonsolvent of the cast film in the coagulation bath adapted from *[9].*

Where m is the position coordinate in the polymer fixed frame; M is the support; X is the location of the interface between the film and the coagulation bath; x is the spatial position coordinate normal to the membrane surface, and y is the position coordinate that moves with the interface. The exchange of solvent and nonsolvent occurs at position X (top of the cast film), which induces the demixing process and results in the top of the film solidifying and slowing down the exchange within the sublayer. The pore formation, favoured in the polymer lean phase, now occurs in the sub-layer close to the support of the fabricated membrane. The process can be modelled by considering the mass transfer to describe the diffusion process that occurs during the immersion process of the cast film. The prediction of the membrane formation was divided into two groups, namely instantaneous demixing and delayed demixing system, to describe the process and concluded that the concentration of the nonsolvent and the interaction between the solvent and nonsolvent determines which mechanism controlled the formation [128]. Presented in figure (2.10) is the schematic ternary phase diagram of the demixing process that occurs during the membrane formation. Polymer solutions tend to have lower energy when their phase is separated rather than in a uniform state [129]. The instantaneous demixing occurs when there is a rapid exchange between the cast film and the nonsolvent after immersion in the coagulation bath. The composition path crosses the binodal curve into the unstable miscibility gap region, and phase separation occurs by spinodal decomposition. The membrane formed generally shows a finger-like structure of a highly porous sub-structure (with macro voids) and a finely porous thin or dense top layer. The delayed demixing occurs due to the slow diffusion exchange rate between the cast film and nonsolvent. The composition path of demixing is not spontaneous; as nucleation and growth occur, the homogeneous solution becomes metastable. As a result, the formed membrane tends to have a porous spongy-like structure. The different demixing processes tend to be influenced by several factors, such as the viscosity of the polymer solution and the affinity between the solvent and nonsolvent [130], which affects the precipitation process resulting in a wide range of microstructure and properties of prepared membranes. Presented in figure 2.11 are illustrative descriptions of expected membrane morphologies that can be obtained based on the membrane separation mechanism process.

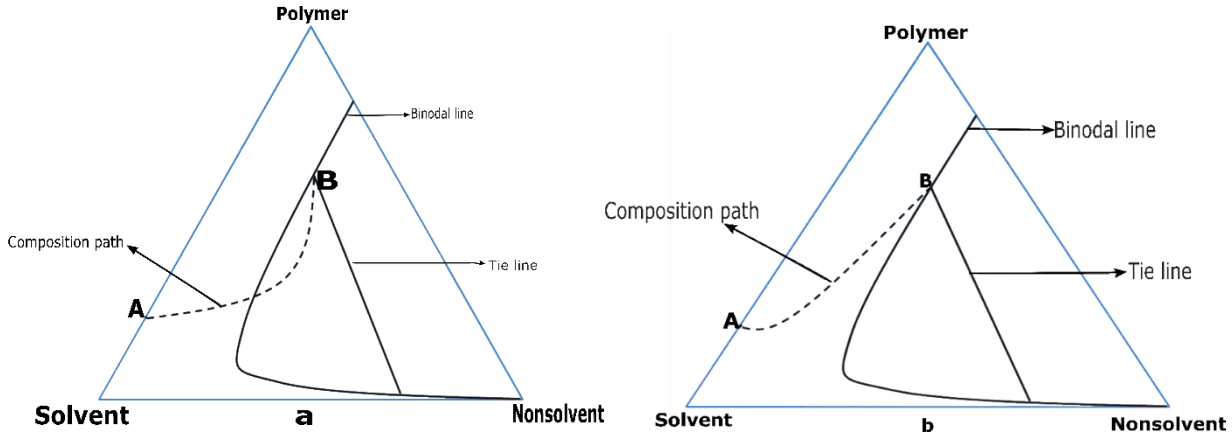

Figure 2.10: Schematic composition paths of the cast film when immersed in the nonsolvent bath. (a) Instantaneous demixing (b) delayed demixing [9]

A fabricated membrane can be categorised as either symmetric or asymmetric depending on whether it has an even porosity throughout the membrane cross section, or a thin microporous layer on top of a spongy/ porous layer with large voids and finger-like cavities as a substructure. The different layers in the asymmetric membrane provide additional functionality that includes selectivity and mechanical strength. The NIPS method has also been applied to fabricate thin film composite membranes, with the performance of these membranes typically exhibiting a trade-off between selectivity and permeability.

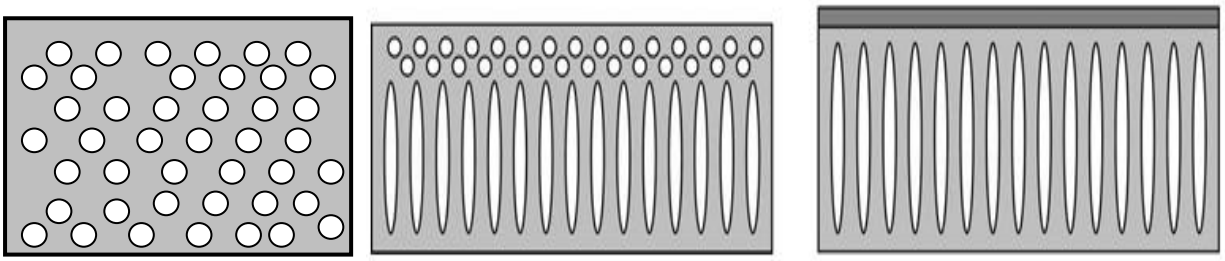

a b c

Figure 2.11: Schematic illustration of the most common types of polymeric membrane, which include- (a) symmetric, (b) asymmetric membrane, (c) thin film composite (TFC) membranes [131]

The membrane morphology considerably affects the mechanical strength and performance of the developed separation process. Also, membranes with different structures can be applied for specific separation processes. There have been a lot of experimental studies done recently on how to tailor the membrane's morphology by taking into account variables such as varying the polymer's concentration, selecting an appropriate solvent and

nonsolvent system, altering the coagulation bath temperature or composition, altering the casting thickness etc. [9,]. In some situations, a combination of two methods is used to fabricate membranes of desired characteristics for membrane application. However, it is also likely that just one mechanism can be selected to control the process. In such a situation, determining a correlation between a single parameter and the obtainable membrane structure will be very interesting.

The development of experimental techniques to study the structural evolution during membrane formation remains a challenge that is required to merge the theories about membrane formation reported in the literature. Modelling of the membrane formation is still complicated due to the complex interplay in describing the diffusion process of the first moments of immersion. The lack of detailed literature on the kinetics of the membrane-forming process is a setback. Many researchers have to correlate the membrane-forming process to the interaction between nonsolvent and solvent in the coagulation bath or use some complex computational approach to predict this phenomenon [132].

In the case of a quaternary system, it has been reported that due to favourable interactions between the additive and blends to the nonsolvent in the polymer system, the miscibility gaps would likely be located inside the tetrahedron and composed of phase triangles with all components of the polymer system represented. In addition, studies have shown that selecting an additive miscible with nonsolvent would avert delayed demixing due to the initial separation between the polymer and additive [133]. However, the additive and a component in the polymer system are considered one when a pseudo ternary phase diagram is used to represent the polymer system. Results for conditions using a pseudo ternary diagram showed that the demixing boundary (binodal curve) was located inside the quaternary diagram. When the additive content increases within the polymer solution, a shift towards the region poorer in nonsolvent occurs, thus increasing the miscibility gap. When the phase separation occurs slowly, the polymer and the additive begin to separate. At this point, the composition of the solution may be in the unstable region of the quaternary diagram, resulting in spinodal demixing with typical membrane morphology leading to interconnected pores.

Theoretically, the Flory Huggins theory has been reported to describe the Gibbs energy of mixing such a multicomponent polymer system and a methodology that allows the phase diagram calculation for quaternary mixtures without assuming a pseudo ternary system [134,135]. However, this thesis will not investigate theoretical modelling relating to the ternary or quaternary system for polymer systems with GVL as solvent.

Many studies on PVDF membranes have examined the relationship between membrane morphology and performance. In those research work, several preparation factors such as the influence of polymer molecular weight and concentration, composition of polymer solution (dope); coagulation medium, dissolved polymer temperature, coagulation and casting temperature, solvent, evaporation rate, casting thickness, casting speed and choice of polymer or nonsolvent additives [136,137,138] were investigated and used to modify the membrane morphological structure & performance. Furthermore, the consideration of polymer/nonsolvent additives and inorganic salt has been used to improve membrane porosity and hydrophilicity, influence mechanical properties, and modify the morphological structure [9]. Typically, these additives are used as pore-forming agents in membrane preparation and have hydrophilic or amphiphilic groups. Common examples of additives used are polyvinylpyrrolidone (PVP), polyethylene glycol (PEG), propionic acid (PA), water, Lithium chloride (LiCl), polyethylene oxide (PEO) and zinc chloride (ZnCl) [139,140]. However, adding these additives has been reported to increase the dope solution's viscosity and hinder the phase separation kinetics while significantly enhancing the thermodynamics for the phase separation [141,142]. Table 2.3 highlights several parameters frequently examined for commercial and lab-based literature studies in the fabrication of PVDF membranes via the NIPS approach, including conditions of casting temperature, dissolution temperatures, and polymer concentration.

Majority of the time, it is interesting to evaluate and study the properties of the synthesised PVDF membrane since it provides insight into the relationship between the membrane structure, physical features and performance. Among the different characterisation methods is scanning electron microscopy (SEM), an imaging tool used to provide detailed micro- and nano-scale dimension information of the surface and cross section of the morphological structure of membrane materials. Typically, PVDF membranes prepared have been observed to exhibit a dense sponge-like, finger-like cross section morphology or globule-like nodular surface structure, depending on the process parameters investigated and its influence on the demixing process that occurred during the fabrication [143]. Other techniques used to evaluate polymeric membranes includes physical measurement such as membrane thickness, pore size distribution and porosity [144,145].

Table 2-3: Effect of different process parameters influencing PVDF membrane via the NIPS approach.

Process parameter	Impact variable	Membrane morphology	Porosity (%)	Contact angle (°)	Degree of crystallinity (%)	Flux ($L.m^{-2}.h^{-1}$)	Ref.
Solvent	Stronger solvent power results in increased gravimetric porosity and pore size	Macrovoids & finger-like structure	75.1 - 90.2	80-88.3	35.2 – 46	12.5-620	[146, 147, 39]
	Weak solvent power. Reduced porosity values	Dense with a sponge-like structure					
Polymer concentration	Low concentration (10 -12.5%wt) Higher water flux due to the formation of membrane structure	Macrovoids and high overall porosity	68 -82%	85 - 92	57-62%	5 - 160	[148, 58, 149, 150]
	High concentration (20-25%wt). Reduced overall membrane porosity and water flux	Sponge-like structure; macrovoids progressively disappear with increasing polymer concentration;		77-145			
Coagulation bath temperature	low temperature (≤30°C)	Finger-like with large macrovoids	34-83%	84- 150	38-69	40-152	[151, 152]
	high temperature (>30°C - 60°C)	Sponge-like or globule-like structure with increasing coagulation bath temperature				15-70	
dissolution temperature	Increasing temperature between 50-120°C	Bi-continuous network with cross section cavities	60-92	60 -88	32 - 59	0.4 - 5.2	[153, 154, 155]
Additives (PVP)	Low concentration of additive (≤7.5wt%)	larger finger-like macrovoids increased gravimetric porosity and mean pore size	86 - 90	76 -95	-	145-800	[156, 140, 157]
	High concentration of additive (>7.5wt%)	Reduced gravimetric porosity, fewer macrovoids					

The use of Fourier transform infrared (FTIR) spectroscopy, water contact angle instrument, differential scanning calorimeter (DSC), and atomic force microscopy (AFM) have also been utilised used as valuable tools to provide quantitative and qualitative analysis of the surface properties of fabricated membranes [158]. The FTIR allows the determination of functional groups and molecular bonds in membrane materials by understanding the positions of the infrared (IR) absorption bands. The water contact angle analysis allows the characterisation of the membrane hydrophilicity and hydrophobicity property [159].

The DSC is a thermal analytical technique that evaluates the change of heat flow on a material and is measured as a function of temperature. The DSC compares the amount of heat energy it takes to heat an empty pan, referred to as the “reference”, with a pan containing the sample to be analysed. The equipment heats up both reference and sample pan holders and maintains the temperature by heating at a constant rate during the experiment. The heat absorption and release are measured, and the difference between reference and sample pans, which is proportional to the temperature, is recorded. In addition, standard material calibration is conducted to provide quantitative measurements of analysed sample material. Thus, the DSC analysis allows the transition observation of the examined material's melting temperature, phase changes, thermal stability, glass transition and crystallisation temperature. Typically the technique is employed in characterising the different fabricated PVDF materials. In the presented study, the DSC is used to analyse the thermal behaviour and degree of crystallinity of the membrane [160,161] to analyse any difference in thermal properties of the sample materials. Discussed characteristics are not an exhaustive effort in accounting for all membrane characterisation techniques. However, the mentioned methods will be used to obtain essential information about fabricated PVDF membranes. Furthermore, the knowledge acquired will help guide the design of PVDF membranes with desired properties for specific applications [104].

Since the development of PVDF membrane fabrication using green bio solvent is not well explored. The study presented in subsequent chapters would prepare PVDF membrane using GVL as solvent via the widely employed NIPS technique. The PVDF membrane properties will be evaluated to examine how the selected process parameters affect membrane morphology and performance. In addition, results will be contrasted with reported PVDF membranes prepared using toxic solvents and discussed. An overview of the research presented in the thesis will be to combine specific process fabrication factors and optimise the morphology and performance of fabricated PVDF membranes that meet or exceed existing membrane performance criteria for water separation applications.

2.4 References

[1] Mulder, J. (2012). Basic principles of membrane technology. Springer Science & Business Media.

[2] W.S.W., Sirkar K.K. (1992) Overview. In: Ho W.S.W., Sirkar K.K. (eds) Membrane Handbook (pp. 3-15). Springer, Boston, MA.

[3] Sutherland, K. (Ed.). (2003). Profile of the International Membrane Industry-Market Prospects to 2008. Elsevier.

[4] L. Eykens, K. De Sitter, C. Dotremont, L. Pinoy, B. Van der Bruggen, Membrane synthesis for membrane distillation: A review, Separation and Purification Technology, 182 (2017) 36-51

[5] Dao, T. D., Mericq, J. P., Laborie, S., & Cabassud, C. (2013). A new method for permeability measurement of hydrophobic membranes in Vacuum Membrane Distillation process. *water research*, *47*(6), 2096-2104.

[6] Figoli A., Simone S., Drioli E. Polymeric membranes. In: Hilal, N., Ismail, A. F., & Wright, C. (Eds.). (2015). *Membrane fabrication*. CRC Press. pp. 1–42.

[7] Kang, G. D., & Cao, Y. M. (2014). Application and modification of poly (vinylidene fluoride)(PVDF) membranes–a review. *Journal of membrane science*, *463*, 145-165.

[8] Lalia, B. S., Kochkodan, V., Hashaikeh, R., & Hilal, N. (2013). A review on membrane fabrication: Structure, properties and performance relationship. *Desalination*, *326*, 77-95.

[9] Guillen, G. R., Pan, Y., Li, M., & Hoek, E. M. (2011). Preparation and characterization of membranes formed by nonsolvent induced phase separation: a review. *Industrial & Engineering Chemistry Research*, *50*(7), 3798-3817.

[10] Loeb, S., & Sourirajan, S. (1962). High-flow semipermeable membranes for separation of water from saline solutions. *Adv Chem Ser*, *38*(1), 117-132.

[11] Wang, D. M., & Lai, J. Y. (2013). Recent advances in preparation and morphology control of polymeric membranes formed by nonsolvent induced phase separation. *Current Opinion in Chemical Engineering*, *2*(2), 229-237.

[12] Altinkaya, S. A., & Ozbas, B. (2004). Modeling of asymmetric membrane formation by dry-casting method. *Journal of Membrane Science*, *230*(1-2), 71-89.

[13] J. Jansen, M. Macchione and E. Drioli, High flux asymmetric gas separation membranes of modified poly (ether ether ketone) prepared by the dry phase inversion technique, *J. Membr. Sci.*, 2005, 255, 167–18

[14] Kim, J. F., Kim, J. H., Lee, Y. M., & Drioli, E. (2016). Thermally induced phase separation and electrospinning methods for emerging membrane applications: A review. *AIChE Journal*, *62*(2), 461-490.

[15] Su, Y., Chen, C., Li, Y., & Li, J. (2007). PVDF membrane formation via thermally induced phase separation. *Journal of Macromolecular Science Part A: Pure and Applied Chemistry*, *44*(1), 99-104.

[16] Figoli, A., Marino, T., Simone, S., Di Nicolo, E., Li, X. M., He, T., ... & Drioli, E. (2014). Towards non-toxic solvents for membrane preparation: a review. *Green Chemistry*, *16*(9), 4034-4059.

[17] M. Liu, Y.-M. Wei, Z.-L. Xu, R.-Q. Guo, L.-B. Zhao, Preparation and characterization of polyethersulfone microporous membrane via thermally induced phase separation with low critical solution temperature system, Journal of Membrane Science 437 (2013) 169–178.

[18] Lloyd, D.R., K.E. Kinzer, and H.S. Tseng, Microporous Membrane Formation Via Thermally Induced Phase-Separation .1. Solid Liquid-Phase Separation. Journal of Membrane Science, 1990. 52(3): p. 239-261.

[19] Mat Nawi, N. I., Chean, H. M., Shamsuddin, N., Bilad, M. R., Narkkun, T., Faungnawakij, K., & Khan, A. L. (2020). Development of hydrophilic PVDF membrane using vapour induced phase separation method for produced water treatment. *Membranes*, *10*(6), 121.

[20] Tsai, J. T., Su, Y. S., Wang, D. M., Kuo, J. L., Lai, J. Y., & Deratani, A. (2010). Retainment of pore connectivity in membranes prepared with vapor-induced phase separation. *Journal of Membrane Science*, *362*(1-2), 360-373.

[21] Khare, V. P., Greenberg, A. R., & Krantz, W. B. (2005). Vapor-induced phase separation—Effect of the humid air exposure step on membrane morphology: Part I. Insights from mathematical modeling. *Journal of Membrane Science*, *258*(1-2), 140-156.

[22] Li, C. L., Wang, D. M., Deratani, A., Quémener, D., Bouyer, D., & Lai, J. Y. (2010). Insight into the preparation of poly (vinylidene fluoride) membranes by vapor-induced phase separation. *Journal of membrane science*, *361*(1-2), 154-166.

[23] Zhao, N., Xie, Q., Weng, L., Wang, S., Zhang, X., & Xu, J. (2005). Superhydrophobic surface from vapor-induced phase separation of copolymer micellar solution. *Macromolecules*, *38*(22), 8996-8999.

[24] M. Pagliero, A. Bottino, A. Comite, C. Costa, Novel hydrophobic PVDF membranes prepared by nonsolvent induced phase separation for membrane distillation, Journal of Membrane Science, 596 (2020) 117575.

[25] Khulbe, K. C., Feng, C. Y., & Matsuura, T. (2007). *Synthetic polymeric membranes: characterization by atomic force microscopy*. Springer Science & Business Media.

[26] Annamalai, P. K., Pochat-Bohatier, C., Bouyer, D., Li, C. L., Deratani, A., & Wang, D. M. (2011). Kinetics of mass transfer during vapour-induced phase separation (VIPS) process and its influence on poly-(vinylidene fluoride)(PVDF) membrane structure and surface morphology. *Desalination and Water Treatment*, *34*(1-3), 204-210.

[27] Baker, R. W., & Updated by Staff. (2000). Membrane technology. *Kirk-Othmer Encyclopedia of Chemical Technology*.

[28] Marchetti, P., Jimenez Solomon, M. F., Szekely, G., & Livingston, A. G. (2014). Molecular separation with organic solvent nanofiltration: a critical review. *Chemical reviews*, *114*(21), 10735-10806.

[29] Ladewig, B., & Al-Shaeli, M. N. Z. (2017). Fundamentals of membrane processes. In *Fundamentals of membrane bioreactors* (pp. 13-37). Springer, Singapore.

[30] Zhu, Y., Romain, C., & Williams, C. K. (2016). Sustainable polymers from renewable resources. *Nature*, *540*(7633), 354-362.

[31] Galiano, F., Briceño, K., Marino, T., Molino, A., Christensen, K. V., & Figoli, A. (2018). Advances in biopolymer-based membrane preparation and applications. *Journal of Membrane Science*, *564*, 562-586.

[32] H.A. Le Phuong, N.A. Izzati Ayob, C.F. Blanford, N.F. Mohammad Rawi, G. Szekely, Nonwoven Membrane Supports from Renewable Resources: Bamboo Fiber Reinforced Poly(Lactic Acid) Composites, ACS Sustainable Chemistry & Engineering, 7 (2019) 11885-11893.

[33] Colburn, A., Vogler, R. J., Patel, A., Bezold, M., Craven, J., Liu, C., & Bhattacharyya, D. (2019). Composite membranes derived from cellulose and lignin sulfonate for selective separations and antifouling aspects. *Nanomaterials*, *9*(6), 867.

[34] Cui, L., Gao, S., Song, X., Huang, L., Dong, H., Liu, J., ... & Yu, S. (2018). Preparation and characterization of chitosan membranes. *RSC Advances*, *8*(50), 28433-28439.

[35] Lee, D. W., Lim, H., Chong, H. N., & Shim, W. S. (2009). Advances in chitosan material and its hybrid derivatives: a review. *The Open Biomaterials Journal*, *1*(1).

[36] Wang, Q., Wang, Z., & Wu, Z. (2012). Effects of solvent compositions on physicochemical properties and anti-fouling ability of PVDF microfiltration membranes for wastewater treatment. *Desalination*, *297*, 79-86.

[37] Tao, M. M., Liu, F., Ma, B. R., & Xue, L. X. (2013). Effect of solvent power on PVDF membrane polymorphism during phase inversion. *Desalination*, *316*, 137-145.

[38] Nejati, S., Boo, C., Osuji, C. O., & Elimelech, M. (2015). Engineering flat sheet microporous PVDF films for membrane distillation. *Journal of Membrane Science*, *492*, 355-363.

[39] Yeow, M. L., Liu, Y. T., & Li, K. (2004). Morphological study of poly (vinylidene fluoride) asymmetric membranes: effects of the solvent, additive, and dope temperature. *Journal of Applied Polymer Science*, *92*(3), 1782-1789.

[40] Lin, D. J., Chang, H. H., Chen, T. C., Lee, Y. C., & Cheng, L. P. (2006). Formation of porous poly (vinylidene fluoride) membranes with symmetric or asymmetric morphology by immersion precipitation in the water/TEP/PVDF system. *European polymer journal*, *42*(7), 1581-1594.

[41] Shih, H. C., Yeh, Y. S., & Yasuda, H. (1990). Morphology of microporous poly (vinylidene fluoride) membranes studied by gas permeation and scanning electron microscopy. *Journal of membrane science*, *50*(3), 299-317.

[42] Marino, T., Russo, F., & Figoli, A. (2018). The formation of polyvinylidene fluoride membranes with tailored properties via vapour/non-solvent induced phase separation. *Membranes*, *8*(3), 71.

[43] Jung, J. T., Wang, H. H., Kim, J. F., Lee, J., Kim, J. S., Drioli, E., & Lee, Y. M. (2018). Tailoring nonsolvent-thermally induced phase separation (N-TIPS) effect using triple spinneret to fabricate high performance PVDF hollow fiber membranes. *Journal of Membrane Science*, *559*, 117-126.

[44] Hassankiadeh, N. T., Cui, Z., Kim, J. H., Shin, D. W., Lee, S. Y., Sanguineti, A., ... & Drioli, E. (2015). Microporous poly (vinylidene fluoride) hollow fiber membranes fabricated with PolarClean as water-soluble green diluent and additives. *Journal of Membrane Science*, *479*, 204-212.

[45] Cha, B. J., & Yang, J. M. (2007). Preparation of poly (vinylidene fluoride) hollow fiber membranes for microfiltration using modified TIPS process. *Journal of membrane science*, *291*(1-2), 191-198.

[46] Ghasem, N., Al-Marzouqi, M., & Rahim, N. A. (2012). Effect of polymer extrusion temperature on poly (vinylidene fluoride) hollow fiber membranes: Properties and performance used as gas–liquid membrane contactor for CO2 absorption. *Separation and purification technology*, *99*, 91-103.

[47] Rajabzadeh, S., Maruyama, T., Sotani, T., & Matsuyama, H. (2008). Preparation of PVDF hollow fiber membrane from a ternary polymer/solvent/nonsolvent system via thermally induced phase separation (TIPS) method. *Separation and Purification Technology*, *63*(2), 415-423.

[48] Van Goethem, C., Magboo, M. M., Mertens, M., Thijs, M., Koeckelberghs, G., & Vankelecom, I. F. (2020). A scalable crosslinking method for PVDF-based nanofiltration membranes for use under extreme pH conditions. *Journal of Membrane Science*, *611*, 118274.

[49] Marino, T., Russo, F., Criscuoli, A., & Figoli, A. (2017). TamiSolve® NxG as novel solvent for polymeric membrane preparation. *Journal of Membrane Science*, *542*, 418-429.

[50] Saidi, S., Macedonio, F., Russo, F., Hannachi, C., Hamrouni, B., Drioli, E., & Figoli, A. (2021). Preparation and characterization of hydrophobic P (VDF-HFP) flat sheet membranes using Tamisolve® NxG solvent for the treatment of saline water by direct contact membrane distillation and membrane crystallization. *Separation and Purification Technology*, *275*, 119144.

[51] Marino, T., Galiano, F., Molino, A., & Figoli, A. (2019). New frontiers in sustainable membrane preparation: Cyrene™ as green bioderived solvent. *Journal of Membrane Science*, *580*, 224-234.

[52] Russo, F., Galiano, F., Pedace, F., Aricò, F., & Figoli, A. (2019). Dimethyl isosorbide as a green solvent for sustainable ultrafiltration and microfiltration membrane preparation. *ACS Sustainable Chemistry & Engineering*, *8*(1), 659-668.

[53] Capello, C., Fischer, U., & Hungerbühler, K. (2007). What is a green solvent? A comprehensive framework for the environmental assessment of solvents. *Green Chemistry*, *9*(9), 927-934.

[54] Fedors, R. F. (1974). A method for estimating both the solubility parameters and molar volumes of liquids. *Polymer Engineering & Science*, *14*(2), 147-154.

[55] Hansen, C. M. (2004). 50 Years with solubility parameters—past and future. *Progress in Organic Coatings*, *51*(1), 77-84.

[56] Hansen, C. M. (2002). Hansen solubility parameters: a user's handbook. CRC press.

[57] Lubasova, D., & Martinova, L. (2011). Controlled morphology of porous polyvinyl butyral nanofibers. *Journal of Nanomaterials*, *2011*.

[58] Jung, J. T., Kim, J. F., Wang, H. H., di Nicolo, E., Drioli, E., & Lee, Y. M. (2016). Understanding the non-solvent induced phase separation (NIPS) effect during the fabrication of microporous PVDF membranes via thermally induced phase separation (TIPS). *Journal of Membrane Science*, *514*, 250-263.

[59] Barton, A. F. (2017). CRC handbook of solubility parameters and other cohesion parameters. Routledge.

[60] Van Krevelen, D. W., & Hoftyzer, P. J. (1967). Practical evaluation of the [η]–M relationship. III. Estimation of the exponent A. *Journal of Applied Polymer Science*, *11*(11), 2189-2200.

[61] Eroğlu, M. S., Baysal, B. M., & Güven, O. (1997). Determination of solubility parameters of poly (epichlorohydrin) and poly (glycidyl azide) networks. *Polymer*, *38*(8), 1945-1947.

[62] Özdemir, C., & Güner, A. (2007). Solubility profiles of poly (ethylene glycol)/solvent systems, I: Qualitative comparison of solubility parameter approaches. *European Polymer Journal*, *43*(7), 3068-3093.

[63] Sperling, L. H. (2005). *Introduction to physical polymer science*. John Wiley & Sons.

[64] Errede, L. A. (1986). Polymer swelling. 5. Correlation of relative swelling of poly (styrene-co-divinylbenzene) with the Hildebrand solubility parameter of the swelling liquid. *Macromolecules*, *19*(6), 1522-1525.

[65] Flory, P. J. (1942). Thermodynamics of high polymer solutions. *The Journal of chemical physics*, *10*(1), 51-61.

[66] Fredenslund, A., Jones, R. L., & Prausnitz, J. M. (1975). Group-contribution estimation of activity coefficients in nonideal liquid mixtures. *AIChE Journal*, *21*(6), 1086-1099.

[67] Fredenslund, A. (1989). UNIFAC and related group-contribution models for phase equilibria. *Fluid Phase Equilibria*, *52*, 135-150.

[68] Sandler, S. I. (2017). Chemical, biochemical, and engineering thermodynamics. John Wiley & Sons.

[69] Benazzouz, A., Moity, L., Pierlot, C., Sergent, M., Molinier, V., & Aubry, J. M. (2013). Selection of a greener set of solvents evenly spread in the Hansen space by space-filling design. *Industrial & Engineering Chemistry Research*, *52*(47), 16585-16597.

[70] Magueijo et al. University of Strathclyde chemical Day poster, 2016

[71] Figoli, A., Marino, T., Simone, S., Di Nicolo, E., Li, X. M., He, T., & Drioli, E. (2014). Towards non-toxic solvents for membrane preparation: a review. *Green Chemistry*, *16*(9), 4034-4059.

[72] Kerton, F., & Marriott, R. (2013). Alternative solvents for green chemistry.

[73] Nunes, S. P., & Peinemann, K. V. (Eds.). (2006). *Membrane technology: in the chemical industry*. John Wiley & Sons.

[74] Regulation, E. C. (1999). No 1907/2006 of the European Parliament and of the Council of 18 December 2006 concerning the Registration. Evaluation, Authorisation and Restriction of Chemicals (REACH), establishing a European Chemicals Agency, amending Directive, 1999/45/EC and Repealing Council Regulation (EEC) No 793/93 and Commission Regulation (EC) No 1488/94 as well as Council Directive 76/769/EEC and Commission Directives 91/155/EEC, 93/67/EEC, 93/105/EC and 2000/21/EC. Available online: http://eur-lex.europa.eu/LexUriServ/LexUriServ.do?uri=OJ:L:2007:136:0003: 0280:en:PDF (accessed on 16 January 2019).

[75] F.P. Byrne, S. Jin, G. Paggiola, T.H.M. Petchey, J.H. Clark, T.J. Farmer, A.J. Hunt, C. Robert McElroy, J. Sherwood, Tools and techniques for solvent selection: green solvent selection guides, Sustainable Chemical Processes 4 (2016) 7.

[76] Randová, A., Bartovská, L., Morávek, P., Matějka, P., Novotná, M., Matějková, S., ... & Friess, K. (2016). A fundamental study of the physicochemical properties of Rhodiasolv® Polarclean: A promising alternative to common and hazardous solvents. *Journal of Molecular Liquids*, *224*, 1163-1171.

[77] Wang, H. H., Jung, J. T., Kim, J. F., Kim, S., Drioli, E., & Lee, Y. M. (2019). A novel green solvent alternative for polymeric membrane preparation via nonsolvent-induced phase separation (NIPS). *Journal of Membrane Science*, *574*, 44-54.

[78] Medina-Gonzalez, Y., Aimar, P., Lahitte, J. F., & Remigy, J. C. (2011). Towards green membranes: preparation of cellulose acetate ultrafiltration membranes using methyl lactate as a biosolvent. *International Journal of Sustainable Engineering*, *4*(01), 75-83.

[79] Russo, F., Ursino, C., Avruscio, E., Desiderio, G., Perrone, A., Santoro, S., ... & Figoli, A. (2020). Innovative Poly (Vinylidene Fluoride)(PVDF) electrospun nanofiber membrane preparation using DMSO as a low toxicity solvent. *Membranes*, *10*(3), 36.

[80] Meringolo, C., Mastropietro, T. F., Poerio, T., Fontananova, E., De Filpo, G., Curcio, E., & Di Profio, G. (2018). Tailoring PVDF membranes surface topography and hydrophobicity by a sustainable two-steps phase separation process. *ACS Sustainable Chemistry & Engineering*, *6*(8), 10069-10077.

[81] Alonso, D. M., Wettstein, S. G., & Dumesic, J. A. (2013). Gamma-valerolactone, a sustainable platform molecule derived from lignocellulosic biomass. *Green Chemistry*, *15*(3), 584-595.

[82] Valentini, F., Brufani, G., Di Erasmo, B., & Vaccaro, L. (2022). γ-Valerolactone (GVL) as a green and efficient dipolar aprotic reaction medium. *Current Opinion in Green and Sustainable Chemistry*, 100634.

[83] Hengst, K., Schubert, M., Kleist, W., & Grunwaldt, J. D. (2014). Hydrodeoxygenation of lignocellulose-derived platform molecules. *Catalytic Hydrogenation for Biomass Valorization; Rinaldi, R., Ed.; The Royal Society of Chemistry: Cambridge, UK*, 125-150.

[84] Chia, M., & Dumesic, J. A. (2011). Liquid-phase catalytic transfer hydrogenation and cyclization of levulinic acid and its esters to γ-valerolactone over metal oxide catalysts. *Chemical Communications*, *47*(44), 12233-12235.

[85] Piskun, A. S., Van de Bovenkamp, H. H., Rasrendra, C. B., Winkelman, J. G. M., & Heeres, H. J. (2016). Kinetic modeling of levulinic acid hydrogenation to γ-valerolactone in water using a carbon supported Ru catalyst. *Applied Catalysis A: General*, *525*, 158-167.

[86] Havasi, D., Mizsey, P., & Mika, L. T. (2016). Vapor–Liquid Equilibrium Study of the Gamma-Valerolactone–Water Binary System. *Journal of Chemical & Engineering Data*, *61*(4), 1502-1508.

[87] Horváth, I. T., Mehdi, H., Fábos, V., Boda, L., & Mika, L. T. (2008). γ-Valerolactone—a sustainable liquid for energy and carbon-based chemicals. *Green Chemistry*, *10*(2), 238-242.

[88] Ravotti, R., Fellmann, O., Lardon, N., Fischer, L. J., Stamatiou, A., & Worlitschek, J. (2019). Investigation of lactones as innovative bio-sourced phase change materials for latent heat storage. *Molecules*, *24*(7), 1300.

[89] Fegyverneki, D., Orha, L., Láng, G., & Horváth, I. T. (2010). Gamma-valerolactone-based solvents. *Tetrahedron*, *66*(5), 1078-1081.

[90] Tang, X., Zeng, X., Li, Z., Hu, L., Sun, Y., Liu, S. ... & Lin, L. (2014). Production of γ-valerolactone from lignocellulosic biomass for sustainable fuels and chemicals supply. *Renewable and Sustainable Energy Reviews*, *40*, 608-620.

[91] Rasool, M. A., & Vankelecom, I. F. (2021). γ-Valerolactone as Bio-Based Solvent for Nanofiltration Membrane Preparation. *Membranes*, *11*(6), 418.

[92] Pârvulescu, V. I., & Hardacre, C. (2007). Catalysis in ionic liquids. *Chemical Reviews*, *107*(6), 2615-2665.

[93] D.Y. Xing, W.Y. Dong, T.-S. Chung, Effects of Different Ionic Liquids as Green Solvents on the Formation and Ultrafiltration Performance of CA Hollow Fiber Membranes, Ind. Eng. Chem. Res., 55 (2016) 7505-7513.

[94] Livazovic, S., Li, Z., Behzad, A. R., Peinemann, K. V., & Nunes, S. P. (2015). Cellulose multilayer membranes manufacture with ionic liquid. *Journal of Membrane Science*, *490*, 282-293.

[95] Li, C., Zhu, Y., Lv, R., Na, B., & Chen, B. (2014). Poly (vinylidene fluoride) membrane with piezoelectric β-form prepared by immersion precipitation from mixed solvents containing an ionic liquid. *Journal of Applied Polymer Science*, *131*(15).

[96] Xing, C., Zhao, M., Zhao, L., You, J., Cao, X., & Li, Y. (2013). Ionic liquid modified poly (vinylidene fluoride): crystalline structures, miscibility, and physical properties. *Polymer Chemistry*, *4*(24), 5726-5734.

[97] Colburn, A., Wanninayake, N., Kim, D. Y., & Bhattacharyya, D. (2018). Cellulose-graphene quantum dot composite membranes using ionic liquid. *Journal of membrane science*, *556*, 293-302.

[98] Rogers, R. D., & Seddon, K. R. (2003). Ionic liquids--solvents of the future?. *Science*, *302*(5646), 792-793.

[99] Kim, D.; Vovusha, H.; Schwingenschlögl, U.; Nunes, S. P. Polyethersulfone Flat Sheet and Hollow Fiber Membranes from Solutions in Ionic Liquids. J. Membr. Sci. 2017, 539, 161−171.

[100] Xing, D. Y., Chan, S. Y., & Chung, T. S. (2014). The ionic liquid [EMIM] OAc as a solvent to fabricate stable polybenzimidazole membranes for organic solvent nanofiltration. *Green Chemistry*, *16*(3), 1383-1392.

[101] Romero, A., Santos, A., Tojo, J., & Rodríguez, A. J. J. O. H. M. (2008). Toxicity and biodegradability of imidazolium ionic liquids. *Journal of hazardous materials*, *151*(1), 268-273.

[102] Mullins, E., Oldland, R., Liu, Y. A., Wang, S., Sandler, S. I., Chen, C. C., ... & Seavey, K. C. (2006). Sigma-profile database for using COSMO-based thermodynamic methods. *Industrial & engineering chemistry research*, *45*(12), 4389-4415.

[103] Magueijo, V. M., Anderson, L. G., Fletcher, A. J., & Shilton, S. J. (2013). Polysulfone mixed matrix gas separation hollow fibre membranes filled with polymer and carbon xerogels. *Chemical Engineering Science*, *92*, 13-20.

[104] Matsuyama, H., Nishiguchi, M., & Kitamura, Y. (2000). Phase separation mechanism during membrane formation by dry-cast process. *Journal of applied polymer science*, *77*(4), 776-783.

[105] Tompa, H. (1949). Phase relationships in polymer solutions. *Transactions of the Faraday Society*, *45*, 1142-1152.

[106] Altena, F. W., & Smolders, C. A. (1982). Calculation of liquid-liquid phase separation in a ternary system of a polymer in a mixture of a solvent and a nonsolvent. *Macromolecules*, *15*(6), 1491-1497.

[107] Mohsenpour, S., Esmaeilzadeh, F., Safekordi, A., Tavakolmoghadam, M., Rekabdar, F., & Hemmati, M. (2016). The role of thermodynamic parameter on membrane morphology based on phase diagram. *Journal of Molecular Liquids*, *224*, 776-785.

[108] Yilmaz, L., & McHugh, A. J. (1986). Analysis of nonsolvent–solvent–polymer phase diagrams and their relevance to membrane formation modelling. *Journal of applied polymer science*, *31*(4), 997-1018.

[109] Romay, M., Diban, N., & Urtiaga, A. (2021). Thermodynamic modeling and validation of the temperature influence in ternary phase polymer systems. *Polymers*, *13*(5), 678.

[110] Young, T. H., & Chuang, W. Y. (2002). Thermodynamic analysis on the cononsolvency of poly (vinyl alcohol) in water–DMSO mixtures through the ternary interaction parameter. *Journal of membrane science*, *210*(2), 349-359.

[111] Kamide, K. (1990). Thermodynamics of Polymer Solutions Phase Equilibria and Critical Phenomena. *Polymer Science Library*, *9*.

[112] Strathmann, H., & Kock, K. (1977). The formation mechanism of phase inversion membranes. *Desalination*, *21*(3), 241-255.

[113] Broens, L., Altena, F. W., Smolders, C. A., & Koenhen, D. M. (1980). Asymmetric membrane structures as a result of phase separation phenomena. *Desalination*, *32*, 33-45.

[114] van de Witte, P. J. D. P., Dijkstra, P. J., Van den Berg, J. W. A., & Feijen, J. (1996). Phase separation processes in polymer solutions in relation to membrane formation. *Journal of membrane science*, *117*(1-2), 1-31.

[115] Ariono, D., Aryanti, P. T. P., Hakim, A. N., Subagjo, S., & Wenten, I. G. (2017, May). Determination of thermodynamic properties of polysulfone/PEG membrane solutions based on Flory-Huggins model. In *AIP Conference Proceedings* (Vol. 1840, No. 1, p. 090008). AIP Publishing LLC.

[116] L. Keshavarz, M.A. Khansary, S. Shirazian, Phase diagram of ternary polymeric solutions containing nonsolvent/solvent/polymer: Theoretical calculation and experimental validation, Polymer 73 (2015) 1–8.

[117] Ismail, A. F., & Yean, L. P. (2003). Review on the development of defect-free and ultrathin-skinned asymmetric membranes for gas separation through manipulation of phase inversion and rheological factors. *Journal of Applied Polymer Science*, *88*(2), 442-451.

[118] Guenet, J. M. (1992). Thermoreversible gelation of polymers and biopolymers. Academic Press.

[119] Wienk, I. M., Boom, R. M., Beerlage, M. A. M., Bulte, A. M. W., Smolders, C. A., & Strathmann, H. (1996). Recent advances in the formation of phase inversion membranes made from amorphous or semi-crystalline polymers. *Journal of Membrane Science*, *113*(2), 361-371.

[120] Stropnik, C., Germic, L., & Zerjal, B. (1996). Morphology variety and formation mechanisms of polymeric membranes prepared by wet phase inversion. *Journal of applied polymer science*, *61*(10), 1821-1830.

[121] Barth, C., & Wolf, B. A. (2000). Quick and reliable routes to phase diagrams for polyethersulfone and polysulfone membrane formation. *Macromolecular Chemistry and Physics*, *201*(3), 365-374.

[122] Cohen, C., Tanny, G. B., & Prager, S. (1979). Diffusion-controlled formation of porous structures in ternary polymer systems. *Journal of Polymer Science: Polymer Physics Edition*, *17*(3), 477-489.

[123] Lloyd, D. R., Kinzer, K. E., & Tseng, H. S. (1990). Microporous membrane formation via thermally induced phase separation. I. Solid-liquid phase separation. *Journal of Membrane Science*, *52*(3), 239-261.

[124] Reuvers, A. J., Van den Berg, J. W. A., & Smolders, C. (1987). Formation of membranes by means of immersion precipitation: Part I. A model to describe mass transfer during immersion precipitation. *Journal of membrane science*, *34*(1), 45-65.

[125] Radovanovic, P., Thiel, S. W., & Hwang, S. T. (1992). Formation of asymmetric polysulfone membranes by immersion precipitation. Part I. Modelling mass transport during gelation. *Journal of membrane science*, *65*(3), 213-229.

[126] Tsay, C. S., & McHugh, A. J. (1990). Mass transfer modeling of asymmetric membrane formation by phase inversion. *Journal of Polymer Science Part B: Polymer Physics*, *28*(8), 1327-1365.

[127] Cheng, L. P., Dwan, A. H., & Gryte, C. C. (1995). Membrane formation by isothermal precipitation in polyamide-formic acid-water systems I. Description of membrane morphology. *Journal of Polymer Science Part B: Polymer Physics*, *33*(2), 211-222.

[128] H.H. Wang, J.T. Jung, J.F. Kim, S. Kim, E. Drioli, Y.M. Lee, A novel green solvent alternative for polymeric membrane preparation via nonsolvent-induced phase separation (NIPS), Journal of Membrane Science, 574 (2019) 44-54.

[129] Tran Duc, V. N., & Chan, P. K. (2019). Using the Cahn–Hilliard Theory in Metastable Binary Solutions. *ChemEngineering*, *3*(3), 75.

[130] Kahrs, C., Gühlstorf, T., & Schwellenbach, J. (2020). Influences of different preparation variables on polymeric membrane formation via nonsolvent induced phase separation. *Journal of Applied Polymer Science*, *137*(28), 48852.

[131] Freeman, B. D. (1999). Basis of permeability/selectivity tradeoff relations in polymeric gas separation membranes. *Macromolecules*, *32*(2), 375-380.

[132] Hopp-Hirschler, M., & Nieken, U. (2018). Modeling of pore formation in phase inversion processes: Model and numerical results. *Journal of Membrane Science*, *564*, 820-831.

[133] Boom, R. M. (1994). Membrane formation by immersion precipitation: The role of a polymeric additive.

[134] Horst, R., & Wolf, B. A. (1995). Phase diagrams calculated for quaternary polymer blends. *The Journal of chemical physics*, *103*(9), 3782-3787.

[135] Boom, R. M., Van den Boomgaard, T., & Smolders, C. A. (1994). Equilibrium thermodynamics of a quaternary membrane-forming system with two polymers. 1. Calculations. *Macromolecules*, *27*(8), 2034-2040.

[136] Sugihara, M., Fujimoto, M., & Uragami, T. (1979, January). Effect of casting solvent on permeation characteristics of polyvinylidene fluoride membranes. In *ABSTRACTS OF PAPERS OF THE AMERICAN CHEMICAL SOCIETY* (No. APR, p. 296). 1155 16TH ST, NW, WASHINGTON, DC 20036: AMER CHEMICAL SOC.

[137] Morphological study of poly(vinylidene fluoride) asymmetric membranes: effects of the solvent, additive, and dope temperature

[138] Pinnau, I. F. B. D., & Freeman, B. D. (2000). Formation and modification of polymeric membranes: overview.

[139] Wang, D., Li, K., & Teo, W. K. (2000). Porous PVDF asymmetric hollow fiber membranes prepared with the use of small molecular additives. *Journal of Membrane Science*, *178*(1-2), 13-23.

[140] Fontananova, E., Jansen, J. C., Cristiano, A., Curcio, E., & Drioli, E. (2006). Effect of additives in the casting solution on the formation of PVDF membranes. Desalination, 192(1-3), 190-197.

[141] Tan, X., & Rodrigue, D. (2019). A review on porous polymeric membrane preparation. Part I: production techniques with polysulfone and poly (vinylidene fluoride). *Polymers*, *11*(7), 1160.

[142] Han, M. J., & Nam, S. T. (2002). Thermodynamic and rheological variation in polysulfone solution by PVP and its effect in the preparation of phase inversion membrane. *Journal of Membrane Science*, *202*(1-2), 55-61.

[143] Lin, D. J., Chang, C. L., Lee, C. K., & Cheng, L. P. (2006). Preparation and characterization of microporous PVDF/PMMA composite membranes by phase inversion in water/DMSO solutions. *European polymer journal*, *42*(10), 2407-2418.

[144] Wyart, Y., Georges, G., Deumie, C., Amra, C., & Moulin, P. (2008). Membrane characterization by microscopic methods: multiscale structure. *Journal of Membrane Science*, *315*(1-2), 82-92.

[145] Wang, P., Tan, K. L., Kang, E. T., & Neoh, K. G. (2002). Plasma-induced immobilization of poly (ethylene glycol) onto poly (vinylidene fluoride) microporous membrane. *Journal of membrane science*, *195*(1), 103-114.

[146] Li, Q., Xu, Z. L., & Yu, L. Y. (2010). Effects of mixed solvents and PVDF types on performances of PVDF microporous membranes. *Journal of applied polymer science*, *115*(4), 2277-2287.

[147] Yao, M., Ren, J., Akther, N., Woo, Y. C., Tijing, L. D., Kim, S. H., & Shon, H. K. (2019). Improving membrane distillation performance: Morphology optimization of hollow fiber membranes with selected non-solvent in dope solution. *Chemosphere*, *230*, 117-126.

[148] Pezeshk, N., Rana, D., Narbaitz, R. M., & Matsuura, T. (2012). Novel modified PVDF ultrafiltration flat-sheet membranes. *Journal of Membrane Science*, *389*, 280-286.

[149] Sukitpaneenit, P., & Chung, T. S. (2021). Molecular elucidation of morphology and mechanical properties of PVDF hollow fiber membranes from aspects of phase inversion, crystallization, and rheology. In *Hollow Fiber Membranes* (pp. 333-360). Elsevier.

[150] Munirasu, S., Banat, F., Durrani, A. A., & Haija, M. A. (2017). Intrinsically superhydrophobic PVDF membrane by phase inversion for membrane distillation. *Desalination*, *417*, 77-86.

[151] Ahmad, A. L., Ideris, N., Ooi, B. S., Low, S. C., & Ismail, A. (2011). Morphology and polymorph study of a polyvinylidene fluoride (PVDF) membrane for protein binding: Effect of the dissolving temperature. *Desalination*, *278*(1-3), 318-324.

[152] Wang, X., Zhang, L., Sun, D., An, Q., & Chen, H. (2008). Effect of coagulation bath temperature on formation mechanism of poly (vinylidene fluoride) membrane. *Journal of Applied Polymer Science*, *110*(3), 1656-1663

[153] Teixeira, J., Cardoso, V. F., Botelho, G., Morão, A. M., Nunes-Pereira, J., & Lanceros-Mendez, S. (2021). Effect of polymer dissolution temperature and conditioning time on the morphological and physicochemical characteristics of poly (Vinylidene fluoride) membranes prepared by non-solvent induced phase separation. *Polymers*, *13*(23), 4062.

[154] Gugliuzza, A., & Drioli, E. (2009). New performance of hydrophobic fluorinated porous membranes exhibiting particulate-like morphology. *Desalination*, *240*(1-3), 14-20.

[155] Wang, X., Wang, X., Zhang, L., An, Q., & Chen, H. (2009). Morphology and formation mechanism of poly (vinylidene fluoride) membranes prepared with immerse precipitation: effect of dissolving temperature. *Journal of Macromolecular Science, Part B*, *48*(4), 696-709.

[156] Mavukkandy, M. O., Bilad, M. R., Giwa, A., Hasan, S. W., & Arafat, H. A. (2016). Leaching of PVP from PVDF/PVP blend membranes: Impacts on membrane structure and fouling in membrane bioreactors. *Journal of Materials Science*, *51*, 4328-4341.

[157] Xu, C., Huang, W., Lu, X., Yan, D., Chen, S., & Huang, H. (2012). Preparation of PVDF porous membranes by using PVDF-g-PVP powder as an additive and their antifouling property. *Radiation Physics and Chemistry*, *81*(11), 1763-1769.

[158] Hilal, N., Ismail, A. F., Matsuura, T., & Oatley-Radcliffe, D. (Eds.). (2017). *Membrane characterization*. Elsevier.

[159] Fontananova, E., Bahattab, M. A., Aljlil, S. A., Alowairdy, M., Rinaldi, G., Vuono, D., ... & Di Profio, G. (2015). From hydrophobic to hydrophilic polyvinylidenefluoride (PVDF) membranes by gaining new insight into material's properties. *RSC Advances*, *5*(69), 56219-56231.

[160] Saxena, P., Shukla, P., & Gaur, M. S. (2021). Thermal analysis of polymer blends and double layer by DSC. *Polymers and Polymer Composites*, *29*(9_suppl), S11-S18.

[161] Supaphol, P., & Lin, J. S. (2001). Crystalline memory effect in isothermal crystallization of syndiotactic polypropylenes: effect of fusion temperature on crystallization and melting behavior. *Polymer*, *42*(23), 9617-9626.

Chapter 3
Overview of Experimental Methods for Membrane Fabrication

3.1 Materials and chemicals

Polyvinylidene fluoride (PVDF, pellets, product code: 1002616042; M_w 275,000 g.mol^{-1}, M_n 107,000 g.mol^{-1}), gamma-Valerolactone (GVL, ≥ 99%), and 2-Propanol (IPA) were all purchased from Sigma-Aldrich, UK. Deionised water was used with a resistivity of 18.4 MΩ cm at 25 °C (Milli-Q). All materials and solvents were used as received for the experimental membrane fabrication without further purification.

3.2 Thermodynamic experiment

The determination of the cloud point of the homogenous polymer mixture provides the equilibrium information about the precipitation process of the polymer system. Typically, a titration method is commonly implemented to investigate the cloud phenomenon and requires the addition of the nonsolvent in this situation water until the titration endpoint is reached. However, the process is slow and time consuming. In chapter 4, a proposed method called polymer dissolution in vial method (PDV) is introduced and presented to examine the cloud points. The process involves preparing different PVDF/GVL/water mixture ratio samples. These samples are heated to an elevated temperature to obtain a homogeneous polymer solution and slowly cooled at a constant rate to a lower temperature until polymer solutions are no longer thermodynamically stable, resulting in the polymer mixture becoming turbid or a gel. The measurement of turbidity or gel is conducted visually and defined as observed conditions polymer sample vials become cloudy (change from a clear solution and remain turbid) or if a gel shows no flow movement of polymer solution vial sample when tilted upside down. The technique will save material, reduce solvent loss due to evaporation and provide informative data on the turbidity of the polymer mixtures.

However, the implemented approach only provides a qualitative analysis. The method is also subjective of the researcher's judgement on the cloud point of the samples. Precise measurements using light transmission detection techniques have been proposed to determine the cloud point [1]. However, the design of a suitable temperature controlled turbidity measuring device setup that could allow for simultaneous measurements of the cooling rate span is required to evaluate the polymer solution's cloud point. In addition, the design should be able to achieve reproducibility of analysis and limit subjective errors of the operator.

The design of the PVDF membrane using the NIPS approach is based on first obtaining a homogenous polymer (dope solution), then casting the polymer liquid solution and immersing it into a coagulation bath with a nonsolvent. Based on this technique, the solubility of the PVDF/GVL/water system was first carried out, and the analysis recorded is depicted using a ternary phase diagram. Furthermore, obtained homogenous compositions were used to construct the experimental ternary phase diagram to analyse the phase change and determine the cloud points of the PVDF system by the PDV method.

3.3 Lab-scale fabrication of Flat sheet PVDF membranes

The materials and procedure presented in this section cover the “base recipe” used to prepare the PVDF membranes. The base recipe used PVDF/GVL binary solutions as casting solutions. In Chapter 7, the base recipe was modified to incorporate dimethyl sulfoxide (DMSO) as a co-solvent and to prepare membranes using PVDF/GVL/DMSO ternary solutions as casting solutions. In Chapter 8, the base recipe was modified to incorporate polyvinylpyrrolidone (PVP) (MW=10000) as a pore former and to prepare membranes using PVDF/PVP/GVL ternary solutions as casting solutions. The corresponding chapters will provide the details of the modifications to the base recipe. All membrane fabrication is based on the NIPS approach discussed in section 3.3.1.

3.3.1 Procedure used in the fabrication of the membranes

The asymmetric PVDF membranes were fabricated using the nonsolvent induced phase separation. The PVDF pellet was dried for 1 hour at 85°C and a 15wt.% polymer concentration is dissolved in GVL at 90°C under continuous stirring at 200rpm for 24 h using a glass vial. The homogeneous polymer (dope) solution was degassed to remove air bubbles that may exist and cooled using either an ice bath or at room temperature to a fixed casting temperature. Once cooled, the dope solution is spread uniformly onto a casting knife block with a 200µm thickness at a constant speed of 18mm/sec and cast on a glass plate using automated cast film equipment. The casting knife and the glass plate were pre-heated to the casting temperature to minimise the effect of the surrounding temperature and avoid phase separation during casting. The cast films were exposed to air at room temperature for 30 seconds and then immersed in a coagulation bath of deionised water set up at the same temperature as the cast solution. The solidified membranes were washed thoroughly with deionised water to remove the residual solvent using a two-batch exchange bath of water/2-propanol (1:1) and a 2-propanol bath for 24 h at room temperature. Afterwards, the

membrane is air-dried and stored at room temperature for 24 h before further characterisation. A schematic description of the fabrication process is presented in figure 3.1.

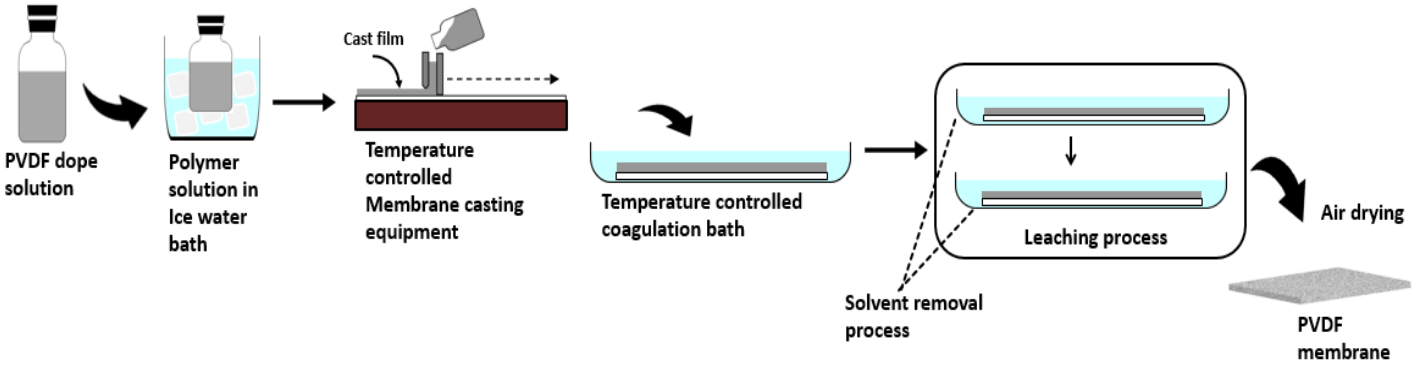

Figure 3.1: Schematic drawing illustrating the preparation of flat sheet PVDF membrane

3.4 Characterisation of the PVDF Membranes

3.4.1 PVDF membrane morphology study (SEM imaging)

The fabricated membrane surface and cross-sectional morphologies were examined using scanning electron microscopy (SEM), Hitachi TM3000. First, the flat sheet membrane samples were frozen in liquid nitrogen and fractured to obtain fragments. Afterwards, the membrane samples were placed on a holder and sputter-coated with gold/platinum in a vacuum before SEM analysis to ensure the material was conductive. Finally, further qualitative characterisation was conducted to analyse membrane morphologies.

3.4.2 Thickness and surface geometric pore size measurement

An open-sourced processing software tool, ImageJ, was used to measure the membrane thickness and surface pore size by devising a method on obtained cross-sections and top surface SEM micrographs. First, the measurement scale was initially set using the software, and a vertical line to the cross-section SEM image was drawn manually to measure the overall thickness. Afterwards, four measurements across the SEM cross-section image were taken to obtain an average thickness value reported for each membrane sample. Similarly, the surface pore size was measured using the top surface micrographs. In addition, the direct observation of SEM micrographs allowed for measuring the top and sublayer thickness and the surface pore size of the membrane samples [2].

3.4.3 Overall Membrane Porosity Analysis

The overall membrane porosity of the prepared membrane (ε) is estimated using the gravimetric method at room temperature by measuring the weight of kerosene in the membrane pores. The assumption is that the flow path depends on the open ended pores within the free standing membrane. Analysis of the overall porosity would provide insight into the mechanical integrity and performance properties of the fabricated PVDF membranes. First, small squares with an area of 1 cm^2 were cut, and the weight of the dry membranes (W_d) was measured. Membrane samples are thus wetted by immersing each piece in a vial containing 1mL of kerosene for 24 h. it was assumed that the specific gravity of PVDF materials did not change once wetted with kerosene, and no air was trapped in the membrane pores. The wet membrane(W_w), is removed from the vials and carefully bolted with filter paper. The porosity (ε) of the membrane is mathematically determined using equation (1) [3,4].

$$\varepsilon(\%) = \frac{\frac{(W_w - W_d)}{\rho_L}}{\left(\frac{W_w - W_d}{\rho_L}\right) + \left(\frac{W_d}{\rho_P}\right)} \times 100 \qquad (1)$$

ρ_L and ρ_P are the densities of wetting liquid (kerosene; 0.80g/mL) and polymer (PVDF; 1.78g/mL). The mean porosity of each membrane sample was obtained as the average of the values determined from the three samples. Typically, water is used as the wetting liquid for the porosity test. However, kerosene was selected as the wetting liquid because it thoroughly wetted the hydrophobic PVDF membrane and did not swell it. A technique widely used to determine the porosity of solid material is the BrunauereEmmetteTeller (BET), which exploits the behaviour of adsorption and desorption of gas once moisture from the membrane has been removed by degassing at 338K for a given period. However, a monolithic sample of weight greater than 500mg is needed to obtain a reliable result. Thus, the method was not used because the fabricated flat sheet membrane sample did not meet the weight requirement.

3.4.4 Contact Angle

The surface wettability of the PVDF membranes prepared was determined by contact angle measurement using the sessile drop method. The contour of a droplet of 5µL milli-Q-water on the membrane surface from a needle tip was recorded using a high definition camera at room temperature. Static contact angle measurement between the meniscus formed by the water droplet and the membrane surface was obtained using computer

calculation software (Krüss company, Hamburg, Germany). The experiment was conducted for six different regions on each membrane sample at room temperature (21±2)°C, and the average and standard deviation values were calculated. However, the contact angle measurement approach has several drawbacks. It is often impacted by factors such as roughness, heterogeneity and capillary forces within the pores of the fabricated membranes.

3.4.5 Atomic force microscopy (AFM)

The application of atomic force microscopy (AFM) has been employed to examine the physical characteristics of membrane surfaces. The PVDF membrane film surface morphology and roughness measurement were carried out using the atomic force microscopy (AFM) Hitachi AFM5000 II model device.

A 10 µm x 10 µm scale AFM image of the top surface was performed in dynamic force mode to examine the impact of various process parameters that influences the membrane surface structure. The samples were placed on a sample holder and set up on the equipment for testing, with all measurements conducted at ambient room temperature. The imaging is obtained using a Tapping mode in air with resonance frequencies of the cantilever set at hundreds of kHz. The practical method allows the heterogeneity of the surface's membrane properties to be emphasised. However, a drawback of this technique is that quantitative data can be challenging to obtain due to several factors, including long-range interaction force, scan speed, adhesion forces and mechanical properties of the membrane surface [5]. The key parameters describing the membrane surface topology are the average roughness, root-mean-square roughness and surface area difference that can be obtained through supplied software with AFM Hitachi AFM5000 II model equipment.

The working principle of AFM involves using a sharp probe tip (made from silicon) mounted on a flexible cantilever arm in scanning the membrane surface, such that the van der Waals forces, due to the proximity of the tip and the material surface, resulting from the interaction. The change in interaction force is detected using a position sensitive photodetector (as some deflection or vibrating frequency of the probe tip) and measured through the cantilever’s deflection. The data obtained can be quantified in a two-dimension (2D) or three-dimensional (3D) map of the investigated membrane material surface topology. In addition, the tip calibration helps improve the reliability of obtained data, and a deformed or contaminated tip affects the resulting topographic image.

3.4.6 Thermal characterisation of the PVDF membrane

The thermal analysis of the prepared PVDF membrane is examined using a differential scanning calorimeter (DSC) to determine the melting and crystallisation temperature of the

pure polymer sample and the PVDF membranes. The DSC experiments were conducted under nitrogen air at a 50 mL/min flow rate to minimise oxidative degradation. The DSC equipment was calibrated with the melting temperature and enthalpy of five (5) high purity standards (biphenyl; benzoic acid, indium; tin; and rubidium nitrate). First, before all DSC experiments are conducted, an empty aluminium crucible is conditioned by undergoing the heating cycle required to analyse the PVDF membrane samples to minimise any heating effect on the crucible and obtain a consistent measurement. Then, samples are cut into smaller pieces, placed in a tared aluminium pan, and heated from room temperature to 250°C using the NETZSCH 449 F3 Jupiter STA.

All measurements were conducted in the standard DSC mode using the following method. The samples were initially heated to 250 °C at a rate of 10°C/min and then held for 5 minutes to eliminate any thermal history, followed by a cooling process to 25 °C. The samples are held at 25 °C for 5 minutes and then reheated at 250 °C at a 10 °C/min rate. Melting endotherms are acquired from the second run of the thermal protocol and analysed to obtain the melting temperature (Tm) and latent heat of fusion (ΔHm). The melting temperature (Tm) and the crystallisation temperature (Tc) were defined as the peak of the melting endotherm and cooling exotherms, respectively. The degree of crystallinity (X_C) of the polymer is determined by integrating the area of the obtained melting endotherm, and the value recorded is compared to the theoretical melting enthalpy of pure crystalline PVDF given as 104.5 J g^{-1} [6,7] and calculated using formulation in equation (2).

$$X_C = \left(\frac{\Delta_{H_m}}{\Delta_{H_{100}}}\right) \times 100 \qquad (2)$$

Where Δ_{H_m} the melting enthalpy of the PVDF membranes is measured in DSC; $\Delta_{H_{100}}$ denotes the theoretical melting enthalpy of crystalline PVDF at 100%. All melting curve results presented are normalised.

3.4.7 Fourier transform infrared spectroscopy with attenuated total reflection

The Fourier transform infrared (FTIR) spectroscopy equipped with an attenuated total reflection (ATR) was performed using a Shimadzu QATR-s IRSpirit spectrophotometer. The prepared membrane's top surface spectra were recorded on a diamond crystal, with each measurement at a resolution of 4 cm^{-1} and 64 scans per spectrum between 4000 - 400 cm^{-1}. All the PVDF sample film measurements were performed at room temperature, and the spectra were normalised and adjusted in the same plot. Study shows that the fraction of crystalline form in a crystal can be estimated by using the absorbance of the characteristics

peaks from the spectra and their absorption coefficients [8]. The α- and β- phases are found to have characteristic infrared absorption bands at 763 cm^{-1} and 840 cm^{-1}

The evaluation of the β-phase crystalline fraction of the PVDF membrane surface layer is determined from the FTIR spectra and numerically determined using equation (3) for all prepared membranes.

$$F(\beta) = \left(\frac{A_{\beta}^{840}}{\left(K_{\beta}^{840}/K_{\alpha}^{763}\right)A_{\alpha}^{763} + A_{\beta}^{840}} \right) \qquad (3)$$

Where A_{α}^{763} and A_{β}^{840} the corrected baseline absorption peaks of the α- and β- phases are 763 cm^{-1} and 840 cm^{-1}, respectively. $F(\beta)$ is the relative fractions of the β phases, and *K* and *d* are the absorption coefficient and penetration depth with corresponding values obtained from the literature study [9,10] and given as: $\left(K_{\alpha}^{763} = 6.1 \times 10^{4}\ cm^{2}/mol\ ;\ K_{\beta}^{840} = 7.7 \times 10^{4}\ cm^{2}/mol \right)$.

3.4.8 Experimental membrane compaction, Gas and water permeation Test

Each prepared membrane's performance is evaluated using a laboratory dead-end membrane cell (316 stainless steel holder) with a diameter of 29mm and a support screen. Filtration setup experiments were conducted at room temperature, and gas and water permeation measurements were recorded. The feed inlet of the membrane cell was connected to a pressure gauge and a feed reservoir. The permeate end was connected to a bubble flow meter for the gas permeation test and a beaker (used as a collection tank) for the water permeation test.

The PVDF membrane samples were cut to fit the membrane module holder size with an effective area of 3.8 cm^2, inserted and then tightly secured. The membrane cell is initially pressurised at 0.2 bar with nitrogen gas. Afterwards, the stabilisation flux of the change in transmembrane pressure was determined after 5mins for each pressure increment. The stabilisation process is the time taken to obtain a steady soap bubble flow as it moves through the bubble flow meter at a set volume. The gas permeation measurements were repeated for pressure between 0.2 -1.0 bar with an increment of 0.2 bar. At 1 bar, the pressure is maintained for 10 minutes, and measurements were taken for 1.0, 0.8, 0.6, 0.4 and 0.2 bar.

Two independent duplicates of each prepared membrane sample were tested. In addition, all measurements for each pressure between 0.2-1.0 bar were carried out thrice for increasing and decreasing pressure conditions to determine if any inconsistency or hysteresis would be observed with the fabricated PVDF membranes. The flux measurement is determined using equation (4), with average and standard deviation determined using formula functions "*AVERAGE*" and "*STDEV*" in Microsoft Excel, respectively.

$$J = \frac{v}{At} \quad (4)$$

J is the flux (L/m^2.min) at a normalised temperature of 25°C, (v) is the volume of Nitrogen gas that permeates through the membrane for a given effective membrane area (A) at a given time (t). The "*STDEV*" function is a measure of how widely the parameter values are dispersed relative to the average value and can be computed using equations (5) and (6) [11].

$$y = f(x_1, x_2, x_3), \varepsilon_y = \sqrt{\left(\frac{dy}{dx_1}\right)^2 \varepsilon_{x1}^2 + \left(\frac{dy}{dx_2}\right)^2 \varepsilon_{x2}^2 + \left(\frac{dy}{dx_3}\right)^2 \varepsilon_{x3}^2} \quad (5)$$

The x_1, x_2, x_3 represent independent variables, with y defining the dependent variable. The ε_x represents an error in variable 'x', and ε_y the corresponding error in variable 'y'. Further simplification to determine the standard deviation of a data set can be computed using equation (6) with 'x' denoting the sample average and 'n' the sample size. All error values associated with average values in the thesis have been determined using the "*STDEV*" function.

$$\sqrt{\frac{\Sigma(x - \bar{x})}{(n-1)}} \quad (6)$$

The schematic apparatus set for the gas permeation test is illustrated in figure 3.2. A similar apparatus setup and procedure were carried out to evaluate the permeation of water. The cut PVDF membrane inside the cell was initially pressurised with deionised water for 30 mins before pure water flux measurements were performed for pressure ranging between (1- 10) bars for each PVDF membrane sample evaluated. All readings were recorded under steady state flow at room temperature, with measurements repeated thrice and flux determined using equation (4). In addition, analysis to determine the liquid entry pressure of water (LEP_w) was conducted before water flux experiments were performed for pressure values between 0.2 to 10 bar at an increment of 0.2 bar. The test rig set up for the experimental study for water permeation analysis is presented in figure 3.3.

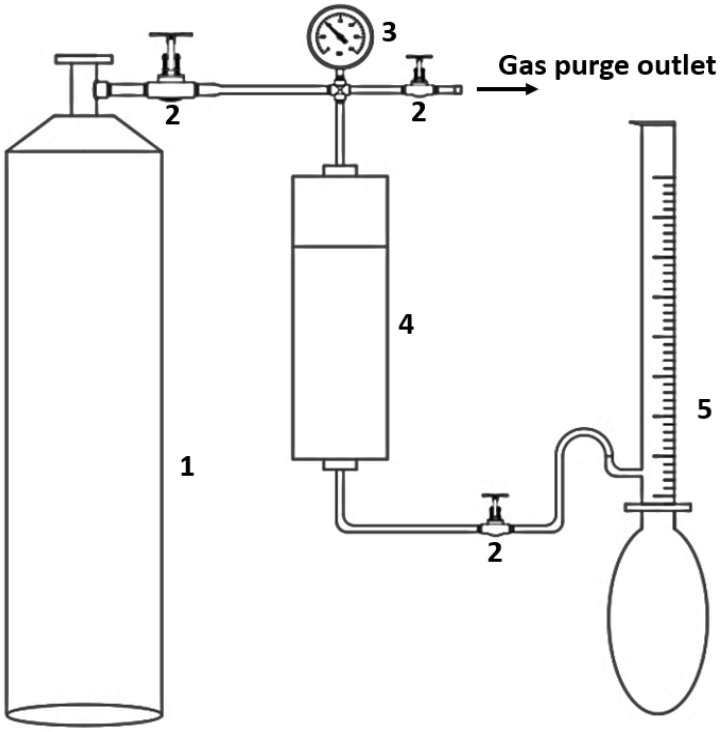

Figure 3.2: Gas permeation test rig where (1) Nitrogen cylinder, (2) valve, (3) pressure gauge, (4) membrane module cell, (5) bubble flow meter, and (6) Soapy water.

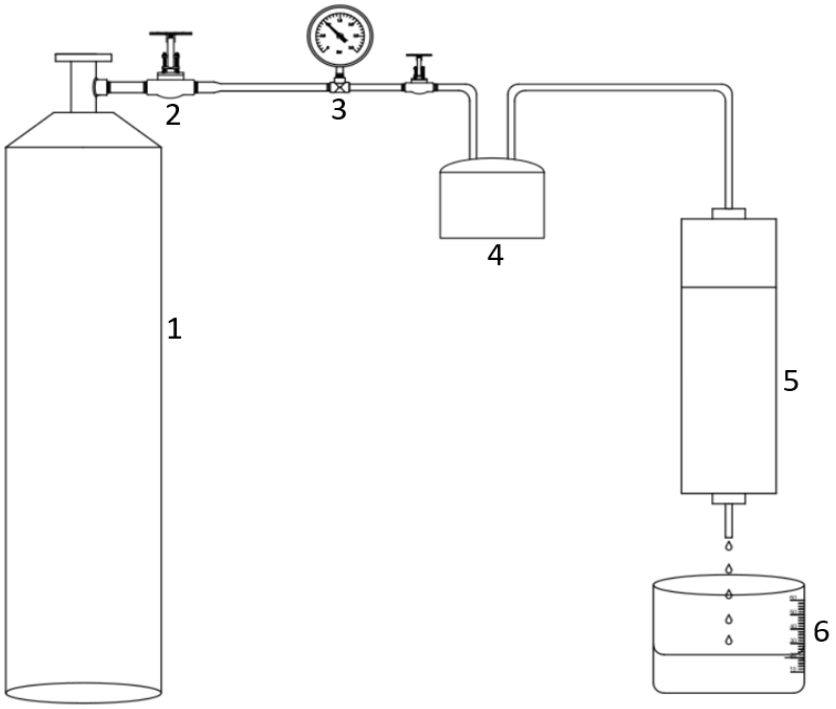

Figure 3.3: The water filtration rig setup is depicted schematically with (1) Nitrogen cylinder, (2) valve, (3) pressure sensor, (4) water feed tank, (5) membrane module cell, and (6) collection tank.

3.4 Reference

[1] Kim, J. W., Taki, K., Nagamine, S., & Ohshima, M. (2009). Preparation of porous poly (L-lactic acid) honeycomb monolith structure by phase separation and unidirectional freezing. *Langmuir*, *25*(9), 5304-5312.

[2] Sun, W., Chen, T., Chen, C., & Li, J. (2007). A study on membrane morphology by digital image processing. *Journal of Membrane Science*, *305*(1-2), 93-102.

[3] Marino, T., Galiano, F., Molino, A., & Figoli, A. (2019). New frontiers in sustainable membrane preparation: Cyrene™ as green bio derived solvent. *Journal of membrane science*, *580*, 224-234.

[4] Hou, D., Fan, H., Jiang, Q., Wang, J., & Zhang, X. (2014). Preparation and characterization of PVDF flat-sheet membranes for direct contact membrane distillation. *Separation and Purification Technology*, *135*, 211-222.

[5] McLean, R. S., & Sauer, B. B. (1997). Tapping-mode AFM studies using phase detection for resolution of nanophases in segmented polyurethanes and other block copolymers. *Macromolecules*, *30*(26), 8314-8317.

[6] Liu, J., Lu, X., & Wu, C. (2013). Effect of preparation methods on crystallization behavior and tensile strength of poly (vinylidene fluoride) membranes. *Membranes*, *3*(4), 389-405.

[7] Gebrekrstos, A., Sharma, M., Madras, G., & Bose, S. (2016). New physical insights into shear history dependent polymorphism in poly (vinylidene fluoride). *Crystal Growth & Design*, *16*(5), 2937-2944..

[8] Mohammadi, B., Yousefi, A. A., & Bellah, S. M. (2007). Effect of tensile strain rate and elongation on crystalline structure and piezoelectric properties of PVDF thin films. *Polymer testing*, *26*(1), 42-50.

[9] Cheng, L. P., Lin, D. J., Shih, C. H., Dwan, A. H., & Gryte, C. C. (1999). PVDF membrane formation by diffusion-induced phase separation-morphology prediction based on phase

behaviour and mass transfer modelling. *Journal of Polymer Science Part B: Polymer Physics*, *37*(16), 2079-2092.

[10] Lin, D. J., Beltsios, K., Young, T. H., Jeng, Y. S., & Cheng, L. P. (2006). Strong effect of precursor preparation on the morphology of semicrystalline phase.

[11] Nuzzo, R. (2014). Statistical errors. *Nature*, *506*(7487), 150.

CHAPTER 4.
Experimental study on the thermodynamics of PVDF/GVL/water system.

4.1 Introduction

The phase separation behaviour of the ternary PVDF/GVL/H_2O system is examined to understand the formation mechanism process to produce PVDF membranes via the phase inversion process. The equilibrium thermodynamics properties of a ternary polymer system play a critical role in describing and controlling the membrane preparation process [1]. Understanding the polymer solution thermodynamics necessitates knowing what happens when a polymer is dissolved in a solvent. Initially, the solvent molecules slowly diffuse into the polymer to form a swollen gel, which disintegrates into a solution due to increased polymer/solvent intermolecular interactions.

The Flory-Huggins theory and several other models proposed over the last eight decades [2,3] are often used to predict the thermodynamic behaviour of polymer mixtures. The analysis provides good descriptions of the thermodynamics of polymer systems. However, the techniques employed by these models involve difficult mathematical complexity, less predictive capability and occasionally demand modifications, which are needed to increase accuracy [4,5,6]. There are different experimental methods [7,8,9,10] available to examine the phase behaviour in polymer solutions and predict the phenomena interplay during membrane fabrication. The optical approach measurement is one of the most common methods employed to determine when polymer solutions with known compositions undergo phase separation. Preliminary studies to evaluate the polymeric system's thermodynamics are the measurement of the cloud points with the boundary able to identify stable compositions from the polymer mixtures' meta- or unstable compositions. Typically, for conditions of membrane fabrication via the NIPS method, the initial casting polymer solution (dope) is identified within the stable region. It was therefore determined that the evaluation of the thermodynamics of the PVDF/GVL/water system was best represented using a ternary phase diagram.

The concept of phase inversion is characterised as the transformation of a homogenous polymer solution into two distinct liquid phases, one with a high concentration of polymer (polymer-*rich* phase) and another with a low concentration of polymer (polymer *lean* phase) [11,12]. The phase diagram offers a convenient depiction to examine the polymer system's thermodynamics and predict the polymer's suitability in a particular solvent during the production of membranes via phase separation. Several phase separation phenomena in

polymer solutions have been reported [13,14], including liquid-liquid phase separation crystallisation and gelation. Furthermore, the observation of the miscibility gap location and the compositions of the cloud points that correspond to the demixing curve of the polymer system on the phase diagram provides a guide for the membrane fabrication process [15,16].

The experimental cloud point approach reported in the literature requires carrying out a large number of titrations, which are time-consuming, time-sensitive and limited by the viscosity of the polymer mixture [17,18]. Therefore, this chapter aims to propose a simple method dubbed as "polymer dissolution in vial method" (PDV) for the phase diagram prediction of the PVDF/GVL membrane forming system and overcome the drawbacks of the cloud point titration method. First, the proposed PDV method prepares pre-defined polymer concentrations at a high temperature. Then, the homogeneous samples were gradually cooled while observing phase transitions and noting when each PVDF solution turned cloudy.

The construction of a ternary phase diagram and analysis of the phase behaviour of PVDF dissolved in GVL/water mixtures is presented and employed to understand the phenomena of the polymer system for the membrane formation process. The Ternary Phase diagram is first used to show solubility analysis of PVDF mixtures and extended to provide an understanding of the thermodynamic and kinetic aspects of the phase inversion approach. The suggested PDV method provides reliable information content and reproducible data compared to the established titration method. In addition, it allows for qualitative description and characterisation of the PVDF/GVL/water system. Experimental cloud point measurements via the widely adopted titration method for PVDF/DMSO/water system [9] were compared to valid results obtained using the proposed PDV method. Furthermore, results obtained based on thermodynamic analysis are used to deduce practical process parameter values that can be used to prepare PVDF membranes.

4.2 Thermodynamics Experiments

4.2.1 Materials

Commercial polyvinylidene fluoride (PVDF, pellets, product code: 1002616042; M_w 275,000 g.mol^{-1}, M_n 107,000 g.mol^{-1}) was pre-dried at 85°C before use. Dimethyl sulfoxide (DMSO ≥ 99.5%), Triethyl phosphate (TEP, ≥ 98.8%) and gamma-Valerolactone (GVL, ≥ 99%) were all purchased from Sigma-Aldrich™. All materials and solvents were used as received for the experiment without further purification. Aqueous solutions were prepared using water with a resistivity of 18.4 MΩ.cm at 25 °C (Milli-Q).

4.2.2 Preparation of Polymer solutions and solution equilibration.

A simple approach is adopted to prepare a homogeneous polymer mixture [19] by adding predetermined PVDF concentrations (1-20wt.%) and appropriate solvents and nonsolvent concentrations in a clean glass vial at room temperature. The initial condition was to dry the polymer pellets using an oven at 85°C. Next, the mass of the polymer was measured using a weight scale (Mettler Toledo AM100), and both solvent and nonsolvent were measured using an adjustable volume micropipette. Polytetrafluoroethylene (PTFE) Teflon tape was used to seal the prepared sample vials to reduce solvent loss due to evaporation. Next, the mixtures were gradually heated to an elevated temperature of 90°C for 48 h to obtain a homogenous solution with no stirring or shaking of polymer mixtures involved. Finally, two samples were prepared for analysis of the phase behaviour of the PVDF system.

4.2.3 Cloud point approach and Gelation points

A formulation process was devised using the polymer dissolution in vial method (PDV) that measures the appropriate known mass weight of polymer, solvent and nonsolvent following solubility analysis of different polymer concentrations and solvents. The polymer mixtures were kept in a thermostatically controlled oven over the range of 30-90°C. The polymer mixtures were cooled at isothermal conditions, and visual observation determined cloud points. The cloud points were identified at isothermal conditions as the compositions at which the homogeneous solution transitions from a colourless clear liquid to a turbid/milky solution in a series of samples prepared with different ratios of PVDF/GVL/water. Furthermore, homogenous solutions that transited from liquid to turbid gel (which was the absence of flow upon 90° tilting the sample in a vial for 2 min) were identified as gelation points in the ternary phase diagram. The cloud and the gelation point observation of PVDF/GVL/water samples were analysed after 2 hrs and 48 hrs. Thus, using a ternary phase diagram, the analysis of samples was depicted as homogeneous, stable phase, or the cloud and gelation line depending on the observation of the unstable phases. The experiment was conducted under controlled temperature conditions to ensure reproducibility with test sample vials of each PVDF system maintained for 48 h after cooling from dissolution temperature.

4.3 Results and Discussion

4.3.1 Solubility of parameters of components

Figure 4.1 compares the Hansen solubility parameters (HSP) of various conventional and green solvents that are used to synthesise polymeric (PVDF) membranes. Results indicate a close interaction distance within the depicted illustrated Hansen 3D sphere. Based on equation (1), the Hansen relation values of the three parameters of the component can be evaluated and represented as a point on the three-dimensional axis to demonstrate the principle of "like-dissolves-like" properties when comparing individual components. The HSPs of many conventional solvents and the polymer are well-known (see Table 4-1). Hence, comparing the solubility parameters of a solute or component provides a quantitative measure used to deduce the solubilising properties and interpreted on the basis of total solubility and the interaction of polymer mixtures.

$$\delta_t = \sqrt{(\delta_{d,i})^2 + (\delta_{p,i})^2 + (\delta_{h,i})^2} \qquad (1)$$

The subscript *i* denotes the component.

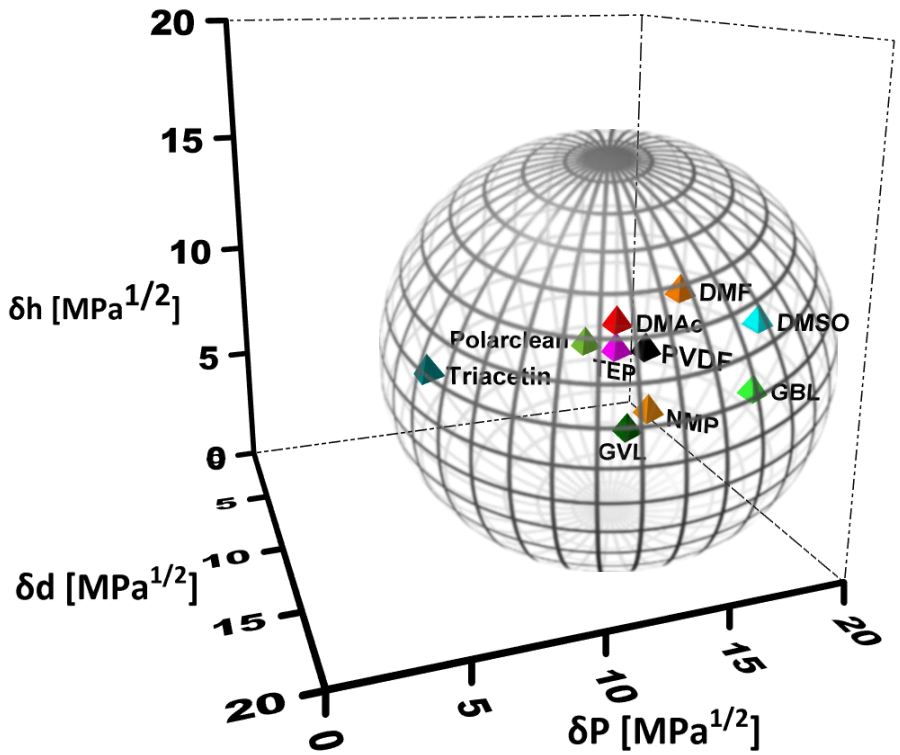

Figure 4.1: 3D Hansen space of GVL, PVDF and some commonly used solvents for membrane fabrication

Solubility of mixtures is mainly considered by theoretical computing, the Hansen solubility parameters (HSPs) as the total molecular interaction distance (R_a) using the independent interactions parameters expressed in equation (2), to reasonably predict the solubility of polymer and solvent interaction mixture, with δ_d, δ_p, and δ_h terms accounting for the dispersive, polar and hydrogen bonding interactions, respectively.

$$R_a = \sqrt{4(\delta_{d1} - \delta_{d2})^2 + (\delta_{p1} - \delta_{p2})^2 + (\delta_{h1} - \delta_{h2})^2} \qquad (2)$$

Subscripts 1 and 2 indicate the polymer and solvent, respectively.

A threshold range of $R_a \leq 5\mathrm{MP}a^{1/2}$ has been proposed as a set of arbitrary values that predicts polymer solubility; however, several studies have suggested that higher threshold range values could indicate that a homogenous mixture can be obtained [20]. Therefore, the result is further evaluated using the proposed relative energy difference (RED) [21] in equation (2) as an indicator to quantify the affinities between polymer and solvent.

$$RED = \frac{R_a}{R_o} \qquad (2)$$

$\boldsymbol{R_o}$ is the radius of a Hansen solubility parameter sphere. The likelihood of achieving solubility of the polymer mixture increases with decreasing $\boldsymbol{R_a}$ values [22]. The closer the interaction distance between the solute and solvent parameters (the lower $\boldsymbol{R_a}$ Value), the more excellent the polymer's solubility in the associated solvent will be achieved

Table 4-1: HSP, Ra and RED values for polymer, toxic & non-toxic aprotic polar solvent [23,24]

Solvent	$\boldsymbol{\delta_d}$ $(\boldsymbol{MPa^{1/2}})$	$\boldsymbol{\delta_p}$ $(\boldsymbol{MPa^{1/2}})$	$\boldsymbol{\delta_h}$ $(\boldsymbol{MPa^{1/2}})$	$\boldsymbol{\delta_t}$ $(\boldsymbol{MPa^{1/2}})$	$\mathbf{R_a}$ $(\boldsymbol{MPa^{1/2}})$	RED
DMAc	16.8	11.5	10.2	22.77	1.62	0.40
DMF	17.4	13.7	11.3	24.86	2.45	0.60
DMSO	18.4	16.4	10.2	26.68	4.69	1.14
GBL	19.0	16.6	7.4	26.29	5.75	1.40
GVL	17.1	11.9	6.2	21.74	3.07	0.75
NMP	18.0	12.3	7.2	22.96	2.57	0.63
TEP	16.7	11.4	9.2	22.34	1.28	0.31
Triacetin	16.5	4.5	9.1	19.37	8.12	1.98
Polarclean	15.8	10.7	9.2	21.18	3.3	0.81
PVDF	17.2	12.5	9.2	23.17	-	

A limitation of the theoretical solubility measurement is the determination of the solubility parameter, which could be harder to determine for polymers with large and variable molecular weights despite considering the total molecular volume when determining the polymer solubility parameter. Secondly, theoretical solubility measurement could be challenging for conditions of partial solubility, typically because the HSP parameters used are obtained from distinct polymer units. However, a preliminary roadmap for polymer/solvent mixtures is provided by the theoretical determination of the solubility of considered components.

The solubility of polymer mixtures has significant advantages in fabricating the PVDF membranes via non-induced phase separation (NIPS). The homogeneity study of the polymer mixtures tends to characterise and predict how the PVDF/GVL/H_2O system will behave, identify appropriate compositions that can yield a homogeneous solution, and the specific temperature at which the polymer mixtures are dissolved. Typically, the polymer and solvent mixture is governed by internal energy interactions, with the most common theory of solute interaction based on cohesive energy [25]. The formation of a homogeneous mixture from a polymer and solvent/nonsolvent is a physical process that depends on whether the system's overall interaction free energy change is negative.

4.3.2 Solubility of PVDF/ɣ-valerolactone/water system

The experimental study is conducted by selecting suitable polymer concentrations commonly used to fabricate polymeric membranes [26]. Several predetermined concentrations/compositions of the polymer system were dissolved at temperatures between 30-90°C, with a maximum dissolving temperature maintained at 90 °C due to the boiling point of the nonsolvent (water). A solubility map of the polymer system is depicted using a ternary phase diagram shown in figure 4.2.1 - 4.2.3 to identify the solubility boundary and allow for a qualitative evaluation of possible compositions suitable for the membrane fabrication. Using a ternary phase diagram, a traffic colour code (green, amber, and red) qualitatively depicted the polymer mixture's solubility.

Contrary to HSP theoretical theory, experimental mixtures of the polymer system were insoluble at room temperature after 48 h. The solubility of a very low polymer concentration mixture was observable at a relatively mild temperature of 50°C for compositions closer to the polymer-solvent axis. The molecular dissolution and mobility of the PVDF mixtures increase at elevated temperatures resulting in a gradual transition of soluble polymer mixture to the right side of the ternary diagram [27,28] with several samples remaining infinitely thermodynamically stable at high temperatures. The solubility data result

of the polymer system offers far-reaching information about the physical nature of the dissolved polymer due to temperature change (Tdissol). Typically, many features of polymer solutions are temperature dependents, such as the driving force for phase separation, system viscosity, polymer mobility, and demixing mechanism. The identified homogeneous polymer mixtures compositions samples will be utilised to analyse the behaviour of the PVDF system, focusing on the influence of temperature change in the determination of experimental cloud point curves.

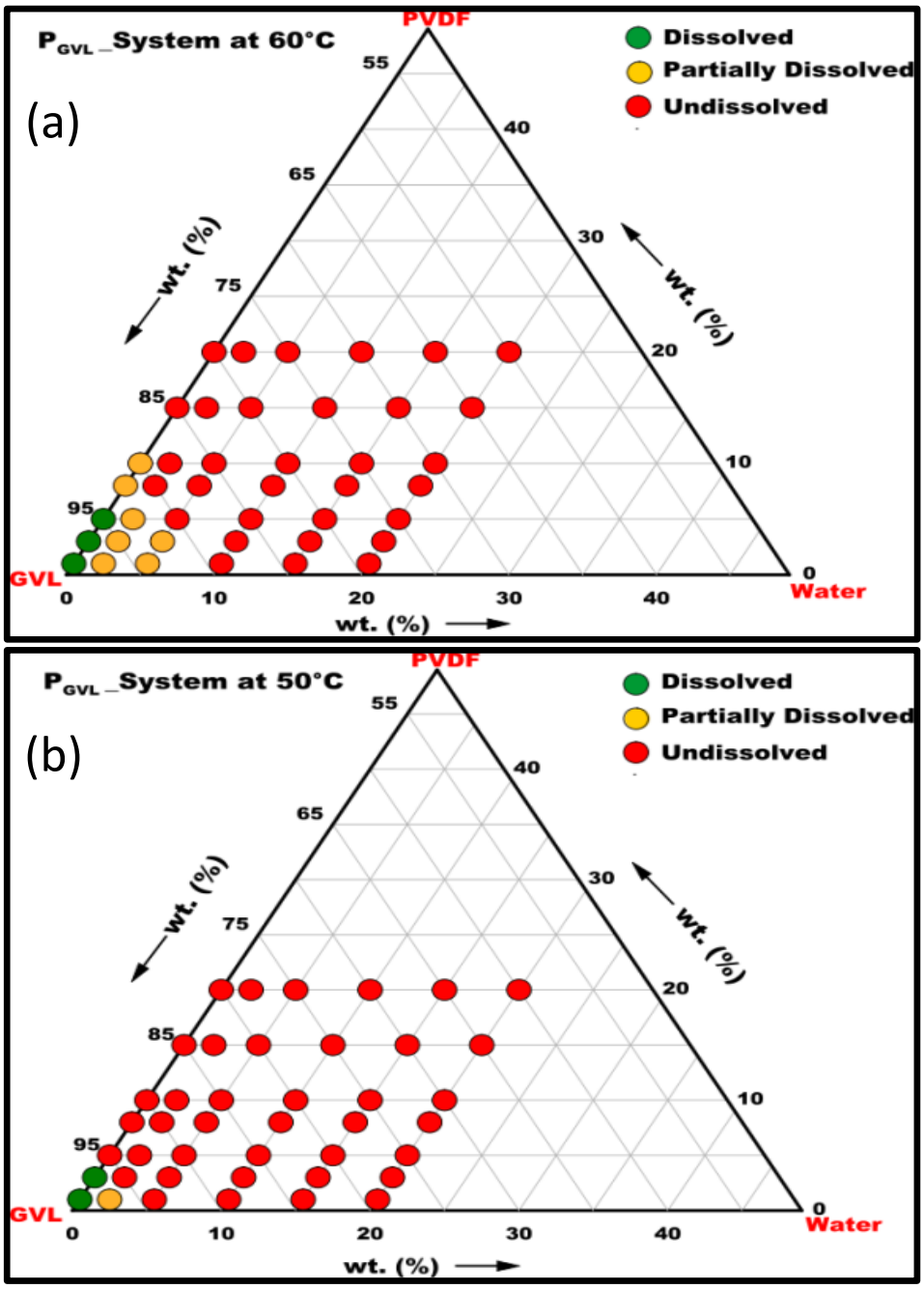

Figure 4.2.1: Solubility of PVDF/solvent/nonsolvent mixtures at different dissolution temperatures [(a) 50°C; (b) 60°C;

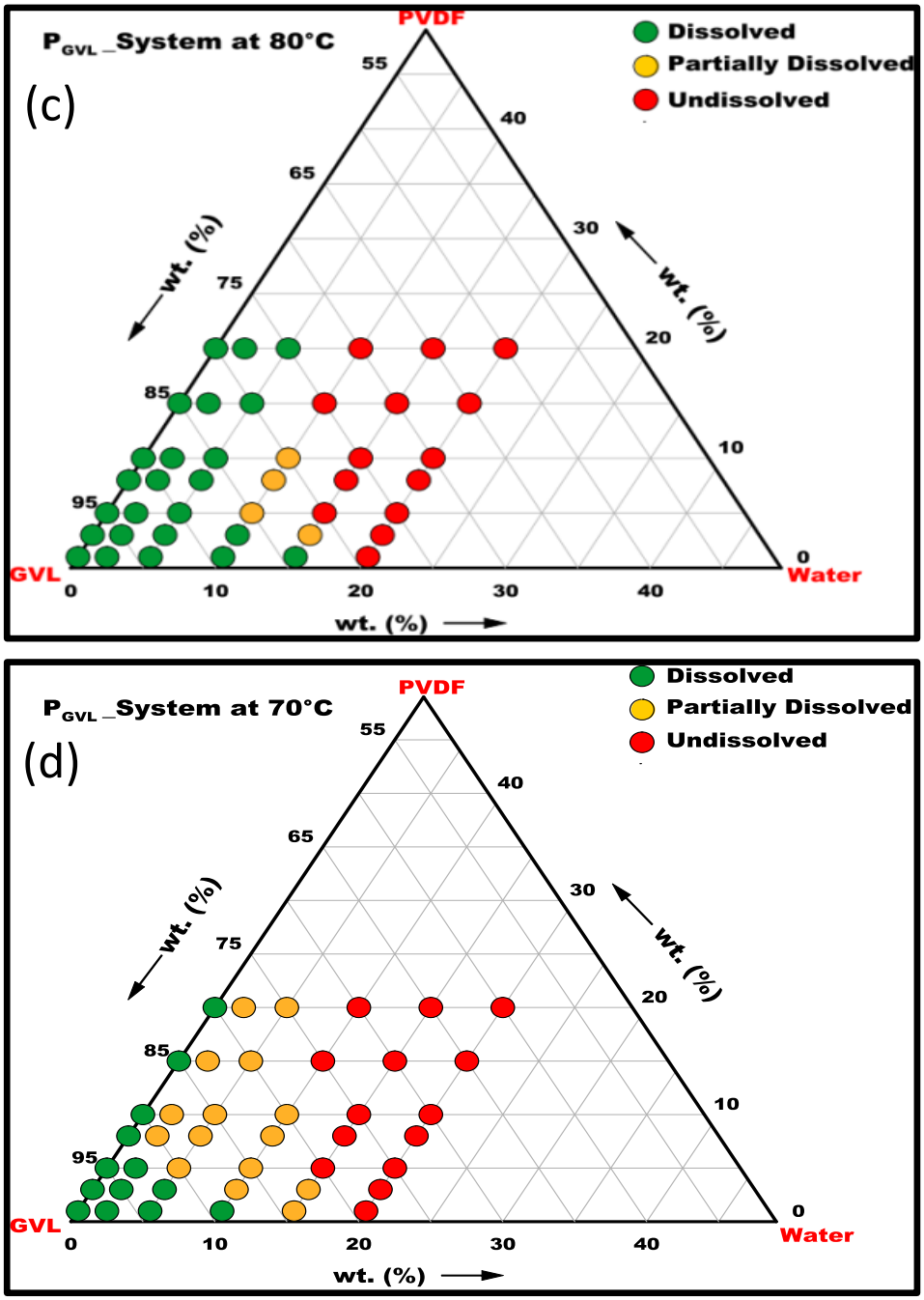

Figure 4.1.2: Solubility of PVDF/solvent/nonsolvent mixtures at different dissolution temperatures (c) 70°C; (d) 80°C.

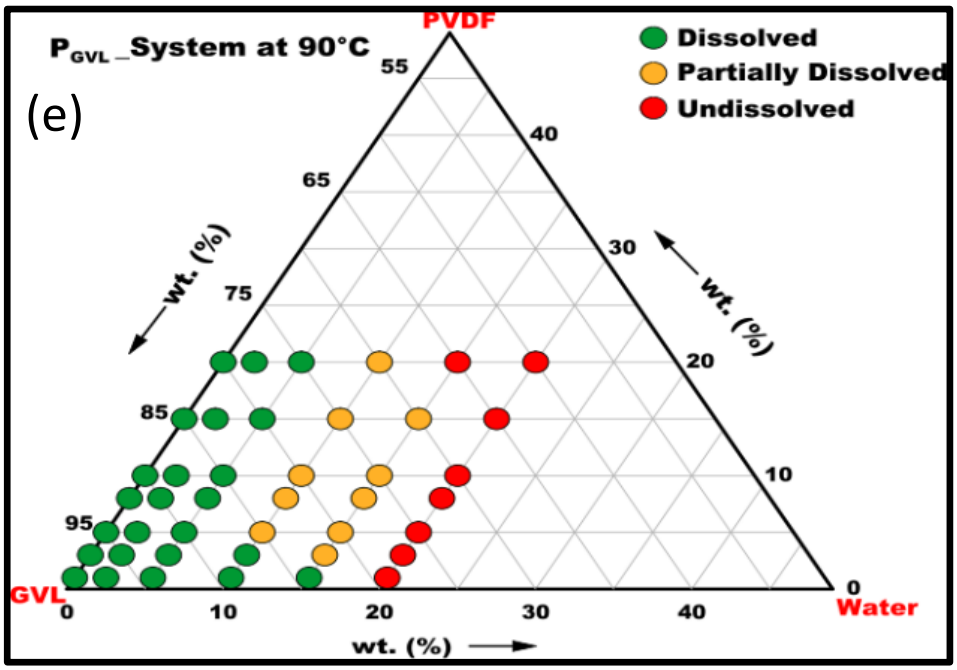

Figure 4.2.2 Solubility of PVDF/solvent/nonsolvent mixtures at different dissolution temperatures (e) 90°C.

4.3.3 Effect of temperature change on dissolved PVDF mixtures at a fixed equilibration period.

A proposed polymer dissolution in the vial method was used to determine the cloud points of the PVDF/GVL/H_2O system. Sealed vial samples were characterised by visually evaluating turbid/cloudiness after a given incubation period (2 days). In addition, the PVDF system's phase transition behaviour and thermodynamics were investigated at isothermal conditions for slow and fast cooling of homogeneous polymer mixtures.

Typically, when phase separation of a polymer mixture is induced, the demixing mechanism often relies on the cooling path (slow or fast) under isothermal conditions to predict the phase transition that is likely to occur due to a temperature change [29]. An illustration of the experimental polymer mixture cooling process (slow and fast) by swiftly reducing the temperature as it evolves over time is shown in Figure 4.3.

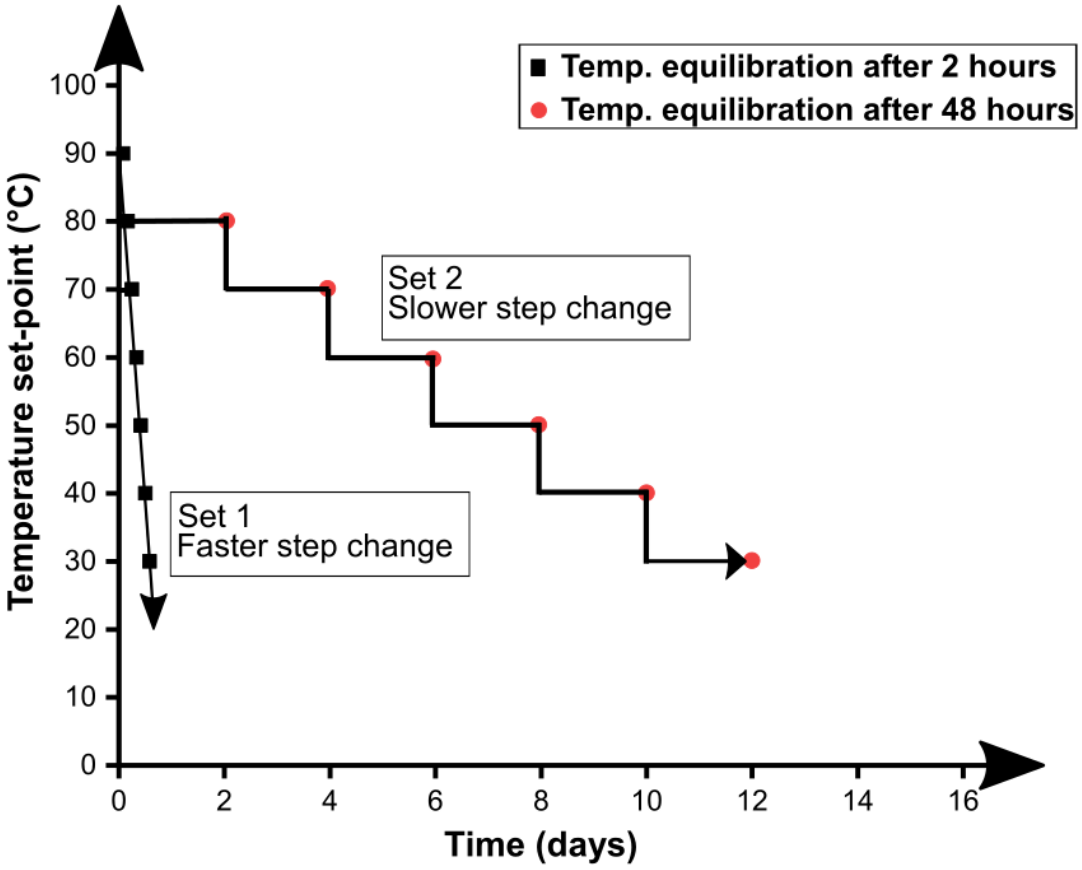

Figure 4.3: Temperature step change process of homogeneous PVDF/GVL/H20 mixtures observed with time evolution.

Two batches of homogeneous polymer mixtures were prepared for testing. The first set (set 1) is cooled with a faster temperature step change and a temperature equilibration of 2hrs. The second set (set 2) is cooled using a slower temperature change with time allowed for temperature equilibration of 48hrs. The implemented temperature gradient step change shows a significant difference between the fast (black Square) and slow (red circle) cooling trajectory path. The symbol represents the time effect conditions required for observed polymer mixture samples to transit from an equilibration temperature step change to another. The concept of a coordinated temperature change is commonly accepted in describing the observation of cloud points of polymer mixture samples. A homogeneous solution undergoes a phase change or begins to agglomerate on a molecular level, giving a cloudy appearance to form either a stable solution or suspension that settles as liquid-solid.

4.3.4 Cloud points based on the PDV method

The experimental phase behaviour study is depicted using a ternary phase diagram for temperature step change for 2h and 48h. The distinct phases are coded using coloured dots, to qualitatively distinguish the different regions and miscibility gap of the PVDF/GVL/H_2O system. Typically, homogeneous polymer mixtures that become thermodynamically unstable upon cooling (turbid/cloudy physical appearance) are considered the experimental cloud point curve [30]. The phase mapping presented in Figures 4.4, 4.5 and 4.6 highlights the distinct compositions and phase conditions of two batch samples of polymer mixtures with the same concentration**.** The green dot denotes a one-phase solution, the yellow dot represents the turbid liquid (two-phase), the blue dot represents a clear gel, and the red represents a turbid gel. The cloud point curve, which often identifies the boundary of the liquid-liquid phase separation, represents the binodal curve and is the same as the demixing curve.

Experimental analysis showed that the initial homogenous solutions are separated into two distinct phases (a liquid turbid phase and a gel phase) as the temperature is reduced and equilibration is maintained for a short or extended period. Analysis of demixing behaviour conditions of the PVDF system due to temperature change shows that the likelihood of phase change was evident for increased polymer or nonsolvent weight concentration. Observation of polymer mixtures due to temperature change and equilibration at 2hrs transited to clear gel. The homogeneous PVDF samples gradually became turbid gel after equilibration for 48hrs, and a few samples separated after a more extended incubation period (one month).

Results indicate that the phase transitions depend on the equilibration time due to temperature change. The onset of turbidity is gradual and not stepwise based on the observed clear gelation point in figure 4.4 – 4.6 and the interpretation of the fitted straight line (set 1) plot (see figure 4.3). However, polymer mixtures equilibrated for extended periods at the same temperature gradient appear to show a stepwise onset of turbidity of gel samples (see figure 4.7).

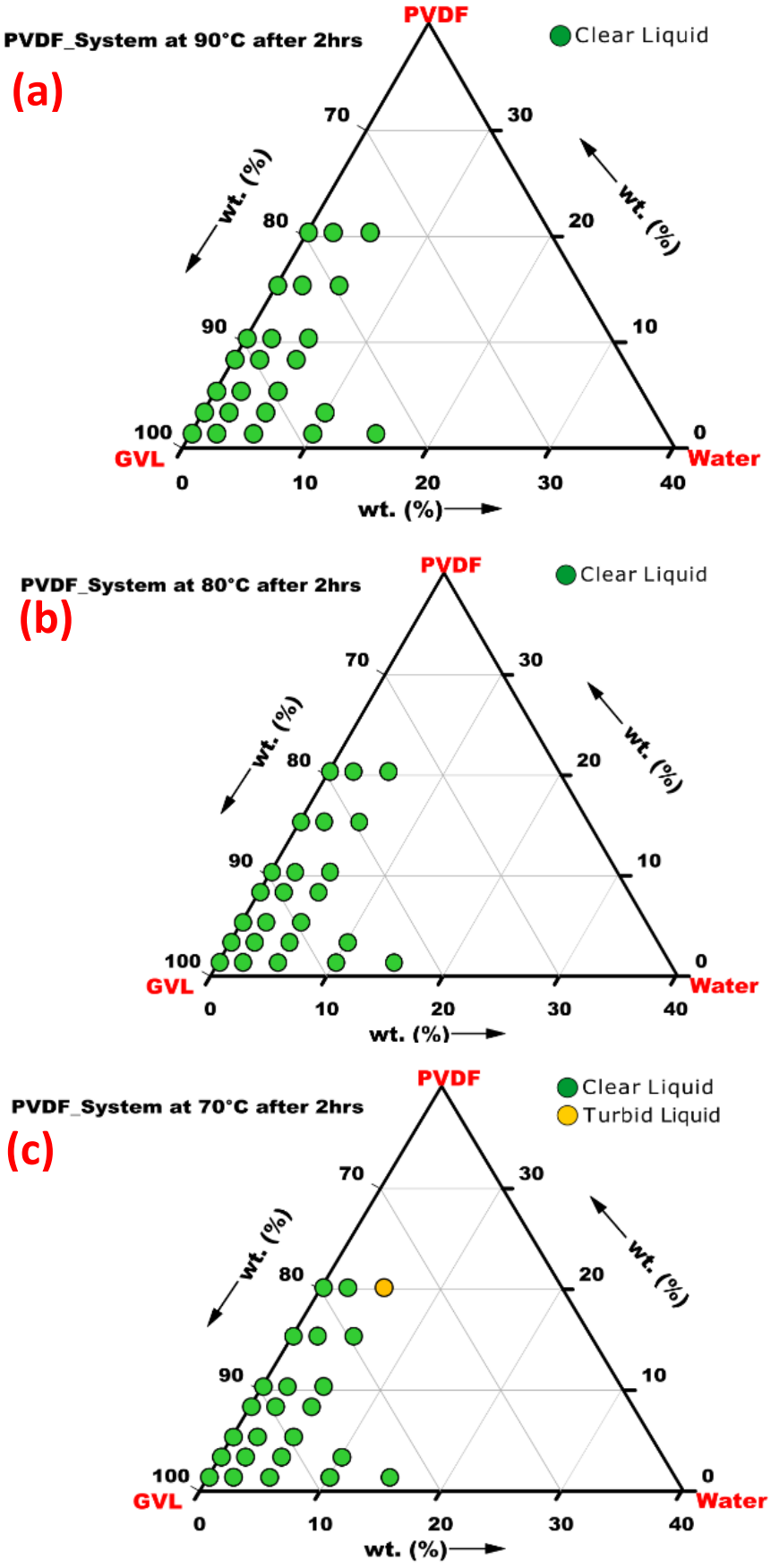

Figure 4.4: Phase behaviour of the PVDF/GVL/H2O system due to step change effect of Gibbs free energy at: (a) 90°C; (b) 80°C; (c) 70°C; and equilibration time evolution for 2hrs.

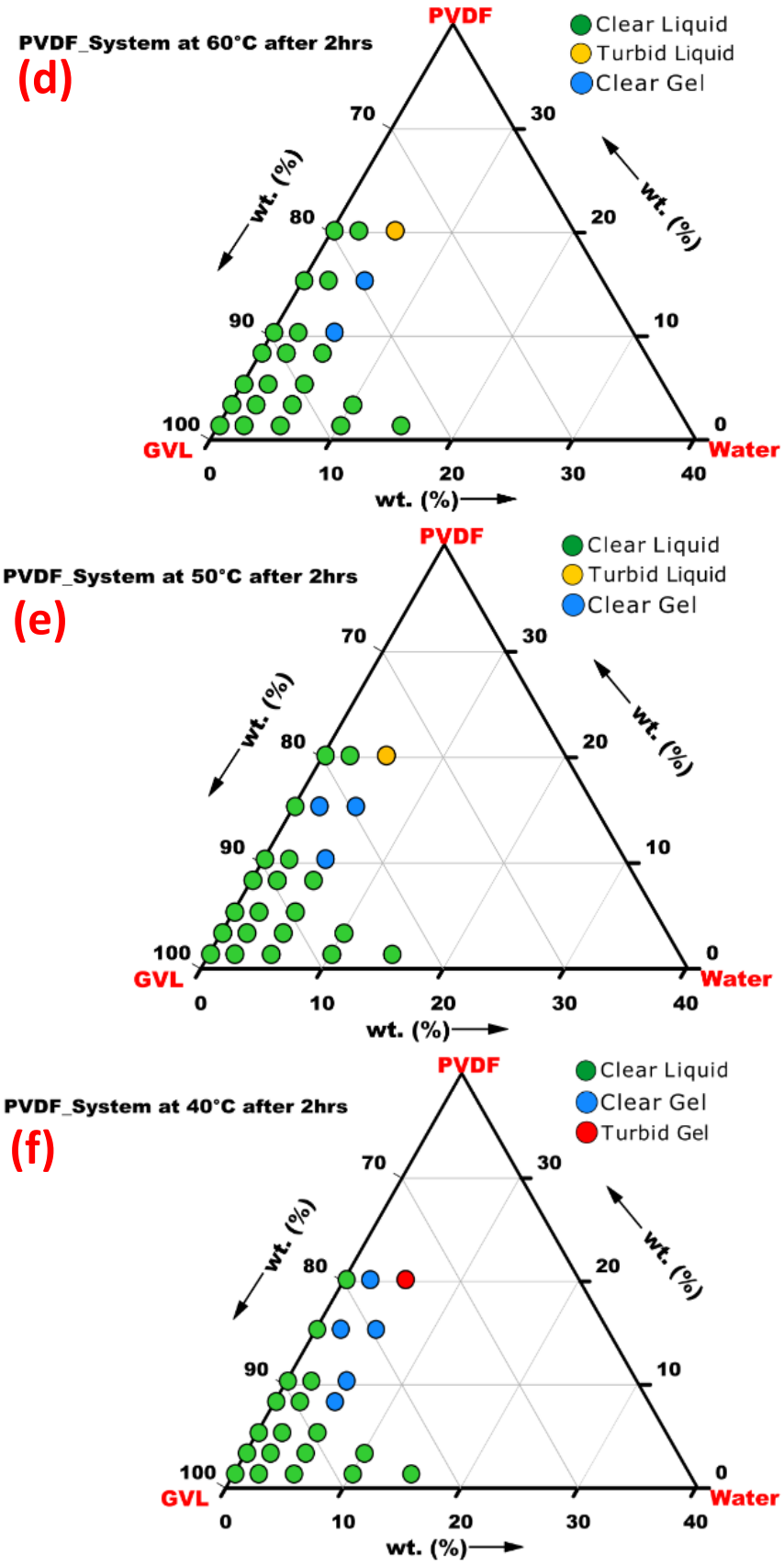

Figure 4.5: Phase behaviour of the PVDF/GVL/H_2O system due to step change effect of Gibbs free energy at: (d) 60°C; (e) 50°C; (f) 40°C; and equilibration time evolution for 2hrs.

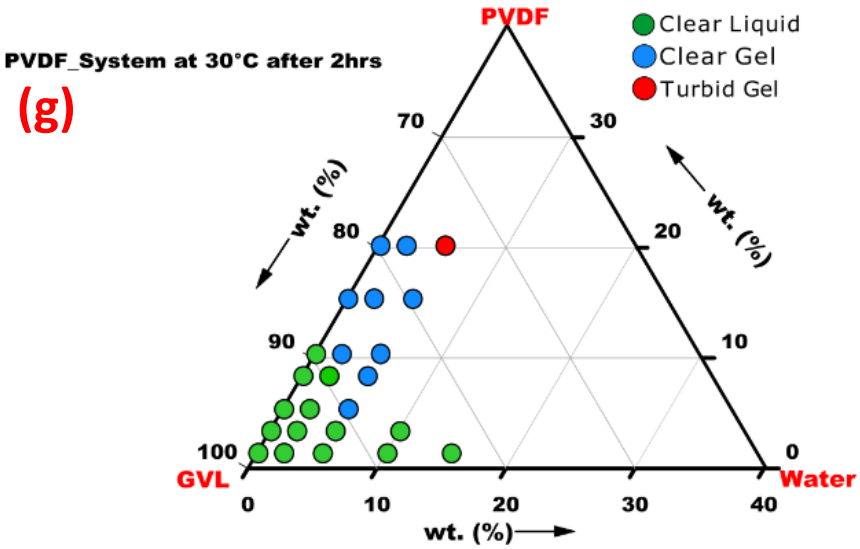

Figure 4.6: Phase behaviour of the PVDF/GVL/H_2O system due to step change effect of Gibbs free energy at (g) 30°C and equilibration time evolution for 2hrs.

The gel samples identified are compositions at which the homogenous solutions precipitated into a gel. Upon tilting the vial, one sample phase showed no flow movement. Gelation has been described as a three-dimensional network formation that occurs when a homogenous solution loses its ability to flow (i.e. turns into a soft solid). Gelation may occur through various mechanisms depending on factors such as the interaction of polymer/solvent, solvent/nonsolvent and temperature change. Many polymers exhibit gelation behaviour due to the potential of microcrystallite to form in some polymer mixtures, with the crystals functioning as nuclei for crystallisation [31,32].

Generally, a polymer solution could appear in several states (stable, unstable, or metastable) as the temperature is lowered with polymer mixtures (see figure 4.7), predominantly in the stable or metastable state. The experimental results show that gelation points were identified at certain temperatures as homogeneous solutions began to precipitate into a gel.

Several studies [33,34] reveal that the composition of polymer mixtures beyond the cloud point boundary demixes into two phases that differ in composition but are in thermodynamic equilibrium with each other. However, gel formation is usually metastable and undergoes imperceptible changes after a long period. The distinct observations have been reported for other PVDF systems and are mainly associated with semi-crystallinity and crystalline polymers [35,36]. Samples in the metastable state must overcome an activation barrier for phase separation to proceed spontaneously, unlike unstable solutions that result in a spontaneous phase separation process.

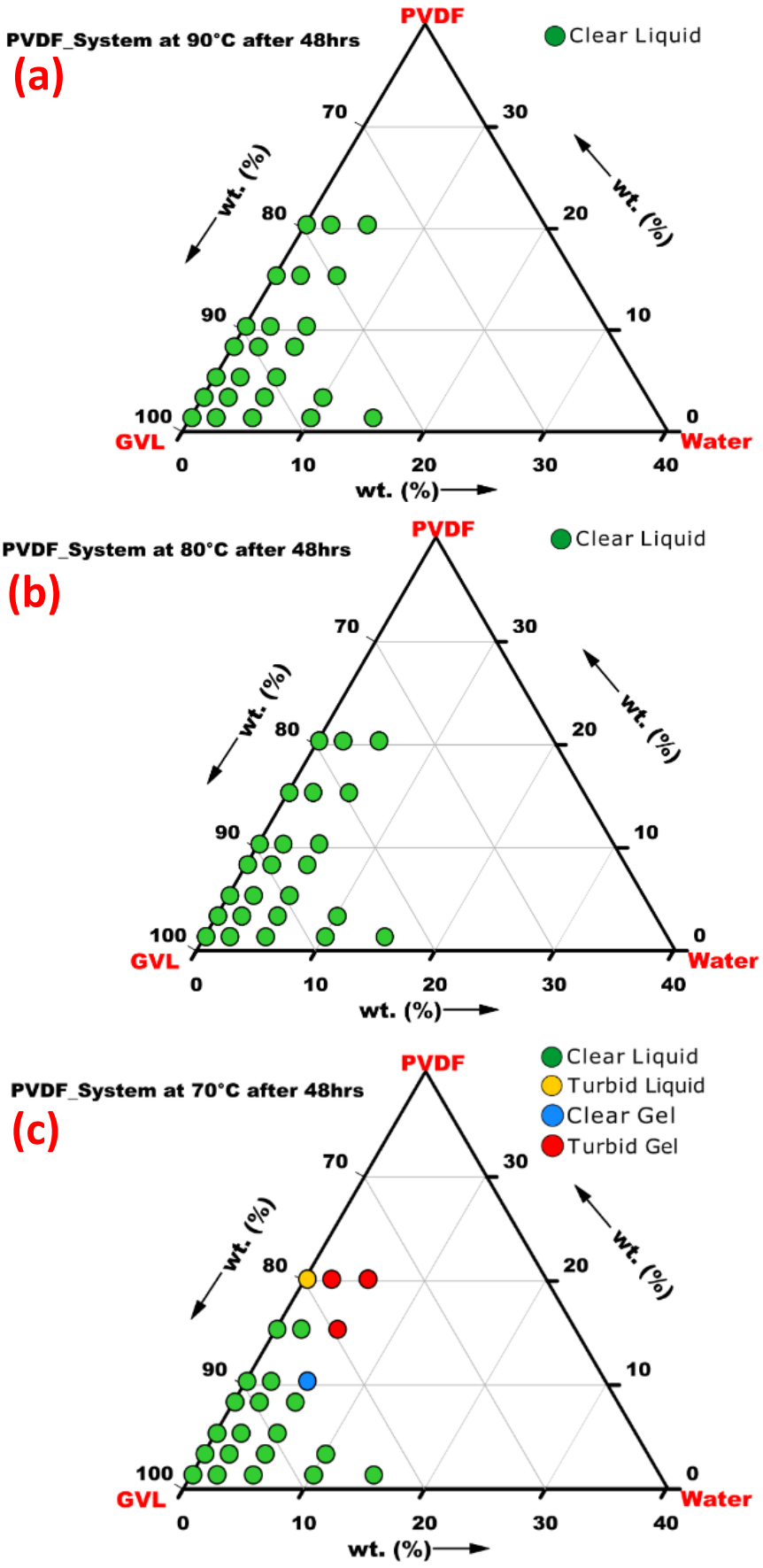

Figure 4.7: Phase behaviour of the PVDF/GVL/H_2O system due to step change effect of Gibbs free energy at: (a) 90 °C; (b) 80 °C; (c) 70 °C and equilibration time evolution for 48hrs.

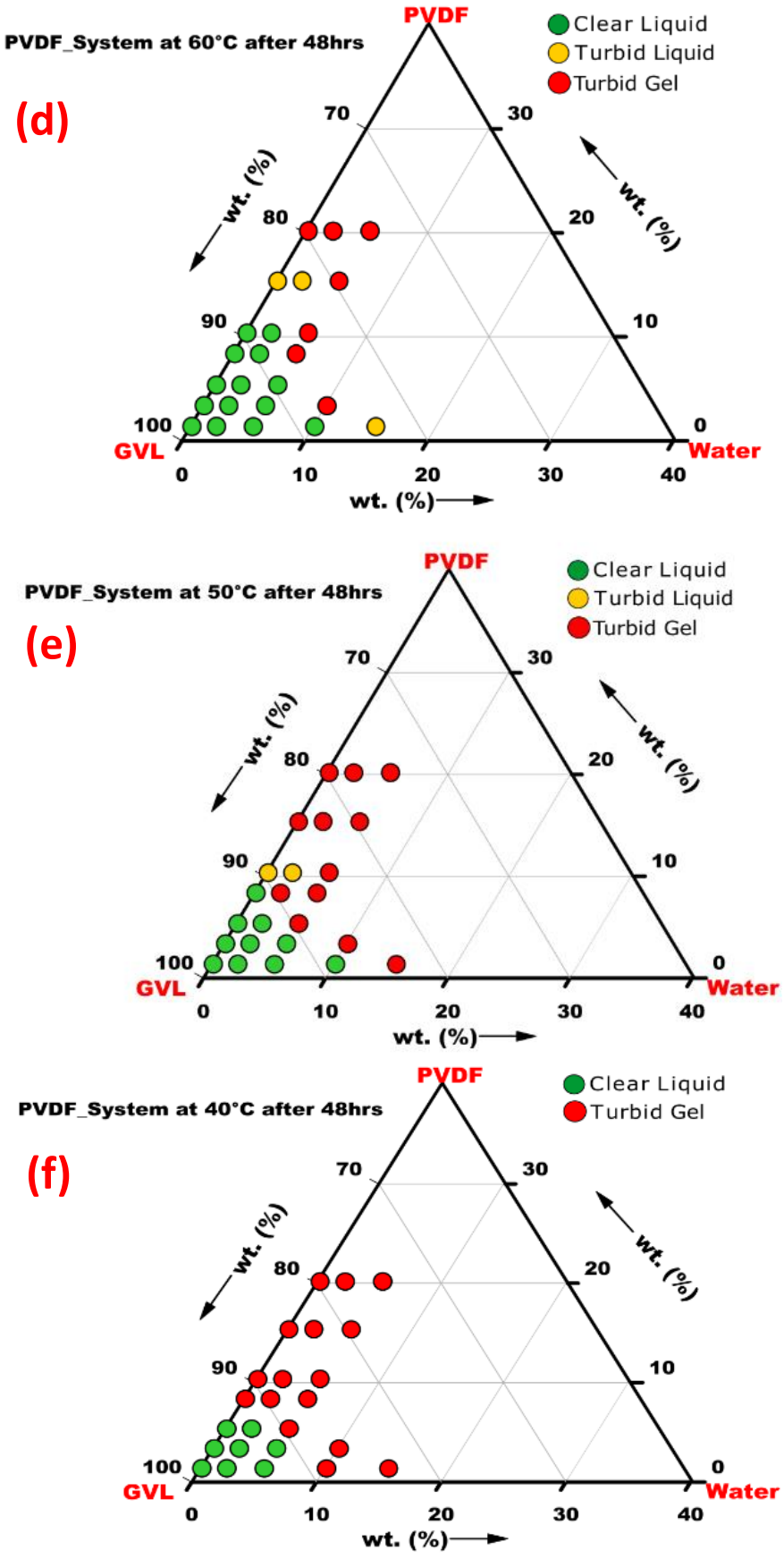

Figure 4.8: Phase behaviour of the PVDF/GVL/H_2O system due to step change effect of Gibbs free energy at: (d) 60°C; (e) 50°C; (f)40°C and equilibration time evolution for 48hrs.

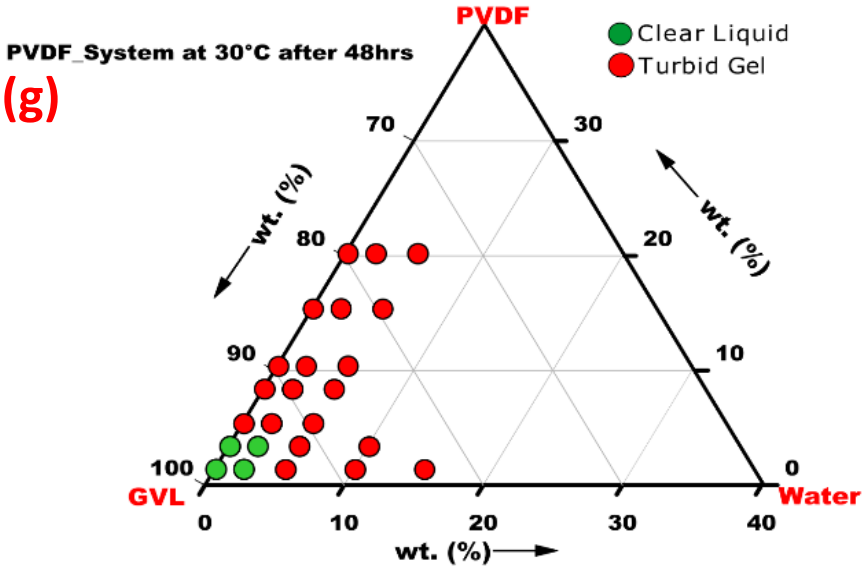

Figure 4.9: Phase behaviour of the PVDF/GVL/H_2O system due to step change effect of Gibbs free energy at: (g) 30°C and equilibration time evolution for 48hrs.

Equilibration analysis of the PVDF/GVL/H_2O showed it was difficult to determine the cloud point boundary due to the gellification of homogeneous polymer mixture samples. Although, it has been reported that gelation points represent cloud points for specific demixing polymer systems [37]. The observation of samples from a purely thermodynamic point of view reveals that gelation and liquid-liquid separation appear to occur concurrently with the solution-gel transition phenomenon linked to interactions between the polymer mixtures and indicative of temperature perturbations [16].

The equilibrium behaviour of the PVDF/GVL/H_20 system of the homogeneous polymer mixtures equilibrated at 48hrs reveals much closer equilibrium conditions for the PVDF system. However, it should be noted that the actual membrane formation process is always speedy and unquestionably different from the PVDF system equilibrium process. In addition, the kinetics of the system and the mass transfer between polymer mixtures may affect how the final membrane structure can be controlled. A map of the thermodynamically considered PVDF system phase transitions indicating the demixing curve due to temperature change is presented in figure 4.10. The result reveals that temperature plays a vital role in the thermodynamic stability of the PVDF system, as transition shifts can be observed in the demixing curve for the PVDF/GVL/H_2O system. The turbid gels observed are often reported to indicate that gelation is crystallisation induced due to the addition of the nonsolvent. However, the type of crystallisation taking place could vary and depend on either the polymer chain folding of the PVDF/GVL complexes involved [38]

Determining the demixing curve based on the equilibration of the temperature step change was necessary to understand the membrane formation and potential morphology structure of the PVDF/GVL/H_2O system. Based on the ternary phase diagram in figure 4.10, it is believed that the length of time the polymer mixtures take to enter into the metastable region dictates how the PVDF system phase separates.

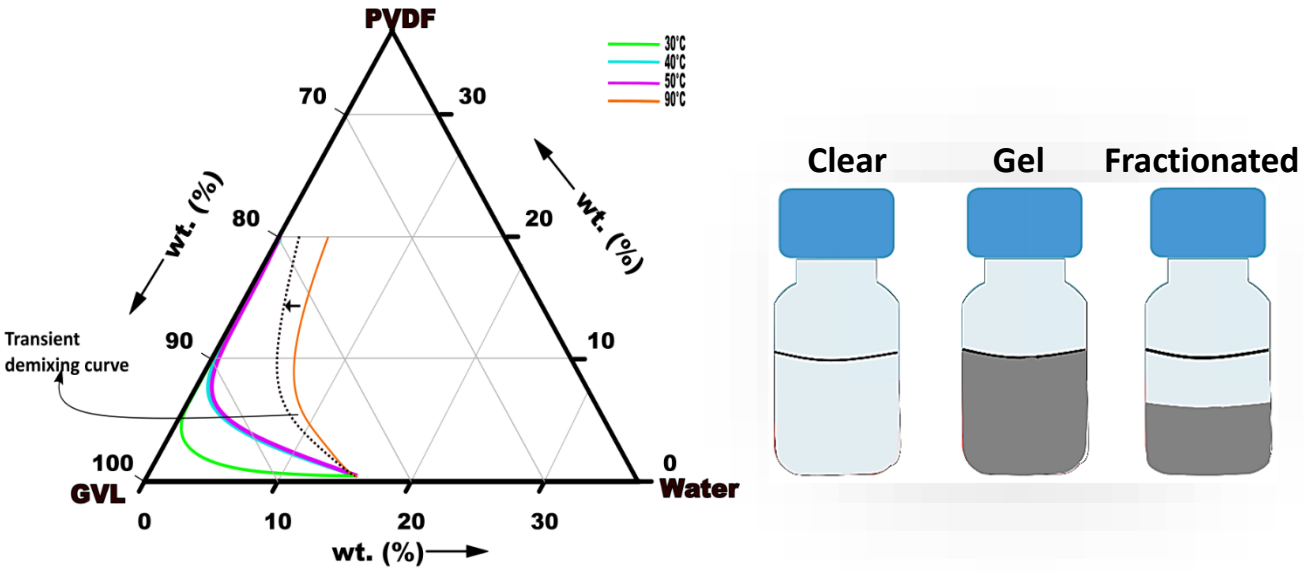

(a) (b)

Figure 4.10: (a) Ternary phase transition curves of the PVDF/GVL/H_2O system upon cooling from 90°C to 30°C after 48 h. (b) The illustrative transition of PVDF mixture samples changes at equilibrium over time.

Therefore, the influence of the equilibration time on the temperature gradient plays a significant role in understanding the turbidity of the PVDF system, and the determination of the gelation or cloud point does not quantify how quickly the phase changes or the demixing curve transits. Nevertheless, the ternary phase diagram reveals the potential experimental demixing pathway of the PVDF system. Temperature changes in dissolved polymer mixtures on samples with increased polymer or nonsolvent concentration promote thermodynamic instability and increase the miscibility gap of the PVDF system to shift to the polymer/solvent axis. The demixing curves transition is probably due to the difference in density, the polydispersity of polymer, or the refractive index of the co-exiting phases, as the temperature is lowered, causing turbidity and, in most cases, phase stratification (see 4.10 (b)) [39,40]. Hence, at isothermal conditions, after some time, the polymer becomes fractionated at equilibrium between two phases, with the higher molecular weight fractions being the *rich* phase and the lower molecular fractions of the dissolved PVDF system representing the polymer *lean* phase. Therefore, observing the demixing curves suggests that it is very likely that different kinds of membrane morphology can be obtained by controlling the influence of

temperature during the fabrication process. Furthermore, observing the PVDF system's phase behaviour can be considered a measure of the system resistance/tolerance to polymer precipitation by the nonsolvent (water) and solvent power.

The validation of the PDV method was experimentally examined for PVDF systems using dimethyl sulfoxide (DMSO) and triethyl phosphate (TEP) as solvents and water as the nonsolvent (See appendix S3). The experimental data for PVDF dissolved in DMSO based on the PDV method is presented in figure 4.11 (a) and shows distinct demixing data point results that reveal similarities with reported data in figure 4.11 (b) that is based on widely employed titration method [41,42,43]. Furthermore, the PDV method is helpful as it provides a discretised demixing boundary of the cloud point region. However, the drawback is that it does not give complete insight concerning other data points that might identify the exact cloud point for a specific polymer system. One way to resolve the issue is to increase the number of discrete points investigated.

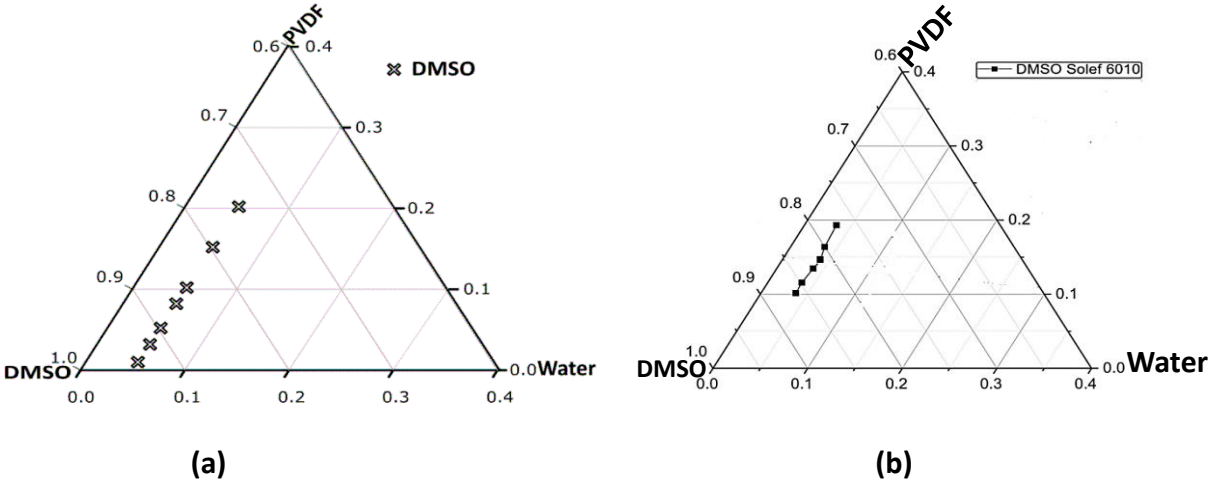

Figure 4.11: (a) Cloud data points of PVDF/DMSO/water system using the PDV method. (b) Cloud points of water/DMSO/PVDF system based on titration experiment [44].

4.3.5 Phase behaviour of the dope solution.

Polymer dissolution plays a crucial role in a wide range of industrial applications. Understanding the dissolution process allows for the optimisation of design and processing conditions and the selection of suitable compositions of polymer mixtures. The phase transition behaviour of the PVDF/GVL/H_2O system encouraged the experimental analysis of the effect of temperature on the polymer/solvent solutions. The objective was to investigate the long-term stability of the homogenous solution before phase separation or gelation and fully comprehend the effect of the solvent (GVL) in dissolving the polymer due to the influence of temperature. Therefore, a fixed PVDF concentration of 15wt% was dissolved in GVL, and

the thermal behaviour of the dope solution was examined for a temperature range between 70-180°C with samples nomenclature as P70-P180, respectively.

The dissolved PVDF at specific temperature conditions were rapidly cooled using an ice bath, and samples were maintained in a thermostatically controlled oven at isothermal conditions of 30°C. Table 4-2 summarises visually examined samples of dissolved PVDF in GVL at temperatures between 70-180°C.

Table 4-2: Thermodynamic analysis and stability of polymer solution at an isothermal temperature

Duration	Preparative dope solution temperature (°C)				
Time after quenching (day(s))	**70 (P70)**	**90 (P90)**	**120 (P120)**	**150 (P150)**	**180 (P180)**
1	Turbid gel	Turbid gel	Clear liquid	Clear liquid	Clear liquid
2	Turbid gel	Turbid gel	Phase separation	Phase separation	Clear liquid
3	Turbid gel	Turbid gel	Phase separation	Phase separation	Clear liquid
4	Turbid gel	Turbid gel	Phase separation	Phase separation	Phase separation
7	Turbid gel	Turbid gel	Phase separation	Phase separation	Phase separation
30	Turbid gel	Turbid gel	Phase separation	Phase separation	Phase separation

The result shows that dissolved polymer at temperatures between 70-90°C precipitated and formed a turbid gel within 24 hours. However, dissolved polymer at temperatures between 120-180°C remained homogeneous for a more extended period before separating into a liquid and gel phase. Typically, many thermodynamic properties of polymer solutions, such as the driving force for phase separation and viscosity, are temperature dependent. The transient behaviour of homogeneous polymer mixtures indicates that the time evolution of the samples observed after homogenisation is believed to depend on the initial state of the solutions based on the preparation process. Hence, upon cooling, once the gelation boundary is crossed, the polymer mixture prepared at high Tdissol (120-180)°C (temperature close to the melting point of the polymer) appears to phase

separate primarily due to crystallisation with the evolution of time. However, samples prepared at low Tdissol (70-90)°C become gel due to polymer chain folding and crystallisation happening with time. Thus, the gelation can affect the phase separation of these samples. Figure 4.12 shows a flow chart of the analysis.

The gelation and liquid-solid phase separations are two different phenomena that compete with each other in polymer solutions. Table 4-2 suggests that gelation is favoured at low solution preparation temperatures as polymer solution observed macroscopically goes from homogeneous liquid to gel state without passing through the liquid-liquid demixing state. The direct change could be explained due to the induced crystallisation of the PVDF-*rich* phase upon cooling close to or below the upper critical solution temperature (UCST). Therefore, the rapid temperature change rate may have caused thermal lags and non-equilibrium phase separation for the polymer mixtures.

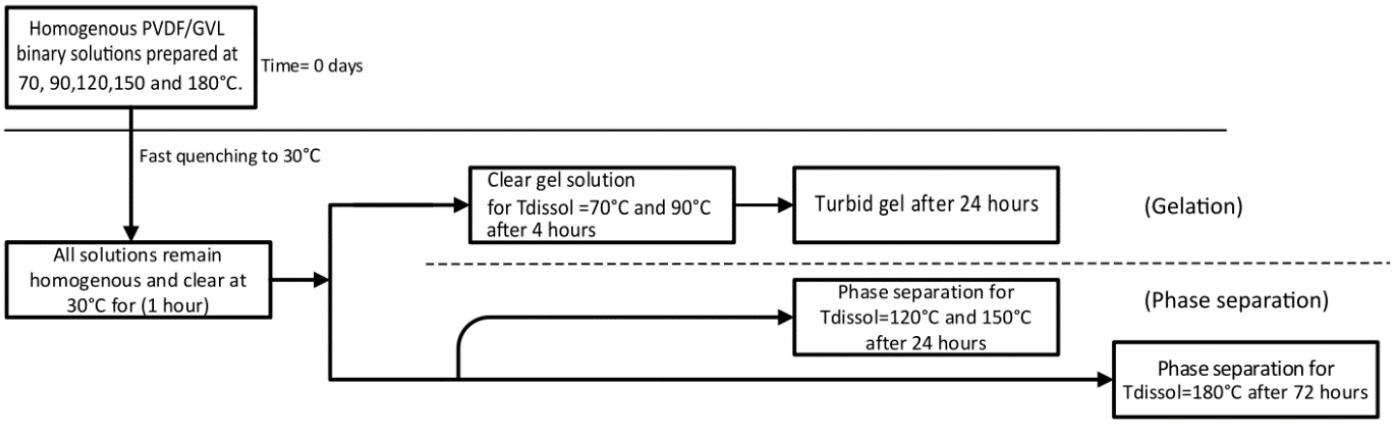

Figure 4.12: Experimental observations of the thermal history of polymer (dope) solution

Meanwhile, the dissolved polymer at temperatures >90°C phase separates once cooled to 30°C, with all PVDF solution-gel transitions being temperature and time dependent. Furthermore, the ageing of the polymer/solvent mixture maintained under isothermal conditions of 30°C can give some significant insight into the thermal history and potentially influence the kinetics effect of the PVDF system.

The experimental study showed that the dope solution's solution-gel evolution is thermoreversible [45]. Typically, the energy removed/released during cooling is counteracted by the time required for the dissolved polymer at different temperatures to phase separate. The phenomenon is consistent with a system's minimum and free energy principles. Hence, the more heat required to change the temperature of the polymer mixture, the slower it cools due to drastic temperature changes. Therefore, it is assumed that the sudden temperature drop of the dissolved polymer in GVL to an isothermal temperature of 30°C after cooling would have caused the formation of gel/crystals in the samples. The degree crystallinity of

the polymer solution was determined using the thermo-analytical technique known as differential scanning calorimetry (DSC) to gain insight into the influence of crystallinity in the PVDF dope solutions used to prepare membranes.

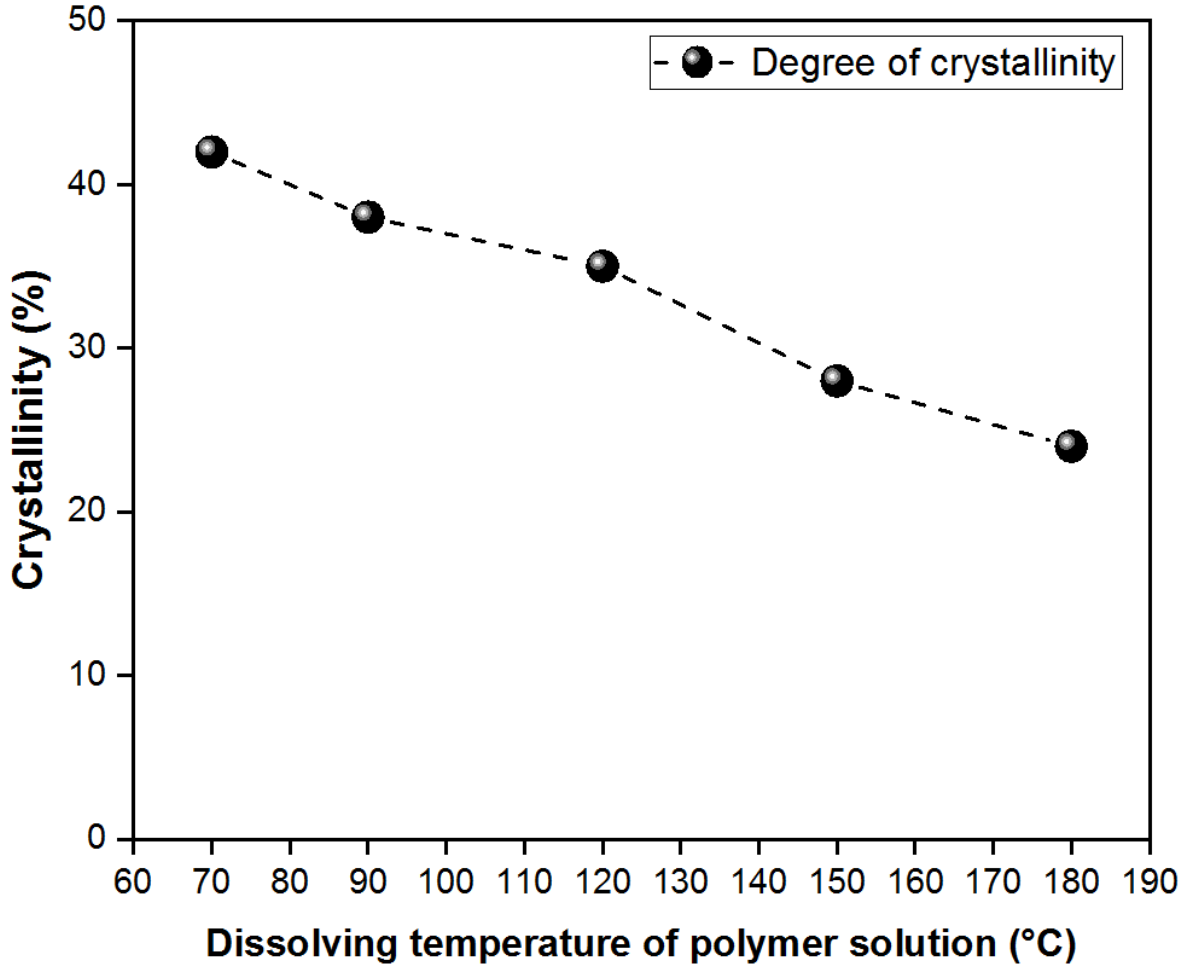

Figure 4.13: Comparison of total crystallinity of dissolved polymer solution at different temperatures.

Crystallisation affects a wide range of polymer properties, including thermal and optical conductivity, dissolved polymer tacticity, and the sample's phase behaviour. Crystallinity is typically induced by cooling a dilute solution or a material melting below its melting point, resulting in the growth of single crystals. The degree of the structural order in the dissolved PVDF solution could influence the phase separation process. Therefore, the results in figure 4.13 reveal the degree of crystallinity of dissolved polymer at a fixed concentration as a function of temperature, which supports the assumption that crystalline domains act as nuclei for gelation to occur in the PVDF solution once cooled to a lower temperature [46]. The fast cooling process allows for a uniform restriction of the crystallisation process and calorimetric measurement, indicating that at a lower Tdissol, the polymer did not crystallise completely. The crystalline region is likely responsible for the physical crosslink in

the samples such that the gelation of the PVDF/GVL samples contributes to the demixing process. However, the gelation phenomenon is due to microcrystallites forming once dope samples are cooled to a lower temperature. The exothermic curves obtained via calorimetric measurement (DSC) (see appendix S4.1) show that the crystallisation temperature of the polymer mixtures decreases slightly with increasing dissolved polymer temperature, which will affect the growth of crystals observed for each PVDF sample (P70-P180). Furthermore, the kinetic aspect of the PVDF system, which relates to the Gibbs energy of the dissolved polymer, is likely to influence the membrane fabrication process based on the crystalline relaxation of the PVDF samples and possible solvent trap in the polymer mixture due to gelation. However, the mechanisms of gelation due to the effect of temperature remain poorly understood for the PVDF system

4.4 Summary

The presented study showed that the bio-based solvent GVL could not solvate PVDF at ambient temperature, contrary to the predicted theoretical HSP analysis and that temperature plays a vital role in the dissolution and thermodynamic stability of the PVDF system. In addition, the solubility study suggests that the solvent power of GVL in dissolving PVDF is weak. The cloud point experimental investigation for the PVDF/GVL/H_2O system was carried out using the proposed “polymer dissolving in vial method” (PDV). Analysis of the PVDF system reveals the demixing boundary and gelation points, which were represented using a ternary phase diagram. It was shown that a small concentration volume of nonsolvent is needed to induce a phase change. The thermodynamic behaviour of the PVDF system was evaluated and presented using a ternary phase diagram to predict the favourable phase transitions and understand the mechanism of the phase separation phenomena. The experimental study shows there is a lag time to solubilise the polymer solutions and reach an equilibration state with the PVDF dope solution primarily influenced by temperature and an ageing time.

The observation of the turbid gel PVDF samples was dependent on the ageing of the solution, demonstrating that the PVDF system’s kinetic process also plays a function in how the components interact. Furthermore, the temperature time plot and the ternary diagram used to observe the cooling conditions of PVDF mixtures show a stack difference between the state of the rapidly cooled samples and those aged samples due to slow cooling conditions. Based on the experimental study, It is evident that the membrane fabrication process is never conducted in a condition of complete thermodynamic equilibrium and deals with phase conditions that constantly change until the solidification of the cast polymer solution. Hence,

the conditions of the membranes prepared differ entirely from the thermodynamic equilibration conditions.

The observed gelation boundary of PVDF/GVL/water splits the ternary phase diagram into two regions, a homogeneous one-phase at low polymer concentration and a turbid gel phase. PVDF is semi-crystalline, and the concept that crystallites are involved in gel formation is undoubtedly not new. However, the mechanisms of gelation in the study presented remain poorly understood. The determined degree of crystallinity at a fixed polymer concentration demonstrates the presence of crystallites, which may have initiated gelation when dissolved polymer mixture samples were cooled. These crystalline domains would likely influence the mass transfer of the polymer mixtures and the isothermal immersion precipitation process of the PVDF system.

Experimentally, the demixing boundary of several PVDF systems composed of different solvents was determined and compared to the conventional cloud point method via titration. The results showed a reasonably good agreement, indicating the reliability of the PDV method. However, the PDV approach has an advantage over the traditional titration approach in that it allows for the experimental monitoring and the time evolution of the thermal phase behaviour of various compositions of polymer mixtures. In addition, the prepared polymer mixture samples can be preserved to save material cost, examine the induced phase separation and evaluate the solubility and stability of the polymer system

Overall, the experimental phase behaviour result using GVL to dissolve PVDF revealed that liquid-liquid demixing would dominate in the early stages of the precipitation process, with induced crystallisation occurring later, which would likely impact the final membrane morphology. The binodal was hardly distinguishable due to the simultaneous occurrence of liquid-liquid separation and gelation of the sample. However, it assumed that the cloud point samples' location is at least very close to that of the gelation points. The thermodynamic analysis is expected to contribute to understanding membrane formation via the nonsolvent induced phase separation (immersion precipitation) for the PVDF/GVL/H_2O system and act as a helpful tool in discussing fabricated PVDF membranes.

The experimental study of the thermodynamics of PVDF/GVL/water system also serves as the foundation for the assessment of a few key process variables, such as the effect of the polymer concentration, use of solvent blends, the addition of additives to the polymer solution and the impact of temperature at which the polymer solution is dissolved or cast. In addition, the study provides the selected range of parameter values considered when assessing the few process variables covered in subsequent chapters (6-8) of the thesis.

4.5 References

[1] Ayman, E. G., Heba, A., & Sahar, A. (2012). Construction of ternary phase diagram and membrane morphology evaluation for polyamide/formic acid/water system. *Aust. J. Basic Appl. Sci*, *6*, 62-68.

[2] Flory, P. J. (1941). Thermodynamics of high polymer solutions. *The Journal of chemical physics*, *9*(8), 660-660.

[3] Sanchez, I. C., & Panayiotou, C. G. (1993). Equations of state thermodynamics of polymer and related solutions. *CHEMICAL INDUSTRIES-NEW YORK-MARCEL DEKKER-*, 187-187.

[4] Romay Romero, M., Diban Gómez, N., & Urtiaga Mendia, A. M. (2021). Thermodynamic modeling and validation of the temperature influence in ternary phase polymer systems.

[5] Barzin, J., & Sadatnia, B. (2007). Theoretical phase diagram calculation and membrane morphology evaluation for water/solvent/polyethersulfone systems. *Polymer*, *48*(6), 1620-1631.

[6] Altena, F. W., & Smolders, C. A. (1982). Calculation of liquid-liquid phase separation in a ternary system of a polymer in a mixture of a solvent and a nonsolvent. *Macromolecules*, *15*(6), 1491-1497.

[7] Lalia, B. S., Kochkodan, V., Hashaikeh, R., & Hilal, N. (2013). A review on membrane fabrication: Structure, properties and performance relationship. *Desalination*, *326*, 77-95.

[8] Ong, Y. K., Widjojo, N., & Chung, T. S. (2011). Fundamentals of semi-crystalline poly (vinylidene fluoride) membrane formation and its prospects for biofuel (ethanol and acetone) separation via pervaporation. *Journal of membrane science*, *378*(1-2), 149-162.

[9] Bottino, A., Camera-Roda, G., Capannelli, G., & Munari, S. (1991). The formation of microporous polyvinylidene difluoride membranes by phase separation. *Journal of membrane science*, *57*(1), 1-20.

[10] Alexowsky, C., Bojarska, M., & Ulbricht, M. (2019). Porous poly (vinylidene fluoride) membranes with tailored properties by fast and scalable non-solvent vapor induced phase separation. *Journal of Membrane Science*, *577*, 69-78.

[11] Bărdacă Urducea, C., Nechifor, A. C., Dimulescu, I. A., Oprea, O., Nechifor, G., Totu, E. E., ... & Bungău, S. G. (2020). Control of nanostructured polysulfone membrane preparation by phase inversion method. *Nanomaterials*, *10*(12), 2349.

[12] Kesting, R. E. (1985). Phase inversion membranes.

[13] Broens, L., Altena, F. W., Smolders, C. A., & Koenhen, D. M. (1980). Asymmetric membrane structures as a result of phase separation phenomena. *Desalination*, *32*, 33-45.

[14] van de Witte, P. J. D. P., Dijkstra, P. J., Van den Berg, J. W. A., & Feijen, J. (1996). Phase separation processes in polymer solutions in relation to membrane formation. *Journal of membrane science*, *117*(1-2), 1-31.

[15] L. Zeman, G. Tkacik, Thermodynamic analysis of a membrane-forming system water/N-methyl-2-pyrrolidone/polyethersulfone, Journal of Membrane Science 36 (1988) 119–140.

[16] M. Mulder, Basic Principles of Membrane Technology, Kluwer Academic Publishers, Dordrecht, Boston, London, 1996.

[17] Mazinani, S., Darvishmanesh, S., Ehsanzadeh, A., & Van der Bruggen, B. (2017). Phase separation analysis of Extem/solvent/non-solvent systems and relation with membrane morphology. *Journal of Membrane Science*, *526*, 301-314.

[18] Boom, R. M., Van den Boomgaard, T., & Smolders, C. A. (1994). Equilibrium thermodynamics of a quaternary membrane-forming system with two polymers. 1. Calculations. *Macromolecules*, *27*(8), 2034-2040.

[19] Wijmans, J. G., Kant, J., Mulder, M. H. V., & Smolders, C. A. (1985). Phase separation phenomena in solutions of polysulfone in mixtures of a solvent and a nonsolvent: relationship with membrane formation. *Polymer*, *26*(10), 1539-1545.

[20] Benazzouz, A., Moity, L., Pierlot, C., Sergent, M., Molinier, V., & Aubry, J. M. (2013). Selection of a greener set of solvents evenly spread in the Hansen space by space-filling design. *Industrial & Engineering Chemistry Research*, *52*(47), 16585-16597.

[21] Barton, A. F. (2018). Handbook of polymer-liquid interaction parameters and solubility parameters. Routledge.

[22] Jung, J. T., Kim, J. F., Wang, H. H., di Nicolo, E., Drioli, E., & Lee, Y. M. (2016). Understanding the non-solvent induced phase separation (NIPS) effect during the fabrication of microporous PVDF membranes via thermally induced phase separation (TIPS). *Journal of Membrane Science*, *514*, 250-263.

[23] Bottino, A., Capannelli, G., Munari, S., & Turturro, A. (1988). Solubility parameters of poly (vinylidene fluoride). *Journal of Polymer Science Part B: Polymer Physics*, *26*(4), 785-794.

[24] Barton, A. F. (2017). CRC handbook of solubility parameters and other cohesion parameters. Routledge.

[25] Van Krevelen, D. W., & Te Nijenhuis, K. (2009). Properties of polymers: their correlation with chemical structure; their numerical estimation and prediction from additive group contributions. Elsevier.

[26] Mulder, J. (2012). Basic principles of membrane technology. Springer Science & Business Media.

[27] Sanchez, I. C., & Lacombe, R. H. (1978). Statistical thermodynamics of polymer solutions. *Macromolecules*, *11*(6), 1145-1156.

[28] Yilmaz, L., & McHugh, A. J. (1986). Analysis of nonsolvent–solvent–polymer phase diagrams and their relevance to membrane formation modeling. *Journal of applied polymer science*, *31*(4), 997-1018.

[29] Su, S. L., Wang, D. M., & Lai, J. Y. (2017). Critical residence time in metastable region–a time scale determining the demixing mechanism of nonsolvent induced phase separation. *Journal of membrane science*, *529*, 35-46.

[30] Tao, M. M., Liu, F., Ma, B. R., & Xue, L. X. (2013). Effect of solvent power on PVDF membrane polymorphism during phase inversion. *Desalination*, *316*, 137-145.

[31] Gaides, G. E., & McHugh, A. J. (1989). Gelation in an amorphous polymer: a discussion of its relation to membrane formation. *Polymer*, *30*(11), 2118-2123.

[32] Rozelle, L. T., Cadotte, J. E., Corneliussen, R. D., Erickson, E. E., Cobian, K. E., & Kopp Jr, C. V. (2000). Phase inversion membranes. *Encyclopedia of Separation Science; Mulder, M., Ed.; Academic Press: Cambridge, MA, USA*, 3331-3346.

[33] Barth, C., Goncalves, M. C., Pires, A. T. N., Roeder, J., & Wolf, B. A. (2000). Asymmetric polysulfone and polyethersulfone membranes: effects of thermodynamic conditions during formation on their performance. *Journal of Membrane Science*, *169*(2), 287-299.

[34] Van de Witte, P., Dijkstra, P. J., Van den Berg, J. W. A., & Feijen, J. (1996). Phase separation processes in polymer solutions in relation to membrane formation. *Journal of membrane science*, *117*(1-2), 1-31.

[35] Cheng, L. P. (1999). Effect of temperature on the formation of microporous PVDF membranes by precipitation from 1-octanol/DMF/PVDF and water/DMF/PVDF systems. *Macromolecules*, *32*(20), 6668-6674.

[36] Soh, Y. S., Kim, J. H., & Gryte, C. C. (1995). Phase behaviour of polymer/solvent/non-solvent systems. *Polymer*, *36*(19), 3711-3717.

[37] Cheng, L. P., Lin, D. J., Shih, C. H., Dwan, A. H., & Gryte, C. C. (1999). PVDF membrane formation by diffusion-induced phase separation-morphology prediction based on phase behavior and mass transfer modeling. *Journal of Polymer Science Part B: Polymer Physics*, *37*(16), 2079-2092.

[38] Akkoyun, M., Carrot, C., & Blottière, B. (2012). Ternary Diagrams of Poly (vinylidene fluoride) and Poly [(vinylidene fluoride)-co-hexafluoropropene] in Propylene Carbonate and Dimethyl Sulfoxide. *Macromolecular Chemistry and Physics*, *213*(5), 587-593.

[39] Tang, Y., Lin, Y., Ma, W., & Wang, X. (2021). A review on microporous polyvinylidene fluoride membranes fabricated via thermally induced phase separation for MF/UF application. *Journal of Membrane Science*, *639*, 119759.

[40] Stropnik, Č., Musil, V., & Brumen, M. (2000). Polymeric membrane formation by wet-phase separation; turbidity and shrinkage phenomena as evidence for the elementary processes. *Polymer*, *41*(26), 9227-9237.

[41] Enayatzadeh, M., & Mohammadi, T. (2018). Morphology and performance of poly (vinylidene fluoride) flat sheet membranes: Thermodynamic and kinetic aspects. *Journal of Applied Polymer Science*, *135*(27), 46419.

[42] Fashandi, H., Yegane, A., & Abolhasani, M. M. (2015). Interplay of liquid-liquid and solid-liquid phase separation mechanisms in porosity and polymorphism evolution within poly (vinylidene fluoride) nanofibers. *Fibers and Polymers*, *16*(2), 326-344.

[43] Yeow, M. L., Liu, Y. T., & Li, K. (2003). Isothermal phase diagrams and phase-inversion behavior of poly (vinylidene fluoride)/solvents/additives/water systems. *Journal of Applied Polymer Science*, *90*(8), 2150-2155.

[44] Alexowsky, C., Bojarska, M., & Ulbricht, M. (2019). Porous poly (vinylidene fluoride) membranes with tailored properties by fast and scalable non-solvent vapor induced phase separation. *Journal of Membrane Science*, *577*, 69-78.

[45] Domszy, R. C., Alamo, R., Edwards, C. O., & Mandelkern, L. (1986). Thermoreversible gelation and crystallization of homopolymers and copolymers. *Macromolecules*, *19*(2), 310-325.

[46] Kim, S. S., & Lloyd, D. R. (1992). Thermodynamics of polymer/diluent systems for thermally induced phase separation: 3. Liquid-liquid phase separation systems. *Polymer*, *33*(5), 1047-1057.

CHAPTER 5

Investigation of the Use of γ-Valerolactone via NIPS for Fabrication of PVDF Membranes

5.1 Introduction

The nonsolvent induced phase separation (NIPS) technique is one of the most commonly used industrial membrane fabrication approaches to prepare asymmetric polymeric membranes, which will be employed in this project to fabricate PVDF membranes. The technique entails preparing a dope solution by dissolving a polymer in the solvent and casting it on a substrate. Typically the NIPS technique is associated with the phase separation behaviour of the polymer solution to obtain asymmetric membranes. In addition, several factors such as polymer concentration, polymer molecular weight, dissolution temperature of polymer solution, types of additives to the polymer solution, and solubility interaction of components have been reported to play a significant effect in polymeric membrane fabrication [1,2,3,4].

The phase separation behaviour of polymer solution has been discussed in chapter 4; hence the need to fabricate PVDF membranes using an alternative replacement or possibly substitution of commonly used toxic solvent is proposed and forms the preliminary analysis investigated in this chapter. Gamma valerolactone (GVL), a bio-derived solvent from lignocelluloses biomass, is offered as a suitable replacement based on its similar physicochemical properties (see figure 5.1 for the structure of solvents and properties highlighted in Table 5.1) to traditional polar, aprotic solvent *N*-methyl pyrrolidinone (NMP) used industrially for the preparation of polymeric (PVDF) membranes ultrafiltration and microfiltration processes.

In this chapter, studies will be carried out to investigate the feasibility of GVL as a potential bio-based green solvent for the synthesis of flat sheet freestanding PVDF membrane via the NIPS method and examine the effect of polymer concentration. The polymer concentration investigated is based on the analysis presented in chapter 4 and commonly investigated polymer concentrations reported [5,6]. In addition, the fabrication of PVDF membranes using a toxic aprotic solvent such as *N*-methyl pyrrolidinone (NMP) is considered. It is consistently compared to the prepared PVDF membrane using GVL as solvent. The characterisation and performance of the fabricated PVDF membranes are also examined and discussed.

Table 5-1: Different solvent Chemical and physical properties [7,8]

Solvent Properties	**Gamma-valerolactone** (GVL)	***N*-Methyl-2-pyrrolidone**(NMP)
CAS-No	108-29-2	872-50-4
Molecular Formula	$C_5H_8O_2$	C_5H_9NO
Boiling point (°C)	207	202
Molecular weight	100.12	99.13
Solubility in water (mg/ml)	Miscible	Miscible
Melting point (°C)	-31	-24
Density (g mL^{-1})	1.05	1.03
Flashpoint (°C)	96	91
Standard enthalpy change of vapourisation ΔHvap (kJ mol^{-1})	54.8	61.9
Enthalpy of combustion ΔcH°liquid (kJ mol^{-1})	-2649.6	-2991.7
Refractive index (n20/D)	1.432	1.479
Viscosity at 25°C (cP)	2.18	1.67
Kinematic viscosity (m^2/s) at (40°C)	2.1×10^{-6}	1.32×10^{-6}
Hazard code/Signal	Not a hazardous substance	H315, H319, H335, H360D/ Danger
Acute Toxicity (LD50 Oral)-(mg/kg) (Rat)	8800	4150
Hodge and Sterner's classification	5-practically non-toxic	4- Slightly toxic

ΔHvap – Enthalpy of vaporisation; ΔcH° - Standard enthalpy of combustion.

Gamma-valerolactone (GVL) *N*-Methyl-2-Pyrrolidone (NMP)

Figure 5.1: Schematic diagram showing the chemical structure of considered aprotic solvents.

5.2 Experimental analysis

5.2.1 Preparation of PVDF dope solution and Membrane preparation

The process of preparing the PVDF casting (dope) solutions required for membrane fabrication is covered in chapter 3. First, PVDF concentration (15wt.%) dissolved in GVL and NMP was used to obtain a homogenous PVDF dope solution. Then, a predetermined concentration of PVDF (10-20wt.%) was dissolved in GVL, and dope solutions were utilised to fabricate PVDF membranes via the nonsolvent induced phase separation (NIPS) method. Table 5.2 shows the formulation conditions of the PVDF solutions and the membrane identification nomenclature.

Table 5-2: Compositions of polymer and solvent concentrations to prepare PVDF membranes

Membrane nomenclature	Polymer (PVDF) (wt. %)	GVL (wt.%)	NMP (wt.%)	Evaporation time to air (seconds)	Casting/coagulation bath temperature (°C)
M10-GVL	10	90	0	30	30
M15-GVL	15	85	0	30	30
M15-NMP	15	0	85	30	30
M20-GVL	20	80	0	30	30

The experimental characterisation study was examined in two stages. First was the analysis of membranes fabricated using solvents (GVL, NMP) with comparable properties. Secondly, investigate the influence of polymer concentration using GVL as an alternative replacement to obtain tailored polymeric membranes for micro or ultrafiltration membrane processes.

5.3 Results and discussion

5.3.1 PVDF membrane morphology due to the effect of solvents.

All prepared PVDF membranes using GVL or NMP selected as solvents favoured an asymmetric structure. The morphological structure of the synthesised PVDF membranes was studied through SEM analysis with the top surface and cross-section images presented in figure 5.2. The SEM image features a finger-like cavity dominated by macrovoids and cellular spongy porous substructure for PVDF membranes prepared using NMP. In contrast, the PVDF/GVL dope membrane showed a dense top layer and a spongy, globule-like bi-continuous structure. The morphology via the NIPS method tends to be governed by the solvent/nonsolvent diffusion rate, the polymer system's solubility and concentration. With a

fast exchange rate of solvent/nonsolvent, an instantaneous demixing occurs with the formation of a finger-like/macrovoid structure.

On the other hand, if the solvent/nonsolvent diffusion rate is slow, delayed demixing phase separation and a spongy-like bicontinuous structure is observed mainly for conditions where a strong nonsolvent such as water is used [9,10]. The membrane formation process via the NIPS method has been described to induce a "sudden shock" phenomenon when a thermodynamically cast film is immediately immersed into a nonsolvent coagulation bath. The exchange of solvent/nonsolvent occurs perpendicular to the cast film and transforms the thermodynamically stable binary polymer solution into a meta or unstable solution.

The PVDF/GVL system's observed morphology is associated with a slow solvent/nonsolvent exchange inducing a delayed liquid-liquid demixing phase separation. On the other hand, NMP, regarded as a strong but toxic solvent [11], features a thin dense top layer with a finger-like and irregular macrovoids structure underneath. The formation of the PVDF/NMP is related to the faster exchange of solvent/nonsolvent, inducing an immediate, demixing process. The rapid desolvation of solvent from cast film [9,12] results in macrovoids within the sublayer. In contrast, the slow exchange of solvent/nonsolvent afterwards results in a spongy, porous structure. The Cahn-Hilliard theory [13] has been used to better understand the phase separation kinetics via NIPS and justify the phenomenon that occurs within the early phase separation stage.

The PVDF morphologies are easily distinguished from one another by their distinct structural differences, which suggest that the phase separation mechanism involving immersion/precipitation was probably caused by liquid-liquid demixing via nucleation and growth mechanisms or/and crystallisation of the polymer. Semi-crystalline polymers generally consist of both an amorphous phase (without any crystal ordering) and a crystalline phase (ordered), and most times, the interplay of formation mechanism due to the selection of solvents offers a broad spectrum of structures [14, 15]. Additionally, the location of the miscibility gap region of both PVDF/GVL and PVDF/NMP systems highlights these differences observed during the fabrication process. Based on the observed morphology of the PVDF membranes, it was possible to discern the influence of the thermodynamic analysis of the PVDF/GVL/water system and correlate the solvent strength power in the PVDF system [16].

I. - Membrane Top Surface

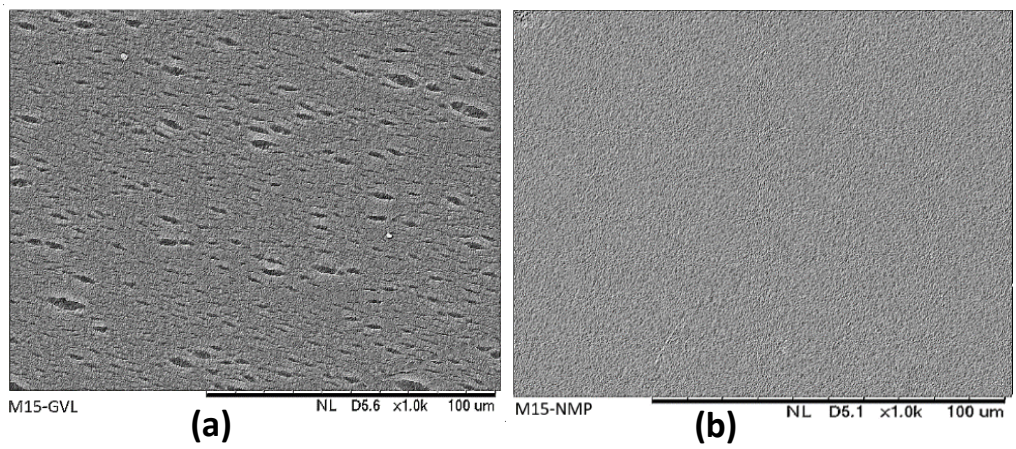

II. - Membrane Cross-section

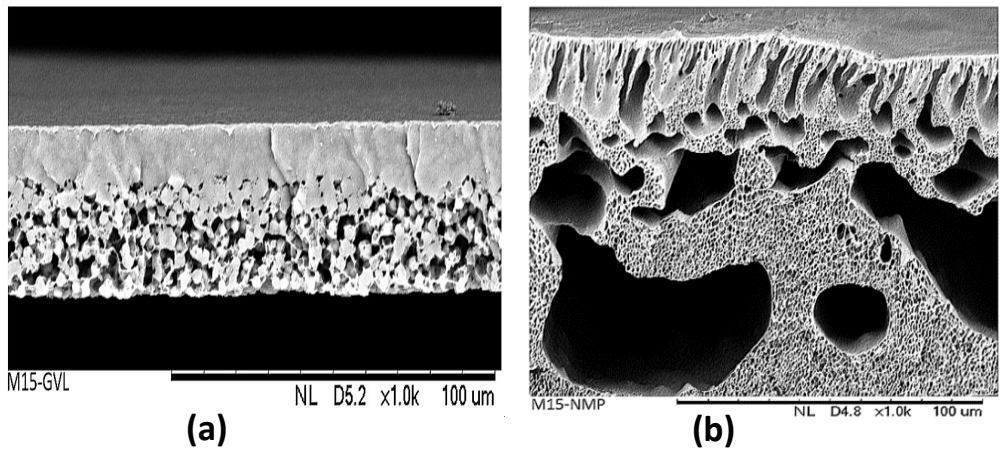

Figure 5.2 (I) and (II): SEM images showing the top surface and cross-section of PVDF membranes. Components of polymer dope are (a) 15wt% PVDF and GVL and (b) constitutes 15wt% PVDF and NMP

The influence of the solvent/nonsolvent mutual diffusivity was examined to determine if it plays a significant factor in the distinct membrane morphology observed in figure 5.2. Experimental assessment of the diffusivities for the different solvent/nonsolvent systems is time consuming and difficult. However, predicting an average value using the Wilke-chang method [17] was suggested to estimate the diffusivities of solvent/nonsolvent as expressed in equation (3). The expression is derived from a mathematical correlation of existing diffusivities for various solvents in water or vice-versa may be acceptable to support the qualitative reasoning of the obtained morphology of the PVDF membrane. The computational parameters considered are the temperature, the solute's molar volume and the solvent's viscosity and molecular mass. The difference in diffusivity between solute and solvent

(solvent/water or water/solvent) is primarily controlled by the molar volume of the solute, with temperature dependency having an insignificant influence on components analysis.

$$D_{A-B} = 7.4 \times 10^{-8} \times \frac{(\Phi M_B)^{0.5} T}{\eta_B V_A^{\,0.6}} \qquad (3)$$

The symbols indicators A and B are solute and solvent, respectively. D_{A-B} is the liquid mutual diffusivity of the solvent (A) in pure water (nonsolvent) (B); Φ is a dimensionless association factor given as 2.26 for solvent-water and 1.1 for water–solvent association factor. η is the viscosity of the solvent (centipoise), with *M* the molecular weight of solvent (g/mol), T is the Temperature (kelvin) and V - the molar volume of the solute (cm^3 /mol). A proposed harmonic mean value between the (D_{A-B}) and (D_{B-A}), considered the optimum parameter for predicting the structure of a polymer membrane prepared from a given solvent, is expressed in equation (4). Results of calculated mutual diffusivity of the solvent in water (D_{A-B}), water in the solvent (D_{B-A}) at 25°C and the calculated precise harmonic mean value (D_m) are presented in table 5.5.

$$D_m = \frac{2D_{A-B} \times D_{B-A}}{D_{A-B} + D_{B-A}} \qquad (4)$$

Table 5-3: Diffusion coefficient values for different solvent/water systems at 25°C [18]

Solvent	$\boldsymbol{D_{A-B}}$ **(Solvent/water)** $(\boldsymbol{10^{-6}\ cm^2/sec})$	$\boldsymbol{D_{B-A}}$**(water/solvent)** $(\boldsymbol{10^{-6}\ cm^2/sec})$	$\boldsymbol{D_m}$ $(\boldsymbol{10^{-6}\ cm^2/sec})$
GVL	10.26	8.18	9.10
NMP	11.26	10.65	10.43

The obtained values of D_m shown in table 5.3 gives the average diffusion value, which is in the order of NMP>GVL, and explains the obtained morphology of the PVDF membrane in figure 5.2. The GVL/water system has a low harmonic mean value, indicating that a prolonged cast film/nonsolvent exchange process contributed to the delayed demixing phase separation during the membrane formation process of the PVDF membranes using GVL as solvent. In addition, the low mutual diffusivity of solvent in water (D_{A-B}) is assumed to result in the compositional concentration path entry in the ternary diagram during the membrane formation into a demixing region at a higher polymer concentration [16], resulting in a dense top layer.

5.3.2 Effect of polymer concentration on the PVDF membrane morphology

The effect of the polymer concentration with GVL was considered with cross section and top surface image results shown in figure 5.3. The different morphology structures observed for the prepared membranes favour a phase separation transition phenomenon of solid-liquid demixing over the liquid-liquid demixing process for increased polymer concentration. The mass transfer phenomena and precipitation composition path that occurs due to increased polymer concentration via the NIPS process have previously been investigated for other polymer/solvent systems [19]. In addition, increased polymer concentration is associated with a more concentrated solution's high viscoelasticity due to closely packed molecular polymer chains.

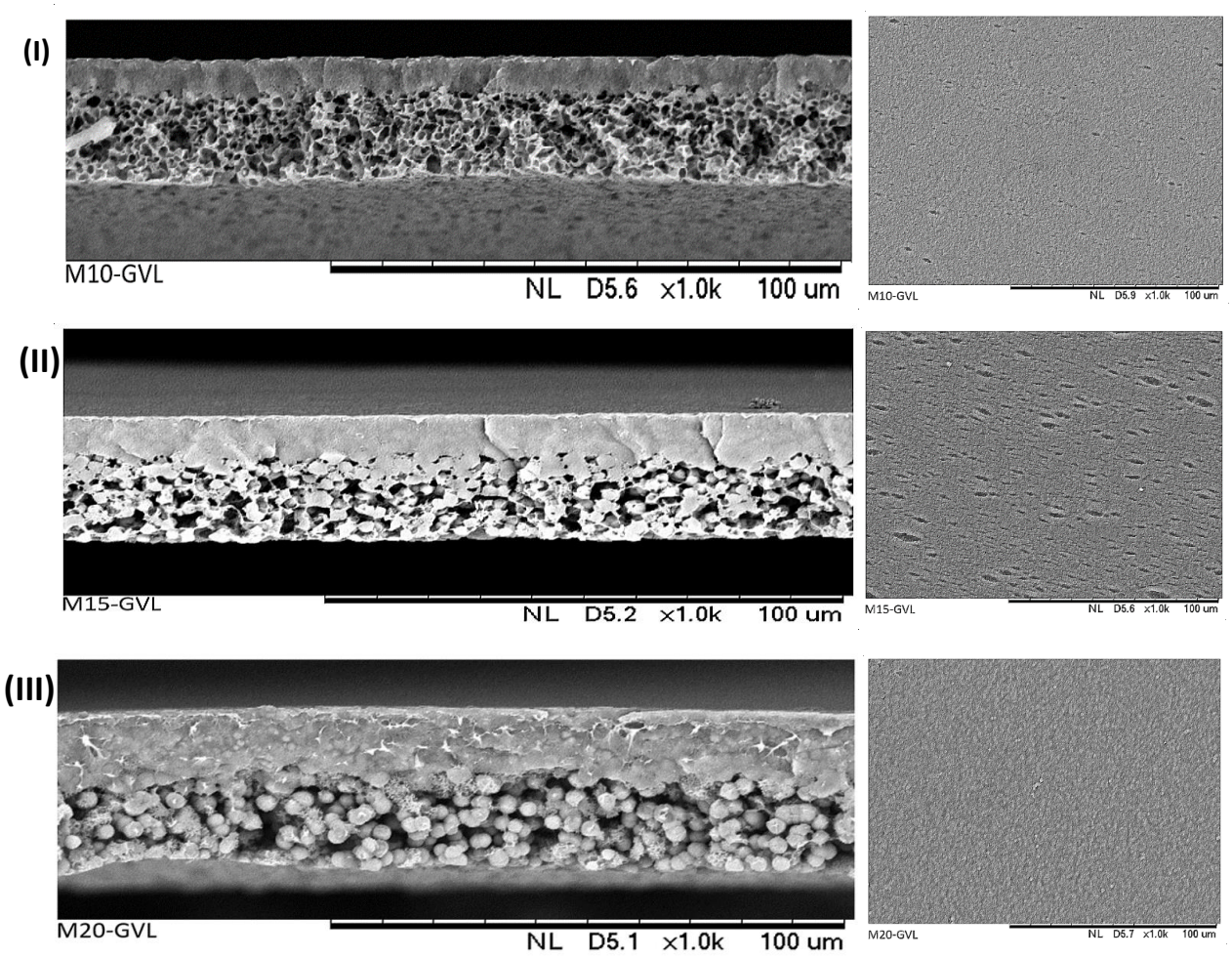

Figure 5.3 (a) and (b) are the cross section and top surface morphologies of the membrane prepared with GVL with different polymer concentrations: (I) 10wt%;(II) 15wt%; (III) 20wt%.

The polymer chain mobility and the mutual diffusion of the effective segments of polymer chain movements substantially influenced the mass transfer phenomena between components and the precipitation process for the PVDF/GVL system [20]. The increased polymer concentration decreases the polymer chain mobility of the cast film as the macromolecules huddle into a dense distribution due to less nonsolvent diffusing into the system.

The formation of the top active layer can be associated with the low mutual affinity determined by the significant difference in the Hildebrand solubility parameter between GVL (δ_t=21.74MPa$^{1/2}$) and water (δ_t=47.81MPa$^{1/2}$), as well as the cast solution and nonsolvent exchange. The phenomenon causes a high ratio of GVL outflow compared to the inflow of the nonsolvent at the cast film/nonsolvent interface, resulting in a high concentration of PVDF at the interface. The solidification of the polymer-rich phase domain enables the formation of a suppressive porous structure and directly affects the structure of the final membrane obtained, as shown in figure 5.4. Subsequently, the dense formation of the top layer results in a few pores forming at the top surface layer [21]. Results show that a spongy-like honeycombed interconnected pore for a low PVDF concentration (10wt.%) emerges in the cross-section membrane.

In contrast, a prepared membrane from 20wt% of PVDF exhibits a bilayer of globular/particulate and dense layer structure, which is formed by the nucleation growth mechanism of the polymer crystals from a solid-liquid phase separation [22]. The globule-like structure appears independently and forms an interconnected polymer-rich matrix. Several other studies have associated polymer crystallisation during the phase separation process as the driving force during fabrication [23,24,25].

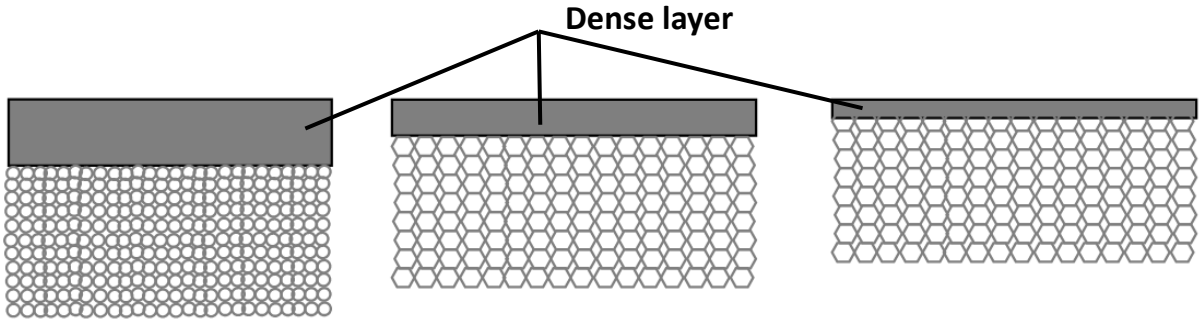

Figure 5.4: Schematic construction of asymmetric cross-section using PVDF/GVL membrane with grey area dense layer and porous sublayer underneath

Generally, polymer chains behave in their natural sequence by expanding and contracting when heated or cooled. However, at low polymer concentrations, the polymer

chain tends to be unaffected by intermolecular attraction and repulsion making polymer chains randomly coil when cooled. In contrast, higher concentration polymer solutions continue to be influenced by forces of attraction and repulsion, which tend to accelerate the coiling of the polymer chains during the demixing phase separation and enhance the formation of globules [26].

In summary, the different PVDF concentrations significantly impact the demixing process and demonstrate that intermolecular interaction differences occur between the cast film and nonsolvent during the membrane fabrication process via NIPS. Furthermore, the membrane morphology depicts a situation where the increased PVDF concentration impacted the top surface of the membrane. Finally, the ternary phase diagram of the PVDF/GVL/H20 system consisting of gelation boundaries provides information regarding the unexpected inhibition growth phenomenon of macrovoids.

5.3.3 Analysis of overall porosity and thickness properties of the PVDF membranes

The overall porosity and thickness of the prepared PVDF membranes were evaluated to examine the influence of different solvents and the effect of polymer concentration. The PVDF membranes prepared from GVL had a smaller film thickness than membranes fabricated using the NMP as the solvent, which showed a higher membrane thickness. The variation in membrane thickness, despite the solvent having similar properties, is associated with the solvent's strength in the PVDF system. Typically, polymer solvation in a “good” solvent maximises surface exposure and promotes expansion. However, solvency in a poor solvent minimises the surface exposure of the polymer solution and results in contraction and polymer coil formation. These phenomena can be correlated with the demixing process, the mutual affinity values, and the observed morphological PVDF membrane structure obtained from either GVL, macrovoid free or NMP, which showed finger-like and macrovoids structure.

Presented in figure 5.5 is the average overall thickness of the thin PVDF membrane obtained from SEM images for increasing polymer concentration of (10-20%wt PVDF) and membranes prepared from NMP at a fixed PVDF concentration of (15%wt). The average thickness of the dense membrane layer from the cross section of SEM images of the PVDF membranes prepared using GVL as solvent was approximately 8µm, 16 µm and 19 µm for the different PVDF concentrations of 10wt.%, 15wt.% and 20wt.% respectively.

The membrane porosity pertains to the membrane void volume fraction, defined as the number of pores divided by the total volume of the membrane [27]. However, not all voids are open at both ends, and the membrane's effective porosity is the ratio of the connected pore volume to the overall sample volume. The experimental porosity results demonstrate

that the overall porosity of produced membranes shown in figure 5.5 can correlate to the phase separation during the membrane formation process. The porosity varied between 54% and 72% for PVDF membranes prepared at a fixed PVDF concentration of 15wt% with GVL and NMP. The overall porosity of PVDF membranes produced by NMP typically ranges from 70% to 83% [28], primarily due to their finger-like macrovoid structure as opposed to the macrovoid-free membrane produced by using GVL. The various PVDF membranes' increased porosity properties correlate with the films' observed morphologies. Therefore, the increased porosity for the PVDF/NMP system can be explained by the observation of large macrovoids as opposed to PVDF/GVL films that feature a macroscopic dense structure layer with no large macrovoids. Invariably, as the PVDF concentration (10-20wt.%) increased for the PVDF/GVL system, the membrane porosity decreased, primarily due to the increased thickness of the dense top layer and substructure of the corresponding PVDF membranes. The relationship between these PVDF membranes' overall porosity and thickness properties as a function of polymer concentration is interesting. The results demonstrate that increasing the polymer concentration leads to decreased PVDF membrane porosity and increased thickness.

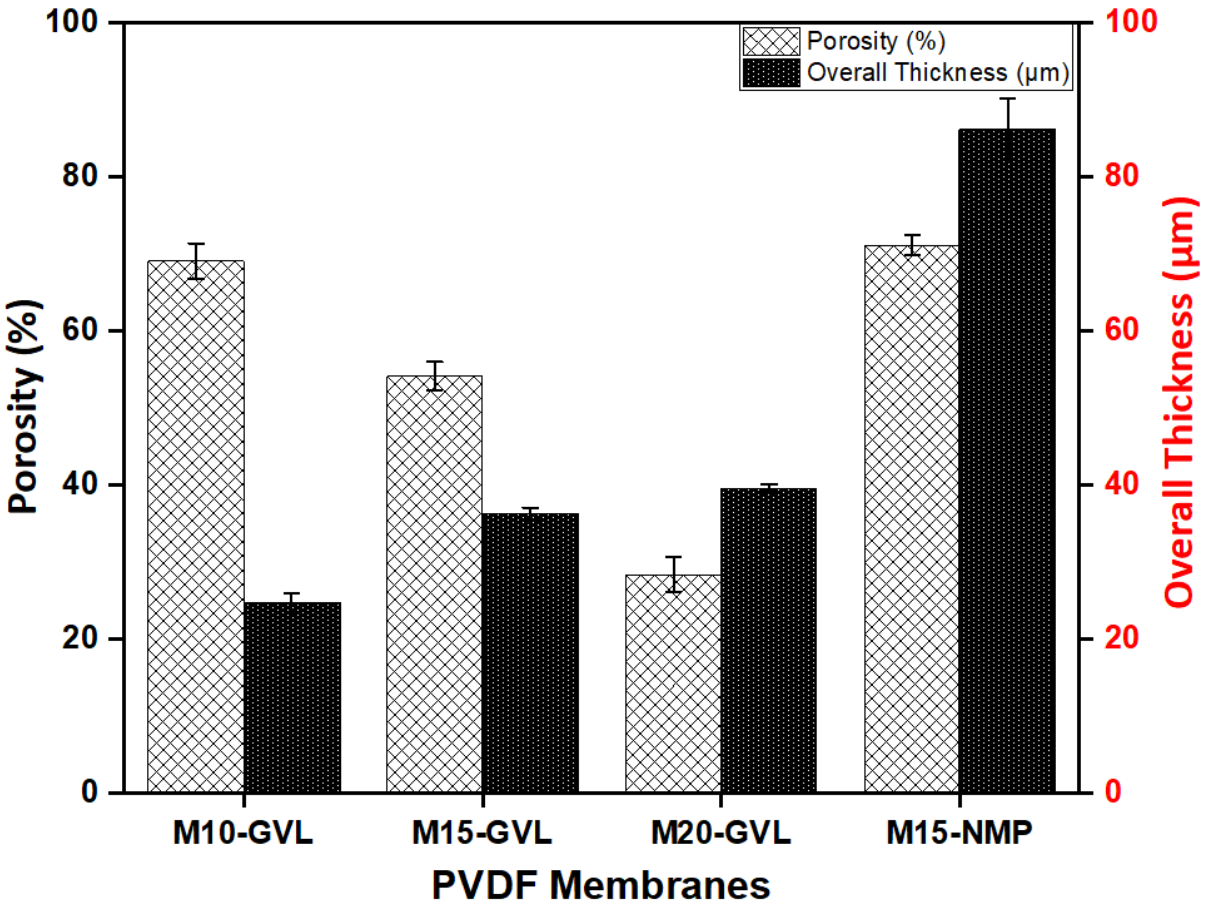

Figure 5.5: Overall Porosity and Thickness measurement of PVDF membranes using different solvent and polymer concentrations.

5.3.4 Contact angle and surface topology analysis

The fabricated PVDF membrane's wettability behaviour was examined using a sessile drop approach and a polar liquid (water) to determine the contact angle [29]. The water contact angle measurement showed different hydrophilicity values for membranes prepared with conventional solvent (NMP) or more variable polymer (PVDF) concentration. Results show that the PVDF membrane prepared using GVL as solvent had a higher water wetting angle that could indicate possible resistivity to water than membranes prepared using NMP. Furthermore, the increase of PVDF concentration to prepare membranes using GVL showed an increasing trend of water contact angle values, which can be related to several factors, such as the surface roughness or the porosity of the membrane [30]. Presented in figure 5.6 are the macroscopically measured water contact angles, root mean surface roughness of the fabricated membrane for different solvents considered, and the increasing PVDF concentration using GVL as solvent. The water contact angle measurements for each data point were carried out on five different regions on three different PVDF membrane samples and reported averaged values presented. Contact angle values were relatively similar to results obtained in the literature using other aprotic solvents and NMP to prepare PVDF membranes via the NIPS technique [31].

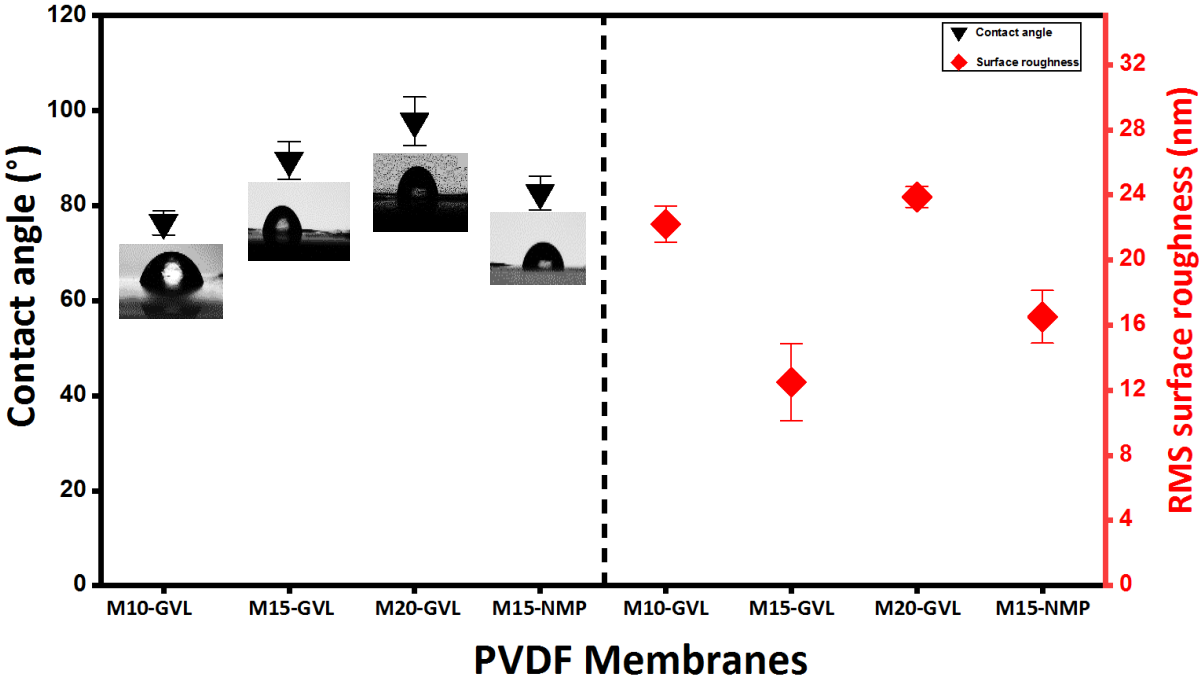

Figure 5.6: Water contact angle (black) and surface (root mean square) roughness (red) of PVDF membranes prepared at increasing PVDF concentration using GVL as a solvent and other solvents.

Regarding the effect of PVDF concentration, the inverse relation of porosity and water contact angles indicates that the decreasing porosity property of the PVDF membrane material would likely impact the wetting property and membrane performance. Therefore, the average surface roughness profile on the PVDF membrane was estimated over a 10 µm×10 µm sample area. Results are depicted in an x-y-z dimensional plane to show the captured surface topology image for both PVDF membranes prepared by NMP and the variation of the PVDF concentration and images presented in figures 5.7 and 5.8.

The three-dimensional (3D) AFM images revealed that the surfaces of polymeric PVDF membranes possess nodule-like and valley-like structures that allow estimation of the roughness of the top surface of the flat sheet membranes, which are explained in several studies [32,33]. The AFM results indicate that surface roughness plays a valuable role in the analysis of the surface hydrophobicity/hydrophilicity, such that an enhanced roughness of the membrane surface could promote hydrophobicity, which agrees with the cassie-Baxter's wetting model that anticipated that for a rough surface, a non-wetting liquid might not penetrate into the surface cavities [34]. The surface topography and wetting ability are related to nodule size and roughness of the membrane. Following the results presented, the only exception for PVDF/GVL system is the 15% wt. PVDF membrane, which shows a low RMS surface roughness value. However, the PVDF membrane surface contact angles do fall within reported values for PVDF membranes prepared with common molecular solvents [35]

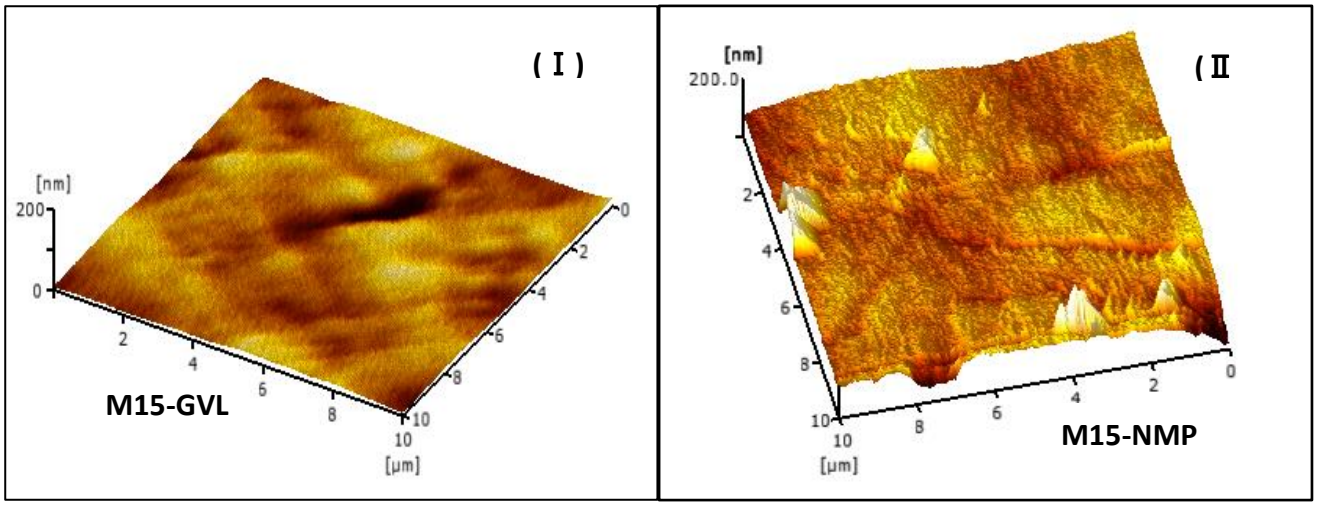

Figure 5.7: AFM images of PVDF flat sheet surface membranes of flat-sheet PVDF membranes as a function of different solvents (Ⅰ-Ⅱ) at 15wt.% PVDF

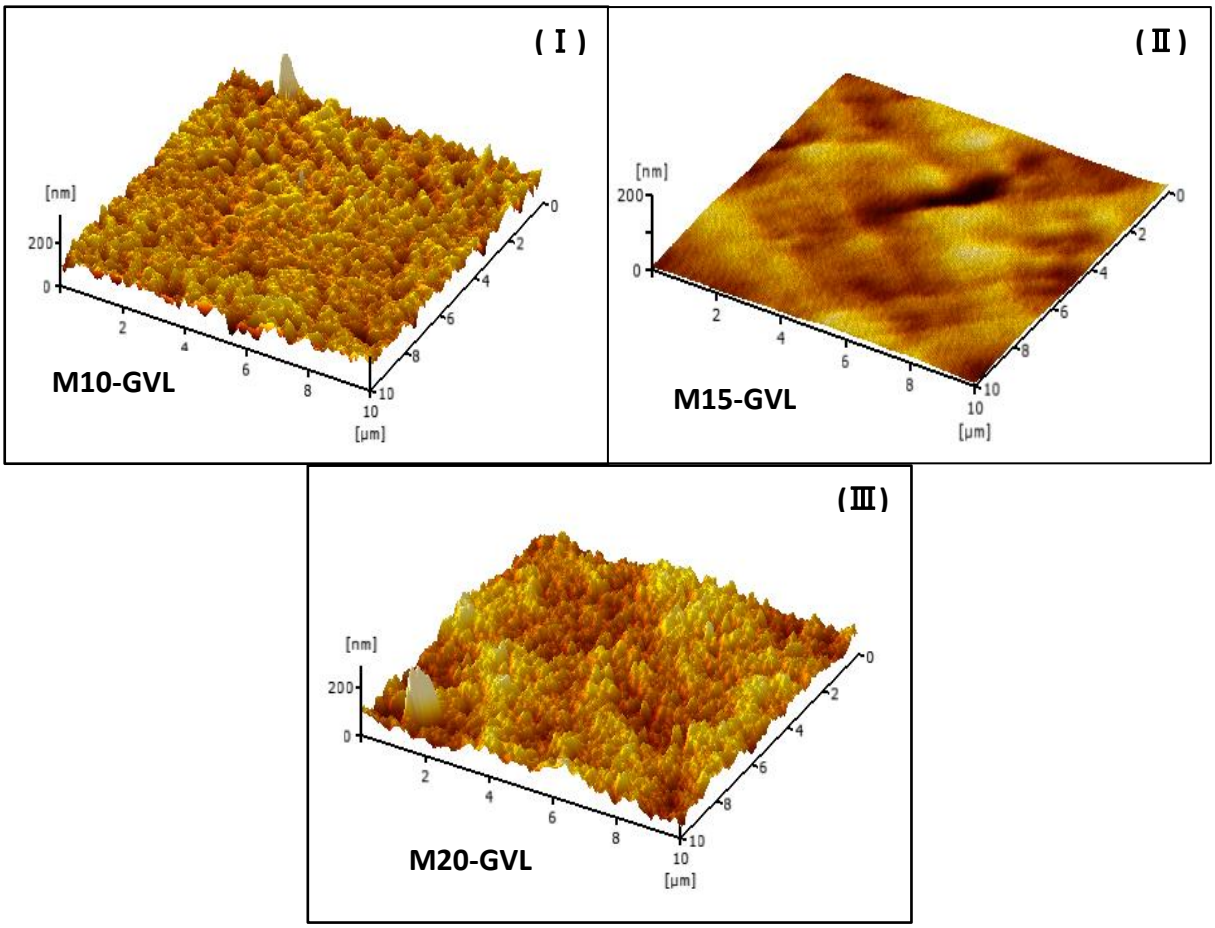

Figure 5.8: AFM images of PVDF flat sheet surface membranes prepared (Ⅰ-Ⅲ) from different polymer concentrations (10 -20) wt.% and GVL as a bio-based solvent.

5.3.5 Thermal behaviour of fabricated PVDF membranes

PVDF is a semi-crystalline polymer consisting of crystalline and amorphous regions. The polymer chains of PVDF can crystallise into five distinct polymorph phases that exhibit different crystallisation behaviour. These intrinsic features play a role in the synthesised PVDF membranes, especially in determining the mechanical strength properties, thermal durability and impact resistance of the membranes [36,37]. Therefore, understanding the effects of fabrication conditions on the PVDF crystalline phase is vital to properly controlling the fabricated membrane's properties. Typically, the crystalline domains have been reported to influence the performance of PVDF membranes since the crystalline domains should be impermeable to small molecules such as gases, regardless of the molecular organisation of the crystalline lattice [38].

Several methods have been proposed for measuring the degree of crystallinity to determine the fraction of crystallinity, which includes using X-ray diffraction (XRD) [39] and differential scanning calorimetry (DSC) [40,41]. The study presented in this thesis measured the

melting temperature and the total degree of crystallinity of the prepared PVDF membranes using the differential scanning calorimetry (DSC) technique. The melting upon heating of the fabricated PVDF membranes is represented by the DSC heating curves shown in Figure 5.9. The DSC curve exhibits only one melting peak between 167°C and 168°C, indicating a complete melting of the crystalline phase formed during the membrane formation process. The characteristic transition enthalpy was determined, and the melting endotherm area was used to evaluate the degree of crystallinity. The membranes' total crystallinity (X_{CT}) was determined by integrating the DSC melting curves and normalising the value to the 100% PVDF crystalline melting enthalpy of 104.7 J/g [42]. The melting endotherms and the calculated associated enthalpies help qualitatively evaluate the polymorphism variation of the prepared membranes. The heat of fusion(Δ_{H_f}) and the total crystallinity (X_{CT}) using the NIPS method to prepare the PVDF membrane is summarised in Table 5.4.

The DSC spectrums of solution-cast membranes prepared under different conditions show a shift in the melting endotherms. The spectrums also show an increase in the area of melting of the endotherms as the polymer concentration increases, which is mainly due to the slower solvent-nonsolvent exchange rate as polymer concentration increases, thus altering the degree of crystallinity of the coagulated membrane. Several variables, including the molecular weight of the polymer, the dissolving temperature, the thermal history and cooling rate of the dope solution, affect the PVDF membranes' crystallinity. Typically, when a semi-crystalline polymer is dissolved in a solvent below the polymer's melting temperature, it is assumed that some crystalline structures are formed in the solution due to the partial dissolution of the crystals or the refolding of the dissolved polymer chains during the fabrication process. Thus, the resulting polymer dope solutions used to prepare the membranes tends to retain their crystallographic arrangements of crystals.

The results presented in Figure 5.10 shows the changes in terms of the degree of crystallinity of PVDF membranes, with part (a) showing the effect of the solvent substitution and part (b) showing the influence of the PVDF concentration. Results demonstrate an upward trend of crystallinity from 39 to 50% as PVDF concentration increased from 10 to 20wt.% with error bars determined using the calculation presented on page 80-81. The assumption is that higher polymer concentrations lead to slower solvent/nonsolvent exchange rates during membrane formation. This, in turn, results in prolonged periods for polymer chain reorganisation and, thus, membranes with higher degrees of crystallinity.

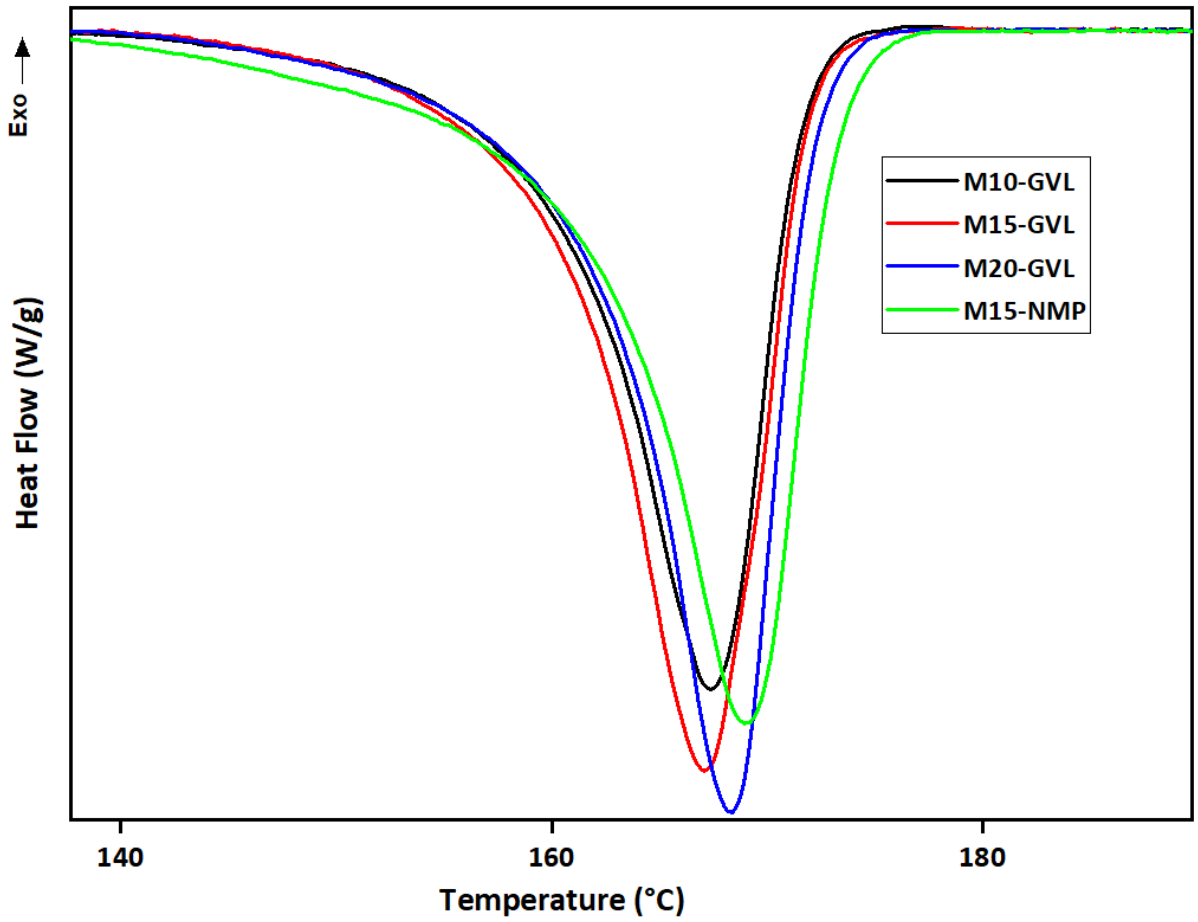

Figure 5.9: Differential scanning calorimeter curves of PVDF membranes prepared from different solvents and polymer concentrations.

Table 5-4: DSC Characterisation of fabricated PVDF membranes

Membrane	Peak Temperature (°C)	Enthalpy (J/g)	Degree of crystallinity (%)
M10-GVL	167 (±1)	41 (±1)	39 (±2)
M15-GVL	167 (±1)	48 (±1)	46 (±1)
M20-GVL	168 (±1)	51 (±1)	48 (±1)
M15-NMP	169 (±1)	43 (±1)	41 (±3)

Membranes produced with different solvents showed different DSC curves, melting temperatures and similar degrees of crystallinity values. The reported data in Figure 5.10 were the average values of triplicates samples for each PVDF membrane. In addition, the degree of crystallinity of the PVDF pellet and prepared membranes obtained using substitute solvent was presented, with results ranging from 41%-46%. Reported degrees of crystallinity

have been found to occur between 35% to 65% for PVDF membranes using NMP as solvents [43,44]. Furthermore, evaluation of the observed PVDF morphology in Figure 5.4 and porosity of PVDF membranes also provides insight into the increased degree of crystallinity for the membranes prepared with higher polymer concentrations associated to the increased membrane dense top layer assumed to have more straight packed chains.

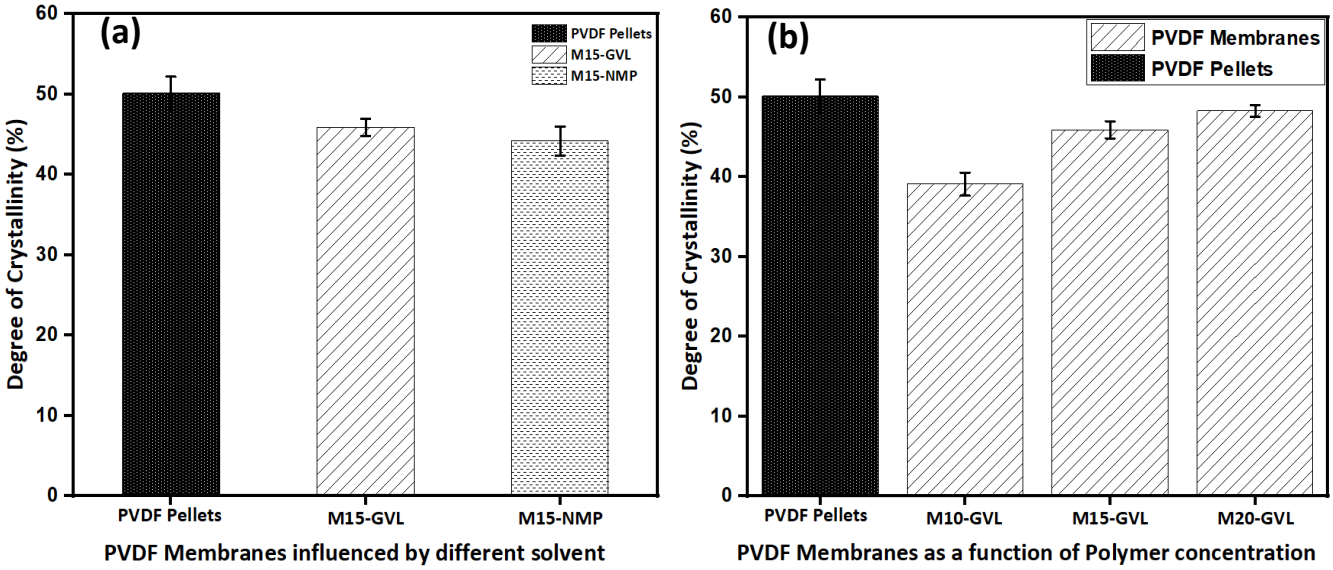

Figure 5.10: Degree of crystallinity as a function of (a) different solvents and (b) polymer concentrations of fabricated PVDF membrane samples and PVDF pellets are presented.

5.3.6 Fourier transform infrared and attenuated total reflectance spectrometry analysis (FTIR-ATR)

The polymorphism of the crystalline phase of the PVDF membrane samples was characterised by FTIR-ATR spectroscopy. The FTIR-ATR is recognised as a powerful technique for detecting information on PVDF crystals based on the different polymorphs the membrane samples crystallise onto, which are identifiable by the different conformations of the polymeric chains phase structure [45]. The transmittance wavenumber peaks at 409, 532, 613, 764, 795 and 972 cm^{-1} indicate that the α-phase and β-phase peaks are 445, 470, 511, respectively 600, and 840 cm^{-1} [46]. The FTIR spectra of the PVDF membrane prepared from GVL and NMP are shown in figure 5.11, focusing on the fingerprint region of the cast film's top surface area. Results show that the PVDF membrane samples possess a mixture of standard vibration bands of the orthorhombic β-phase at 840cm^{-1} and the α-phase at 762cm^{-1} [47] with varying intensity peaks for both α- and β-phases. The intensity of the β-phase at 840cm^{-1} and the absence of exclusive bands of γ phase at 776, 812 in the FTIR spectra due to increased PVDF concentration indicate that the PVDF/GVL membranes are predominantly

related to the β-crystalline phase. The considerable similarity and locations of intensity peaks would suggest that the solvent effect is assumed to be integrated inside the material during the formation process and eliminated during the washing out stage.

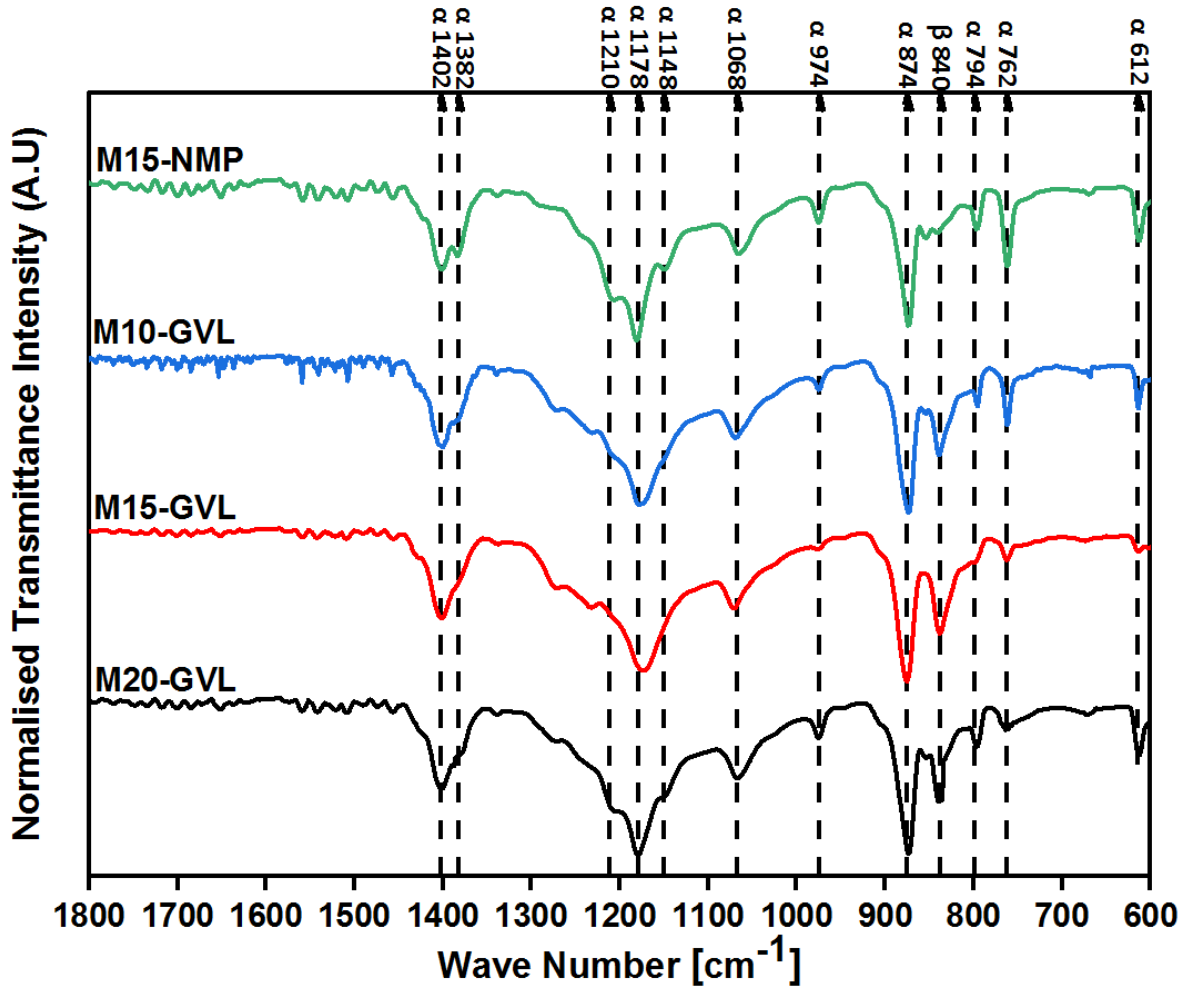

Figure 5.11: The FTIR spectra of the PVDF membrane samples fabricated from different solvents and polymer concentrations.

The relative β phase fraction F(β) of each sample was estimated using a procedure that assumes the IR absorption follows the lambert Beer law and the baseline of corrected absorbance of α- and β-phase at 762cm^{-1} and 840 cm^{-1}. Figure 5.12 shows an increasing F(β) value for increasing PVDF concentration. The PVDF membranes prepared using NMP gives a low value of F(β). The high ratio of β/α (F(β) in the surface layer of the PVDF membrane samples made with GVL could be explained by the high degree of entanglement and low mobility of the PVDF chains during the fabrication process, hindering the stable α-phase in the PVDF membrane.

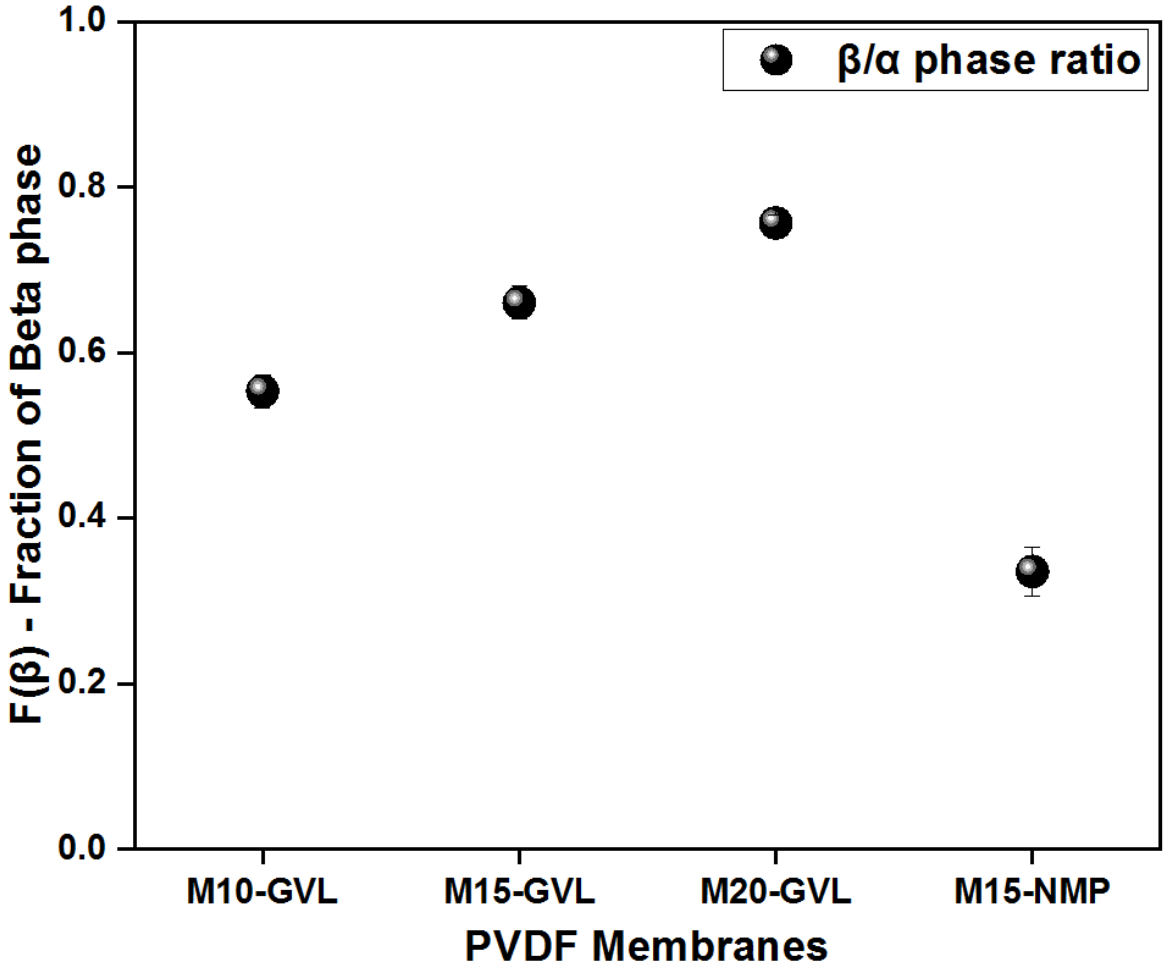

Figure 5.12: The β/α phase ratio (F(β)) in the surface layer of the PVDF membrane samples determined from the FTIR-ATR spectra

5.3.7 Permeation experiments analysis

Results presented in section 5.3.1 and 5.3.2 demonstrates that the solvent and the polymer concentration conditions visibly influence the membrane structure. Furthermore, since the membrane structure and performance are closely related, analysis of the membrane performance was also affected by the change in fabrication conditions.

The liquid entry pressure (LEP) water points and the fluxes of the PVDF membranes were determined using a dead end flow cell module using pure water as feed and applying a stepwise pressure increase of 0.2 bar necessary to drive water through the pores of the tested PVDF membrane sample. The slightest pressure required to force water through the membrane's pores is recorded as the liquid entry pressure of water (LEPw). The analysis allows for the evaluation of the wettability of the membrane sample to be determined at specific pressure [48,49]. In addition, the appearance of water droplets was checked by

monitoring the water flow at constant pressure for 30 mins. Results show PVDF membranes prepared from NMP had a LEPw of 1.2 bar, compared to the reported value of 1.0 bar [50], while membranes prepared using GVL had LEPw values >10 bar.

The corresponding gas and water flux measurements of PVDF membranes obtained using different solvents and polymer concentrations are presented in Figures 5.13 and 5.14. The gas and water fluxes are based on the effect of other solvents, NMP and GVL, with PVDF. The performance of the finger-like membrane obtained using PVDF/NMP and dense morphology obtained from PVDF/GVL is linked to the precipitation phase in the coagulation bath, which has been `discussed in chapter 4. Similar morphological observations for PVDF membranes using other solvents have also been previously reported [51,52].

Comparison of PVDF/GVL membranes and PVDF/NMP membranes demonstrated in 5.13 (a) and 5.13 (b) shows the gas and water flux performance differed considerably with the PVDF/GVL membrane underperforming. The measured gas flux was the steady state fluxes obtained after the compaction of each evaluated PVDF membrane sample. Two different membrane samples were tested with analysis conducted in triplicate and averaged values reported. Further experimental investigation of the gas flux test showed no hysteresis-like phenomenon was observed for increasing and decreasing pressure of the gas flow test.

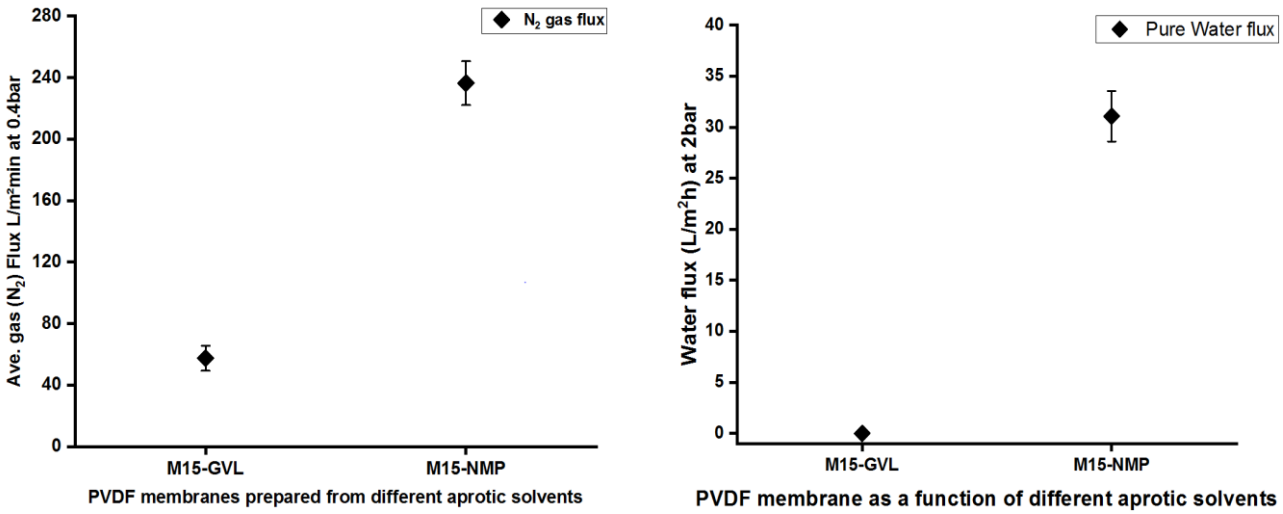

Figure 5.13: (a) N2 gas Flux (at 0.4 bar) and 5.13(b) pure water flux (at 2 bar) for PVDF membrane fabricated using different solvents.

Typically, PVDF/NMP membranes have been reported to exhibit high values of pure water flux owing to their finger-like membrane structure [24]. However, it was difficult to

compare directly due to the varying polymer concentration in reported studies for PVDF membranes prepared using NMP.

The water flux test for PVDF membranes prepared using different solvents (GVL or NMP) was measured using pure deionised water, as shown in figure 5.11(b). The PVDF membranes prepared using GVL and NMP display a water and gas permeation difference that could be associated with the membrane's pore geometry and morphology. The flux results reveal that the mass transfer resistance through the liquid-filled pores is much higher than through the gas-filled pores because the liquid phase diffusivity is lower than the gas phase diffusivity. The flux performance due to the effect of the polymer concentration was carried out for both gas and water test. The gas (nitrogen) flux of the fabricated PVDF/GVL membranes as a function of PVDF polymer concentration is presented in figure 5.14. The increased polymer concentration resulted in the gas flux significantly decreasing from 112 ± 6.7 to 2.1±4.2 ($L.m^{-2}.min^{-1}$), indicating a reduction of over 50 fold.

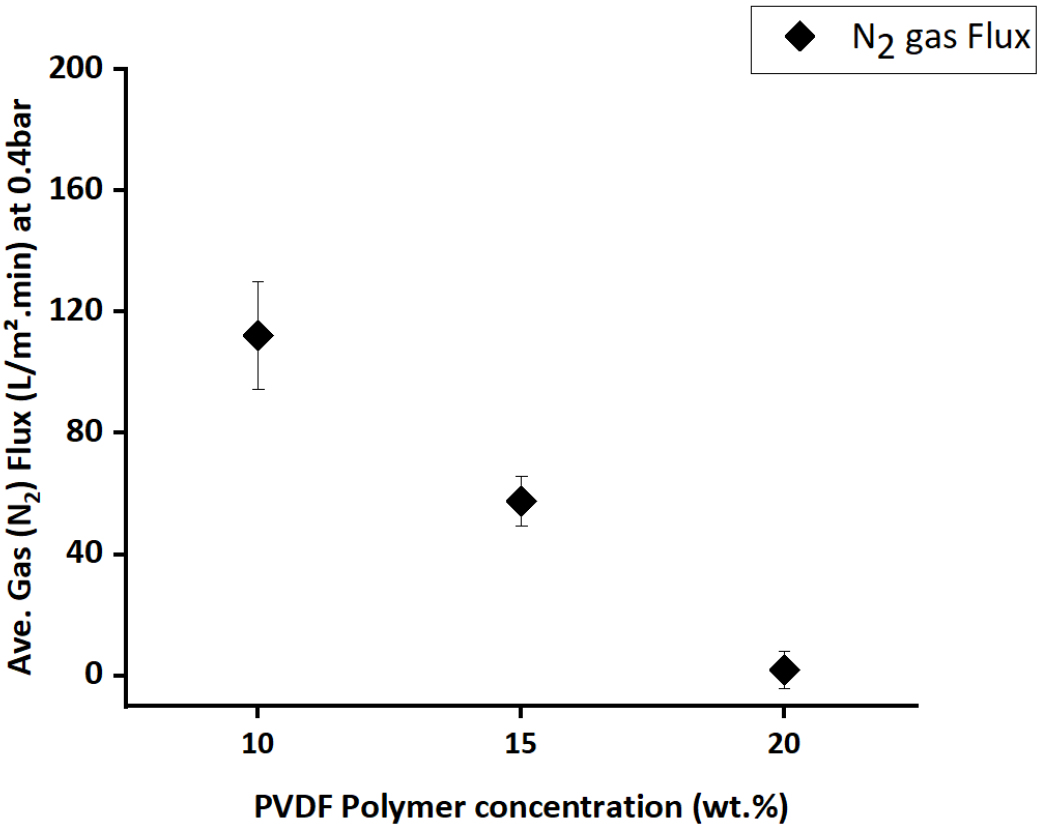

Figure 5.14: Nitrogen gas flux of PVDF membranes fabricated as a function of polymer concentrations at 0.4 bar and temperature of 25°C.

The PVDF membranes prepared using GVL showed no water permeability at pressures between 0 and 10 bar due to the formation of a dense top layer. The high LEPw observed suggests PVDF membranes may be advantageous in membrane processes like membrane distillation or membrane contacts, where the pressure applied to the feed liquid should be below the membrane's LEP_w to prevent liquid from permeating through the membrane [53,54]. The PVDF membranes also have potential uses as gas-liquid contactor membranes for separation processes due to their higher wetting resistance at low applied pressure [55].

The experimental flux results were consistent with observed macrovoid free membrane morphology and associated with the dense active layer, measured membrane overall porosity, and surface roughness [56]. Membranes with a dense active layer are mainly used for reverse osmosis, pervaporation and gas separation because the transport mechanism is primarily via diffusion gradient. Hence, further characterisation and tests should be conducted to define other membrane processes' suitability and industrial application.

5.4 Summary

GVL, a green bio-based, non-toxic and biodegradable solvent, has been used as a suitable and practical alternative to banned and commonly used dipolar solvents such as NMP to prepare PVDF membranes via NIPS. Polymer (dope) solutions were prepared at 90°C, membranes were cast, and studies were devoted to investigating the properties and characterisation of the prepared membranes. The result demonstrates that a green solvent can be used efficiently via the traditional fabrication method to synthesise polymeric membranes. In addition, the wettability behaviour, overall porosity, crystallinity, and morphology of the membranes studied were compared to membranes obtained from conventional toxic solvents. However, despite the similarities in solvent properties between GVL and NMP, the observed cross section and top surface morphology of the membranes formed differed considerably.

Furthermore, the characterisation of the PVDF membrane's overall porosity, crystallinity, and wettability properties prepared with GVL showed substantial differences compared to reported results using NMP in the study presented. The difference in membrane morphology obtained can be related to the binary diffusivity of solvent and nonsolvent and the solubility parameter between the polymer and solvent. Furthermore, the driving force for the phase separation during membrane preparation via NIPS is primarily the kinetics (exchange of solvent and nonsolvent in the coagulation bath) and thermodynamic aspects,

which leads to a phase transition of the homogenous cast film and formation of membrane structure.

The PVDF/NMP had finger-like top layer structures with macro voids sublayer, whereas PVDF/GVL consisted of a dense top layer and a spongy-like honeycomb sublayer structure. Typically, membranes with finger-like and macrovoid structures tend to have higher fluxes than a dense and spongy membrane structure. Irrespective of the initial polymer concentration using GVL, a dense top layer and an interconnected spongy, globule-like substructure was observed with a progressive increase in polymer concentration. The morphology of the membrane using PVDF/GVL shows that the increase in PVDF concentration affects the mass transfer diffusion resulting in a less porous PVDF membrane and low flux performance. Therefore, such parameters can be used to fabricate tailored PVDF membranes for specific industrial applications.

In summary, GVL shows promising alternative solvent prospects that can replace common toxic polar solvents for membrane production to reduce the environmental and health impact of the fabrication process. In addition, the characteristics assessment of the PVDF membrane obtained with traditional solvents published in the literature were generally comparable. However, further investigation is needed to improve the membrane performance to meet those obtained using conventional solvents, especially for micro- and ultra-filtration processes. Therefore, examining other independent controlling parameters, such as the coagulation bath and dissolved polymer temperature, can be implemented to improve the PVDF performance and achieve an enhanced performance of the PVDF membrane made using GVL.

5.5 References

[1] Bottino, A., Capannelli, G., Munari, S., & Turturro, A. (1988). Solubility parameters of poly (vinylidene fluoride). *Journal of Polymer Science Part B: Polymer Physics*, *26*(4), 785-794

[2] Wang, Q., Wang, Z., & Wu, Z. (2012). Effects of solvent compositions on physicochemical properties and anti-fouling ability of PVDF microfiltration membranes for wastewater treatment. *Desalination*, *297*, 79-86.

[3] Liu, F., Hashim, N. A., Liu, Y., Abed, M. M., & Li, K. (2011). Progress in the production and modification of PVDF membranes. *Journal of membrane science*, *375*(1-2), 1-27.

[4] Thuyavan, Y. L., Anantharaman, N., Arthanareeswaran, G., & Ismail, A. F. (2016). Impact of solvents and process conditions on the formation of polyethersulfone membranes and its fouling behavior in lake water filtration. *Journal of Chemical Technology & Biotechnology*, *91*(10), 2568-2581..

[5] Pezeshk, N., Rana, D., Narbaitz, R. M., & Matsuura, T. (2012). Novel modified PVDF ultrafiltration flat-sheet membranes. *Journal of Membrane Science*, *389*, 280-286.

[6] Guillen, G. R., Pan, Y., Li, M., & Hoek, E. M. (2011). Preparation and characterization of membranes formed by nonsolvent induced phase separation: a review. *Industrial & Engineering Chemistry Research*, *50*(7), 3798-3817.

[7] Aparicio, S., & Alcalde, R. (2009). Characterization of two lactones in liquid phase: an experimental and computational approach. *Physical Chemistry Chemical Physics*, *11*(30), 6455-6467

[8] Sigma-Aldrich, 2018. [Online] Available at: http://www.sigmaaldrich.com/united-kingdom.html [Accessed 25 August 2018].

[9] Strathmann, H., Kock, K., Amar, P., & Baker, R. W. (1975). The formation mechanism of asymmetric membranes. *Desalination*, *16*(2), 179-203.

[10] Smolders, C. A., Reuvers, A. J., Boom, R. M., & Wienk, I. M. (1992). Microstructures in phase-inversion membranes. Part 1. Formation of macrovoids. *Journal of Membrane Science*, *73*(2-3), 259-275.

[11] Chang, J., Zuo, J., Zhang, L., O'Brien, G. S., & Chung, T. S. (2017). Using green solvent, triethyl phosphate (TEP), to fabricate highly porous PVDF hollow fiber membranes for membrane distillation. *Journal of Membrane Science*, *539*, 295-304.

[12] Ray, R. J., Krantz, W. B., & Sani, R. L. (1985). Linear stability theory model for finger formation in asymmetric membranes. *Journal of membrane science*, *23*(2), 155-182.

[13] Gameiro, M., Mischaikow, K., & Wanner, T. (2005). Evolution of pattern complexity in the Cahn–Hilliard theory of phase separation. *Acta Materialia*, *53*(3), 693-704.

[14] Kesting, R. E. (1985). Phase inversion membranes.

[15] McKelvey, S. A., & Koros, W. J. (1996). Phase separation, vitrification, and the manifestation of macrovoids in polymeric asymmetric membranes. *Journal of Membrane Science*, *112*(1), 29-39.

[16] Bottino, A., Camera-Roda, G., Capannelli, G., & Munari, S. (1991). The formation of microporous polyvinylidene difluoride membranes by phase separation. *Journal of membrane science*, *57*(1), 1-20.

[17] Wilke, C. R., & Chang, P. (1955). Correlation of diffusion coefficients in dilute solutions. *AIChE journal*, *1*(2), 264-270.

[18]https://www.chemicalbook.com/ChemicalProductProperty_EN_CB4285373.htm (accessed March 2019).

[19] Radovanovic, P., Thiel, S. W., & Hwang, S. T. (1992). Formation of asymmetric polysulfone membranes by immersion precipitation. Part I. Modelling mass transport during gelation. *Journal of membrane science*, *65*(3), 213-229.

[20] Van den Berg, G. B., & Smolders, C. A. (1992). Diffusional phenomena in membrane separation processes. *Journal of membrane science*, *73*(2-3), 103-118.

[21] Abed, M. M., Kumbharkar, S. C., Groth, A. M., & Li, K. (2012). Ultrafiltration PVDF hollow fibre membranes with interconnected bicontinuous structures produced via a single-step phase inversion technique. *Journal of membrane science*, *407*, 145-154.

[22] Ma, W., Zhang, J., Bruggen, B. V. D., & Wang, X. (2013). Formation of an interconnected lamellar structure in PVDF membranes with nanoparticles addition via solid-liquid thermally induced phase separation. *Journal of applied polymer science*, *127*(4), 2715-2723.

[23] Jung, J. T., Kim, J. F., Wang, H. H., Di Nicolo, E., Drioli, E., & Lee, Y. M. (2016). Understanding the non-solvent induced phase separation (NIPS) effect during the fabrication of microporous PVDF membranes via thermally induced phase separation (TIPS). *Journal of Membrane Science*, *514*, 250-263.

[24] Hołda, A. K., & Vankelecom, I. F. (2015). Understanding and guiding the phase inversion process for synthesis of solvent resistant nanofiltration membranes. *Journal of Applied Polymer Science*, *132*(27).

[25] Lin, D. J., Chang, C. L., Chen, T. C., & Cheng, L. P. (2002). On the structure of porous poly (vinylidene fluoride) membrane prepared by phase inversion from water-NMP-PVDF system. *Journal of applied science and Engineering*, *5*(2), 95-98.

[26] Van de Witte, P., Dijkstra, P. J., Van den Berg, J. W. A., & Feijen, J. (1996). Phase separation processes in polymer solutions in relation to membrane formation. *Journal of membrane science*, *117*(1-2), 1-31..

[27] Li, Q., Xu, Z. L., & Liu, M. (2011). Preparation and characterization of PVDF microporous membrane with highly hydrophobic surface. *Polymers for Advanced Technologies*, *22*(5), 520-531..

[28] Ike, I. A., Zhang, J., Groth, A., Orbell, J. D., & Duke, M. (2017). Effects of dissolution conditions on the properties of PVDF ultrafiltration membranes. *Ultrasonics sonochemistry*, *39*, 716-726.

[29] Kubiak, K. J., Wilson, M. C. T., Mathia, T. G., & Carval, P. (2011). Wettability versus roughness of engineering surfaces. *Wear*, *271*(3-4), 523-528.

[30] Chau, T. T., Bruckard, W. J., Koh, P. T. L., & Nguyen, A. V. (2009). A review of factors that affect contact angle and implications for flotation practice. *Advances in colloid and interface science*, *150*(2), 106-115.

[31] Mittal, K. L. (Ed.). (2003). *Contact Angle, Wettability and Adhesion, Volume 3* (Vol. 3). CRC Press.

[32] Khayet, M., Cojocaru, C., & García-Payo, M. D. C. (2010). Experimental design and optimization of asymmetric flat-sheet membranes prepared for direct contact membrane distillation. *Journal of membrane science*, *351*(1-2), 234-245.

[33] Khayet, M., Feng, C. Y., Khulbe, K. C., & Matsuura, T. (2002). Preparation and characterization of polyvinylidene fluoride hollow fiber membranes for ultrafiltration. *polymer*, *43*(14), 3879-3890.

[34] Cassie, A. B. D., & Baxter, S. (1944). Wettability of porous surfaces. *Transactions of the Faraday society*, *40*, 546-551.

[35] Mansourizadeh, A., Ismail, A. F., Abdullah, M. S., & Ng, B. C. (2010). Preparation of polyvinylidene fluoride hollow fiber membranes for CO2 absorption using phase-inversion promoter additives. *Journal of Membrane Science*, *355*(1-2), 200-207.

[36] Ando, S., Sato, S., & Nagai, K. (2020). Gas Permeation and Barrier Properties of Liquid Crystalline Polymers. *Liquid Crystalline Polymers*, 523-547.

[37] Liu, J., Lu, X., & Wu, C. (2013). Effect of preparation methods on crystallization behavior and tensile strength of poly (vinylidene fluoride) membranes. *Membranes*, *3*(4), 389-405.

[38] Wu, P., Jiang, L. Y., & Hu, B. (2018). Fabrication of novel PVDF/P (VDF-co-HFP) blend hollow fiber membranes for DCMD. *Journal of Membrane Science*, *566*, 442-454.

[39] Tiwari, V., & Srivastava, G. (2014). Effect of thermal processing conditions on the structure and dielectric properties of PVDF films. *Journal of Polymer Research*, *21*, 1-8.

[40] Gregorio, Jr, R., & Cestari, M. (1994). Effect of crystallization temperature on the crystalline phase content and morphology of poly (vinylidene fluoride). *Journal of Polymer Science Part B: Polymer Physics*, *32*(5), 859-870.

[41] Wunderlich, B. (2012). *Thermal analysis*. Elsevier.

[42] Rosenberg, Y., Siegmann, A., Narkis, M., & Shkolnik, S. (1991). The sol/gel contribution to the behavior of γ-irradiated poly (vinylidene fluoride). *Journal of applied polymer science*, *43*(3), 535-541.*polymer science*, *43*(3), 535-541.

[43] Yao, M., Ren, J., Akther, N., Woo, Y. C., Tijing, L. D., Kim, S. H., & Shon, H. K. (2019). Improving membrane distillation performance: Morphology optimization of hollow fiber membranes with selected non-solvent in dope solution. *Chemosphere*, *230*, 117-126.

[44] Ahmad, A. L., Ideris, N., Ooi, B. S., Low, S. C., & Ismail, A. (2011). Morphology and polymorph study of a polyvinylidene fluoride (PVDF) membrane for protein binding: Effect of the dissolving temperature. *Desalination*, *278*(1-3), 318-324.

[45] Essalhi, M., Ismail, N., Tesfalidet, S., Pan, J., Wang, Q., Cui, Z., ... & Tavajohi, N. (2022). Polyvinylidene fluoride membrane formation using carbon dioxide as a non-solvent additive for nuclear wastewater decontamination. *Chemical Engineering Journal*, 137300.

[46] Zhang, M., Zhang, A. Q., Zhu, B. K., Du, C. H., & Xu, Y. Y. (2008). Polymorphism in porous poly (vinylidene fluoride) membranes formed via immersion precipitation process. *Journal of Membrane Science*, *319*(1-2), 169-175.

[47] Benz, M., & Euler, W. B. (2003). Determination of the crystalline phases of poly (vinylidene fluoride) under different preparation conditions using differential scanning calorimetry and infrared spectroscopy. *Journal of applied polymer science*, *89*(4), 1093-1100.

[48] E. Guillen-Burrieza, A. Servi, B. S. Lalia, and H. A. Arafat, "Membrane structure and surface morphology impact on the wetting of md membranes," Journal of Membrane Science, vol. 483, pp. 94–103, 2015.

[49] M. d. C. Garcá-Payo, M. A. Izquierdo-Gil, and C. Fernández-Pineda, "Wetting study of hydrophobic membranes via liquid entry pressure measurements with aqueous alcohol solutions," Journal of colloid and interface science, vol. 230, no. 2, pp. 420– 431, 2000.

[50] Abdulla AlMarzooqi, F., Roil Bilad, M., & Ali Arafat, H. (2017). Improving liquid entry pressure of polyvinylidene fluoride (PVDF) membranes by exploiting the role of fabrication parameters in vapor-induced phase separation VIPS and non-solvent-induced phase separation (NIPS) processes. *Applied Sciences*, *7*(2), 181.

[51] Yeow, M. L., Liu, Y. T., & Li, K. (2004). Morphological study of poly (vinylidene fluoride) asymmetric membranes: effects of the solvent, additive, and dope temperature. *Journal of Applied Polymer Science*, *92*(3), 1782-1789.

[52] Penha, F. M., Rezzadori, K., Proner, M. C., Zanatta, V., Zin, G., Tondo, D. W., ... & Di Luccio, M. (2015). Influence of different solvent and time of pre-treatment on commercial polymeric ultrafiltration membranes applied to non-aqueous solvent permeation. *European Polymer Journal*, *66*, 492-501.

[53] Rácz, G., Kerker, S., Kovács, Z., Vatai, G., Ebrahimi, M., & Czermak, P. (2014). Theoretical and experimental approaches of liquid entry pressure determination in membrane distillation processes. *Periodica Polytechnica Chemical Engineering*, *58*(2), 81-91.

[54] Curcio, E., & Drioli, E. (2005). Membrane distillation and related operations—a review. *Separation and Purification Reviews*, *34*(1), 35-86.

[55] Mosadegh-Sedghi, S., Rodrigue, D., Brisson, J., & Iliuta, M. C. (2014). Wetting phenomenon in membrane contactors–causes and prevention. *Journal of Membrane Science*, *452*, 332-353.

[56] Woo, S. H., Park, J., & Min, B. R. (2015). Relationship between permeate flux and surface roughness of membranes with similar water contact angle values. *Separation and purification technology*, *146*, 187-191.

Chapter 6

Effect of the polymer dissolution temperature and casting temperature on the properties of PVDF membranes

6.1 Introduction

Several studies have proposed different parameters to synthesise PVDF membranes via the non-induced phase separation (NIPS) method [1,2] with notable parameters such as coagulation bath or casting temperature, the preparative dope solution, and other fabrication conditions [3,4]. Generally, temperature plays a significant role across the various steps of the NIPS process in membrane fabrication, especially during the interplay between polymer dope solutions and nonsolvent coagulation baths, thus influencing the membrane fabricating process and final membrane structure. Studies [5,6,7,8] have highlighted membrane preparation at room temperature (between 20 to 30°C), primarily to design high performance membranes and minimise operating costs. However, issues on temperature dependency and control of preparation conditions are often obscure, resulting in a temperature gradient between dissolved polymer and casting/coagulation bath. Additionally, it has been noted that the casting/coagulation or dissolving temperature impacts the solution viscosity, which changes the exchange rate during the phase inversion step and affects the membrane surface and interior morphology [9,10,11]. Hence, it is important to focus attention on temperature variations during membrane preparation from the temperature of the dissolved polymer to the casting/coagulation bath to achieve minimal hindrances for the PVDF/GVL system. Based on a limited understanding of the role of temperature during membrane preparation via the non-induced phase separation (NIPS) method for PVDF membranes, the study presented in this chapter examines the influence of temperature on the membrane fabrication process for the PVDF/GVL system.

The study focuses on the dissolved polymer's effect at various temperatures (Tdissol) and at different casting temperatures (Tcast). The temperature ranges for the Tdissol (70-180°C) and Tcast (30-45°C) were selected based on reported studies [12], studies presented in chapter 4 on polymer dissolution. Typically, the NIPS process is driven by the solvent/nonsolvent exchange. Thus, varying the casting/coagulation nonsolvent bath temperature was considered an approach to control the membrane fabrication process. Several temperatures were evaluated in an attempt to increase or slow the solvent/nonsolvent exchange process during the fabrication process. In addition, a controlled casting and nonsolvent coagulation bath temperature were maintained to minimise the effect of any thermal induced gradient that could occur during the membrane fabrication process.

The morphology, porosity, wettability behaviour, surface roughness, crystallinity, and performance of the synthesised PVDF membranes are all evaluated. The results obtained from this study are anticipated to contribute further and provide a better understanding of the membrane formation mechanisms for the polymer system using the non-induced phase separation (NIPS) method.

6.2 Experimental conditions for membrane fabrication

The experimental methodology to synthesise the PVDF membranes via NIPS was carried out under identical conditions presented in chapter three, except for the variations of polymer dissolution or the casting temperature. Thus, the preparative conditions considered using the NIPS method are shown in Table 6-1. The polymer dissolution temperature (Tdissol) was varied between (70-180) °C and maintained for 24h to eliminate variations and ensure a complete homogeneous polymer solution was always obtained. Finally, the homogeneous polymer solutions were rapidly cooled (quenched) using an ice bath and PVDF membranes cast at 30°C. Furthermore, four different PVDF membranes were fabricated by maintaining the temperature of a dissolved polymer given at 90°C and varying the conditions of the casting temperature (Tcast) parameter between (30-45) °C.

Table 6-1: Polymer preparation conditions and PVDF membranes appearance.

Membrane label	Polymer dissolution temperature, Tdissol (°C)	Casting/coagulation temperature, Tcast (°C)
M70-30	70	30
M90-30	90	30
M120-30	120	30
M150-30	150	30
M180-30	180	30
M90-30	90	30
M90-35	90	35
M90-40	90	40
M90-45	90	45

Note: *The casting and coagulation temperatures were maintained for each prepared membrane*

The prepared polymer dope was cooled at room temperature to each Tcast parameter. The polymer dissolution temperature, casting speed, casting temperature and coagulation temperature were all controlled to fabricate reproducible PVDF membranes. The casting process and the coagulation bath were set at the same temperature for all

experiments. The membranes were rinsed thoroughly with deionised water and 2-propanol and air-dried at room temperature.

6.3 Result and discussion

6.3.1 Morphology of the PVDF membranes prepared by NIPS

Scanning electron microscopy (SEM) was used to characterise the microscopic structure of the fabricated PVDF membranes. As presented in figure 6.1, the SEM images show that the dissolved polymer temperature (Tdissol) influences the synthesised PVDF membrane morphologies.

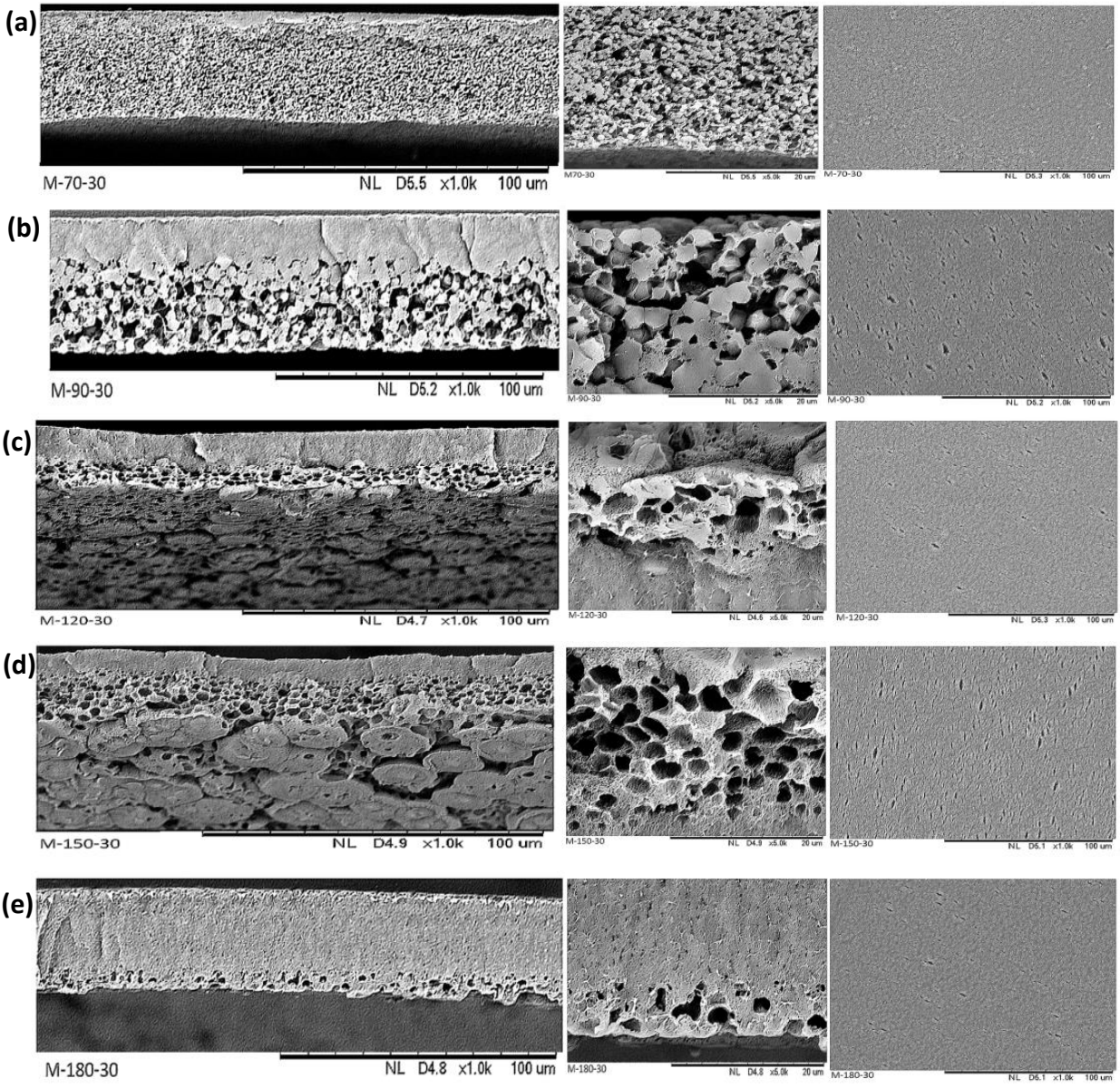

Figure 6.1: SEM micrographs of PVDF membranes fabricated with dope solutions prepared at different temperatures (Tdissol) [(a)70°C; (b)90°C; (c)120°C; (d)150°C; (e)180°C] (Left to right: cross section; sublayer and top surface respectively).

The observed cross section morphology shows that the PVDF membranes possess a spongy-like globular porous substructure and a dense top layer. The morphological changes of the presented PVDF membranes appear to be associated with the phase separation behaviour of the PVDF system due to the influence of the different Tdissol parameters. Typically, the cast film, when immersed in the nonsolvent coagulation bath, undergoes a transformation that results in demixing into two phases, a polymer-rich phase that eventually forms the matrix of the material and a polymer lean phase that forms the pore structure [4]. The demixing occurs due to the polymer system's positive Gibbs free energy state, forming nuclei and coarsening the cast film. The interactions of polymer chains at some point proceed to a state of infinite viscosity leading to solidification taking place via thermodynamic and kinetic hindrance upon phase inversion (crystallisation, or gelation) [13,14].

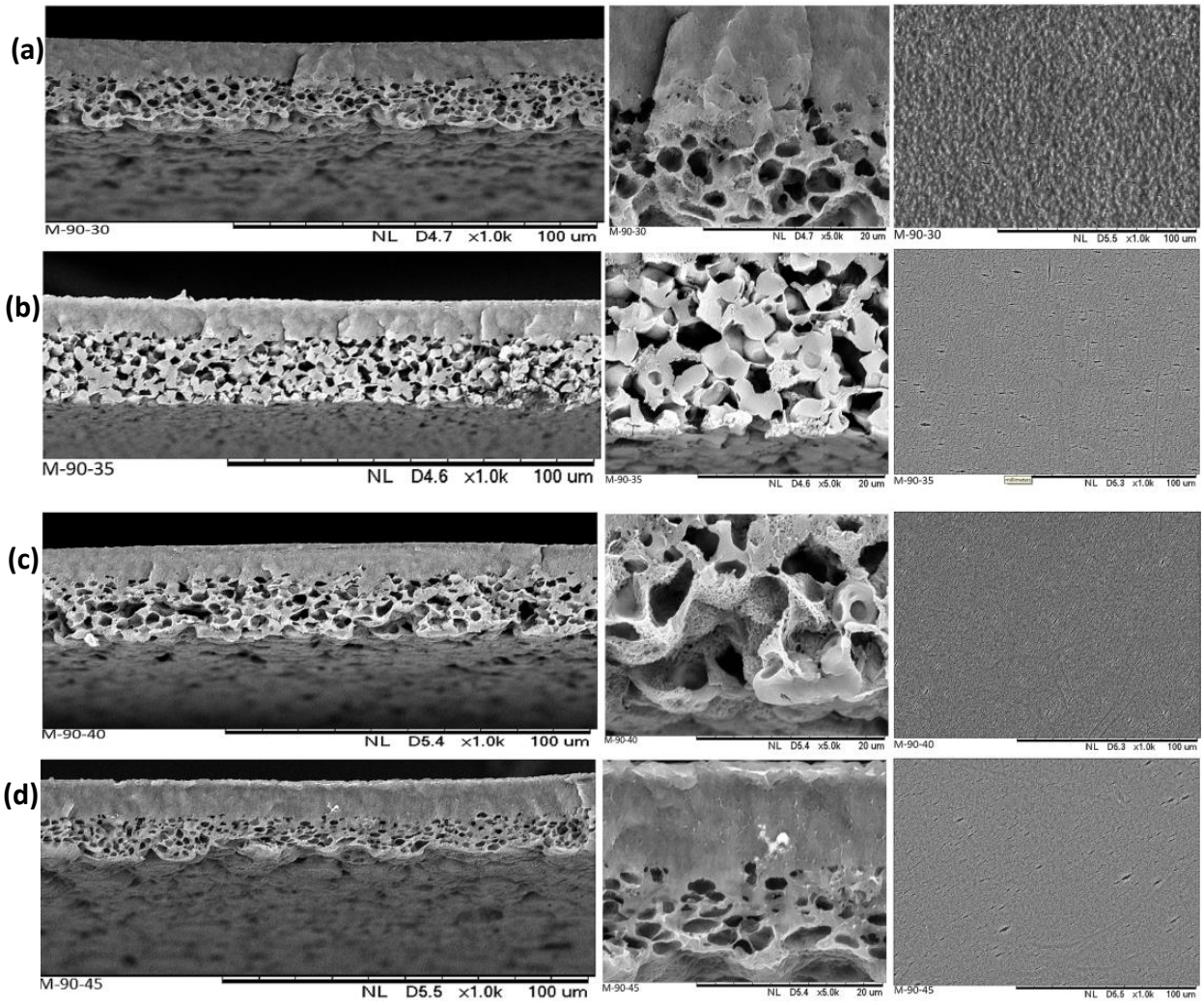

Figure 6.2: From left to right: SEM images of the PVDF membranes as a function of increasing Tcast. [(a)30°C; (b)35°C; (c)40°C; (d)45°C;] Left to right: cross sections; substructure; top surfaces respectively.

Analysis of the PVDF membrane prepared by increasing the Tcast parameters reveals an asymmetric structural morphology with a densely top layer and spongy-like honeycombed interconnected sub-layer structure, as shown in figure 6.2. The morphology of the synthesised PVDF membranes using GVL via the nonsolvent induced phase separation (NIPS) approach suggests that both the equilibrium phase and kinetics must be understood to gain insight into the obtained membrane structure. The membrane morphologies presented in figure 6.1 and 6.2 indicate that the increased Tdissol and Tcast parameters had an influence that resulted in structural changes of obtained PVDF membrane. The correlation with the experimental ternary phase diagram of the PVDF/GVL/water system indicates a thermodynamic effect trade-off between gelation, solid-liquid, and liquid-liquid demixing occurring during the phase separation process of the synthesised PVDF membrane. Based on the scanning electron microscope (SEM) cross section images, the membrane formation mechanism indicates that both solid-liquid and delayed liquid-liquid demixing occurred. The assumption is that the dope solution prepared at high Tdissol loses solvent faster than the inflow of nonsolvent at the cast film/nonsolvent interface in the coagulation bath. Thus, the cast film enters the gelation region with a higher solvent outflow to nonsolvent inflow, forming a dense top layer structure. Typically, within the very first split second after immersion of cast film in a nonsolvent coagulation bath, there is a rapid loss of solvent and a relative penetration of nonsolvent, which increases the polymer concentration at the interface of cast film and nonsolvent in the coagulation bath [15]. The solvent outflow is most significant at the cast film/nonsolvent interface and decreases with cast film depth [16]. The dense layer formed in this way acts as a barrier to solvent outflow. The low polymer and high nonsolvent concentrations resulted in slow precipitation (delayed liquid-liquid demixing) that promotes nucleation growth mechanism [17,18] in the sublayer once the dense top layer is formed.

Furthermore, the experimental time scale measurement was recorded during the membrane fabrication process to evaluate how long it took for the cast film prepared at different Tdissol to transition from transparent to turbid film once immersed into the nonsolvent water coagulation bath. The result showed a decrease in time from 28secs to 18 secs with an increased Tdissol (70-180°C). It appears that the polymer chains continued to act thermodynamically or remained frozen in their dissolved form for a prolonged duration despite the dope solution prepared at different temperatures being rapidly cooled to a fixed casting temperature. The whole cooling process of the dope solution led to increased solvent loss and film solidification. Similarly, it is assumed that increasing the Tcast temperature would result in an accelerated exchange rate of the solvent and nonsolvent. However, the SEM images of the PVDF membranes show that varying the Tcast parameter does not

significantly alter the microstructure of the synthesised cross section of the PVDF membrane. It is generally understood that at lower temperatures or increased demixing gap, the casting solution is closer to its precipitation state and thus requires less water to be thermodynamically disturbed [19,20]. Hence, the final membrane structure for varied Tcast parameters observed a less significant change.

The preceding thermodynamics chapter presents a detailed study of the phase behaviour of the PVDF/GVL/water system. It highlights potential effects regarding mass transfer between polymer mixtures during the membrane fabrication process [21]. It is arguable to infer that PVDF/GVL solution samples prepared at different temperatures and quenched to the specific casting temperature behave differently and depend on the initial memory state of the dissolved polymer. Additionally, the influence of temperature on the behaviour of the PVDF solution can be viewed as transitory and evolves upon cooling to Tcast.

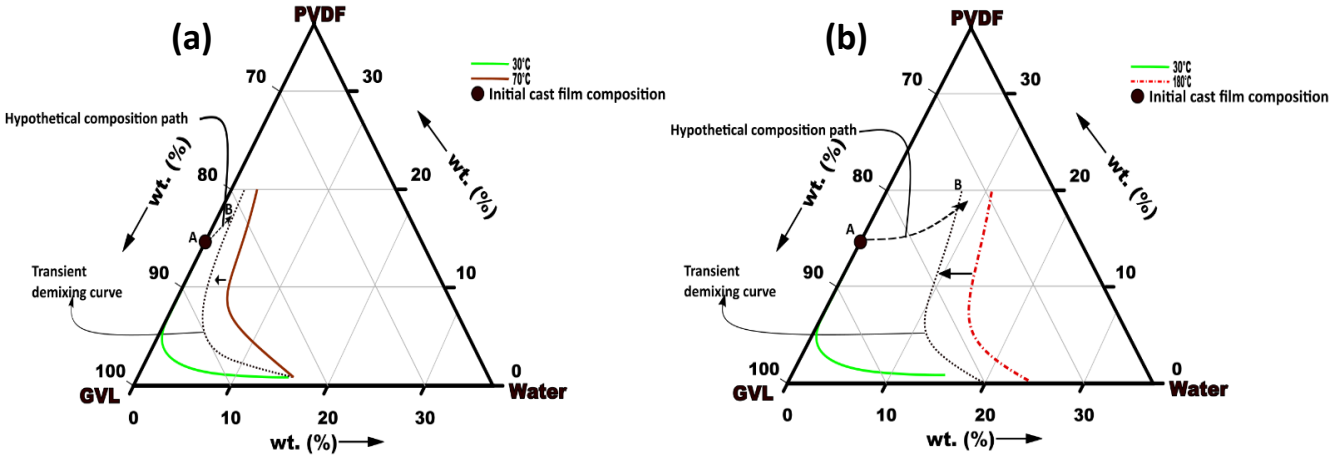

Figure 6.3: The demixing curves based on experimental data obtained by the cloud point approach using the vial dissolution of polymer (VDP) method for Tdissol at (a) 70°C and (b) 180°C.

The presumption is further demonstrated, by examining the experimental demixing phase behaviour of the PVDF/GVL/water system at the different Tdissol and Tcast parameters, as shown in Figures 6.3 and 6.4, respectively. The determined demixing curve at each temperature are compositions at which the solution is no longer thermodynamically stable over time. In figure 6.3, for illustration purposes, the black dotted lines represent the potential location of the estimated transient demixing curve when quenched from Tdissol, the red dashed lines are the demixing curve at dissolved polymer at 180°C while the solid coloured lines are experimental demixing points at the different considered temperature after 48hrs

In summary, the PVDF morphology demonstrates that the Tdissol and Tcast are valuable parameters influencing the phase separation process to obtain tailored PVDF membranes. In addition, the final PVDF membrane is controlled by thermodynamics (phase behaviour at a different specific temperature), the spatiotemporal evolution of cast film compositions and polymer mixture diffusion during the membrane fabrication process [22].

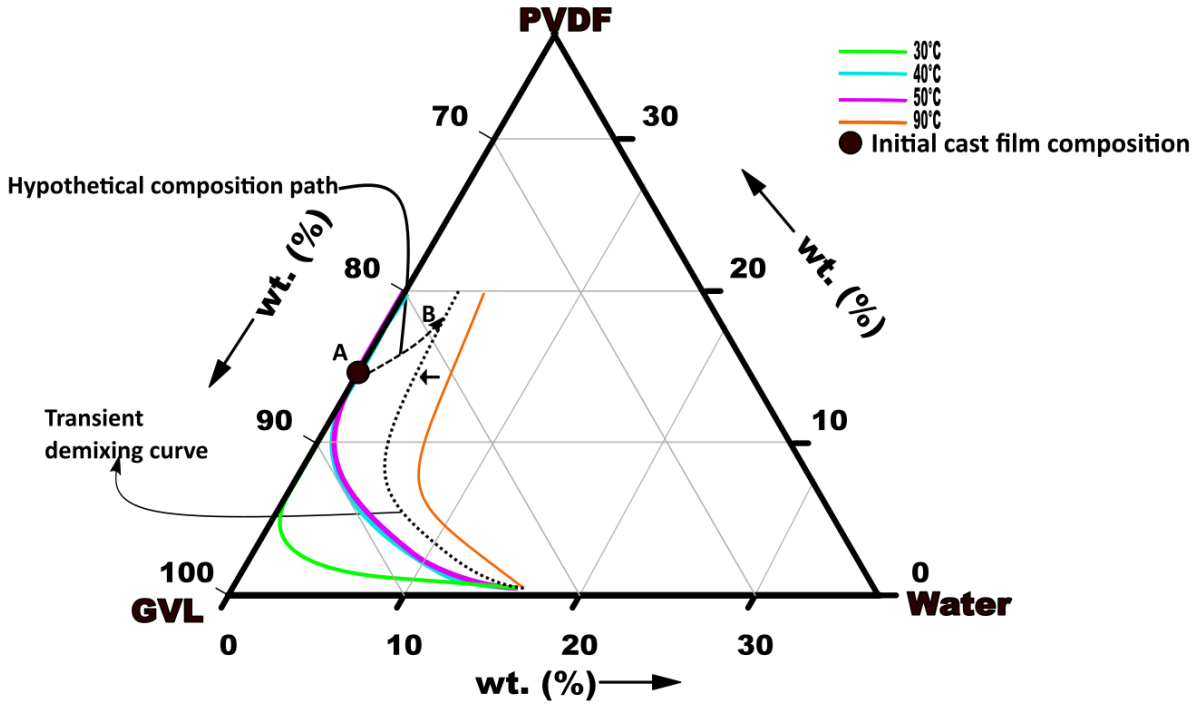

Figure 6.4: Schematic ternary phases diagram for the PVDF/GVL/water system at different temperatures indicating a demixing and phase inversion pathway once cooled between solution preparations to casting

6.3.2 Membrane thickness, surface pore, and porosity measurement

The average thickness and porosity of the PVDF membranes prepared by varying fabrication conditions of casting (Tcast) or polymer dissolution (Tdissol) temperatures are summarised in Table 6-2, with the average thickness of the prepared PVDF membranes ranging between 25-36 (±2) µm. The porosity is an intrinsic property of the material, measured by the percentage of space within a particular porous or semi-porous material. The overall porosity trend shows that increasing either Tdissol or Tcast reduces the PVDF membrane porosity with obtained membrane values between 40%-49%. A similar range of values between 34%-83% has been reported in a few studies [23,24], highlighting that both Tdissol and Tcast parameters play a significant role in the final membrane porosity structure.

Table 6-2: Average overall thickness and porosity of synthesised PVDF membrane

Membrane	Membrane thickness (µm)	Thickness of dense membrane layer (µm)	Overall porosity
M-90-30	36 (±1)	17 (±1)	54 (±3)
M-90-35	33 (±1)	14 (±1)	51 (±1)
M-90-40	40 (±1)	17 (±2)	48 (±2)
M-90-45	26 (±2)	13 (±2)	46 (±2)
M-70-30	33 (±1)	5 (±2)	59 (±2)
M-90-30	36 (±1)	16 (±2)	54 (±3)
M-120-30	28 (±3)	18 (±1)	46 (±3)
M-150-30	30 (±2)	27 (±1)	44 (±3)
M-180-30	28 (±1)	24 (±1)	40 (±3)

The overall thickness of the membranes represents the effective length of the membrane, which decreased as Tdissol/Tcast increased. The PVDF membrane thickness results suggest that dope solutions prepared at different Tdissol, even when cooled to a specific casting temperature, behave differently. The effect of Tcast on the thickness had a comparable influence with the exception of an increase at 40°C, which was an outlier with results presented in figure 6.5.

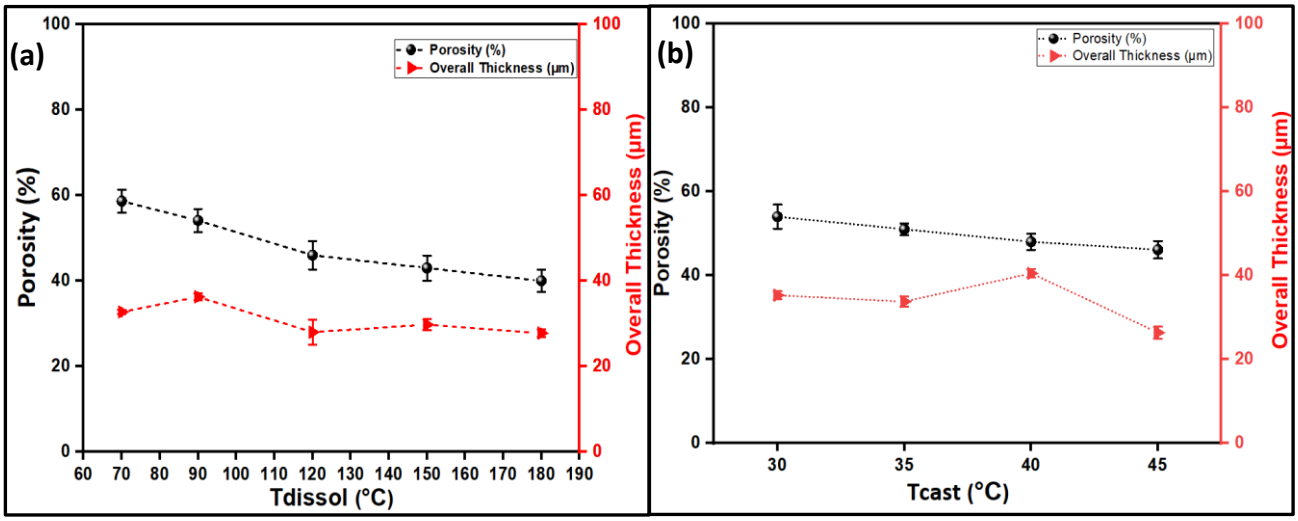

Figure 6.5: Overall porosity and thickness of PVDF membranes as a function of (a) Tdissol and (b) Tcast.

The mass transfer/exchange rate between solvent-nonsolvent is primarily influenced by temperature during the membrane formation process [25]. However, the difference in membrane thickness is justified by the presumption that GVL is a poor solvent based on the thermodynamics behaviour analysis of the PVDF system [21,26]. Hence, for a dope solution prepared at high Tdissol, the cast film interaction and exchange of solvent and nonsolvent during the phase inversion process allows for rapid loss of solvent, resulting in the formation of the dense top layer and polymer coil to contract during the phase separation process. Figure 6.6 depicts the dense layer thickness measurement, emphasising the difference between the effect of Tdissol with an increasing pattern and Tcast, which displayed a random dense layer thickness trend.

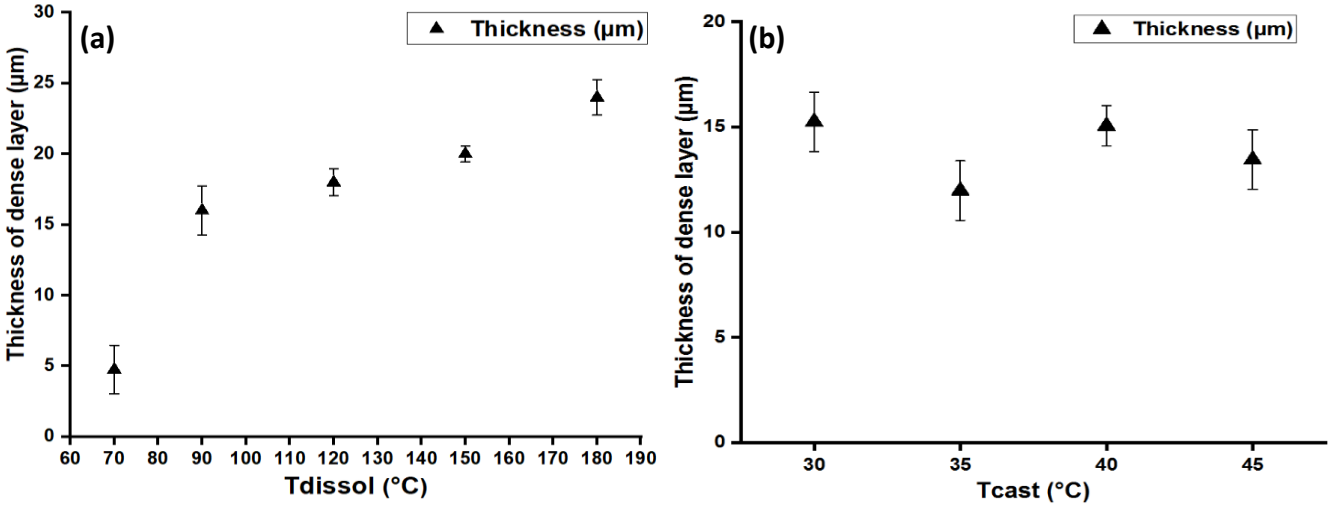

Figure 6.6: Thickness of PVDF membrane dense sublayer as a function of the casting and polymer dissolution temperatures as presented in (a) Tdissol and (b) Tcast.

6.3.3 Wettability and surface roughness analysis of PVDF membrane

The wettability property of PVDF membrane has been reported to affect polymeric membrane performance and fouling behaviour [27,28]. Typically, the low surface tension of PVDF (25 dynes/cm) contributes to the inherent hydrophobicity when characterised by water contact angle [29]. Results summarised in Table 6-3 for water contact angle are within literature values 68-140°C (see Table 2-3) for PVDF membranes prepared by NIPS [30,31]. The water contact angle and roughness of the PVDF membranes are presented in figure 6.7. Results show that increasing the Tdissol of the PVDF membranes influenced the wetting properties of the PVDF membranes. The water contact angles ranged from 76-96°C, proving that Tdissol and Tcast had an impact on the degree of hydrophilicity and hydrophobicity of fabricated PVDF membranes.

Table 6-3: Measurement of PVDF membranes contact angles and surface roughness

Membrane	Contact angle (°)	Average roughness (Ra)	RMS roughness (Rq)
M-90-30	76.8 (±2.2)	3.25	5.011
M-90-35	86.7 (±3.1)	13.08	17.67
M-90-40	77.1 (±2.4)	9.17	11.87
M-90-45	78.9 (±4.3)	10.11	13.59
M-70-30	87.2 (±2.3)	7.86	10.15
M-90-30	89.5 (±3.1)	9.22	12.73
M-120-30	90.6 (±2.6)	11.16	14.72
M-150-30	95.2 (±3.2)	15.35	20.67
M-180-30	96.4 (±4.1)	18.81	28.44

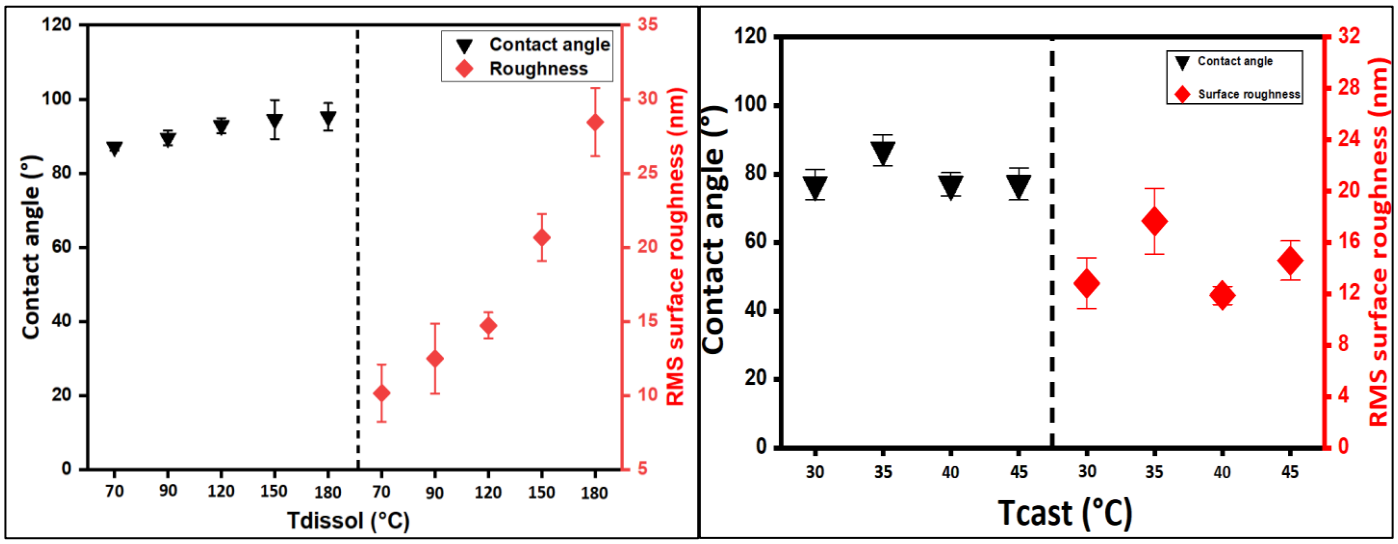

Figure 6.7: wettability characterisation of PVDF and RMS roughness as a function of the casting and polymer dissolution temperatures.

Generally, PVDF membranes synthesised by NIPS using a strong nonsolvent like water result in membranes having low surface contact angles due to a "flattening effect". The phenomenon is described as a process involving the polymer chain's mobility in the cast film due to the large interfacial tension gap and interaction between the cast film and water, which suppresses the polymer chain, thus depressing the hydrophobicity of the membrane [11,32].

Nevertheless, the surface water contact angles obtained for the prepared PVDF membranes are within the expected range of previously reported wettability values for PVDF membranes. In addition, the wetting property has also been reported to be affected by the

surface roughness of the membrane. Studies indicate that an increased surface roughness enhances the hydrophobicity (wettability property) of the membrane due to the design of the membrane surface structure that traps air between the material surface and the liquid [33,34]**.** The topographical analysis of the PVDF membranes was performed using atomic force microscopy (AFM), followed by a roughness analysis. As a result, the surface topology of the PVDF membranes synthesised by varying Tcast or Tdissol showed several rough microprotrusions (see figures 6.8 & 6.9).

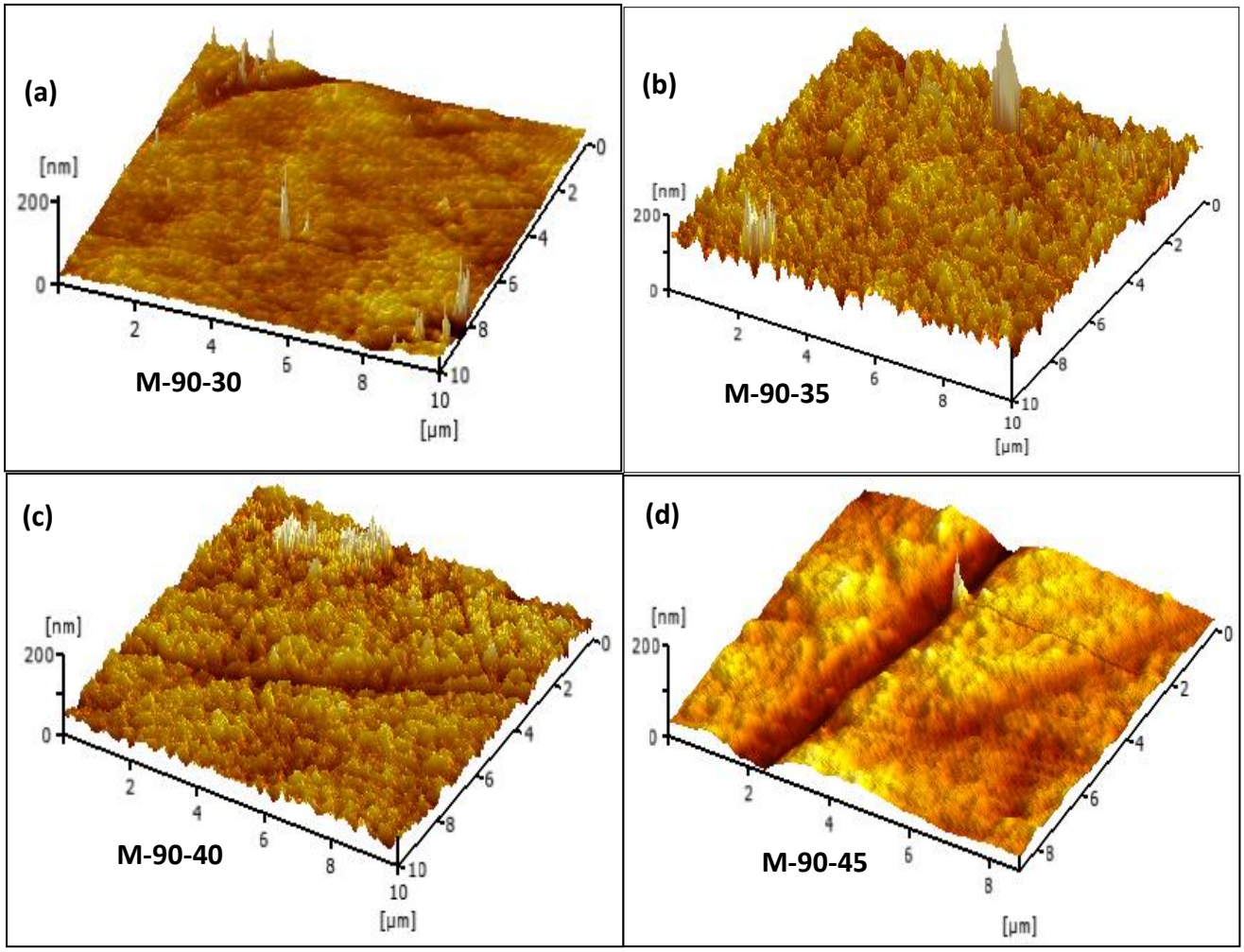

Figure 6.8: AFM three-dimensional images of PVDF membranes prepared by varying the casting temperature from 30 -45°C as presented in figures (a) – (d).

The average surface roughness (Ra) and root mean square (RMS) roughness values (Rq) were quantified over an area of 10 um x 10 um of the PVDF membrane samples are summarised in Table 6-3. Ra and Rq both show similar patterns for PVDF membranes due to the effect of Tdissol and Tcast.

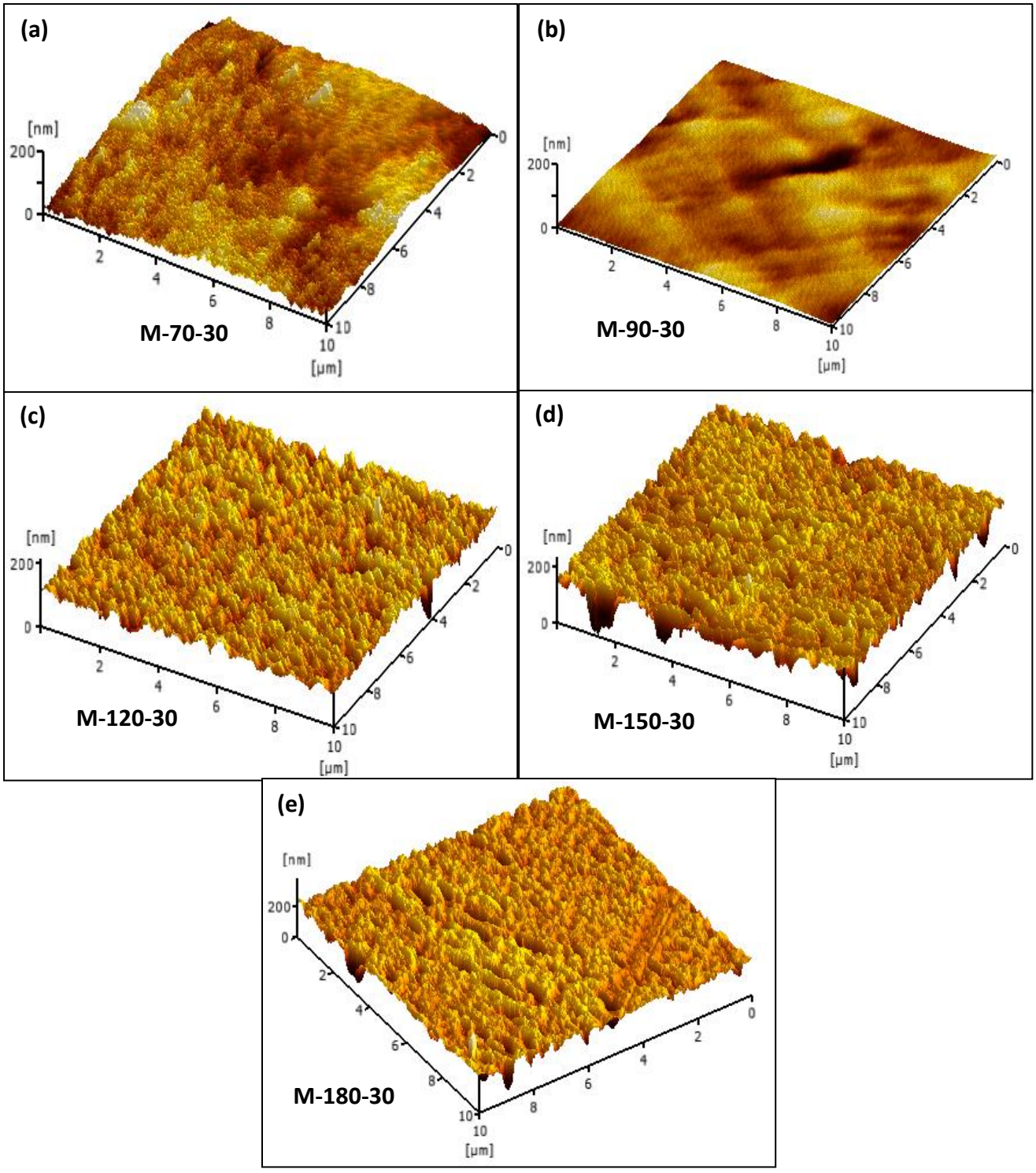

Figure 6.9: AFM three-dimensional images of PVDF membranes prepared by varying the polymer dissolution temperature between 70 -180°C as presented in figures (a) – (e).

The three-dimensional surface images of the flat sheet PVDF membrane suggest that the roughness of the membrane's top surface depends on the structural features due to the influence of Tdissol and Tcast. Furthermore, the results support Cassie-Baxter's wetting hypothesis, which suggests that a non-wetting liquid may not penetrate the surface cavities

of rough surfaces [35]. However, it should be noted that the measurement of the AFM is limited to a few square microscales, which tends to restrict the roughness area observed for each membrane. Additionally, the surface roughness results are challenging to compare with the literature due to a lack of uniformity in the methods applied to determine surface roughness. Nevertheless, results showed that the roughness parameter of the active layer of the asymmetric PVDF membranes increases as the polymer dissolution temperature increases.

In contrast, the asymmetric PVDF membranes prepared under different casting temperature conditions showed various roughness characteristics. Therefore, it is likely that the increase in hydrophobicity due to enhanced roughness on the top surface results from stabilised air gaps at the liquid-solid interface. Such stabilisation of air gaps could be beneficial for membrane distillation process by reducing the possibility of partial wetting of the membranes [36].

Generally, the roughness of the PVDF membranes on such a small scale could be termed as smooth, thus promoting the transport mechanism performance and reducing the susceptibility of fouling. However, the rough surfaces are reported to favour the accumulation of foulant at the surface because foulant particles are more likely to be entrapped by more uneven surfaces than smoother membrane surfaces [37,38]. In addition, the rugged ridged valley structure on the surface of the membranes tends to provide more adsorption sites that result in clogging and increased total surface area of the membrane, which could deteriorate the hydrodynamics near the surface and cause a performance flux decline.

6.3.4 THERMAL ANALYSIS – DSC

PVDF, a semi-crystalline polymer, typically has a degree of crystallinity between 35% - 70%, with melting and glass transition temperatures around 155–192°C and − 40 to – 30°C, respectively [39]. DSC measurements were conducted to characterise the synthesised PVDF membranes and determine the melting temperature (*Tm*), the heat of fusion and the degree of crystallinity, with results summarised in Table 6-4. The normalised DSC thermograms of the synthesised PVDF membrane samples are shown in figure 6.10. Results show no significant change in the melting temperature, with melting points being the peak points of the DSC endothermic curves for the membrane samples. All PVDF membranes exhibit only one endothermic (melting) peak observed between 168-169°C at the scanning rate of 10°C/min, as shown in figure 6.10. A degree of crystallinity between 40-48% was determined for the synthesised PVDF membrane due to the lower energy state during membrane formation. Polymers are long-chain molecules of random coil structures entangled in molten states. At

low polymer dissolution temperatures, the random polymer coil dimension tends to be closely packed together in a regular and parallel array resulting in a high degree of entanglement compared to the polymer coil obtained at high temperatures. In addition, PVDF membranes that feature a macrovoid free morphology are more likely to consist of interlinked semi-crystalline particles due to the resulting phase separation mechanism [40].

Table 6-4: Melting temperature and crystallinity of PVDF membranes

Polymer/membrane Sample	Enthalpy (J/g)	Crystallinity (%)	Melting Temperature (°C)
M-90-30	51 (±1)	48 (±1)	168
M-90-35	50 (±1)	48 (±1)	166
M-90-40	50 (±2)	48 (±2)	167
M-90-45	49 (±1)	47 (±1)	168
M-70-30	48 (±2)	46 (±2)	168
M-90-30	48 (±2)	46 (±2)	168
M-120-30	46 (±2)	44 (±2)	169
M-150-30	45 (±3)	43 (±3)	169
M-180-30	42 (±1)	40 (±1)	168
PVDF pellets	52 (±2)	50 (±2)	172

The membranes prepared using lower polymer dissolution temperatures exhibited higher degrees of crystallinity. The crystallinity is thus related to the phase transition behaviour of the polymer system during membrane formation. Since crystallisation is a slow process, as the PVDF is heated and cooled to a casting temperature below its melting point, the crystals grow slowly as the polymer chains coil back to their natural state. A similar observation has been reported for PVDF/NMP membranes with an investigation on the effect of dissolving temperature [41]. Thus, for conditions of PVDF solution dissolved (<100°C) far away from the PVDF pellet melting temperature (172°C), the thermo-history appears to be retained due to insufficient/partial melting conditions of the PVDF dope and those close or above to the PVDF pellet melting temperature show a resulting difference in the degree of crystallinity of the fabricated PVDF membrane

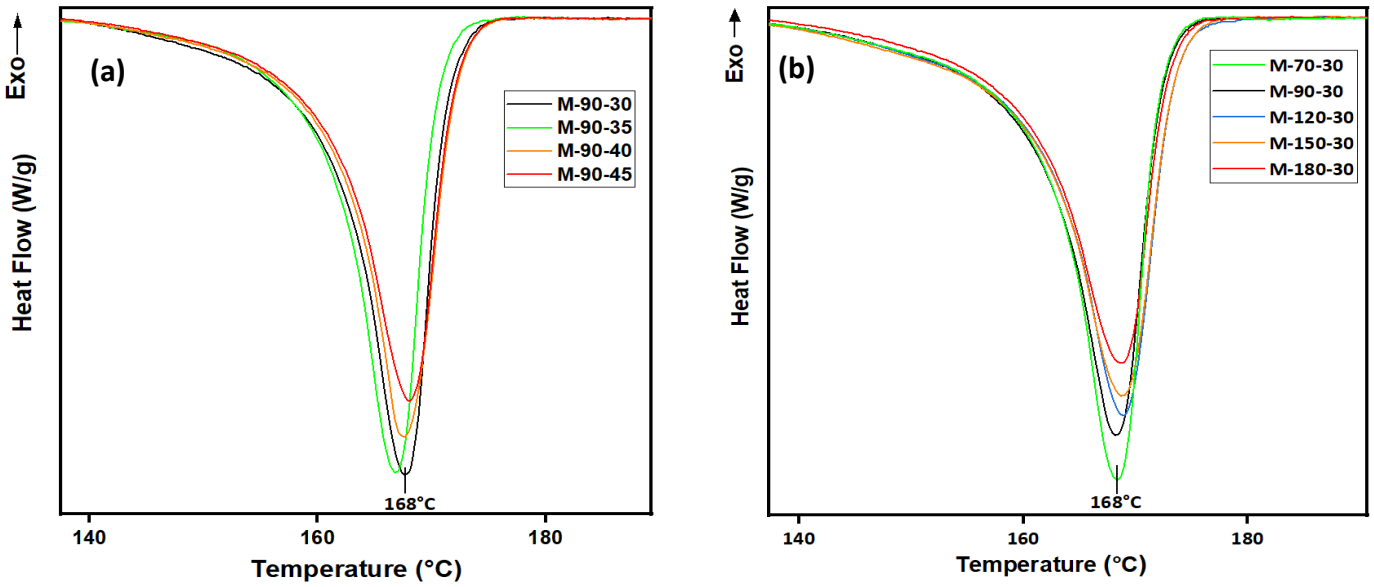

Figure 6.10: Endothermic heat flow curves of PVDF membranes as a function of (a) the casting temperature (Tcast) and (b) the polymer dissolution temperature (Tdissol).

The resulting crystallinity trend shown in figure 6.11 decreased as the polymer dissolution temperature increased due to transient entanglements preserved throughout the cooling process, which seemed to retain its memory state even when cooled to casting temperatures [42]. Therefore, it is possible to predict that the high crystallinity of PVDF membranes occurs at low polymer dissolution temperatures due to micro crystallites connecting sites between the amorphous and crystalline zones. Furthermore, since PVDF has a low glass transition temperature, crystallisation was most likely induced after the liquid-liquid demixing, despite the fast quenching upon cooling to casting temperature.

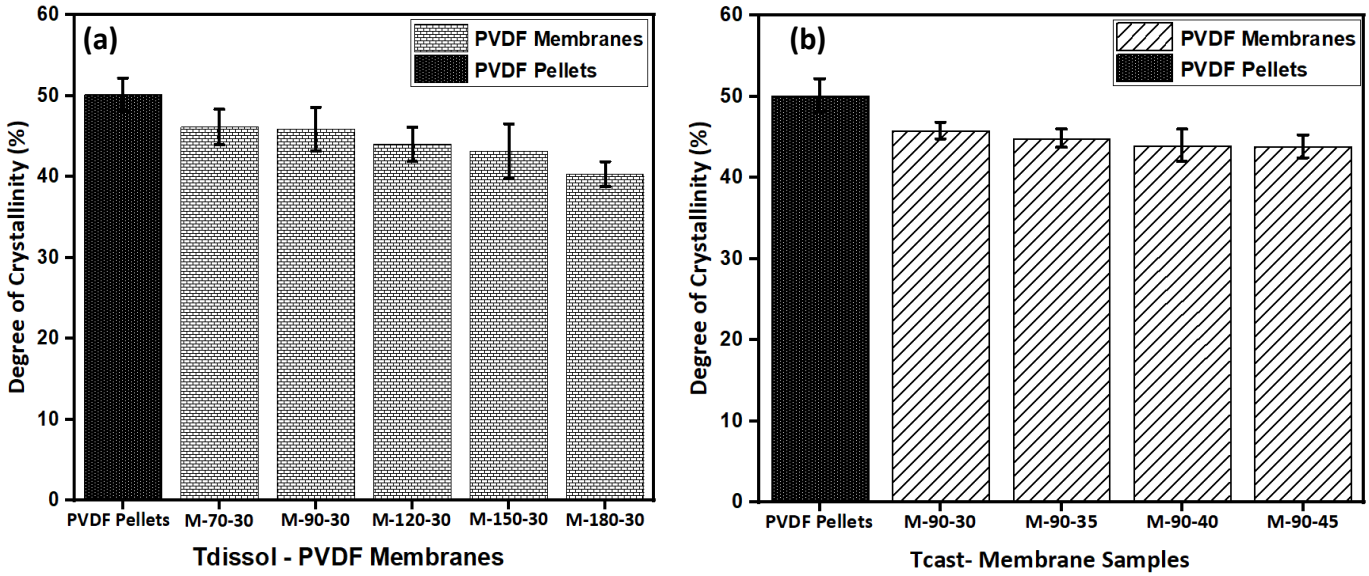

Figure 6.11: Degree of crystallisation of PVDF membranes synthesised at different (a) polymer dissolution temperatures (Tdissol) and (b) different casting temperatures (Tcast).

6.3.5 FTIR ANALYSIS – crystalline forms of synthesised PVDF membranes

The Fourier transform infrared spectroscopy-attenuated total reflection (FTIR-ATR) spectra analyses established the crystalline form. The PVDF membranes obtained from casting and polymer dissolution temperatures were compared to identify the properties resulting from the effect of these two parameters. Generally, PVDF crystallises at temperatures where the solution becomes unstable to induce phase separation, and the crystal phase formation is temperature dependent [43]. Several studies show solvent miscibility, cooling rate, thermal history, and polymer solution quenching process affect crystallisation behaviour [44,45]. PVDF has been reported to crystallise in at least five different polymorphs (α-,β-,γ-,δ-, and ε) under certain conditions, with the most common polymorphs to be the α- and β- phase.

The FTIR-ATR spectra of the synthesised PVDF membrane surfaces are presented in figure 6.12 for a wavenumber range (1800 to 600 cm^{-1}). The spectrum contains typical vibration bands associated with different PVDF phases that have been identified for comparison and visualisation. The bands at 612, 762, 794, 874, 976, 1068, 1148, 1178, 1210, 1382 and 1402 cm^{-1} have been identified as the α-phase while vibration bands associated with the presence of β-phase confined in the membrane as reported are at 840 cm^{-1} [46,47, 48,49].

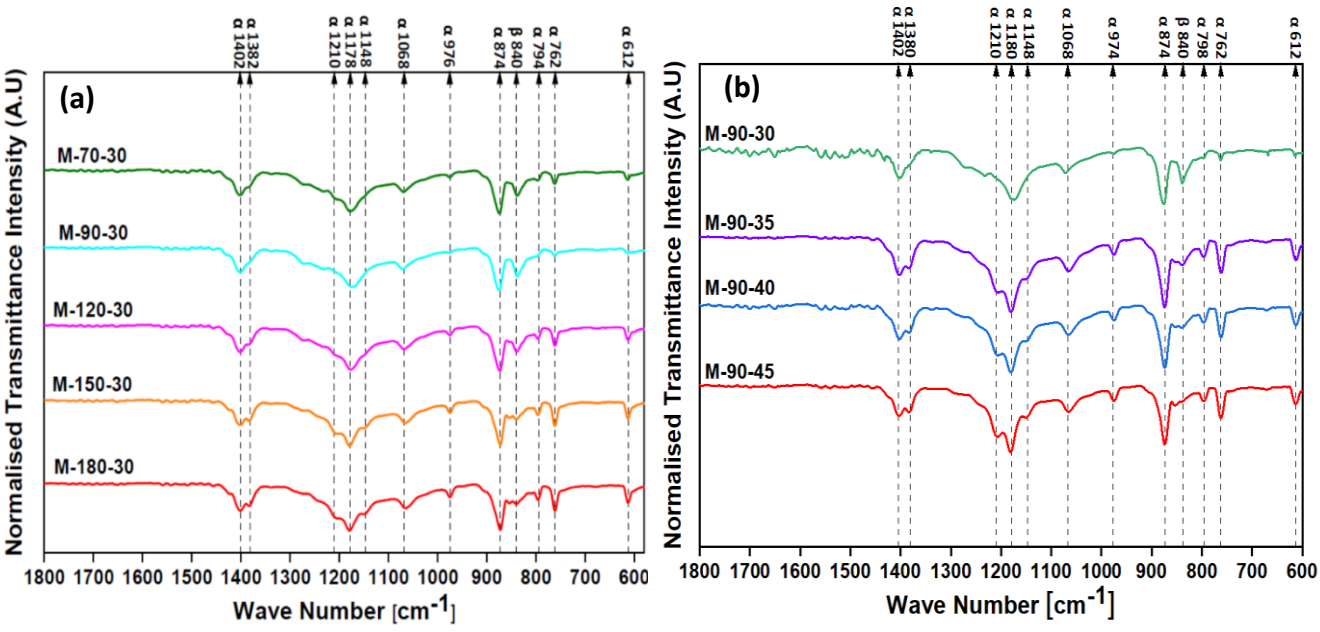

Figure 6.12: FTIR-ATR spectra of the PVDF membranes due to increasing (a) Tdissol and (b) Tcast conditions.

The results show that the synthesised PVDF membranes presented a mixture of α- and β- phases. Furthermore, all membrane samples feature similar peak locations from 1800 to

600 cm^{-1}, with noticeable differences in their peak intensities pattern as observed from the spectra for an increased temperature of considered fabrication parameters.

Typically, the α-phase microcrystal is predominant for PVDF prepared at high temperatures (>120°C) [50]. In contrast, the β-phase has been dominant at mild/low prepared temperatures or noticed from PVDF solution that crystallises rapidly due to high rate quenching at lower temperatures (immersing prepared PVDF solution in ice water/low temperatures) [51,52,53].

The β-PVDF vibration band shown in figure 6.12 is undeniably evident and appears in PVDF membrane spectra prepared from Tdissol between 70 and 120°C. In addition, the spectra results show that the α-phase intensity at 612 and 760 cm^{-1} is diminishing, while the intensity at 840 cm^{-1} (β -phase) peaks dominate when the polymer dissolution temperature decreases. The β-phase is associated with the enhanced mechanical strength of the material and other properties that include piezo- and ferroelectric properties of PVDF films [54].

The FTIR-ATR spectra results suggest the increased Tdissol and Tcast of the PVDF membranes promoted both α- and β- crystalline phase formation with shown spectra displaying exclusive vibration bands. Results for PVDF membranes obtained using conventional solvent (NMP) have been to demonstrate increased α-phase, for conditions of increasing Tdissol parameter [55]. Furthermore, the similarities of the PVDF membrane spectra based on the varying temperature of Tcast and Tdissol suggest that the physical difference cannot be associated with chemical changes. The crystalline mass fraction of the β-phase dominance on the top surface layer of the PVDF membranes was numerically determined using equation (4) for all prepared membranes.

$$F(\beta) = \left(\frac{A_{\beta}^{840}}{\left(K_{\beta}^{840}/K_{\alpha}^{762}\right)A_{\alpha}^{762} + A_{\beta}^{840}}\right) \qquad (4)$$

Where A_{α}^{762} and A_{β}^{840} are the corrected baseline absorption peaks of the α- and β- phases at 762 and 840 cm-1, $F(\beta)$ is the relative fractions of the β phases, and *K* and *d* are the absorption coefficient and penetration depth with corresponding values obtained from the literature study [17,26] and given as: $\left(K_{\alpha}^{762} = 6.1 \times 10^{4}\ cm^{2}/mol\ ;\ K_{\beta}^{840} = 7.7 \times 10^{4}\ cm^{2}/mol\right)$. The fraction of the β-phase in figure 6.13 showed a decreasing trend when the temperature was increased, indicating that the crystal phase is influenced by the Gibbs free energy of the PVDF system.

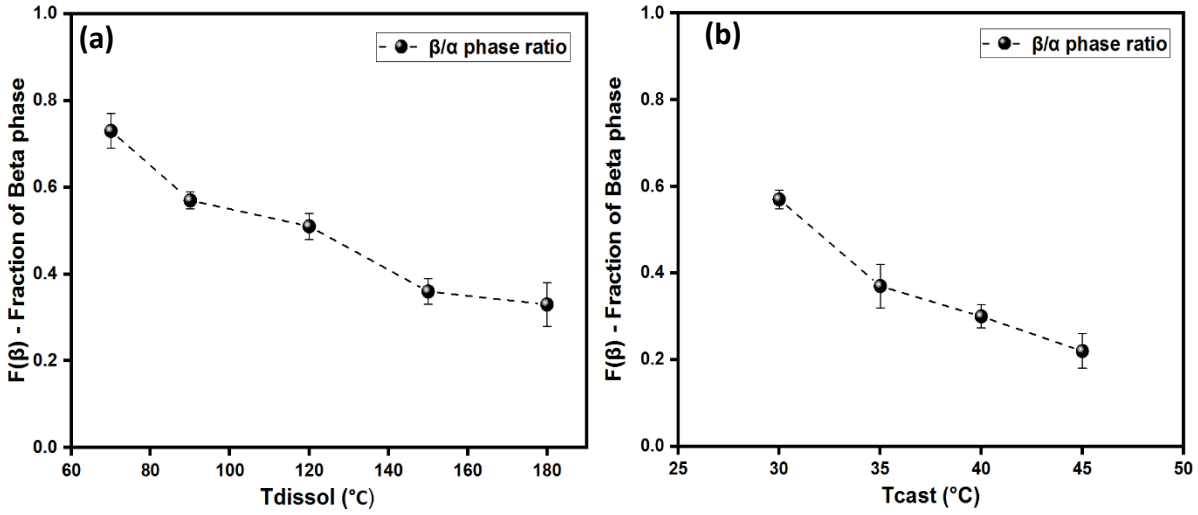

Figure 6.13: The crystalline fraction of the Beta (β) phase in samples of PVDF membranes. (a) Tdissol and (b) Tcast.

Typically, thermodynamic and kinetic factors influence crystallisation. Gibb's free energy is all about altering the state of a system, which involves a change in thermodynamics that may modify the arrangement of polymer chains. Therefore, Gibbs free energy is interpreted as the driving force to describe the crystal phase transformation due to the effect of increased Tdissol and Tcast parameters [56]. The PVDF pellet and membranes fabricated with low Tdissol dope solution prepared between 70-90°C feature a high β-phase fraction. On the other hand, a low fraction of β-phase was observed for PVDF membranes fabricated from a high Tdissol (120-180°C) dope solution. Figure 6.14 illustrates the transition in the crystal phase fraction between the α- and β- noticed from PVDF membranes due to the difference in Gibbs free energy. In addition, PVDF membranes with decreasing polar β- crystal phase exhibits a correlation trend to increased water contact angles (figure 6.7), indicating that the different crystal phases are likely to alter the PVDF membrane's performance.

The observed crystalline phase results agree with the reported observation of PVDF membranes [14]. However, based on assessing the crystalline phase using the x-ray diffraction (XRD) technique, a few studies have reported different results for PVDF membranes achieved by increasing Tdissol parameters. [3,7]. Hence, It is likely that the XRD approach is less sensitive than the FTIR-ATR technique for characterising the PVDF crystalline phase. A visualisation of the behaviour of the crystal phase form in the fabricated membranes once dried in figure 6.14.

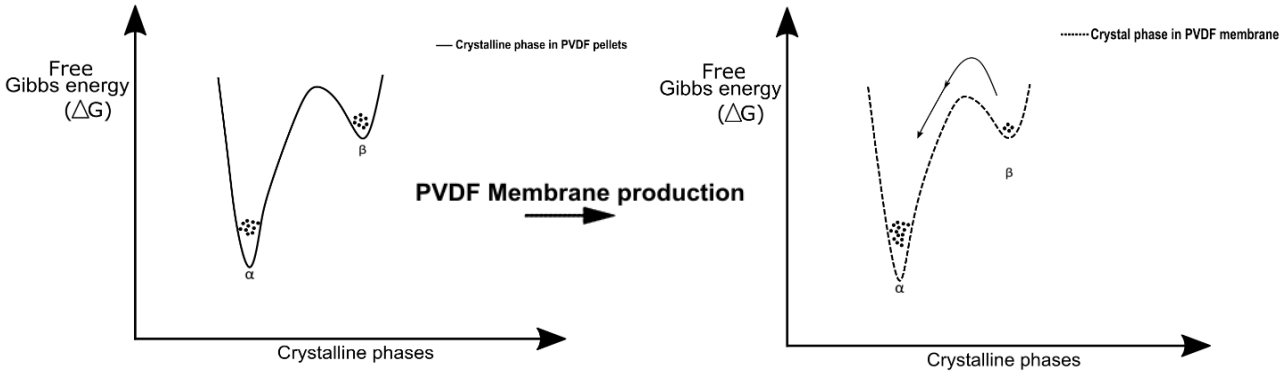

Figure 6.14: Schematic illustration of Gibbs free energy change during crystal phase transition form. The black dots illustrate the form of crystal phase

6.3.6 Gas permeation analysis

The performance of the PVDF membrane was determined by a gas flux test using nitrogen gas as the permeability medium. The schematic arrangement of the membrane filtration setup is presented in chapter three (3). The nitrogen permeation flux was measured at room temperature and plotted as a function of the pressure difference. The experimental study shows that gas permeation through the PVDF membranes decreased with increasing Tdissol and Tcast parameters, as shown in figure 6.16. Furthermore, no hysteresis loop was observed for all synthesised PVDF membranes.

The gas permeation trend correlated with the porosity, which suggests that the PVDF morphological structure plays an important aspect in the performance of the synthesised membrane. However, it must be stated that the nitrogen gas permeation through the PVDF membrane sample (M-90-40) seems an outlier, with reasons associated with the thickness of the dense layer of the PVDF membrane. Therefore, it is arguable that the different thickness of the top layer acts as a separation barrier and influences the PVDF membrane's performance.

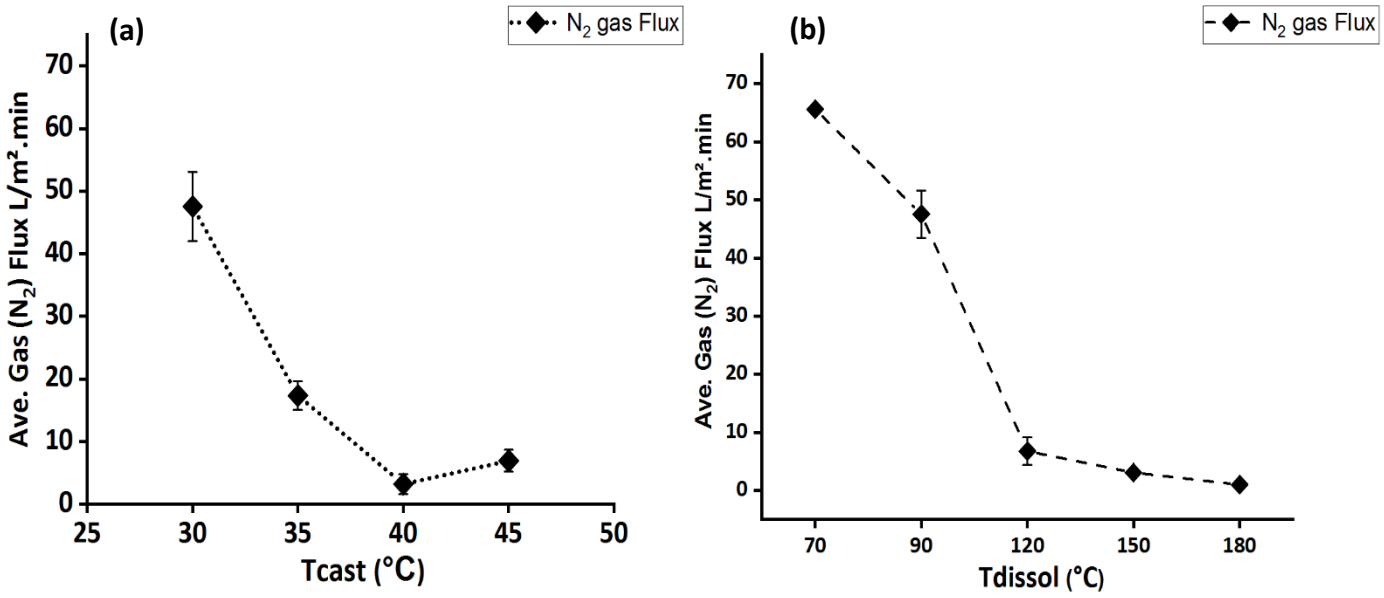

Figure 6.15: Gas (Nitrogen) Flux of PVDF membranes (at 0.4 bar) as a function of (a) Tcast and (b) Tdissol

The synthesised PVDF membrane using GVL exhibited no pure water flux (PWF) for the considered pressure between 1 and 10 bars, making it suitable for gas-liquid membrane contactors.

6.4 Summary

The study demonstrates a sustainable NIPS approach in fabricating freestanding tailored PVDF membrane samples by controlling the temperatures of the dissolved polymer (Tdissol) and casting (Tcast) without using toxic solvents. The analysis demonstrated in chapter 4 showed that the increase in temperature of the PVDF dope solution played a significant role in the thermodynamics and kinetics aspects of the membrane fabrication process. The ternary diagram was used to describe the phase separation behaviour of the PVDF system and interpret the relationship between the membrane formation process and the morphological structures of the PVDF membranes. Typically by varying the conditions of Tcast and Tdissol parameters, it is expected that the phase separation of the PVDF system at higher temperatures would result in synthesising PVDF membrane with increased permeability and performance due to reduced viscous resistance of dope solution and the relaxation dynamics of semi crystalline PVDF structure. However, the solidification process of the cast film was slowed down by the increased temperature due to a slow coagulation exchange rate of cast film and nonsolvent via the immersion precipitation process. In addition, PVDF typically has low surface tension; therefore, the increased temperature of the

process parameters is likely to have restricted the penetration of the nonsolvent (water) into the cast film during the membrane development process due to weak interactions between the PVDF and water, which ultimately had a significant impact on the resulting membrane morphological structure.

The membrane properties were further assessed by characterising and comparing fabricated PVDF membranes obtained by altering the controlled conditions of Tdissol and Tcast. The PVDF membrane characterisations were evaluated by porosity measurement, water contact angle, roughness, degree of crystallinity, crystal phases, and gas flux performance. The altering of Tdissol or Tcast parameters demonstrates that it is feasible to improve the performance of the PVDF membranes, which offer a considerably steady-state high gas flux with correlations to the membrane porosity. The dense top layer and sponge-like or globule-like substructure indicate that the PVDF membrane will be suitable for pervaporation, membrane contactors, or gas separation processes. The final membrane structure and performance were affected by increasing the Tdissol and Tcast parameters offering different novel designed PVDF membranes. The degree of crystallinity highlights the difference in the properties of the PVDF membranes fabricated using GVL. Furthermore, analysis of the polymorphism of the films revealed the influence of temperature as the different forms of crystal associated with PVDF exhibit some transformation, which could have affected the freestanding PVDF membrane performance.

Overall, the results indicate that the thermodynamic conditions of Tdissol significantly impacted the properties of the PVDF membranes compared to the varied Tcast conditions. The properties observed for PVDF membranes synthesised by varying the Tcast parameter can relate to the temperature–time plot analysis in chapter 4. The thermodynamic plot of the polymer mixtures shows that implementing a slow cooling process once heating is stopped results in an immediate change that initially occurs with the polymer mixture. However, the changes appear to take a long time to be visible. Hence, similar membrane morphology properties with the PVDF membrane were prepared via Tcast with the flux performance measurement highlighting the difference between all designed PVDF membranes. In general, the study presented contributes to growing research demonstrating the impact of sustainable solvents on the properties of the membrane. Furthermore, the effect of the process variables investigated shows that it is possible to effectively control the membrane structure's reproducibility effectively.

6.5 References

[1] Liu, F., Hashim, N. A., Liu, Y., Abed, M. M., & Li, K. (2011). Progress in the production and modification of PVDF membranes. *Journal of membrane science*, *375*(1-2), 1-27.

[2] Kang, G. D., & Cao, Y. M. (2014). Application and modification of poly (vinylidene fluoride)(PVDF) membranes–a review. *Journal of membrane science*, *463*, 145-165.

[3] Lin, D. J., Beltsios, K., Young, T. H., Jeng, Y. S., & Cheng, L. P. (2006). Strong effect of precursor preparation on the morphology of semicrystalline phase inversion poly (vinylidene fluoride) membranes. *Journal of Membrane Science*, *274*(1-2), 64-72.

[4] Tao, M. M., Liu, F., Ma, B. R., & Xue, L. X. (2013). Effect of solvent power on PVDF membrane polymorphism during phase inversion. *Desalination*, *316*, 137-145.

[5] Jung, J. T., Kim, J. F., Wang, H. H., Di Nicolo, E., Drioli, E., & Lee, Y. M. (2016). Understanding the non-solvent induced phase separation (NIPS) effect during the fabrication of microporous PVDF membranes via thermally induced phase separation (TIPS). *Journal of Membrane Science*, *514*, 250-263.

[6] Buonomenna, M. G., Macchi, P., Davoli, M., & Drioli, E. (2007). Poly (vinylidene fluoride) membranes by phase inversion: the role the casting and coagulation conditions play in their morphology, crystalline structure and properties. *European Polymer Journal*, *43*(4), 1557-1572.

[7] Wang, X., Wang, X., Zhang, L., An, Q., & Chen, H. (2009). Morphology and formation mechanism of poly (vinylidene fluoride) membranes prepared with immerse precipitation: effect of dissolving temperature. *Journal of Macromolecular Science, Part B*, *48*(4), 696-709.

[8] Teixeira, J., Cardoso, V. F., Botelho, G., Morão, A. M., Nunes-Pereira, J., & Lanceros-Mendez, S. (2021). Effect of polymer dissolution temperature and conditioning time on the morphological and physicochemical characteristics of poly (Vinylidene fluoride) membranes prepared by non-solvent induced phase separation. *Polymers*, *13*(23), 4062.

[9] Tsai, H. A., Ruaan, R. C., Wang, D. M., & Lai, J. Y. (2002). Effect of temperature and span series surfactant on the structure of polysulfone membranes. *Journal of applied polymer science*, *86*(1), 166-173.

[10] Ike, I. A., Zhang, J., Groth, A., Orbell, J. D., & Duke, M. (2017). Effects of dissolution conditions on the properties of PVDF ultrafiltration membranes. *Ultrasonics sonochemistry*, *39*, 716-726.

[11] Nawi, N. I. M., Bilad, M. R., & Nordin, N. A. H. M. (2018, April). Effect of dope solution temperature on the membrane structure and membrane distillation performance. In *IOP Conference Series: Earth and Environmental Science* (Vol. 140, No. 1, p. 012032). IOP Publishing.

[12] Yeow, M. L., Liu, Y. T., & Li, K. (2004). Morphological study of poly (vinylidene fluoride) asymmetric membranes: effects of the solvent, additive, and dope temperature. *Journal of Applied Polymer Science*, *92*(3), 1782-1789.

[13] O'Connell, R. A., Porter, A. E., Higgins, J. S., & Cabral, J. T. (2019). Phase behaviour of poly (2, 6-diphenyl-p-phenylene oxide)(PPPO) in mixed solvents. *Polymer*, *180*, 121652.

[14] Ishigami, T., Nakatsuka, K., Ohmukai, Y., Kamio, E., Maruyama, T., & Matsuyama, H. (2013). Solidification characteristics of polymer solution during polyvinylidene fluoride membrane preparation by nonsolvent-induced phase separation. *Journal of Membrane Science*, *438*, 77-82.

[15] Broens, L., Altena, F. W., Smolders, C. A., & Koenhen, D. M. (1980). Asymmetric membrane structures as a result of phase separation phenomena. *Desalination*, *32*, 33-45.

[16] Sukitpaneenit, P., & Chung, T. S. (2009). Molecular elucidation of morphology and mechanical properties of PVDF hollow fiber membranes from aspects of phase inversion, crystallization and rheology. *Journal of Membrane Science*, *340*(1-2), 192-205.

[17] Cheng, L. P., Lin, D. J., Shih, C. H., Dwan, A. H., & Gryte, C. C. (1999). PVDF membrane formation by diffusion-induced phase separation-morphology prediction based on phase behaviour and mass transfer modelling. *Journal of Polymer Science Part B: Polymer Physics*, *37*(16), 2079-2092.

[18] Bottino, A., Camera-Roda, G., Capannelli, G., & Munari, S. (1991). The formation of microporous polyvinylidene difluoride membranes by phase separation. *Journal of membrane science*, *57*(1), 1-20.

[19] Ashtiani, S., Khoshnamvand, M., Číhal, P., Dendisová, M., Randová, A., Bouša, D., ... & Friess, K. (2020). Fabrication of a PVDF membrane with tailored morphology and properties via exploring and computing its ternary phase diagram for wastewater treatment and gas separation applications. *RSC Advances*, *10*(66), 40373-40383.

[20] Annamalai, P. K., Pochat-Bohatier, C., Bouyer, D., Li, C. L., Deratani, A., & Wang, D. M. (2011). Kinetics of mass transfer during vapour-induced phase separation (VIPS) process and its influence on poly-(vinylidene fluoride)(PVDF) membrane structure and surface morphology. *Desalination and Water Treatment*, *34*(1-3), 204-210.

[21] Kim, Y. D., Kim, J. Y., Lee, H. K., & Kim, S. C. (2001). A new modeling of asymmetric membrane formation in rapid mass transfer system. *Journal of Membrane Science*, *190*(1), 69-77.

[22] van de Witte, P. J. D. P., Dijkstra, P. J., Van den Berg, J. W. A., & Feijen, J. (1996). Phase separation processes in polymer solutions in relation to membrane formation. *Journal of membrane science*, *117*(1-2), 1-31.

[23] Wang, X., Wang, X., Zhang, L., An, Q., & Chen, H. (2009). Morphology and formation mechanism of poly(vinylidene fluoride) membranes prepared with immerse precipitation: effect of dissolving temperature. *Journal of Macromolecular Science, Part B*, *48*(4), 696-709.

[24] Han, J. Y., Oh, H. H., Jun Choi, K., & Min, B. R. (2011). Characterization of poly (vinylidene fluoride) flat sheet membranes prepared in various ratios of water/ethanol for separator of li-ion batteries: Morphology and other properties. *Journal of Applied Polymer Science*, *122*(4), 2653-2665.

[25] Guillen, G. R., Pan, Y., Li, M., & Hoek, E. M. (2011). Preparation and characterization of membranes formed by nonsolvent induced phase separation: a review. *Industrial & Engineering Chemistry Research*, *50*(7), 3798-3817.

[26] Lin, D. J., Beltsios, K., Young, T. H., Jeng, Y. S., & Cheng, L. P. (**2006**). Strong effect of precursor preparation on the morphology of semicrystalline phase inversion poly (vinylidene fluoride) membranes. *Journal of membrane science*, *274*(1-2), 64-72.

[27] Nejati, S., Boo, C., Osuji, C. O., & Elimelech, M. (2015). Engineering flat sheet microporous PVDF films for membrane distillation. *Journal of Membrane Science*, *492*, 355-363.

[28] Cui, Z., Hassankiadeh, N. T., Zhuang, Y., Drioli, E., & Lee, Y. M. (2015). Crystalline polymorphism in poly (vinylidenefluoride) membranes. *Progress in Polymer Science*, *51*, 94-126.

[29] Franken, A. C. M., Nolten, J. A. M., Mulder, M. H. V., Bargeman, D., & Smolders, C. A. (1987). Wetting criteria for the applicability of membrane distillation. *Journal of Membrane Science*, *33*(3), 315-328.

[30] Hou, D., Fan, H., Jiang, Q., Wang, J., & Zhang, X. (2014). Preparation and characterization of PVDF flat-sheet membranes for direct contact membrane distillation. *Separation and Purification Technology*, *135*, 211-222.

[31] AlMarzooqi, F. A., Bilad, M. R., & Arafat, H. A. (2016). Development of PVDF membranes for membrane distillation via vapour induced crystallisation. *European Polymer Journal*, *77*, 164-173.

[32] Moradi, R., Karimi-Sabet, J., Shariaty-Niassar, M., & Koochaki, M. A. (2015). Preparation and characterization of polyvinylidene fluoride/graphene superhydrophobic fibrous films. *Polymers*, *7*(8), 1444-1463.

[33] Quetzeri-Santiago, M. A., Castrejón-Pita, A. A., & Castrejón-Pita, J. R. (2019). The effect of surface roughness on the contact line and splashing dynamics of impacting droplets. *Scientific reports*, *9*(1), 1-10.

[34] Wong, P. C. Y., Kwon, Y. N., & Criddle, C. S. (2009). Use of atomic force microscopy and fractal geometry to characterize the roughness of nano-, micro-, and ultrafiltration membranes. *Journal of Membrane Science*, *340*(1-2), 117-132.

[35] Cassie, A. B. D., & Baxter, S. (1944). Wettability of porous surfaces. *Transactions of the Faraday society*, *40*, 546-551.

[36] Dumée, L. F., Gray, S., Duke, M., Sears, K., Schütz, J., & Finn, N. (2013). The role of membrane surface energy on direct contact membrane distillation performance. *Desalination*, *323*, 22-30.

[37] Kumar, R., & Ismail, A. F. (2015). Fouling control on microfiltration/ultrafiltration membranes: Effects of morphology, hydrophilicity, and charge. *Journal of Applied Polymer Science*, *132*(21).

[38] Yuliwati, E., & Ismail, A. F. (2011). Effect of additives concentration on the surface properties and performance of PVDF ultrafiltration membranes for refinery produced wastewater treatment. *Desalination*, *273*(1), 226-234.

[39] Matsuyama, H., Rajabzadeh, S., Karkhanechi, H., & Jeon, S. (2017). 1.7 PVDF Hollow Fibers Membranes. *Comprehensive Membrane Science and Engineering*, 137-189.

[40] Sukitpaneenit, P., & Chung, T. S. (2011). Molecular design of the morphology and pore size of PVDF hollow fiber membranes for ethanol–water separation employing the modified pore-flow concept. *Journal of membrane science*, *374*(1-2), 67-82.

[41] Ahmad, A. L., Ideris, N., Ooi, B. S., Low, S. C., & Ismail, A. (2011). Morphology and polymorph study of a polyvinylidene fluoride (PVDF) membrane for protein binding: Effect of the dissolving temperature. *Desalination*, *278*(1-3), 318-324.

[42] Seguela, R. (2005). Critical review of the molecular topology of semicrystalline polymers: The origin and assessment of intercrystalline tie molecules and chain entanglements. *Journal of Polymer Science Part B: Polymer Physics*, *43*(14), 1729-1748.

[43] Salimi, A., & Yousefi, A. A. (2004). Conformational changes and phase transformation mechanisms in PVDF solution-cast films. *Journal of Polymer Science Part B: Polymer Physics*, *42*(18), 3487-3495.

[44] Tang, Y., Lin, Y., Ma, W., & Wang, X. (2021). A review on microporous polyvinylidene fluoride membranes fabricated via thermally induced phase separation for MF/UF application. *Journal of Membrane Science*, 119759.

[45] Gregorio, Jr, R., & Cestari, M. (1994). Effect of crystallization temperature on the crystalline phase content and morphology of poly (vinylidene fluoride). *Journal of Polymer Science Part B: Polymer Physics*, *32*(5), 859-870.

[46] Martins, P., Lopes, A. C., & Lanceros-Mendez, S. (2014). Electroactive phases of poly (vinylidene fluoride): Determination, processing and applications. *Progress in polymer science*, *39*(4), 683-706.

[47] Gregorio Jr, R. (2006). Determination of the α, β, and γ crystalline phases of poly (vinylidene fluoride) films prepared at different conditions. *Journal of Applied Polymer Science*, *100*(4), 3272-3279.

[48] Boccaccio, T., Bottino, A., Capannelli, G., & Piaggio, P. (2002). Characterization of PVDF membranes by vibrational spectroscopy. *Journal of membrane science*, *210*(2), 315-329.

[49] Liu, Y., Sun, Y., Zeng, F., Chen, Y., Li, Q., Yu, B., & Liu, W. (2013). Morphology, crystallization, thermal, and mechanical properties of poly (vinylidene fluoride) films filled with different concentrations of polyhedral oligomeric silsesquioxane. *Polymer Engineering & Science*, *53*(7), 1364-1373.

[50] Ribeiro, C., Costa, C. M., Correia, D. M., Nunes-Pereira, J., Oliveira, J., Martins, P., ... & Lanceros-Mendez, S. (2018). Electroactive poly (vinylidene fluoride)-based structures for advanced applications. *Nature protocols*, *13*(4), 681-704.

[51] Inoue, M., Tada, Y., Suganuma, K., & Ishiguro, H. (2007). Thermal stability of poly (vinylidene fluoride) films pre-annealed at various temperatures. *Polymer Degradation and Stability*, *92*(10), 1833-1840.

[52] Song, D., Yang, D., & Feng, Z. (1990). Formation of β-phase microcrystals from the melt of PVF 2-PMMA blends induced by quenching. *Journal of materials science*, *25*(1), 57-64.

[53] Soin, N., Boyer, D., Prashanthi, K., Sharma, S., Narasimulu, A. A., Luo, J., ... & Thundat, T. (2015). Exclusive self-aligned β-phase PVDF films with abnormal piezoelectric coefficient prepared via phase inversion. *Chemical Communications*, *51*(39), 8257-8260.

[54] Mohammadi, B., Yousefi, A. A., & Bellah, S. M. (2007). Effect of tensile strain rate and elongation on crystalline structure and piezoelectric properties of PVDF thin films. *Polymer testing*, *26*(1), 42-50.

[55] Bormashenko, Y., Pogreb, R., Stanevsky, O., & Bormashenko, E. (2004). Vibrational spectrum of PVDF and its interpretation. *Polymer testing*, *23*(7), 791-796.

[56] Pramoda, K. P., Mohamed, A., Yee Phang, I., & Liu, T. (2005). Crystal transformation and thermomechanical properties of poly (vinylidene fluoride)/clay nanocomposites. *Polymer international*, *54*(1), 226-232.

CHAPTER 7

Use of a biobased and a low-hazard solvent blend to fabricate PVDF membranes

7.1 Introduction

In the previous study, synthesised PVDF membranes using a bio based green solvent GVL resulted in mostly spongy/dense membranes with no water flux permeation at low pressures. Typically, membranologists have proposed several efficient techniques for preparing PVDF membranes, which consist of crosslinking [1], surface grafting [2], and blending of polymers [3,4] with solvents to obtain different morphological structures that might offer improved water performance. Solvents blends have previously been researched for fabricating polymeric membranes [5,6] because cosolvent work as materials that can either increase or reduce the solvent power in the polymer dope during fabrication. Cosolvency is a phenomenon broadly reported in ternary systems where polymers are soluble in binary mixtures of two solvents. In addition, cosolvent has been reported as a promising strategy for fabricating the PVDF membrane process and achieving improved performance [7]. Based on the morphological structures obtained from the PVDF/GVL/water system, a cosolvent is introduced to determine if the dense top layer and spongy globule-like structure can be modified or eliminated to improve the membrane performance. Primarily, the mutual affinity between components used to prepare membranes via the NIPS influences the thermodynamics and kinetic aspect of the polymer system during the fabrication stage. The PVDF/GVL system's thermodynamic analysis revealed low mutual affinity, resulting in delayed demixing. Therefore, using a non-toxic cosolvent to influence the diffusive exchange rate between solvent and nonsolvent during the membrane formation process might be advantageous when using the appealing preparative nonsolvent induced phase separation (NIPS) method. The composition of the cosolvent solutions and choice of nonsolvent will influence the solvent exchange rate, define the phase inversion path of the fabrication process [8] and impact the morphology, mechanical properties, interfacial characteristics, and separation performance of the final membrane [9,10].

Polymeric membranes can be particularly attractive if the designed preparative process using green and non-toxic solvents can improve the membrane structure and achieve excellent separation performance (desired applicability) [11]. The closet substitute for traditional toxic solvents such as NMP, DMF and DMAc in terms of polarity and capability of dissolving PVDF is dimethyl sulfoxide (DMSO) which has been used to fabricate PVDF membrane [12,13].

DMSO is derived from lignin, a renewable source, and it is one of the most potent organic solvents that can be found naturally in the environment and natural waters. DMSO is well known for having excellent solvent power for many organic and inorganic compounds [14]**.** The solvent is completely miscible with water, is simple to recycle after use, and contributes significantly to the natural global sulphur cycle due to its widespread presence in nature and rapidly dilutes on exposure to air [15]. DMSO acts as a permeability enhancer and is employed in the medical industry for several drugs to improve skin adsorption [16,17]. It is commercially available and relatively affordable. Its low level of acute toxicity raises some concerns about in vitro assays. However, it is reported to have less adverse health impact and environmental damage [18] when applied in a small-scale application. The solvent's high boiling point enables it to dissolve various polysulfones and fluoropolymers. Several studies demonstrate its successful use as an alternative non-toxic solvent to prepare porous PVDF membranes [19] for ultrafiltration and membrane distillation processes. Characterisation of these membranes reveals polymeric membranes prepared using DMSO to exhibit dense and large porous membranes with water contact angles within 70-85° for PVDF concentration between 10-20 wt%. Characterisation of membrane thickness and porosity were given to be ≥100µm and ≥68%, respectively. Furthermore, the quality of the PVDF membranes prepared using DMSO demonstrated high pure water flux between 116 -390 $L.m^{-2}.h^{-1}$ [20].

Table 7-1 compares the physical and chemical characteristics of GVL with DMSO. The selected non-toxic solvents γ-valerolactone (GVL) and dimethyl sulfoxide (DMSO) with chemical structure shown in figure 7.1 were chosen due to their minimal environmental impact, physical properties, polarity, and capability to dissolve PVDF [21]. These two solvents will be used as a cosolvent to improve membrane morphology and performance function.

.

Gamma-valerolactone (GVL) Dimethyl sulfoxide (DMSO)

Figure 7.1. Schematic diagram showing the chemical structure of considered aprotic solvents.

Table 7-1: Different solvent Chemical and physical properties [22]

Solvent Properties	**Gamma-valerolactone** (GVL)	**Dimethyl sulfoxide** (DMSO)
CAS-No	108-29-2	67-68-5
Molecular Formula	$C_5H_8O_2$	C_2H_6OS
Boiling point (°C)	207	189
Molecular weight	100.12	78.13
Solubility in water (mg/ml)	Miscible	Miscible
Melting point (°C)	-31	18.5
Density (g mL^{-1})	1.05	1.10
Flashpoint (°C)	96	89
Standard enthalpy change of vapourisation ΔHvap (kJ mol^{-1})	54.8	52.9
Enthalpy of combustion ΔcH°liquid (kJ mol^{-1})	-2649.6	-2037.3
Refractive index (n20/D)	1.432	1.479
Viscosity at 25°C (cP)	2.18	1.991
Kinematic viscosity (m^2/s) at (40°C)	2.1×10^{-6}	1.38×10^{-6}
Hazard code/Signal	Not a hazardous substance	Warning/H227
Acute Toxicity (LD50 Oral)-(mg/kg) (Rat)	8800	28300
Hodge and Sterner's classification	5-practically non-toxic	5-practically non-toxic

The study presented in this chapter aims to develop porous PVDF membranes with improved performance for water filtration using selected non-toxic solvent/cosolvent (GVL/DMSO) that have a minimal environmental impact as alternative solvents other than the traditional toxic solvents. Furthermore, it supports the ongoing push for sustainable polymeric membrane production that is environmentally friendly and aims to reduce or eliminate global

climate change by using solvents that are renewable and non-toxic. The initial work focused on theoretical and experimental PVDF/GVL/DMSO solubility analyses to achieve a stable homogenous polymer solution. A predetermined set of selected ratios of the solvent/cosolvent concentration are used to examine the impact of the cosolvent in fabricating free-standing tailored-made PVDF membranes. The chapter examines how the solvent blend affects the membrane's structure, surface roughness, porosity, water contact angle (wettability behaviour) or performance.

7.2 Experimental study

7.2.1 Materials

Polyvinylidene fluoride (PVDF, pellets, product code: 1002616042; M_w 275,000 g.mol^{-1}, M_n 107,000 g.mol^{-1}), gamma-Valerolactone (GVL, ≥ 99%), dimethyl sulfoxide (DMSO ≥ 99.5%), and 2-Propanol (IPA) were all purchased from Sigma-Aldrich, UK. Deionised water was used with a resistivity of 18.4 MΩ cm at 25 °C (Milli-Q). All materials and solvents were used as received for the experimental material fabrication without further purification.

7.2.2 Interaction parameters and solubility assessment of the PVDF/GVL/DMSO system

The premise for phase inversion is to ensure the solvent/cosolvent can dissolve the selected polymer (PVDF). Thus, the polymer, solvent and cosolvent interaction was examined theoretically and experimentally. The ability to predict the solubility/miscibility of components was determined theoretically by evaluating the Hansen solubility parameters (HSPs) due to its simplicity, and it is commonly used in combination with experimental results[23]. Since PVDF was dissolved in a binary solvent, the cosolvent mixture's corresponding solubility parameters were determined using equations (1-3).

$$\delta_d = \frac{x_1 v_1 \delta_{d1} + x_2 v_2 \delta_{d2}}{x_1 v_1 + x_2 v_2} \quad (1)$$

$$\delta_p = \frac{x_1 v_1 \delta_{p1} + x_2 v_2 \delta_{p2}}{x_1 v_1 + x_2 v_2} \quad (2)$$

$$\delta_h = \frac{x_1 v_1 \delta_{h1} + x_2 v_2 \delta_{h2}}{x_1 v_1 + x_2 v_2} \quad (3)$$

Where subscripts 1 and 2 represent the solvent and cosolvent, x and v indicates the molecular fraction and volume of the solvents, while $\delta_d, \delta_p, \delta_h$ represent the dispersive, polar and hydrogen bonding interactions [24,25]. In addition, the HSP distance and a relative energy difference (RED) in equation (4-5) were used as a good evaluation indicator to describe the affinity between the polymer (PVDF) and considered cosolvent (GVL/DMSO) mixture. Theoretical determined solubility interaction distance (R_a) in Hansen space is a small value, and reported studies have suggested the solubility of components with $R_a \leq 8$ MPa$^{1/2}$. Typically, good solvents tend to have their distance from the centre of the sphere between the solvent and polymer R_a less than the radius of the Hansen solubility parameter sphere of the polymer R_o. Thus, a RED value between 0 and 1 indicates the affinity of polymer/solvents to form a homogeneous solution [26,27]. It should be noted that the stated threshold value of R_a is arbitrary as several studies have proposed different acceptable values [28] that showed solvent dissolves the polymer. Due to these components' interaction and influence on the polymer's behaviour in the solution. Therefore, an experimental attempt was conducted to examine the solubility and the ageing effect on different compositions of PVDF and the solvent blend

$$R_a = \sqrt{4\left(\delta_{p,d} - \delta_{s,d}\right)^2 + \left(\delta_{p,p} - \delta_{s,p}\right)^2 + \left(\delta_{p,h} - \delta_{s,h}\right)^2} \quad (4)$$

$$RED = \frac{R_a}{R_o} \quad (5)$$

Where the subscript $P\ and\ S$ represents the polymer and solvent.

7.3 Results and discussion

7.3.1 Solubility and thermodynamic analysis of the PVDF/GVL/DMSO system.

The compatibility of PVDF with binary solvent mixtures was determined by evaluating the theoretical solubility parameters of components of the PVDF system. A rational design parameter was implemented, and different combinations of the binary mixture were assessed with an increased cosolvent concentration. Analysis of the R_a and RED values provided a qualitative indicator to compare the solubility difference of the prepared dope mixtures. The Hansen theory is based on a "like-dissolves-like" principle and δ_T reveals similar relative parameters among polymers and solvents. The calculated result of the Hansen

solubility parameter for varying concentrations of solvent/cosolvent is summarised in Tables 7-2 and 7-3.

Table 7-2: Hansen's solubility parameters of the polymer

Polymer/solvent blends	δ_d $\left(\mathrm{MPa}^{1/2}\right)$	δ_p $\left(\mathrm{MPa}^{1/2}\right)$	δ_h $\left(\mathrm{MPa}^{1/2}\right)$	δ_T $\left(\mathrm{MPa}^{1/2}\right)$	R_o $\left(\mathrm{MPa}^{1/2}\right)$	R_a $\left(\mathrm{MPa}^{1/2}\right)$
PVDF	17.2	12.5	9.2	23.17	4.1	-
GVL	17.6	10.5	9.1	21.74		3.07
DMSO	18.4	16.4	10.2	26.68		4.69

Table 7-3: Calculated HSP and interaction values for binary mixtures and PVDF

Membrane code	GVL - Solvent (wt.%)	DMSO - Cosolvent (wt.%)	δ_d $\left(\mathrm{MPa}^{1/2}\right)$	δ_p $\left(\mathrm{MPa}^{1/2}\right)$	δ_h $\left(\mathrm{MPa}^{1/2}\right)$	δ_T $\left(\mathrm{MPa}^{1/2}\right)$	R_a $\left(\mathrm{MPa}^{1/2}\right)$	RED	$\Delta\delta$(GVL/DMSO-H_2O) $\left(\mathrm{MPa}^{1/2}\right)$
M-GD80-20	80	20	17.4	12.8	7.0	22.68	2.24	0.55	35.6
M-GD60-40	60	40	17.6	13.7	7.8	23.64	2.03	0.49	34.8
M-GD40-60	40	60	17.9	14.6	8.6	24.63	2.57	0.63	34.1
M-GD20-80	20	80	18.1	15.5	9.4	25.64	3.54	0.86	33.3

The small RED values below 1 theoretically indicate better solvent quality for the polymer's solubility. However, the experimental analysis showed that PVDF/GVL/DMSO mixtures were not miscible at ambient temperature despite the small interaction RED values. Results show miscibility was achieved at temperatures above 60°C for low PVDF concentrations. The experimental thermodynamic analysis of predetermined PVDF solutions consisting of PVDF/GVL/DMSO was carried out to identify stable homogenous dope solutions compositions that can be selected to fabricate the PVDF membrane. The thermodynamics is related to the phase equilibria between the components of the considered PVDF system, and the stability of the polymer dope before casting is an essential property in the phase inversion process. Figure 7.2 depicts the PVDF/GVL/DMSO isothermal ternary plot, and identifies potential thermodynamically viable polymer solutions at 30°C.

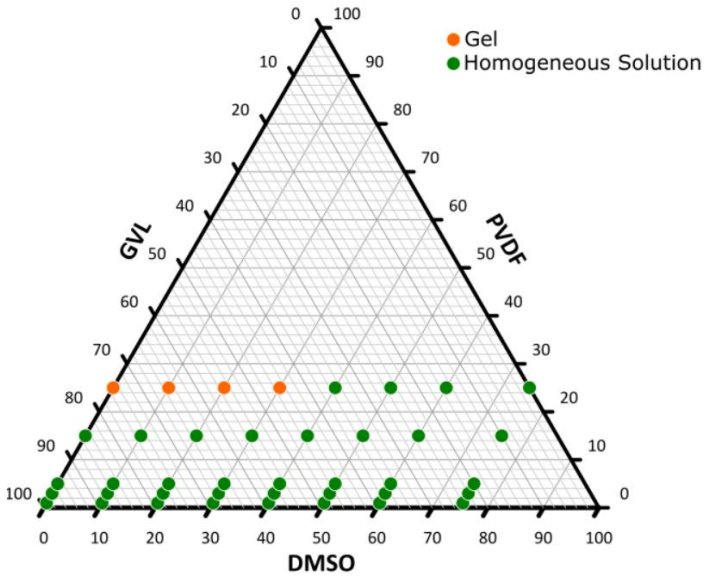

Figure 7.2: Ternary solution map diagram of the PVDF/GVL/DMSO system at 30°C

7.3.2 Conditions of membrane fabrication

The membrane fabrication conditions and compositions of polymer, solvent and cosolvent concentrations are summarised in table 7-4. The fabrication procedure is discussed in chapter 3.

Table 7-4: Composition of PVDF prepared membrane and conditions.

Membrane nomenclature	PVDF (wt.%)	GVL (wt.%)	DMSO (wt.%)	Dissolved Polymer temperature	Gelation/phase separation due to ageing of polymer dope (Days)
M-G80-D20	15	68	17	90	2
M-G60-D40	15	51	34	90	8
M-G40-D60	15	34	51	90	9
M-G20-D80	15	17	68	90	10
M15-DMSO	15	0	85	90	>15 days

Note: The casting (Tcast) and coagulation (Tcoag) temperatures are kept constant at 30°C, and water is used as nonsolvent

The ageing of the different dope solutions at a fixed temperature of 30° predicts the solvent/cosolvent power strength and reveals the thermodynamically stable dope concentration mixture over time. Results indicate an increased concentration of cosolvent

demonstrated a prolonged duration of polymer solution stability before gelation or phase separation of samples.

7.3.3 SEM analysis of flat sheet PVDF membranes

The cross section and top surface of the prepared PVDF membrane as a function of different concentrations of cosolvent addition in the dope solution are presented in figure 7.3. The observed morphologies show a noticeable difference in the structure of the fabricated membranes under the same controlled condition. The membrane morphology transitioned from a dense spongy-like cross-section structure for the "M-G80-D20" sample to membranes with finger-like. These tear-like structures elongated and transcended into macrovoids as the cosolvent concentration increases

The observation of the PVDF membrane morphologies correlates to the idea that both delayed and rapid onset of liquid-liquid demixing in the cast film occurred. Studies have reported that a spongy-like matrix is associated with a delayed demixing process [29,30], and macrovoids formation with a finger-like structure is related to fast precipitation during the membrane formation process [31,32]. Hence, depending on the concentration of cosolvent, one of the two phenomena was the dominant phase separation process. Furthermore, the asymmetric membrane structure of the PVDF membranes prepared from the different cosolvent concentrations consists of a very thin top layer, suggesting the membrane morphology can be controlled using a cosolvent. The coexistence of finger-like macrovoids and sponge layers for PVDF membrane structure shows that the properties of membranes would differ in terms of porosity and membrane performance.

Traditionally, small interaction distance (R_a) values indicate increased mixing tendency based on Hasen solubility parameters. Based on the determined interaction parameter distance of PVDF/GVL and PVDF/DMSO, the quantitative prediction of the polymer-solvent affinity contradicts experimental studies as the PVDF/GVL showed a lower solubility tendency. Thus, comparing the morphological structures of the PVDF membranes prepared from either GVL or DMSO as solvent reveals a significant unexpected difference in macrovoid formation and suppression not anticipated.

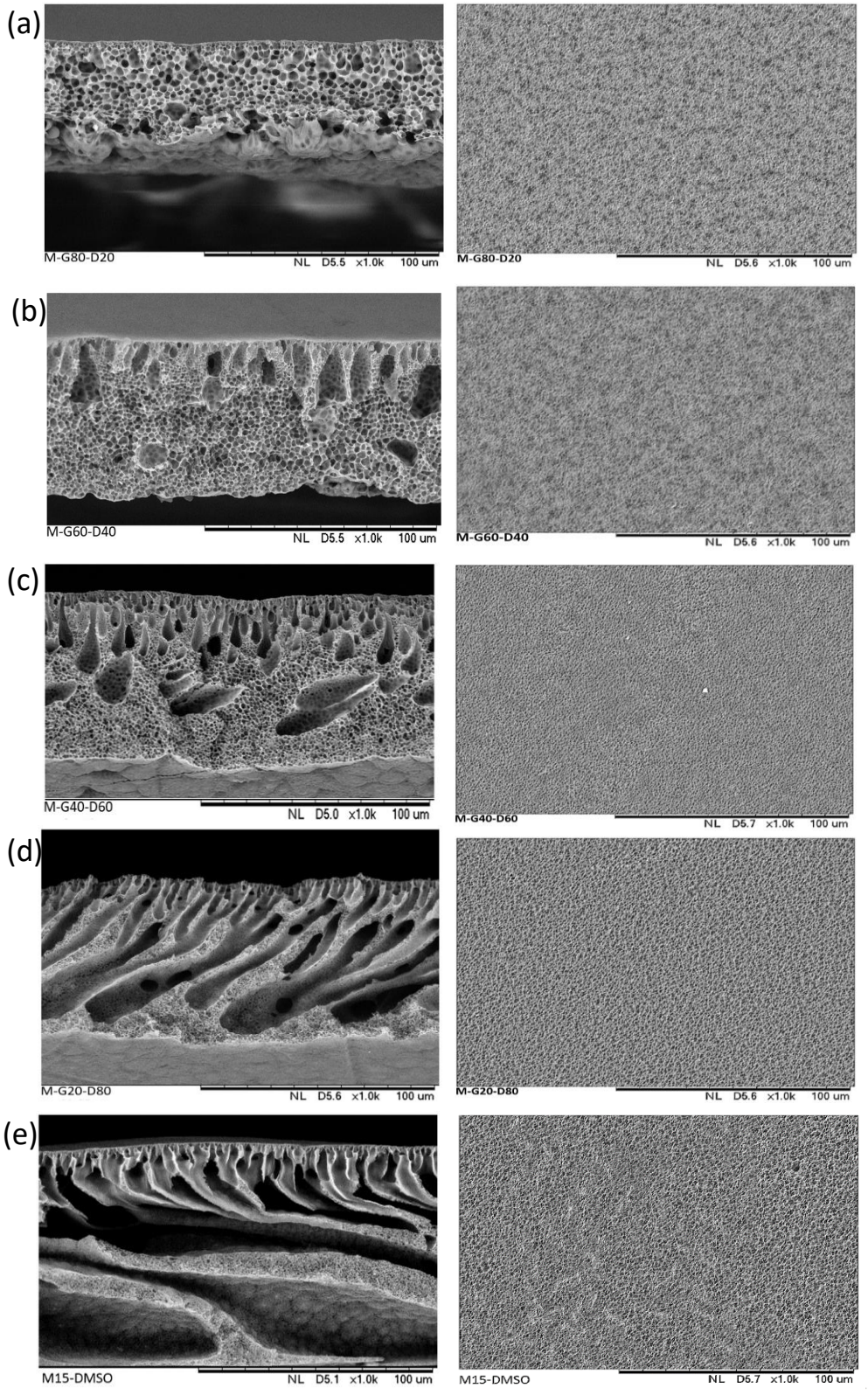

Figure 7.3: SEM images of PVDF membranes prepared using different concentrations of GVL/DMSO as a mixed solvent and DMSO as solvent. [Concentration of DMSO solvent added is given (a) 17wt% DMSO; (b) 34wt% DMSO; (c) 51wt% DMSO; (d) 68wt% DMSO; (e) 85wt% DMSO].

The macrovoids observed in the sublayer of the PVDF/GVL/DMSO system compared to the PVDF/GVL system suggests that the addition of the cosolvent is the main reason for the increased mutual affinity and the diffusional exchange rate between the nonsolvent (water) and the mixed solvent (GVL/DMSO). Thus the composition of the dope solutions and the ability of how well solvent and nonsolvent mix appear to control the liquid-liquid demixing process and dictate the final obtained membrane morphology.

The phase separation phenomenon is a more complex process for a quaternary polymer system due to interactions between polymer components and mutual diffusivities. In addition, the potential gradient and diffusion rate between the cast film and nonsolvent are extremely fast at the onset of the phase inversion, and as the concentration gradient levels out, the diffusion rate gradually decreases, making it difficult to understand [33,34]. However, assessing the top surface for fabricated PVDF membranes using DMSO or mixed solvent showed that an open interconnected pore structure was achieved with increased cosolvent concentration. This observation could be significant in the analysis of the membrane performance.

7.3.4 Membrane Thickness and Porosity Analysis

The fixed PVDF concentration of 15wt% with increased cosolvent concentration showed a final membrane average thickness between 48.36 ±1.2µm and 96.50 ±1.6 µm with data presented in Table 7-5.

Table 7-5: PVDF membrane thickness and porosity of asymmetric PVDF membrane

Membrane	Membrane thickness (µm) SEM	Mean pore size (µm)	Overall porosity (%)
M-GD80-20	48.36 (±1.2)	0.166	62.44 (±1.8)
M-GD60-40	66.09 (±2.4)	0.172	68.21 (±2.1)
M-GD40-60	66.25 (±1.8)	0.272	69.48 (±1.2)
M-GD20-80	93.60 (±1.3)	0.483	74.72 (±2.2)
M15-DMSO	96.50 (±1.6)	0.368	67.43 (±3.4)

The PVDE membrane “M-G80-D20” exhibited the lowest membrane thickness of 48.36µm. On the other hand, “M15-DMSO” had the highest thickness, indicating that the final thickness of the membrane depended on the concentration of the cosolvent since a fixed cast thickness knife was used to fabricate PVDF membranes. Analysis of membrane thickness also

highlights the solvent strength of GVL and DMSO with PVDF, which is opposite to the conclusion of the HSPs evaluation. Furthermore, the observed increased appearance of the finger-like/macrovoids structures due to the demixing rate is likely to have contributed to the increased thickness of the final PVDF membrane compared to a closely packed spongy structure. The PVDF membrane porosity results ranged from 62% to 74% and showed good agreement with values for PVDF membranes made using the NIPS method. There was no direct correlation between the thickness and porosity of the PVDF membrane. However, observation of pore measurement shows that the addition of the cosolvent DMSO enhances the formation of pores in the membrane, which could likely improve the performance of the membrane.

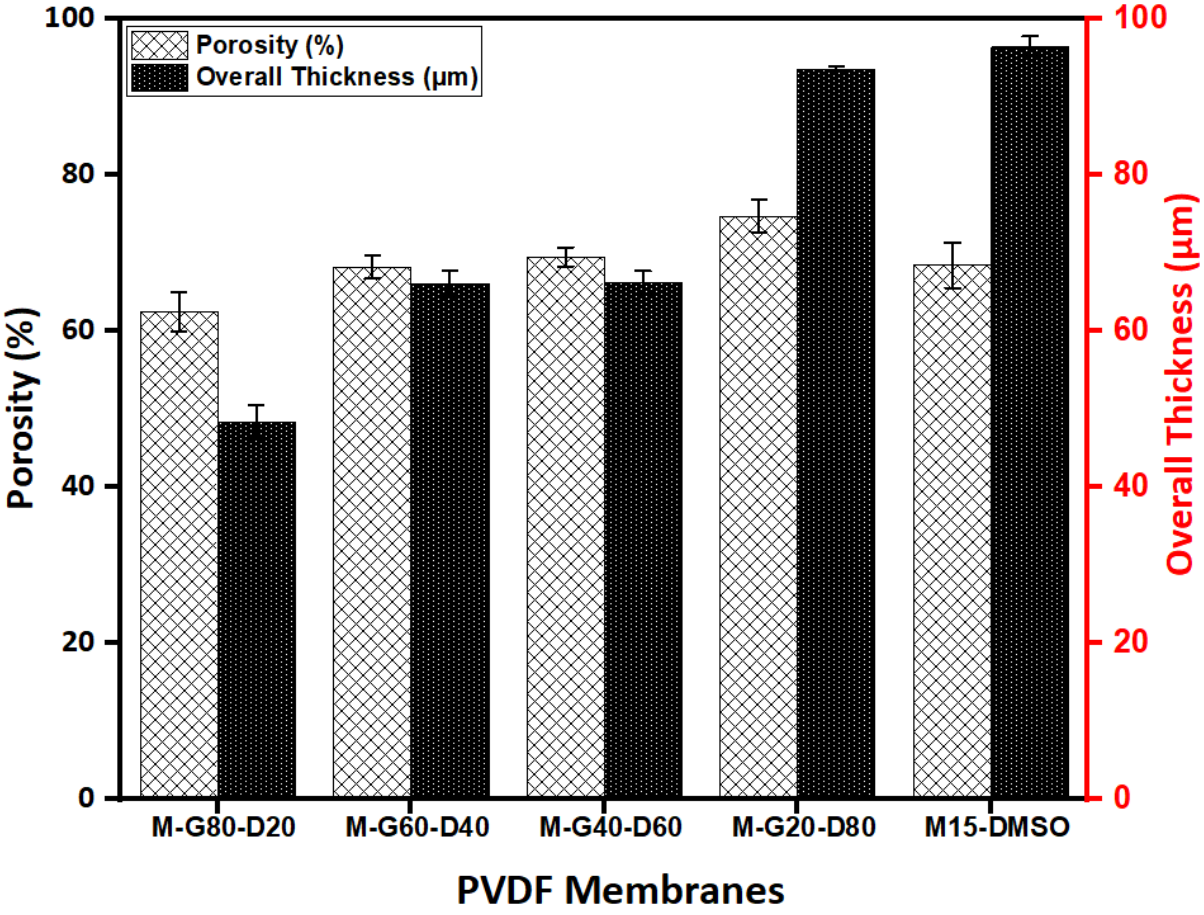

Figure 7.4: Membrane thickness and porosity of PVDF membrane containing different cosolvent concentrations

7.3.5 Surface Roughness and Contact angle measurement

The PVDF membrane's wettability characteristics were measured as the static water contact angle on the top surface, with results in Table 7-6. The wettability analysis of the PVDF membrane is a crucial parameter that highlights the potential suitability of the PVDF

membrane for specific processes such as membrane distillation [35]. The contact angles of the PVDF membranes were between 80.25 (±2.1) and 88.31 (±3.3), which was within borderline regarding reported wettability measurements for PVDF membranes [36,37,38]. However, the contact angle hydrophilicity results have been associated with a flattening effect due to the polymer chain mobility at the top of the cast film when immersed in a strong nonsolvent with high surface tension during the membrane formation process. Hence the large interfacial tension gap forces suppression of the polymer chain downwards into the polymer matrix.
Furthermore, the surface wettability measurement shows that the prepared membranes resulted in a decreased adhesive force between the liquid and membrane. The reduction of membrane contact angle measurement has been related to the membrane's surface roughness and pore structure [39,40,41], which indicates that increased surface roughness suppresses the wettability of the material and increases the hydrophilic behaviour of the membrane.

Table 7-6: Effect of roughness and wettability behaviour on prepared PVDF membrane

Membrane	**Contact angle (°)**	R_a **(nm)**	(R_q) **(nm)**	R_{max} **(nm)**
M-G80-D20	88.31 (±3.3)	12.87	16.18	219.30
M-G60-D40	84.03 (±4.1)	11.18	14.33	216.50
M-G40-D60	79.90 (±1.3)	12.08	15.81	145.10
M-G20-D80	80.25 (±2.1)	8.374	12.85	200.6
M15-DMSO	85.08 (±3.2)	22.97	28.96	282.6

The PVDF membranes became relatively hydrophilic with polymer dope cast as the cosolvent concentration was systematically increased. The water contact angle properties of the developed membranes are encouraging and support the hypothesis that cosolvent could modify the structure of membranes and result in changes in the PVDF membrane's performance. Illustrated in figure 7.5 is the water contact measurement and root mean square roughness values of the PVDF membrane due to the effect of increased cosolvent compositions in the polymer dope.

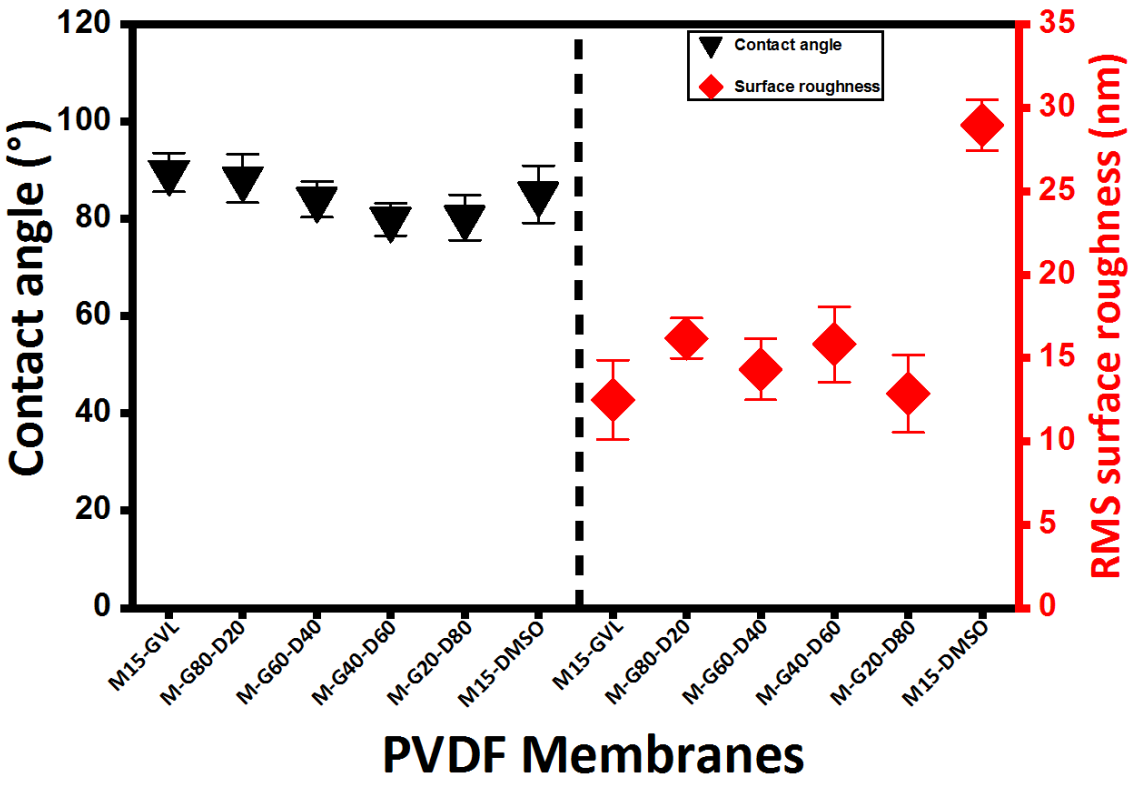

Figure 7.5: Surface roughness and water contact angle for PVDF membranes prepared using non-toxic binary solvents via NIPS.

The surface topology was characterised using atomic force microscopy. The three-dimensional AFM images in figure 7.6 reveal that the PVDF membrane surfaces possess valley-like and nodule-like structural ridges. The denoted dark depressions are appearances that indicate the surface's valleys, such as the relative pore formations on the membrane surface and the bright peaks representing the nodular protrusion of the membrane. The determined surface roughness reveals that the PVDF membranes prepared with a low concentration of DMSO in the solvent mixture featured a higher average roughness (R_a), maximum roughness (R_{max}) and the root mean square (RMS) roughness (R_q), was slightly different in magnitude from ~13nm to ~16nm. An outlier was observed for the "M-G60-D40" membrane sample, but this could be related to artefacts of the membrane [42] or provide further information about the properties of these tailored PVDF membranes. In addition, PVDF membranes prepared with pure DMSO as solvent reveal an increased RMS roughness that is likely related to the kinetic process between the cast film and nonsolvent during fabrication [43]. The difference in wetting property and roughness measurement indicates that the membrane performance would be impacted.

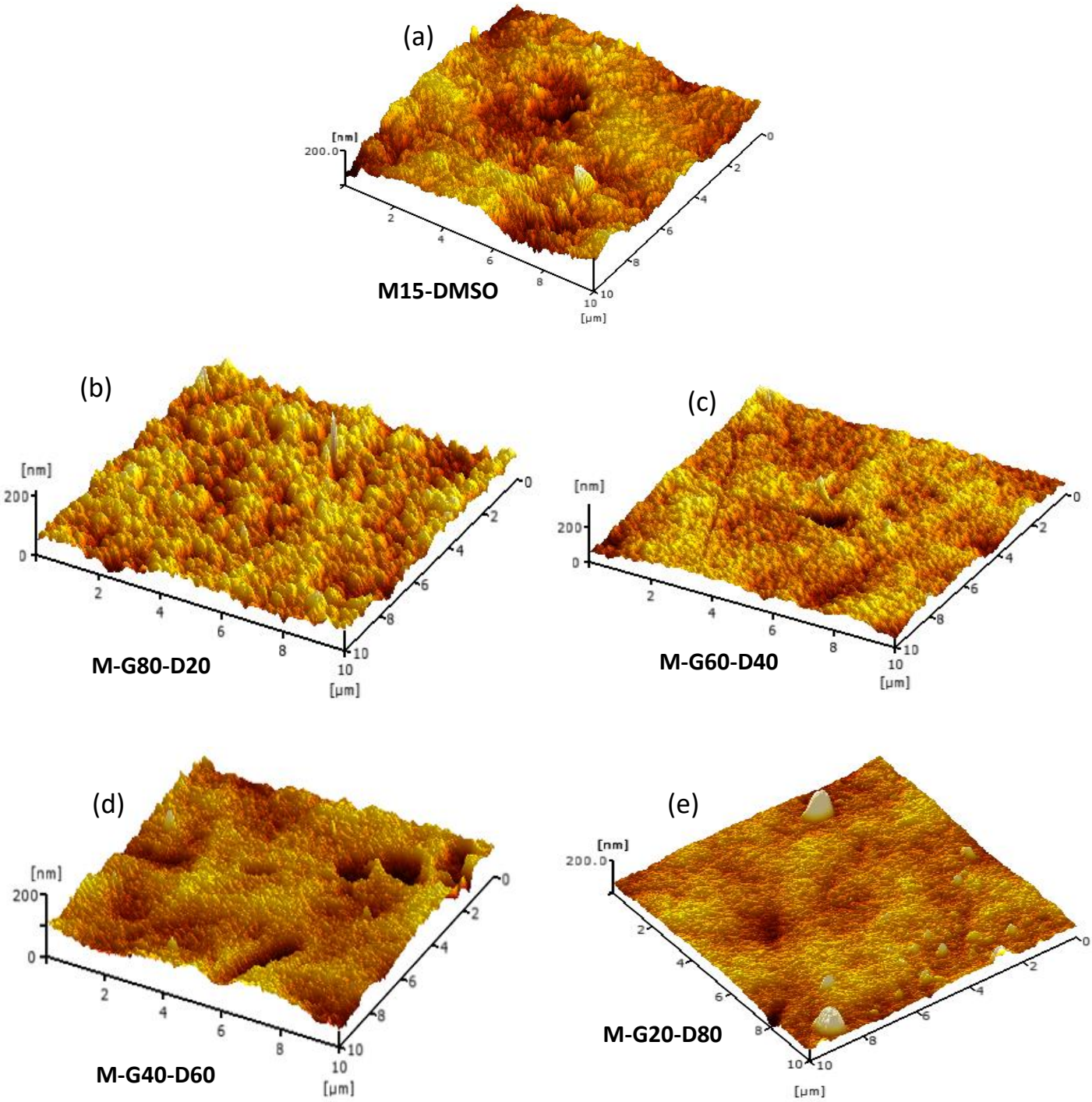

Figure 7.6: 3D AFM images of the top surface morphology for PVDF membrane prepared from pure DSMO and a mix of GVL/DMSO concentrations. [(a) no DMSO added; (b) 20wt% DMSO; (c) 40wt% DMSO; (d) 60wt% DMSO; (e) 80wt% DMSO;]

7.3.6 Crystallinity of PVDF membrane

The differential scanning calorimeter (DSC) was used to study the contribution of the melting temperature and crystallinity percentage of the PVDF membranes due to the

influence of mixed solvent in the casting solution. Presented in Table 7.7 is the data on the melting peak and degree of crystallinity of the PVDF membranes prepared with various concentrations of cosolvent.

Table 7-7: Thermal behaviour properties in different concentrations of binary mixtures

Membrane	Melting temperature (°C)	Crystallisation temperature (°C)	Enthalpy	Degree of crystallinity (%)
M-G80-D20	168(±1)	141.2	46.53 (±3.2)	42.98 (±2.3)
M-G60-D40	169(±1)	141.6	44.58 (±2.4)	38.36 (±2.1)
M-G40-D60	167(±1)	141.8	45.26 (±1.8)	40.22 (±3.3)
M-G20-D80	168(±2)	141.8	45.48 (±2.1)	40.82 (±2.1)
M15-DMSO	167(±2)	141.5	45.74(±2.3)	43.69 (±1.4)

All systems were prepared with an initial polymer concentration of 15wt.%

The thermogram of the prepared membrane shown in figure 7.7 shows a single melting endotherm of the PVDF membranes with an average melting peak at 168°C(±1), which was within the reported values mentioned in the literature for PVDF membranes [44]. However, the PVDF pellet melting temperature was recorded as 172°C (±1), indicating that adding mixed solvent decreased the polymer's melting temperature.

All prepared membranes exhibited crystalline structure with a degree of crystallinity within 39% to 44% (figure 7.8). These crystalline fractions can be linked to the semi-crystalline property of PVDF and the changes in the compositional pathway from the initial polymer solution to the final membrane solidification composition, which occurred during the PVDF membrane formation process via NIPS. The crystallinity results indicate that increased cosolvent concentrations could sterically promote or hinder the growth of individual crystallites and polymer agglomeration during the fabrication process. In addition, the crystallinity result obtained for the PVDF membrane samples indicates that the presence of crystalline domain regions may affect the membrane's permeability and perm-selectivity. The PVDF membrane's crystalline properties might enhance its barrier capabilities and decrease the volume fraction of the membrane that is accessible to permeants.

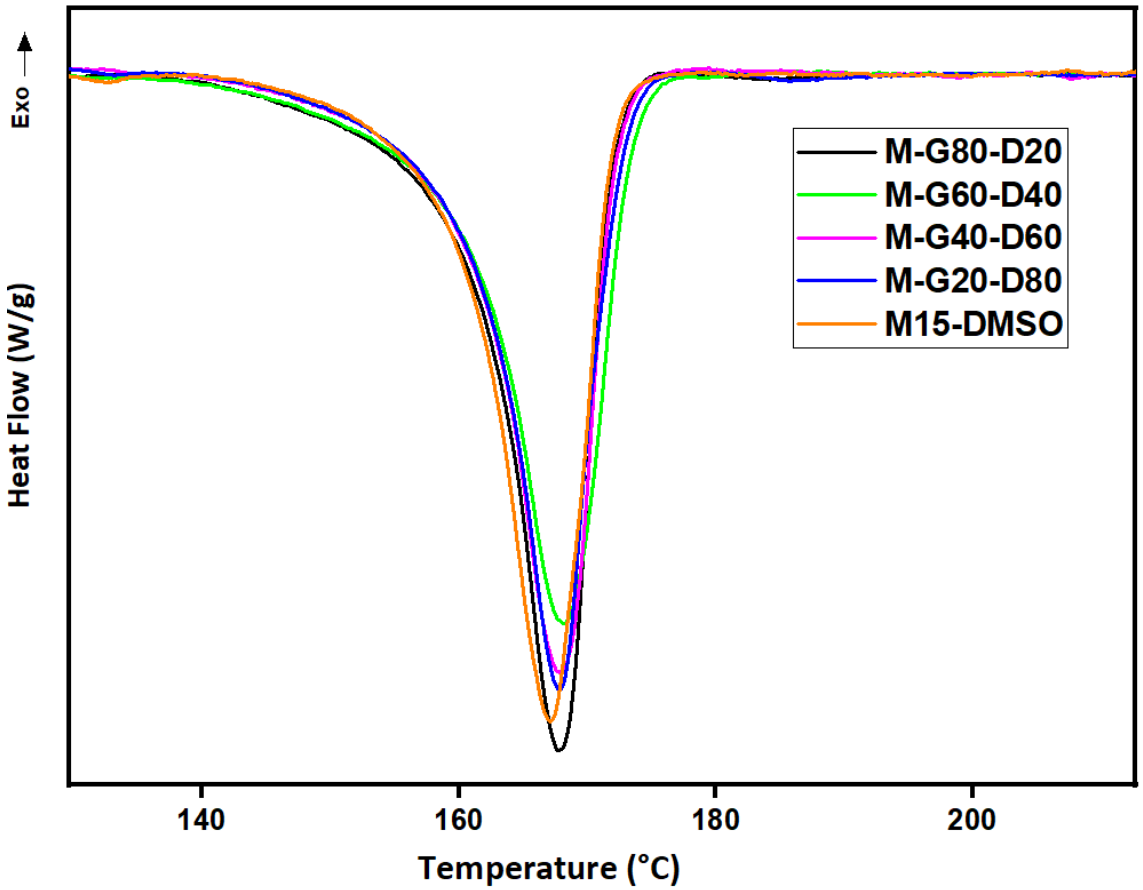

Figure 7.7 : DSC thermograms for PVDF membranes due to solvent/cosolvent blend effect.

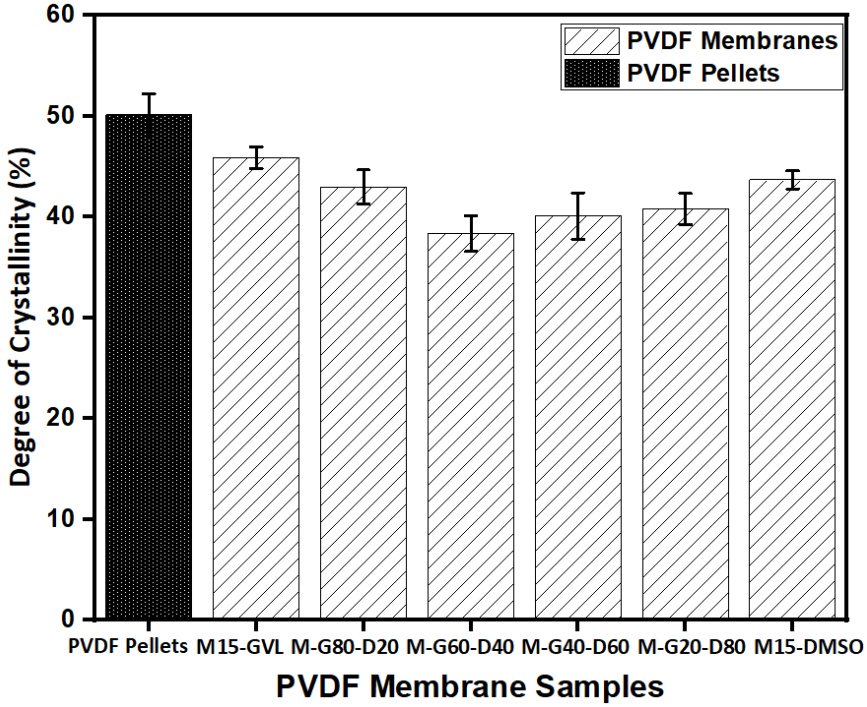

Figure 7.8 : Determined degree of crystallinity for PVDF membranes due to solvent/cosolvent blend effect.

7.3.7 FTIR-ATR Analysis (crystal structure)

The FTIR-ATR is used to evaluate the specific crystalline phases of the prepared PVDF membranes. The differential scanning calorimetric (DSC) analysis revealed that only one endotherm was observed in the PVDF films, corresponding to crystal melting and not correlating to multiple crystal phases. Figure 7.9 displays the FTIR-ATR spectra of the prepared PVDF membrane samples from varying solvent/cosolvent blend and pure cosolvent concentrations within a spectral region of 600 – 1800 cm^{-1}. Several peaks were observed; hence the characteristic band of the crystalline phase was identified using reported information in the literature [45].

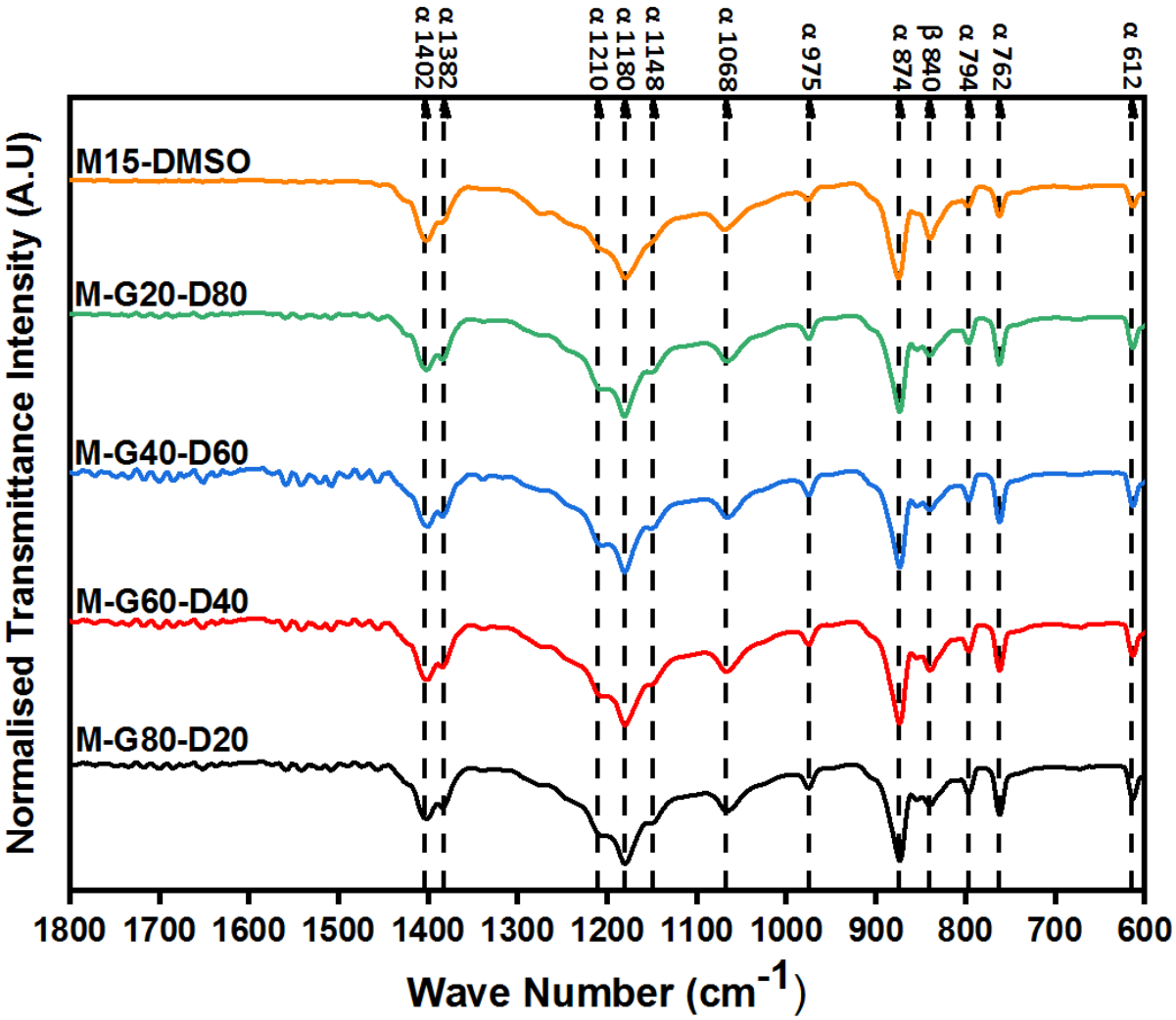

Figure 7.9: FTIR-ATR spectra of top surface PVDF membrane prepared with varying solvent/cosolvent ratios.

The PVDF membrane samples exhibit common polymorphs characteristics of the kinetically favourable trans-gauche-trans-gauche (TGTG) non-polar α-phase form with wavenumbers at 612, 762, 796, 874, 976 and an all-trans conformation (TTTT) stable thermodynamically polar β- phase band with intensity at 840 and 1275 cm-1 [46,47]. Analysis

shows that FTIR spectra were similar for each membrane sample. The difference was the varying range of peak intensity exhibited. The absorbance values of the peak of each PVDF membrane were taken as the reference for calculating relative changes in the intensities of the other peaks. Evaluation of the β-phase crystalline fraction ($F(\beta)$) of the PVDF membrane surface layer was conducted from the FTIR-ATR spectra data for each PVDF membrane. Results are shown in figure 7.10, revealing PVDF membranes prepared from DMSO/GVL mix blend and pure DMSO demonstrated both α-phase and β-phase. In addition, the α-phase looks more like the dominant crystal fraction for all PVDF membranes, which is likely influenced by the solvent power of the mixed solvent. The FTIR-ATR characterisation aids in understanding the changes at the active microstructural layer that are relevant to the PVDF membrane performance.

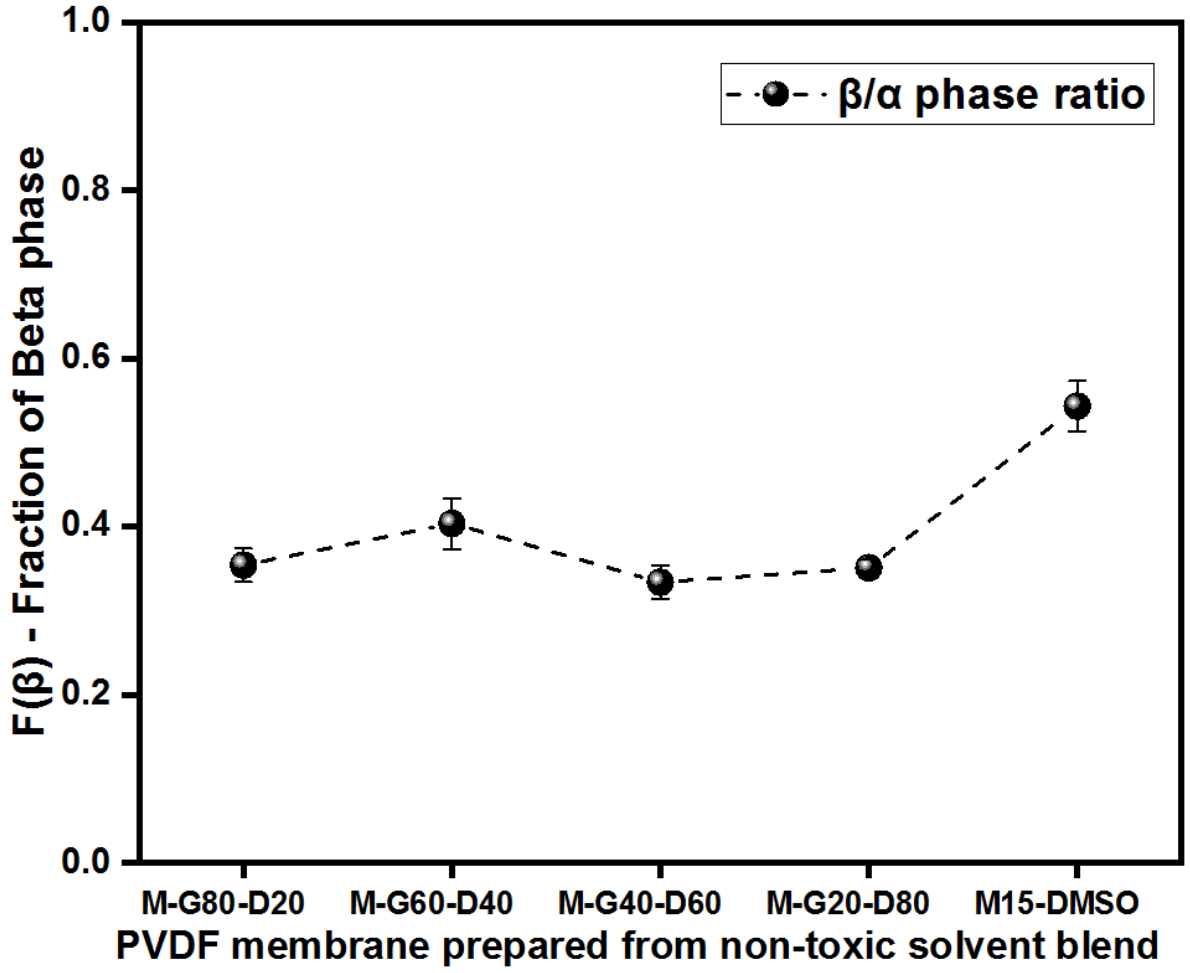

Figure 7.10: Relative beta fraction of PVDF membranes prepared by dopes using different concentrations of DMSO as cosolvent.

7.3.8 Membrane performance – (Gas and Pure water experiments);

The water and gas flux tests through the dry PVDF membranes were measured to evaluate the performance properties of the prepared tailored membranes. Figure 7.11a illustrates the relationship between the nitrogen gas fluxes varied by regulating the pressure between 0.2 to 1.0 bars for each prepared PVDF membrane. The evaluation of two independent batch samples of PVDF membranes at a constant pressure of 0.4 bar is presented in figure 7.11b. The PVDF membranes performance analysis shows the effect of the solvent blend on the sample, which acts as a promising strategy to achieve improved gas flux compared to membranes prepared using PVDF and GVL. The enhanced gas flux was related to the cosolvent with the PVDF membrane prepared from pure cosolvent exhibiting extremely high gas flux primarily associated with finger-like morphological structure. The "M-G60-D40" and "M-G40-D60" permeated increased gas fluxes at higher pressure gradients than "M-G20-D80" despite having a large mean pore size. The low gas flux for "M-G20-D80" could be due to fouling, dead-end pores or tortuous pore path of the membrane. The characterisation of the gas flux performance resulted in further evaluation of the PVDF membrane to determine to what extent it can avoid wetting and withstand certain liquid entry pressure (LEP) [48].

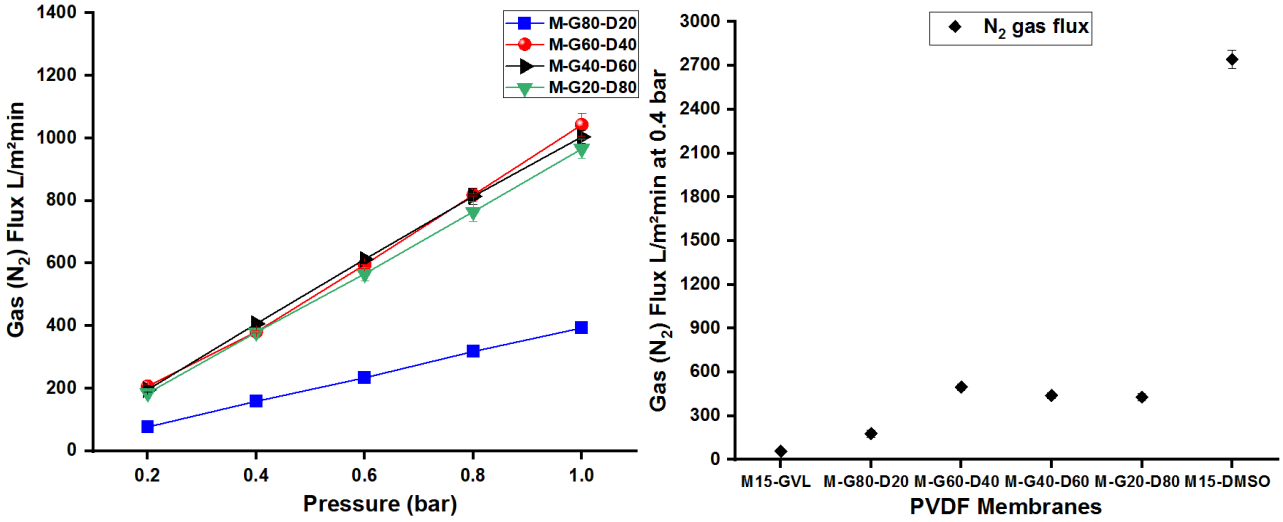

(a) (b)

Figure 7.11 (a): The effect of transmembrane pressure on nitrogen gas flux through the fabricated PVDF membrane. Figure 7.11(b): Nitrogen flux performance by the different PVDF membranes prepared with varying solvent/cosolvent concentrations.

The theoretical LEP can be estimated via the Cantor-Laplace equation [49], expressed as a function of the wetting liquid surface tension, the wettability property described in terms of the contact angle and the maximum pore size of the membrane for conditions of perfectly cylindrical pores. However, morphological observation does not show a constant radius of curvature. Hence experimental evaluation of the liquid entry pressure of water (LEPw) was determined to observe a trade-off between barrier and transport properties [50]. Typically commercial PVDF membranes have LEPw at a pressure between 0.5- 2.9 bar [51,52]; however, experimental results for tailored prepared membranes showed high LEPw values above 6 bars for PVDF membranes "M-G80-D20" and "M-G60-D40" while "M-G40-D60" and "M-G20-D80" had LEPw values at 2 bar with DMSO membrane having a LEPw of 0.8 bar.

The deionised water flux measurement through the membrane showed that the G20-D80 membrane prepared with a higher concentration of DMSO exhibited the most increased pure water flux at 8 bars. The resulting trend of the water flux presented in figure 7.12 can be correlated to the asymmetric cross-section morphological structure of the different prepared PVDF membranes, which possess other pores sizes and increasingly finger-like/macrovoids structures.

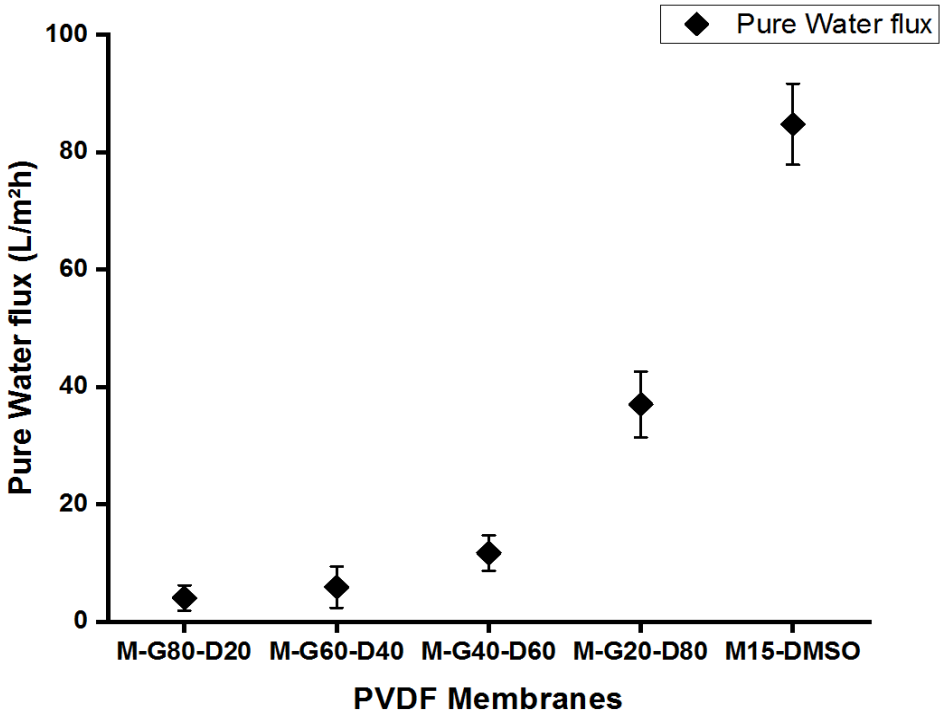

Figure 7.12: The effect of PVDF membranes prepared from varying cosolvent (DMSO) concentrations on the water flux through the membranes at 8 bar.

The PVDF membrane performance correlates with the morphological structure [5]. Using a non-toxic cosolvent (DMSO) concentration in the polymer dope for membrane preparation tends to work as an agent to dissipate the dense globule-like morphology previously observed for PVDF/GVL system and improve the transmembrane water flux through the PVDF membrane. The permeated water flux at low pressure is consistent with research studies for membranes with such microstructure and could be suitable for ultra- and micro-filtration [53]. The lab scale experimental gas and water flux test was conducted for several months without displaying remarkable variation, indicating performance stability over time. The experimental performance analysis demonstrates that the steric qualities of the membrane and feed stream could significantly obtain reduced or enhanced flux performance from PVDF membranes. Furthermore, evidence supporting the potential use of fabricated PVDF membranes as membrane contactors, ultra- and microfiltration membrane processes can be associated with the determined high LEP for some membranes, water and gas flux.

7.4 Summary

The study in this chapter introduces a low-hazard cosolvent (DMSO) and a bio based solvent (GVL) as potential alternatives to toxic petroleum-derived traditional solvents in fabricating PVDF polymeric membranes via the NIPS process. The solvent blend seems appropriate as it alters the PVDF membrane's morphology and enhances performance. The use of non-toxic DMSO as a cosolvent ensures that the process for membrane fabrication is sustainable even though it is not regarded as a green solvent. Furthermore, investigating different solvent/cosolvent concentrations allowed the fabrication of tailored-made PVDF membranes. The obtained membranes resulted in different surface morphology and improved porous structure and performance.

The wettability behaviour, crystalline phase and roughness characterisation of the PVDF membranes were studied to improve the understanding of the structural changes that occur due to the effect of mixed solvent concentrations in the casting solution. The results opened a new dimension for controlling the morphology of PVDF membranes using a non-toxic solvent blend. Furthermore, the gas, liquid entry pressure of water (LEPw) and water flux performance suggest potential membrane applications suitable for membrane processes such as membrane distillation, contactors or ultrafiltration. However, further studies would be necessary to identify the tailored membrane to achieve optimal performance for specific membrane processes. In addition, the high LEPw and low gas flux for some tailored PVDF

membranes indicates that further study is needed to improve hydrophilicity and reduce the fouling of PVDF membranes fabricated with GVL.

The successful fabrication of PVDF membranes demonstrates that the non-toxic solvent blend (GVL/DMSO) can reduce the environmental impact caused by solvent waste during the membrane fabrication process and serve as a suitable substitute for traditional toxic solvents. In addition, the tailor-made PVDF membranes show promising potential for better performance than those prepared using only GVL solvent.

7.5 References

[1] Wang, Y., Lin, H., Xiong, Z., Wu, Z., Wang, Y., Xiang, L., ... & Liu, F. (2016). A silane-based interfacial crosslinking strategy to design PVDF membranes with versatile surface functions. *Journal of Membrane Science*, *520*, 769-778.

[2] Li, M. Z., Li, J. H., Shao, X. S., Miao, J., Wang, J. B., Zhang, Q. Q., & Xu, X. P. (2012). Grafting zwitterionic brush on the surface of PVDF membrane using physisorbed free radical grafting technique. *Journal of membrane science*, *405*, 141-148.

[3] Deng, F., Wang, X., He, D., Hu, J., Gong, C., Ye, Y. S., ... & Xue, Z. (2015). Microporous polymer electrolyte based on PVDF/PEO star polymer blends for lithium ion batteries. *Journal of membrane science*, *491*, 82-89.

[4] Elwan, H. A., Mamlouk, M., & Scott, K. (2021). A review of proton exchange membranes based on protic ionic liquid/polymer blends for polymer electrolyte membrane fuel cells. *Journal of Power Sources*, *484*, 229197.

[5] Li, Q., Xu, Z. L., & Yu, L. Y. (2010). Effects of mixed solvents and PVDF types on performances of PVDF microporous membranes. *Journal of applied polymer science*, *115*(4), 2277-2287.

[6] Su, Y., Chen, C., Li, Y., & Li, J. (2007). Preparation of PVDF membranes via TIPS method: the effect of mixed diluents on membrane structure and mechanical property. *Journal of Macromolecular Science, Part A: Pure and Applied Chemistry*, *44*(3), 305-313.

[7] Rasool, M. A., & Vankelecom, I. F. J. (2019). Use of γ-valerolactone and glycerol derivatives as bio-based renewable solvents for membrane preparation. *Green Chemistry*, *21*(5), 1054-1064.

[8] Chen, X., Hu, Y., Xie, Z., & Wang, H. (2018). Materials and design of photocatalytic membranes. In *Current Trends and Future Developments on (Bio-) Membranes* (pp. 71-96). Elsevier.

[9] Guillen, G. R., Pan, Y., Li, M., & Hoek, E. M. (2011). Preparation and characterization of membranes formed by nonsolvent induced phase separation: a review. *Industrial & Engineering Chemistry Research*, *50*(7), 3798-3817.

[10] Pereira, C. S., Silva, V. M., & Rodrigues, A. E. (2011). Ethyl lactate as a solvent: Properties, applications and production processes–a review. *Green Chemistry*, *13*(10), 2658-2671.

[11] Rogers, Luke, and Klavs F. Jensen. "Continuous manufacturing–the Green Chemistry promise?." *Green chemistry* 21.13 (2019): 3481-3498.

[12] Figoli, A., Marino, T., Simone, S., Di Nicolo, E., Li, X. M., He, T., ... & Drioli, E. (2014). Towards non-toxic solvents for membrane preparation: a review. *Green Chemistry*, *16*(9), 4034-4059.

[13] Alexowsky, C., Bojarska, M., & Ulbricht, M. (2019). Porous poly (vinylidene fluoride) membranes with tailored properties by fast and scalable non-solvent vapor induced phase separation. *Journal of Membrane Science*, *577*, 69-78.

[14] F.P. Byrne, S. Jin, G. Paggiola, T.H.M. Petchey, J.H. Clark, T.J. Farmer, A.J. Hunt, C. Robert McElroy, J. Sherwood, Tools and techniques for solvent selection: green solvent selection guides, Sustainable Chemical Processes 4 (2016) 7.

[15] Vignes, R. (2000, August). Dimethyl Sulfoxide (DMSO)—A “new” clean, unique, superior solvent. In *American Chemical Society Annual Meeting* (No. 228

[16] Marwah, H., Garg, T., Goyal, A. K., & Rath, G. (2016). Permeation enhancer strategies in transdermal drug delivery. *Drug delivery*, *23*(2), 564-578.

[17] Brayton, C. F. (1986). Dimethyl sulfoxide (DMSO): a review. *The Cornell Veterinarian*, *76*(1), 61-90.

[18] Verheijen, M., Lienhard, M., Schrooders, Y., Clayton, O., Nudischer, R., Boerno, S., ... & Caiment, F. (2019). DMSO induces drastic changes in human cellular processes and epigenetic landscape in vitro. *Scientific reports*, *9*(1), 1-12.

[19] Marino, T., Galiano, F., Simone, S., & Figoli, A. (2018). DMSO EVOL™ as novel non-toxic solvent for polyethersulfone membrane preparation. Environmental Science and Pollution Research

[20] Meringolo, C., Mastropietro, T. F., Poerio, T., Fontananova, E., De Filpo, G., Curcio, E., & Di Profio, G. (2018). Tailoring PVDF membranes surface topography and hydrophobicity by a sustainable two-steps phase separation process. *ACS Sustainable Chemistry & Engineering*, *6*(8), 10069-10077.

[21] Thuyavan, Y. L., Anantharaman, N., Arthanareeswaran, G., & Ismail, A. F. (2016). Impact of solvents and process conditions on the formation of polyethersulfone membranes and its fouling behavior in lake water filtration. *Journal of Chemical Technology & Biotechnology*, *91*(10), 2568-2581.

[22] Sigma-Aldrich, 2018. [Online] Available at: http://www.sigmaaldrich.com/united-kingdom.html [Accessed 25 August 2018].

[23] Zhenova, A. (2020). Challenges in the development of new green solvents for polymer dissolution. *Polymer International*, *69*(10), 895-901.

[24] Bottino, A., Capannelli, G., Munari, S., & Turturro, A. (1988). Solubility parameters of poly (vinylidene fluoride). *Journal of Polymer Science Part B: Polymer Physics*, *26*(4), 785-794.

[25] Hansen, C. M. (2007). Hansen solubility parameters: a user's handbook. CRC press.

[26] Benazzouz, A., Moity, L., Pierlot, C., Sergent, M., Molinier, V., & Aubry, J. M. (2013). Selection of a greener set of solvents evenly spread in the Hansen space by space-filling design. *Industrial & Engineering Chemistry Research*, *52*(47), 16585-16597.

[27] Kerkel, F., Markiewicz, M., Stolte, S., Müller, E., & Kunz, W. (2021). The green platform molecule gamma-valerolactone–ecotoxicity, biodegradability, solvent properties, and potential applications. *Green Chemistry*, *23*(8), 2962-2976.

[28] Jung, J. T., Kim, J. F., Wang, H. H., di Nicolo, E., Drioli, E., & Lee, Y. M. (**2016**). Understanding the non-solvent induced phase separation (NIPS) effect during the fabrication of microporous PVDF membranes via thermally induced phase separation (TIPS). *Journal of Membrane Science*, *514*, 250-263.

[29] Abdulla AlMarzooqi, F., Roil Bilad, M., & Ali Arafat, H. (2017). Improving liquid entry pressure of polyvinylidene fluoride (PVDF) membranes by exploiting the role of fabrication parameters in vapor-induced phase separation VIPS and non-solvent-induced phase separation (NIPS) processes. *Applied Sciences*, *7*(2), 181.

[30] Marino, T., Galiano, F., Simone, S., & Figoli, A. (2019). DMSO EVOL™ as novel non-toxic solvent for polyethersulfone membrane preparation. *Environmental Science and Pollution Research*, *26*(15), 14774-14785.

[31] Drioli, E., Ali, A., Simone, S., Macedonio, F., Al-Jlil, S. A., Al Shabonah, F. S., ... & Criscuoli, A. (2013). Novel PVDF hollow fiber membranes for vacuum and direct contact membrane distillation applications. *Separation and Purification Technology*, *115*, 27-38.

[32] Lin, D. J., Chang, C. L., Chen, T. C., & Cheng, L. P. (2002). On the structure of porous poly (vinylidene fluoride) membrane prepared by phase inversion from water-NMP-PVDF system. *Journal of applied science and Engineering*, *5*(2), 95-98.

[33] Hendrix, K., Koeckelberghs, G., & Vankelecom, I. F. (2014). Study of phase inversion parameters for PEEK-based nanofiltration membranes. *Journal of membrane science*, *452*, 241-252.

[34] Ashtiani, S., Khoshnamvand, M., Číhal, P., Dendisová, M., Randová, A., Bouša, D., ... & Friess, K. (2020). Fabrication of a PVDF membrane with tailored morphology and properties via exploring and computing its ternary phase diagram for wastewater treatment and gas separation applications. *RSC Advances*, *10*(66), 40373-40383.

[35] Marino, T., Russo, F., Criscuoli, A., & Figoli, A. (2017). TamiSolve® NxG as novel solvent for polymeric membrane preparation. *Journal of Membrane Science*, *542*, 418-429.

[36] Nawi, N. I. M., Bilad, M. R., Nordin, N. A. H. M., Mavukkandy, M. O., Putra, Z. A., Wirzal, M. D. H., ... & Khan, A. L. (2018). Exploiting the interplay between liquid-liquid demixing and crystallization of the PVDF membrane for membrane distillation. *International Journal of Polymer Science*, *2018*.

[37] Hou, D., Fan, H., Jiang, Q., Wang, J., & Zhang, X. (2014). Preparation and characterization of PVDF flat-sheet membranes for direct contact membrane distillation. *Separation and Purification Technology*, *135*, 211-222.

[38] Mat Nawi, N. I., Chean, H. M., Shamsuddin, N., Bilad, M. R., Narkkun, T., Faungnawakij, K., & Khan, A. L. (2020). Development of hydrophilic PVDF membrane using vapour induced phase separation method for produced water treatment. *Membranes*, *10*(6), 121.

[39] Hebbar, R. S., Isloor, A. M., & Ismail, A. F. (2017). Contact angle measurements. In *Membrane characterization* (pp. 219-255). Elsevier.

[40] Woo, S. H., Park, J., & Min, B. R. (2015). Relationship between permeate flux and surface roughness of membranes with similar water contact angle values. *Separation and purification technology*, *146*, 187-191.

[41] Wenzel, R. N. (1936). Resistance of solid surfaces to wetting by water. *Industrial & Engineering Chemistry*, *28*(8), 988-994.

[42] Wang, X., Zhang, L., Sun, D., An, Q., & Chen, H. (2008). Effect of coagulation bath temperature on formation mechanism of poly (vinylidene fluoride) membrane. *Journal of Applied Polymer Science*, *110*(3), 1656-1663.

[43] Meringolo, Carmen, et al. "Tailoring PVDF membranes surface topography and hydrophobicity by a sustainable two-steps phase separation process." *ACS Sustainable Chemistry & Engineering* 6.8 (2018): 10069-10077.

[44] Kurada, K. V., & De, S. (2018). Role of thermodynamic and kinetic interaction of poly (vinylidene fluoride) with various solvents for tuning phase inversion membranes. *Polymer Engineering & Science*, *58*(7), 1062-1073.

[45] Gregorio Jr, R. (2006). Determination of the α, β, and γ crystalline phases of poly (vinylidene fluoride) films prepared at different conditions. *Journal of Applied Polymer Science*, *100*(4), 3272-3279.

[46] Tao, M. M., Liu, F., Ma, B. R., & Xue, L. X. (2013). Effect of solvent power on PVDF membrane polymorphism during phase inversion. *Desalination*, *316*, 137-145.

[47] Cai, X., Lei, T., Sun, D., & Lin, L. (2017). A critical analysis of the α, β and γ phases in poly (vinylidene fluoride) using FTIR. *RSC advances*, *7*(25), 15382-15389.

[48] Rácz, G., Kerker, S., Kovács, Z., Vatai, G., Ebrahimi, M., & Czermak, P. (2014). Theoretical and experimental approaches of liquid entry pressure determination in membrane distillation processes. *Periodica Polytechnica Chemical Engineering*, *58*(2), 81-91.

[49] Warsinger, D. M., Swaminathan, J., Guillen-Burrieza, E., & Arafat, H. A. (2015). Scaling and fouling in membrane distillation for desalination applications: a review. *Desalination*, *356*, 294-313.

[50] McCullough, E. A., Kwon, M., & Shim, H. (2003). A comparison of standard methods for measuring water vapour permeability of fabrics. *Measurement Science and Technology*, *14*(8), 1402.

[51] Gugliuzza, A., & Drioli, E. (2007). PVDF and HYFLON AD membranes: Ideal interfaces for contactor applications. Journal of Membrane Science, 300(1-2), 51-62.

[52] Abdulla AlMarzooqi, F., Roil Bilad, M., & Ali Arafat, H. (2017). Improving liquid entry pressure of polyvinylidene fluoride (PVDF) membranes by exploiting the role of fabrication parameters in vapor-induced phase separation VIPS and non-solvent-induced phase separation (NIPS) processes. *Applied Sciences*, *7*(2), 181.

[53] Liu, F., Hashim, N. A., Liu, Y., Abed, M. M., & Li, K. (2011). Progress in the production and modification of PVDF membranes. *Journal of membrane science*, *375*(1-2), 1-27.

CHAPTER 8
Effect of PVP concentration on the membrane structure and performance of PVDF membrane

8.1 Introduction

In the membrane industry, modifying the polymer dope without adding extra complexity to the fabrication procedure has been reported as an excellent strategy for designing polymeric membranes [1,2]. Furthermore, several reported studies show that adding polymeric additives to the casting solution can act as a pore former or nonsolvent agent to produce membranes with improved performance and mitigate problems such as fouling, pore constriction or modify the wettability properties of fabricated membranes [3,4,5]. Therefore, in this chapter, a polymer additive as a fore former is pursued to modify the membrane structure of PVDF/GVL membranes.

PVP is a synthetic polymeric additive that is non-toxic, biocompatible and possesses excellent solubility properties in many solvents [6] and a few polymers. Hence, it has been extensively used in the pharmaceutical, medical, biological, fine chemical and manufacturing industries as protective coating material, enhancing agent and as a pore former in the production of polymeric membranes [7,8,9]. Presented in figure 8.1 is the molecular structure of polyvinylpyrrolidone (PVP). The miscibility between PVP and PVDF is primarily due to the quasi-hydrogen bonding interactions between the carbonyl group of PVP and the PVDF's methyl group [10].

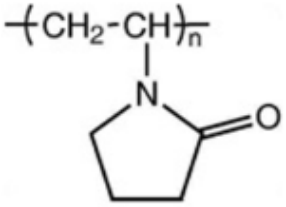

Figure 8.1: Molecular structure of polyvinylpyrrolidone (PVP).

This chapter aims to fabricate PVDF membranes by modifying the composition of the dope solution by adding PVP as a pore former and ultimately changing the membrane structure. It is assumed that adding PVP to the polymer dope would induce noticeable changes, improve hydrophilicity, and regulate the dense surface, size of macrovoids, and spongy-like structure of the resulting membrane. The prepared membranes' morphology, pore size and hydrophilicity were examined and discussed. At the time of the submission of

this thesis, no studies using biobased GVL as a solvent and PVP as a single additive to fabricate PVDF membranes via the NIPS approach have been published in the literature.

8.2 Experimental study

8.2.1 Materials

The base materials used to fabricate the PVDF membrane in this chapter have been presented in chapter 3. Table 8.1 shows the compositions of each casting solution. The NIPS method was employed to prepare the flat sheet membranes. The PVDF membrane prepared from the PVDF/GVL polymer dope is the reference membrane, and the other investigated membranes are crafted from PVDF/PVP/GVL mixtures.

Table 8-1: Compositions of the dope solution to fabricate flat sheet PVDF membranes (PVP used as pore former).

Membrane code	Casting composition (wt.%)		
	PVDF	GVL	PVP
M15-GVL	15	85	0
M15-PVP3	15	82	3
M15-PVP5	15	80	5
M15-PVP7.5	15	77.5	7.5

8.3 Results and discussion

8.3.1 Effect of additive (PVP) concentration on polymer dope state

The evolution of the polymer dopes by ageing at a controlled temperature was investigated. Table 8-2 reveals that the thermodynamic properties of the dope solutions due to ageing will lead to changes in “solution conditions”. The term “solution conditions” refers to the state of aggregation and disposition of polymer chains within the casting solution.

Analysis shows that dope solutions with PVP tend to form gels within a few days rather than a few hours. The study indicates that adding PVP will likely significantly impact the phase inversion process, primarily due to physicochemical properties, which affect the thermodynamic and kinetic driving forces [11]. As the PVP replaces GVL in the PVDF dope solution, the homogenous region of the polymer mixtures due to ageing appears to promote phase separation due to the mutual moment of the PVDF mixtures and the increased molecular effect of added polymer additives. The analysis of a phase inversion process in a

multi-component polymeric system containing an additive is typically very challenging due to several correlated factors, including different interactions, mutual diffusions, and specific bonding between process components. However, the study of aged polymer dope offers data on the polymer mixtures' stability and reveals the PVDF system's potential separation mechanism.

Table 8-2: Ageing of Polymer dope with different PVP concentrations.

Polymer dope code	The physical state of polymer dope	Gelation/phase separation time (hours)
M15-GVL	Gel	4
M15-PVP3	Gel	48
M15-PVP5	Phase separation	48
M15-PVP7.5	Phase separation	48

8.3.2 SEM membrane characterisation

Figure 8.2 shows the cross-section and top surface of the different PVDF membranes with and without the addition of PVP. The cross-section images reveal that the addition of PVP is responsible for a transition from a membrane morphology showing a thick, dense top layer and a globule-like substructure (“M15-GVL” morphology) to a membrane morphology composed of a thin dense top layer and a substructure with large finger-like macrovoids (the “M15-PVP’” membranes). It seems that the induced thermodynamic behaviour of the PVDF system was impacted by the addition of PVP, leading to the morphological formation that favours finger-like and macrovoid structures [12].

Adding PVP at a lower concentration (3wt%) resulted in forming a thin dense top layer and a substructure with macrovoids. In contrast, the addition of PVP at higher concentrations (5 and 7.5 wt%) leads to the gradual thickening of the dense top layer and the gradual transition of the substructure from finger-like macrovoids to a sponge-like morphology. According to the literature, the mutual diffusivities of a polymer system and the thermodynamic phase equilibria effect are decisive factors that influence how the membrane forms when using the phase inversion method [13].

Observed morphological differences were linked to collected data recorded during the solidification period of cast film. The results in Table 8-3 reveal that an incremental addition of PVP leads to a longer “solidification/coagulation period”, i.e. the membranes take progressively more time to solidify/coagulate. These observations provide an assumption that

the contribution of the kinetic hindrance will likely outweigh the thermodynamic behaviour effect of the PVDF/PVP/GVL/water system for increased PVP concentration in polymer dope.

Table 8-3: Observation of PVDF cast film solidification period and precipitation conditions.

Polymer dope code	Coagulation bath temperature (°C)	Time span for the cast film to solidify in the coagulation bath (secs)
M15-GVL	30	28
M15-PVP3	30	35
M15-PVP5	30	38
M15-PVP7.5	30	58

Therefore, it is suggested that the morphology difference is primarily due to the change in the phase separation rate caused by the addition of PVP in the PVDF/PVP/GVL/water system, which impacted the overall structural properties of the produced PVDF membranes [14]. Further analysis of the top surface of the membrane shows pore sizes in the range of 138-650nm (pore sizes determined using ImageJ).

In summary, it can be stated that depending on the concentration of PVP in the PVDF dope, the enhancement or suppression of macrovoid formation is linked to the trade-off between thermodynamic enhancement and kinetic hindrance.

8.3.3 Membrane Thickness and Porosity Analysis

Table 8-4 shows the effect of increased PVP in the PVDF dope solution and its impact on the thickness and porosity of fabricated PVDF membranes. The overall membrane thickness increased with PVP concentration from ~36µm to ~86µm, with the changes in thickness likely influenced by the polymer-additive interactions and increased molecular weight of polymer dope. In addition, PVP acting as a pore-forming agent effectively improved the porosity of the fabricated membranes.

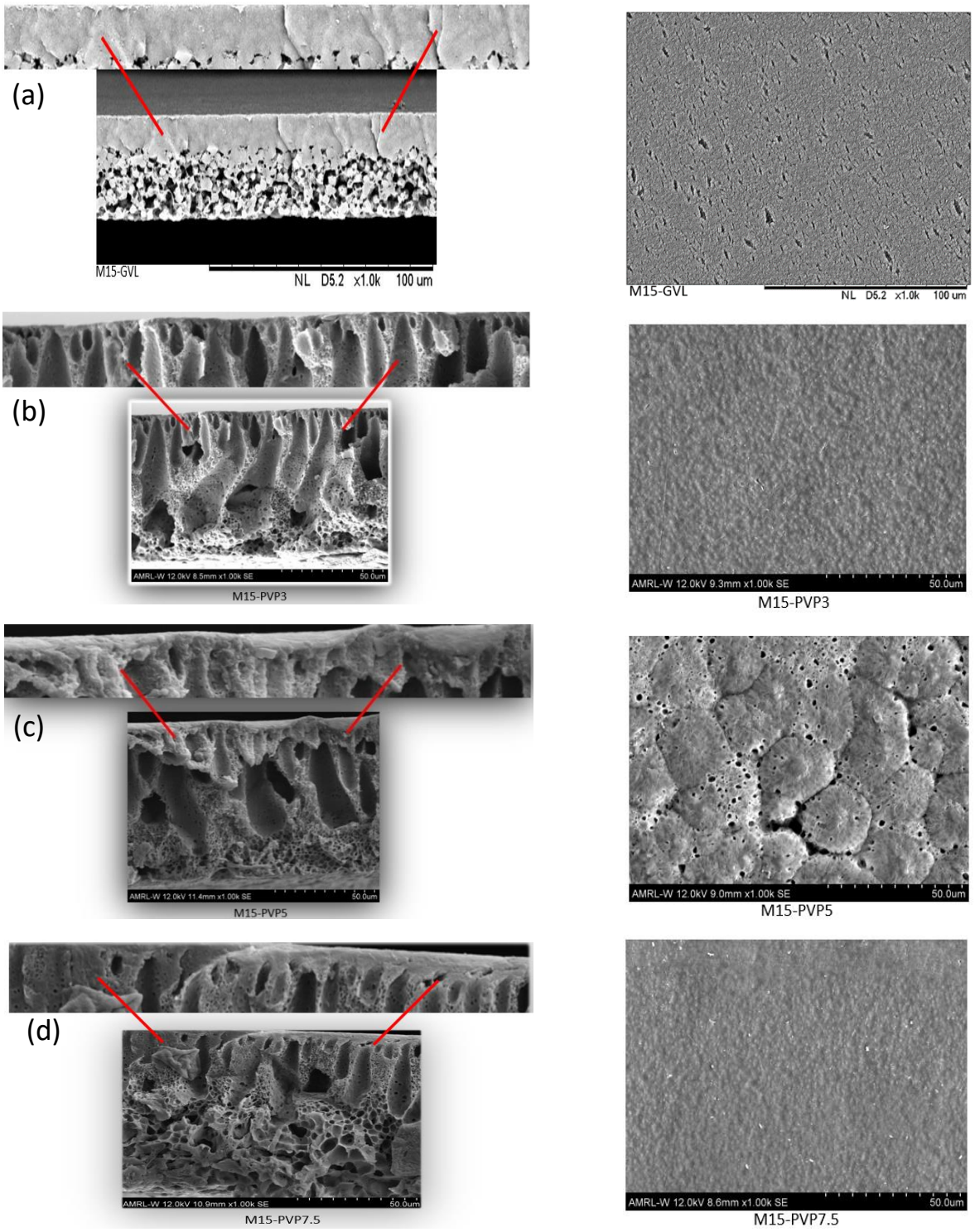

Cross-section of membrane **Top Surface of membrane**

Figure 8.2: SEM images for PVDF membrane with/without the addition of PVP as an additive (a) No PVP added; (b) 3wt% PVP; (c) 5wt% PVP; (d) 7.5wt% PVP).

The result shows that small addition of PVP (3wt.%) led to an increased membrane porosity by approximately 30% when compared to PVDF membrane with no addition of PVP. Overall, the porosity of the PVDF membranes increased with PVP concentration, rising from 53% without PVP to 80% for membranes prepared with 7.5% PVP.

Table 8-4: PVDF membrane thickness and porosity of asymmetric PVDF membrane

Membrane Sample	**Membrane measured thickness (SEM) (µm)**	**Overall porosity (%)**
M15-GVL	36.25 (±1.2)	52.65(±2.2)
M-PVP3%	75.44 (±3.4)	74.24(±1.3)
M- PVP5%	80.22 (±1.1)	76.69(±1.4)
M- PVP7.5%	86.42 (±1.4)	79.81(±3.1)

The result presented in figure 8.3 shows that both overall membrane thickness and porosity have a similar upward trend due to increased PVP concentration. The thickness of polymeric membranes has been associated with enhanced polymer dope thermodynamic instability [15]. In addition, the hydrophilic polymer additive, PVP, has been reported to migrate towards the nonsolvent phase (water) during the demixing stage, enabling a quicker exchange of solvent/nonsolvent and creating a porous membrane as the PVP leaches out during the formation process. Hence, the increased porosity trend of the fabricated membranes is associated with the observed macrovoids and increased finger-like structures of the prepared membranes compared to spongy-like/dense structures obtained for membranes prepared with no addition of PVP.

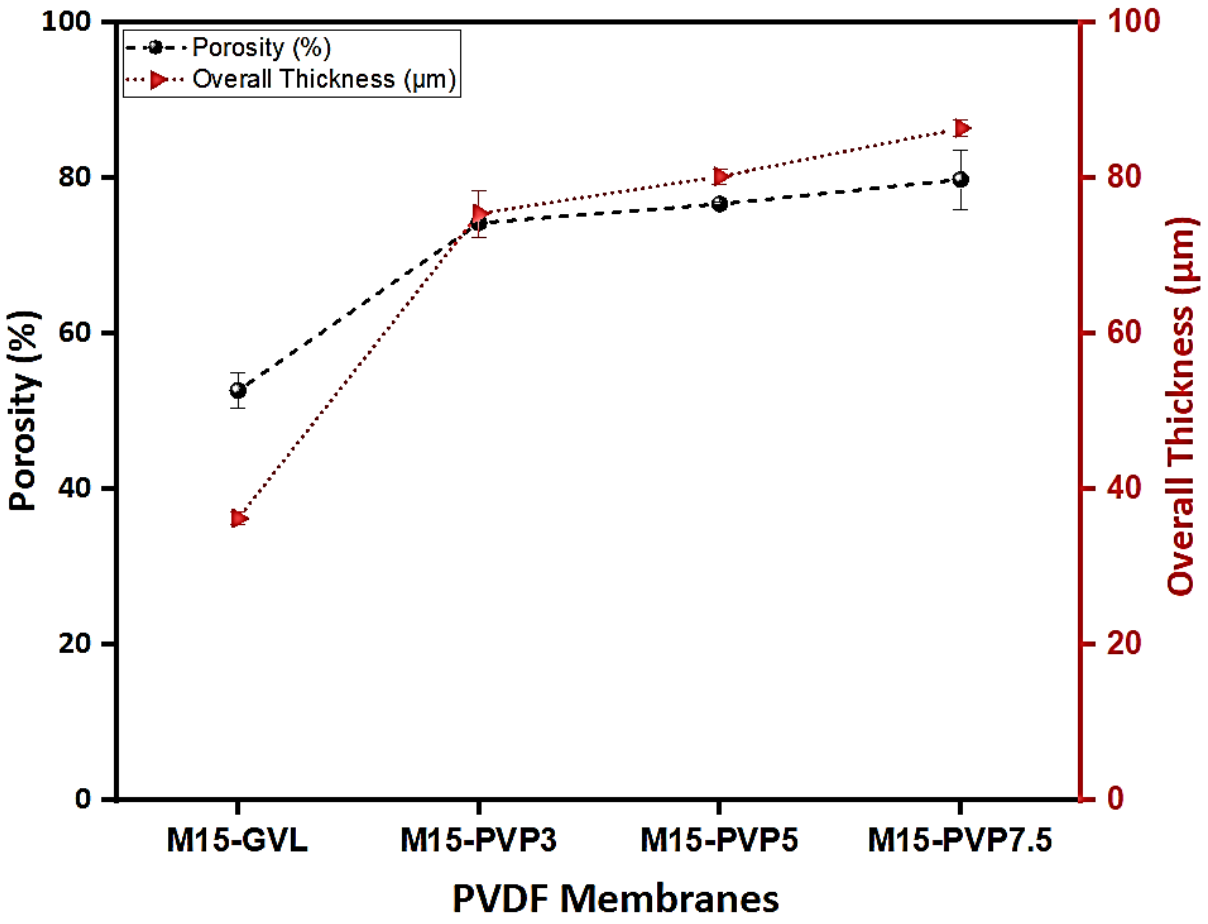

Figure 8.3: Membrane thickness and PVDF membrane porosity containing different PVP concentrations.

8.3.4 Contact angle measurement

The contact angle measurement was used to determine the wettability profile of all four fabricated PVDF membranes. The static water contact angle for each membrane sample is presented in figure 8.4 shows that the addition of PVP resulted in a reduced wetting resistance. PVDF membranes prepared from dope without adding PVP gave a higher contact angle than membranes produced with the pore former agent in the dope solution. However, the change in wettability behaviour with increased PVP concentration did not result in a remarkable difference among the fabricated PVDF membranes. The difference in hydrophilicity of the PVDF membranes prepared from dopes containing PVP hints at the possibility that not all PVP is leached out during the membrane fabrication process, and some residual PVP remains in the polymeric matrix of these membranes. The membranes were analysed using FTIR-ATR spectroscopy to test this hypothesis, and the results are presented in the following section.

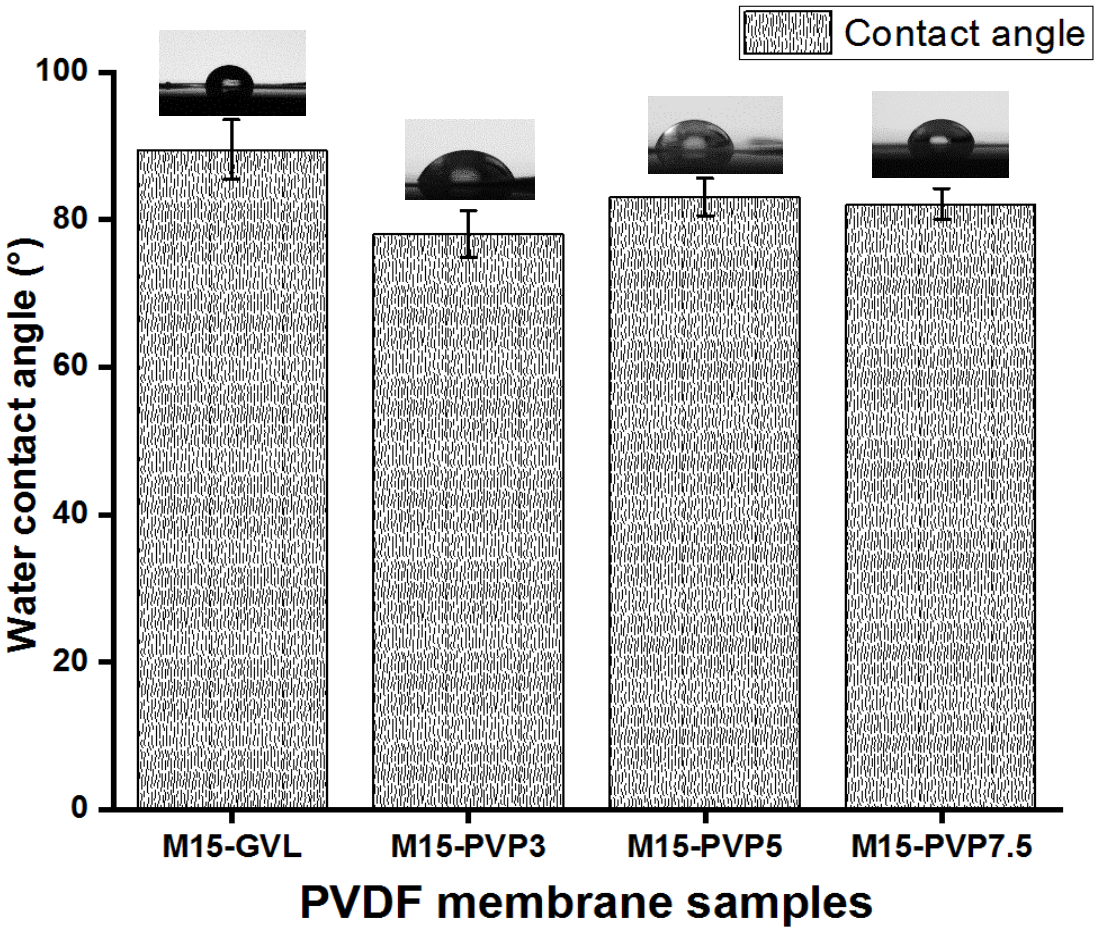

Figure 8.4: Evaluation of fabricated PVDF membrane wettability profile with/without polymeric additive PVP.

8.3.5 FTIR-ATR Analysis

The FTIR-ATR spectra were used to analyse the prepared PVDF membrane surfaces qualitatively. The FTIR-ATR characterisation of the membranes samples prepared from different concentrations of addition of PVP, the PVDF pellet and PVP powder is presented in figure 8.5. The presence of specific vibration bands was evaluated to confirm the occurrence of PVP in the PVDF membrane. Typically, the standard PVP vibrating band is located within the spectra region of 1627-1673 $cm^{-1,}$ indicating a C=O stretch [16,17]. Vibration bands associated with PVDF are located at peak wavenumber of 840cm^{-1} (CF_2 stretching), 1062cm^{-1} (CH_2 bonding) and 1402cm^{-1} (CH_2 wagging).

A significant difference between PVDF and PVP samples was observed at 1658 cm^{-1}. Furthermore, at a wavenumber of 1672, various reduced intensity peaks of the membranes prepared from the PVDF/PVP/GVL blend can be detected, corresponding to a low amount of PVP that still exists in the blended PVDF matrix. The shift from 1658 to 1672 is associated with the adsorbed water during the phase inversion process.

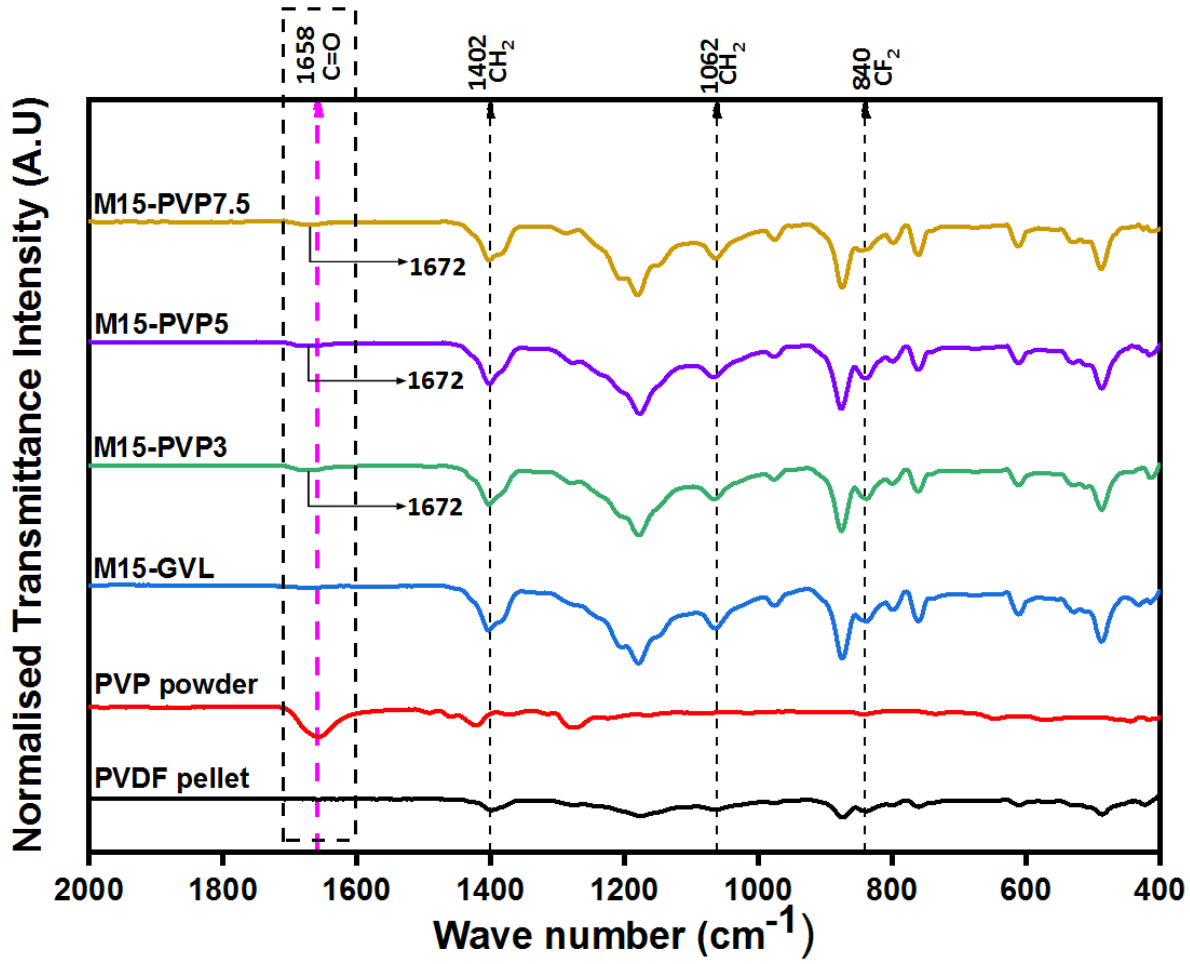

Figure 8. 5: FTIR-ATR spectra of the top surface for PVDF membranes, PVP and PVDF samples.

Typically, it is commonly known that several functional groups contribute to the surface wettability behaviour of membranes, such as hydroxyl, carbonyl and carboxyl functional groups that enhance material hydrophilicity [18]. There is no observed characteristic band of PVP identified at 1658cm^{-1} for the PVDF membrane samples. However, the peak at 1672cm^{-1} is caused by the carbonyl (C=O) stretching, which is sensitive to the hydrogen bond formation, as illustrated in figure 8.6. When PVP is added to PVDF, it is expected to bond through nucleophilic addition and hydrogen interaction, which leads to the attachment of a hydroxyl group (-OH) [19]. Furthermore, the observed FTIR-ATR spectra result is supported by figure 8.4, which demonstrates that the PVP fraction directly alters the membrane surface properties. The increase in PVP concentration results in different degrees of hydrophilic profile that can be compared with PVDF membrane fabricated with no PVP added.

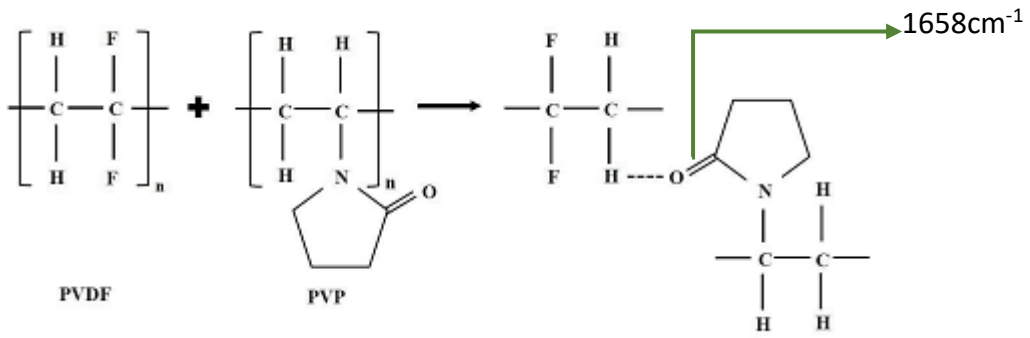

Figure 8.6: Schematic illustration of the chemical structure highlighting the bonding of PVDF and PVP and the C=O stretching of the PVDF membrane.

The peak intensity at 1672cm^{-1} indicates that the carbonyl group is more likely to originate from the PVP. Thus, It is arguable that the increased period observed for membrane solidification conditions during membrane fabrication could account for leached PVP fraction on the surface of the PVDF membrane, and the relative quantity of C=O peaks corresponds to a lower amount of PVP remaining in the membrane. Furthermore, results also presented in figure 8.7 reveal that dope solutions with increased concentration of PVP produced membrane with less residual PVP, as indicated by a slight difference in the intensity of the reflectance, which is interesting.

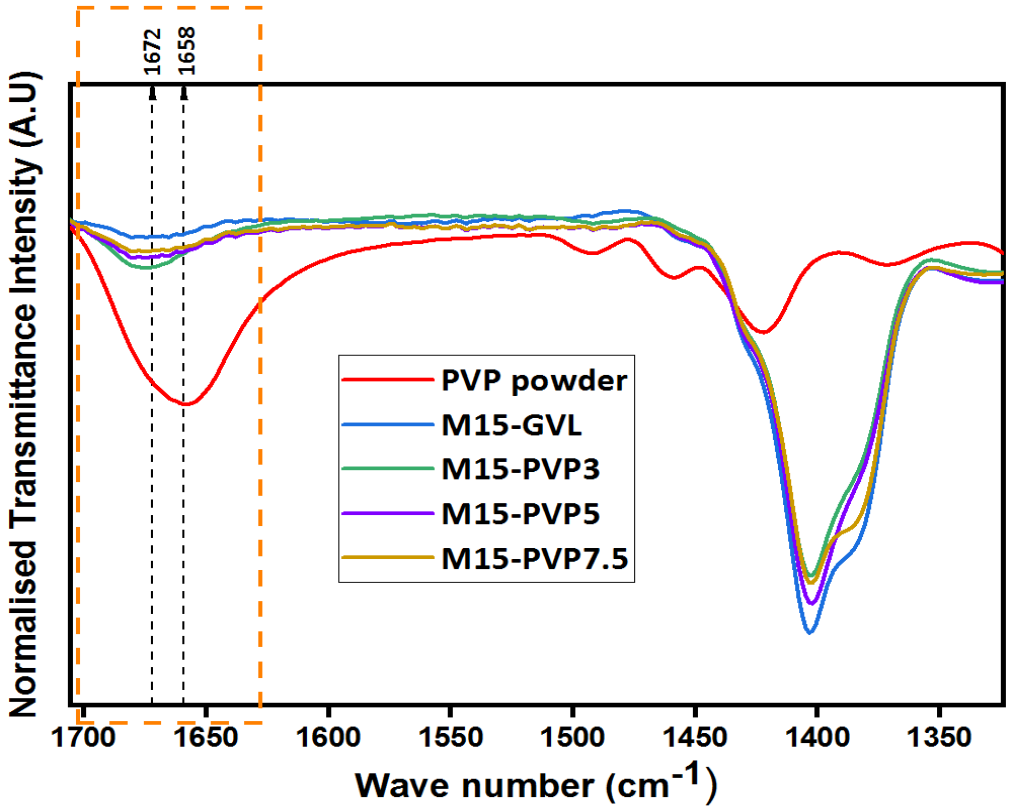

Figure 8.7: FTIR-ATR spectra view of identified C=O double bond stretching vibration peak and CH_2 wagging of PVDF membrane samples

8.3.6 Membrane performance – (Gas and Pure water experiments).

The effect of the addition of PVP on the permeation characteristics of the PVDF membranes was evaluated by measuring the nitrogen gas and water fluxes through the different tailored PVDF membrane samples. Figure 8.8 shows the nitrogen gas flux as a function of the transmembrane pressure for all membranes prepared with the addition of PVP. The membrane M15-GVL was prepared without adding PVP to the polymer dope and was used as the control PVDF membrane material for performance comparison. Improved gas (N_2) permeation fluxes were observed for pressures between 0.2 to 1.0 bars for the PVDF membrane prepared with the addition of PVP for each prepared membrane. The pore forming agent, PVP, seems to increase the interconnectivity pores, which aided the increased gas permeation through the PVDF membrane.

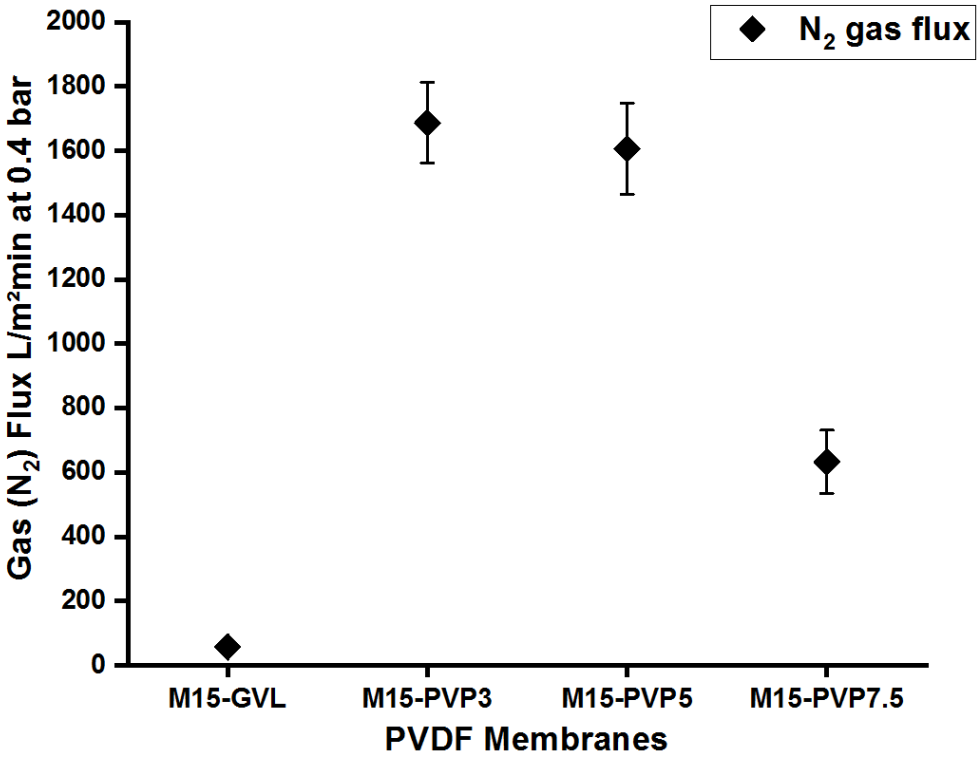

Figure 8.8: Gas flux measurement for PVDF membranes prepared from different concentrations of PVP as a polymeric additive.

The increase of the PVP concentration from 3wt% to 7.5wt% resulted in a decline in gas flux that did not correlate with the measured membrane porosity. However, these results can be ascribed to the thicker, dense top layers observed in the membranes (SEM images) prepared with 5wt% and 7.5wt% PVP. The membranes showed repeatability in terms of the

permeation performance test, with relatively small variations in the gas flux between membrane samples. The maximum gas flux (1686 $L.m^{-2}.min^{-1}$) was considerably higher than most results from earlier chapters and the control membrane.

A similar trend was observed for the water permeation tests (results in figure 8.9). Adding 3wt% PVP to the polymer dope dramatically increased the water permeation flux (note that the membrane prepared without adding PVP, M15-GVL, showed zero water flux at 4 bar). However, adding a higher concentration of PVP leads to a decline in pure water flux correlated with the changes in the morphological structure of the different prepared PVDF membranes. The declining water flux for membrane samples "M15-PVP5" and "M15-PVP7.5" can be associated with the morphological structure limiting pure water permeation. Generally, membranes with spongy structures typically offer a much reduced water flux than finger-like macrovoid structures [20]. In addition, several other properties, such as surface porosity and hydrophilicity, affected pure water fluxes.

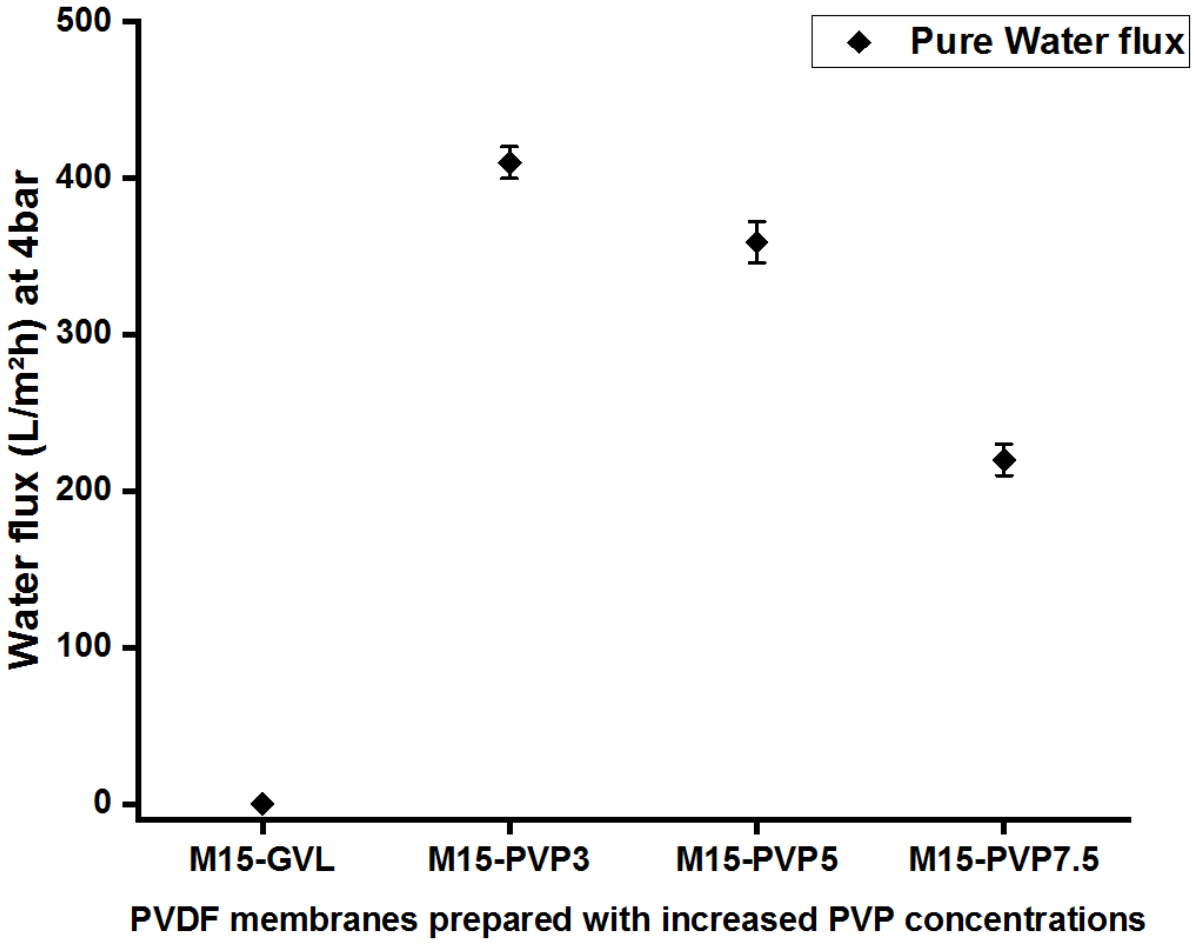

Figure 8.9: Water flux performance measurement due to different PVP concentrations for the PVDF membrane samples.

It is anticipated that PVDF membranes fabricated by adding a small amount of PVP to GVL are suitable for ultrafiltration/microfiltration processes, which are preferred for wastewater treatment applications.

8.4 Summary

The results obtained and discussed in this chapter provide a new window of opportunity for utilising GVL as a green solvent, which can be tailored by adding a cheap and accessible additive material, PVP. The study presented in this chapter highlights the blending of PVP into PVDF and discusses the various properties of the fabricated PVDF membranes. As an additive in the polymer dope, PVP promotes pore formation and slightly improves the surface wettability of the PVDF membranes. Furthermore, the structure of the PVDF membranes was modified with the addition of PVP to the PVDF/GVL system. The presence of residual amounts of PVP in the fabricated membranes was confirmed by the existence of a residual C=O vibration band in the FTIR-ATR spectra of the prepared membranes, and such presence is assumed to impact the properties of the PVDF membranes.

The asymmetric structure obtained comprises a porous substructure topped by a thin dense layer. The porous substructure presents large macrovoids or a spongy-like structure depending on the concentration of PVP added to the PVDF dope. A small amount of increased PVP concentration at 3wt. % induces the formation of large cavities, increases overall membrane thickness and achieves much higher gas and water permeation fluxes when compared with the control membrane with no added PVP. Although not investigated in this study, the presence of finger-like macrovoids may negatively impact the membrane's mechanical strength. In addition, a further increase of PVP above 3wt% promoted the formation of a sponge-like structure, reduced the presence of macrovoids, and led to a decline in the gas and water permeation fluxes.

The tailored PVDF membrane obtained highlights the intriguing nature of PVP on the membrane structure and indicates that the choice of PVP concertation is vital in controlling the final structure and achieving desired membrane performance for specific membrane process applications. In addition, it offers a trade-off regarding membrane structure, performance and wettability behaviour of the PVDF membrane.

In summary, the obtained PVDF membranes highlight the effectiveness of this method in modifying the structure and performance of PVDF membranes without any additional chemical treatments. The addition of a small concentration of PVP to the PVDF/GVL dope potentially improved the porosity, hydrophilicity and flux performance. Although, it has been known that PVP significantly influences membrane formation. Further studies are necessary

to provide an in depth understanding of the formation process of the PVDF/PVP/GVL system with increased PVP concentration.

8.5 References

[1] Arahman, N., Mulyati, S., Fahrina, A., Muchtar, S., Yusuf, M., Takagi, R., ... & Bilad, M. R. (2019). Improving Water Permeability of Hydrophilic PVDF Membrane Prepared via Blending with Organic and Inorganic Additives for Humic Acid Separation. *Molecules*, *24*(22), 4099.

[2] Tofighy, M. A., Mohammadi, T., & Sadeghi, M. H. (2021). High-flux PVDF/PVP nanocomposite ultrafiltration membrane incorporated with graphene oxide nanoribbones with improved antifouling properties. *Journal of Applied Polymer Science*, *138*(4), 49718.

[3] Wypysek, D., Kalde, A. M., Pradellok, F., & Wessling, M. (2021). In-situ investigation of wetting patterns in polymeric multibore membranes via magnetic resonance imaging. *Journal of Membrane Science*, *622*, 119026.

[4] Chen, Y., Zhang, J., & Cohen, Y. (2022). Fouling resistant and performance tunable ultrafiltration membranes via surface graft polymerization induced by atmospheric pressure air plasma. *Separation and Purification Technology*, *286*, 120490.

[5] Prihandana, G. S., Sriani, T., & Mahardika, M. (2022). Effect of Polyvinylpyrrolidone on Polyvinylidene Fluoride/Hydroxyapatite Blended Nanofiltration Membranes: Characterization and Filtration Properties. *Recent Patents on Nanotechnology*.

[6] Ong, C. S., Lau, W. J., Goh, P. S., Ng, B. C., & Ismail, A. F. (2015). Preparation and characterization of PVDF–PVP–TiO2 composite hollow fiber membranes for oily wastewater treatment using submerged membrane system. *Desalination and Water Treatment*, *53*(5), 1213-1223.

[7] Kumar, V., Yang, T., & Yang, Y. (1999). Interpolymer complexation. I. Preparation and characterization of a polyvinyl acetate phthalate-polyvinylpyrrolidone (PVAP-PVP) complex. *International journal of pharmaceutics*, *188*(2), 221-232.

[8] Mohsenpour, S., & Khosravanian, A. (2018). Influence of additives on the morphology of PVDF membranes based on phase diagram: Thermodynamic and experimental study. *Journal of Applied Polymer Science*, *135*(21), 46225.

[9] Ignatova, M., Manolova, N., & Rashkov, I. (2007). Novel antibacterial fibers of quaternized chitosan and poly (vinyl pyrrolidone) prepared by electrospinning. *European polymer journal*, *43*(4), 1112-1122.

[10] Chen, N., & Hong, L. (2002). Surface phase morphology and composition of the casting films of PVDF–PVP blend. *Polymer*, *43*(4), 1429-1436.

[11] Han, M. J., & Nam, S. T. (2002). Thermodynamic and rheological variation in polysulfone solution by PVP and its effect in the preparation of phase inversion membrane. *Journal of Membrane Science*, *202*(1-2), 55-61.

[12] Liu, F., Hashim, N. A., Liu, Y., Abed, M. M., & Li, K. (2011). Progress in the production and modification of PVDF membranes. *Journal of membrane science*, *375*(1-2), 1-27.

[13] Sadrzadeh, M., & Bhattacharjee, S. (2013). Rational design of phase inversion membranes by tailoring thermodynamics and kinetics of casting solution using polymer additives. *Journal of membrane science*, *441*, 31-44.

[14] Marino, T., Russo, F., & Figoli, A. (2018). The formation of polyvinylidene fluoride membranes with tailored properties via vapour/non-solvent induced phase separation. *Membranes*, *8*(3), 71.

[15] Saljoughi, E., Amirilargani, M., & Mohammadi, T. (2010). Effect of PEG additive and coagulation bath temperature on the morphology, permeability and thermal/chemical stability of asymmetric CA membranes. *Desalination*, *262*(1-3), 72-78.

[16] Mohamed, M. A., Jaafar, J., Ismail, A. F., Othman, M. H. D., & Rahman, M. A. (2017). Fourier transform infrared (FTIR) spectroscopy. In *Membrane characterization* (pp. 3-29). elsevier.

[17] Taylor, L. S., Langkilde, F. W., & Zografi, G. (2001). Fourier transform Raman spectroscopic study of the interaction of water vapor with amorphous polymers. *Journal of pharmaceutical sciences*, *90*(7), 888-901.

[18] Ahmad, N. A., Leo, C. P., Ahmad, A. L., & Ramli, W. K. W. (2015). Membranes with great hydrophobicity: a review on preparation and characterization. *Separation & Purification Reviews*, *44*(2), 109-134.

[19] Xu, Z., Li, L., Wu, F., Tan, S., & Zhang, Z. (2005). The application of the modified PVDF ultrafiltration membranes in further purification of Ginkgo biloba extraction. *Journal of Membrane Science*, *255*(1-2), 125-131.

[20] Strathmann, H., Kock, K., Amar, P., & Baker, R. W. (1975). The formation mechanism of asymmetric membranes. *Desalination*, *16*(2), 179-203.

CHAPTER 9
CONCLUSIONS AND RECOMMENDATIONS FOR FUTURE WORK

9.1 Summary

In this study, the enveloping objective of the presented thesis was to investigate the use of non-toxic/green pure solvents to replace traditional toxic petroleum solvents, in this case, NMP, for the fabrication of flat sheet poly (vinylidene fluoride) PVDF membranes via the phase inversion process. The first objective was to investigate GVL as a solvent and understand the thermodynamics of the polymer/solvent/nonsolvent system. A qualitative approach, “polymer dissolution in vial method” (PDV), was proposed rather than the deterministic and quantitative turbidity measurement to examine the thermodynamic behaviour of the PVDF/GVL/water system. The primary reason the turbidity measurement based on light transmittance was not implemented was the difficulty of designing an in-house optical device/apparatus that could control the cooling rate, temperature and provide analysis of phase change for a large amount of samples at the same time.

The experimental study involved using the predetermined concentration of polymer, solvent and solvent to explore the influence of temperature on the solubility of the PVDF system. Results showed that increased temperature resulted in an increased solubility gap of the PVDF ternary system. As a novelty, the present study examined the influence of temperature on potential casting solutions behaviour. The ternary diagrams were used to describe the casting solutions with changing compositions at constant temperature and pressure.

In addition, the evolution with the temperature of the demixing boundary/miscibility gap of the PVDF/GVL/water system was investigated at two different cooling rates. The ternary phase diagram was employed to depict the NIPS process’s equilibrium behaviour and kinetics characteristics (effect of temperature and time). The PVDF/DMSO/water system validated the PDV technique, and experimental cloud point boundaries showed reasonable agreement with the results in the literature. The thermodynamic and kinetic analysis of the PVDF/GVL system via the PDV approach and a literature review were crucial in identifying suitable casting compositions. The PVDF membrane was designed and manufactured based on an understanding of the thermodynamics of the PVDF/GVL system. The resulting structure and performance of the PVDF membranes based on the PVDF/GVL/water system were compared to the structure and performance of PVDF membranes based on the PVDF/NMP/water system. Initial experiments showed that PVDF membranes fabricated from

binary solutions using the green solvent GVL exhibited dense/globular morphological structure with very low gas flux, when compared to the PVDF membranes produced using the traditional, toxic and hazardous solvents, such as NMP.

Further studies focused on investigating the effect of several different process parameters that can be varied during the membrane fabrication process via NIPS to modify the final membrane structure and improve its performance. The various process parameters investigated influence the formation process, and eventually, the structure and performance of the membranes are categorised into two groups. The first examines compositional parameter changes, which include PVDF concentration, the addition of cosolvent and finally, the addition of a pore former. The second aspect is referred to changes in operating parameters consisting of the temperature of different solution preparation (Tdissol) and casting preparation (Tcast) conditions. These examined parameters are summarised in several sections below, and the main conclusion is discussed.

9.1.1 Investigation of the effect of polymer concentration using GVL as solvent via the NIPS approach.

The effect of different polymer concentrations (10-20)wt.% was investigated by preparing polymer dopes at fixed temperature using GVL as solvent. The study showed that the low polymer concentration of PVDF (10wt.%) used to prepare polymer dope resulted in a thin dense top layer and spongy-like structure. However, an increase in polymer concentration by 5-10wt.% lead to a primarily dense top layer with a globule-like membrane structure. The increased polymer concentration affected the exchange between the solvent in the cast film and the nonsolvent (water) due to the activity difference in polymer concentration. The observed membrane morphology with an increased dense top layer created a barrier that affected the diffusional fluxes of the feed material, in this situation, nitrogen gas. The manufactured PVDF membrane's overall thickness was much smaller than those obtained using traditional toxic solvents. The high liquid entry pressure and increased polymer concentration lead to reduced gas flux. There was no water permeation through the PVDF membrane at low pressure. However, the high porosity and flux obtained by reducing the polymer concentration allow the PVDF membrane to be used as a membrane contactor for gas and water separation.

9.1.2 Investigation of the influence of temperature on the dissolved polymer and precipitation conditions in the fabrication of PVDF membrane.

The effect of the temperature, as a process variable in the fabrication of polymeric membranes by the nonsolvent induced phase separation (NIPS) technique, was considered for dissolved polymer (Tdissol), and varying temperature conditions for maintained casting and coagulation bath (Tcast) were studied. A tailored design of PVDF membranes was produced by altering the temperature conditions of Tdissol and Tcast at a fixed polymer (PVDF) concentration. The degree of the polymer molecular chain's unfolding and their entanglement was related to the effect of the Tdissol and Tcast on the fabrication of PVDF membrane by increasing the temperature. In addition, both parameters allowed an understanding of the sequence of the phase separation of the PVDF/GVL/water system via the immersion precipitation process.

The thermodynamic analysis showed that the polymer dope prepared at low Tdissol could not resist gelation within a short period once cooled to casting temperature. Increased Tdissol results in a better disentanglement of polymer chains, and upon cooling to Tcast, the polymer solutions remain homogeneous for a more extended period before phase separating. In addition, the PVDF membrane morphology was impacted by the increase of Tdissol, which decreased the membrane's overall thickness, porosity, crystallinity and hydrophilicity. On the other hand, increasing Tcast only resulted in minimal changes to the properties of the designed PVDF membranes. The effects of Tdissol and Tcast were explained using the experimental ternary phase diagrams.

Furthermore, increasing Tdissol resulted in thicker, dense top layers supported by a spongy-like structure. In addition, the membrane demonstrated a cellular texture consisting of open/closed pores and gradually reduced membrane performance. Despite the membranes showing no pure water permeation at the pressures tested, altering the process parameters (Tdissol and Tcast) allowed PVDF membranes with unique membrane structures and performance to be engineered through the NIPS process. Therefore, the PVDF membranes may also be used for gas membrane operations. However, because of the high energy cost to prepare membranes using higher temperatures and low gas permeation performance obtained, it is challenging to present a financial argument for up-scaling production. Further research was carried out to manage the fabricating process by utilising a low preparation temperature and modifying the fabrication process conditions to produce PVDF membranes that exhibit pure water permeation and increased gas performance.

The industrial scalability of PVDF membrane fabrication can be implemented by transferring the proposed batch lab process to a semi-continuous pilot scale. However, a few

modifications to the fabrication design must be implemented to control the fabrication parameters to achieve membrane reproducibility precisely. The thermal history of the PVDF dope solution, or more specifically, the effect of temperature and time on the evolution of the dope solution, must be considered. In addition, several other process parameters, such as humidity and wait time after casting before immersion into the coagulation bath, must also be considered when fabricating commercial membranes.

Generically, for any polymer-GVL system, the most critical factor is the polymer's solubility in GVL. Therefore, employing a tight, precise fine control of the fabrication parameters such as process temperature and process time before casting must be considered more than perhaps a membrane process that uses a traditional solvent if the use of GVL is to be adopted by the industry. Furthermore, since the solvent GVL (with a viscosity of 1.86 cP at 25°C) is slightly more viscous than the typical traditional solvents used in membrane fabrication, the difference in terms of stirring and pumping requirement during the preparation process of dope solution is expected. In addition, storage of prepared dope solution using GVL at 30°C before casting would only be possible for a short period compared to dope solutions obtained using the traditional toxic solvent, which tends to be stable for a prolonged period. Therefore minor equipment changes (e.g. storage conditions of dope solution before casting, stirrer paddles and pumps) will be required in commercial membrane fabrication for GVL to be taken up by the industry.

9.1.3 Use of solvent/cosolvent blend to fabricate PVDF membrane

A solvent blend was considered a simple approach to designing tailored PVDF membranes by modifying the morphology of PVDF membranes fabricated using GVL as a green solvent and DMSO as a cosolvent. The objective was to develop PVDF membranes with better/different permeation performance using a non-toxic cosolvent that will provide synergetic properties in the blended polymer dope. Literature studies show that solvent blends used in the preparation of polymer dopes are effective in fabricating PVDF membranes. The solubility of PVDF in different mixtures of GVL and DMSO and the stability of the resultant polymer solutions were investigated as it is necessary to fabricate tailored PVDF membranes. The PVDF membranes exhibited very thin top dense layers supported by finger-like, spongy and macrovoid structures. The results demonstrated that using a solvent blend to prepare the polymer dope can change the fundamental membrane formation mechanisms that occur during the NIPS formation process and modify the final membrane morphology. The combination of the physicochemical properties of the solvent and cosolvent

resulted in higher membrane permeability in terms of gas and liquid water permeation, allowing designed PVDF films to be used for various membrane processes and applications.

9.1.4 Investigation of the effect of additives on PVDF membrane performance using GVL as a bio based solvent

This study compares neat PVDF membranes fabricated from GVL and membranes obtained with the addition of poly (vinylpyrrolidone) (PVP), which acts as a pore former. The PVDF membranes were synthesised by the NIPS technique using a fixed 15wt% PVDF. The objective of this study was to obtain improved PVDF membrane performance using green solvent (GVL) by directly altering the membrane structure by adding a pore former (PVP). Several tailored-made PVDF membranes were obtained by varying the concentration of the additive PVP. The different compositions of the polymer dope resulted in the fabrication of unique PVDF membranes that demonstrated thin dense layers with finger-like and spongy structures. Analysis showed that adding a small concentration of PVP dramatically changed the membranes' morphology and improved overall performance. However, further increase above 3wt% PVP concentration resulted in higher resistance of transmembrane flux, which was associated with membrane structure and especially the progressive thickening of the dense top layer. The resulting membrane modification introduced a promising new concept for eco-friendly PVDF membrane production/design using GVL, which possesses distinct properties and high performance and can be used for different membrane processes.

9.1.5 CONCLUSIONS

Research objectives were achieved by investigating and assessing the influencing process parameter to fabricate PVDF membranes using GVL as a green solvent. As a result, all novel PVDF membranes fabricated exhibited asymmetric structures with unique wettability behaviour, surface roughness, porosity, thickness and performance properties. The tailored conditions were able to provide an expanded understanding of the formation mechanism of the PVDF/GVL system via the phase inversion method. The process allowed the membrane morphological structure to be controlled to achieve improved performance flux. Furthermore, it demonstrated the suitability of fabricated PVDF membrane materials for various membrane processes, including ultrafiltration, membrane distillation and membrane contactors.

A snapshot of the assessed performance of each fabricated novel PVDF membrane is presented in figure 9.1. It guides how to replace a hazardous solvent with a green, non-toxic or environmentally friendly substitute that meets specific membrane processes and desired industrial applications.

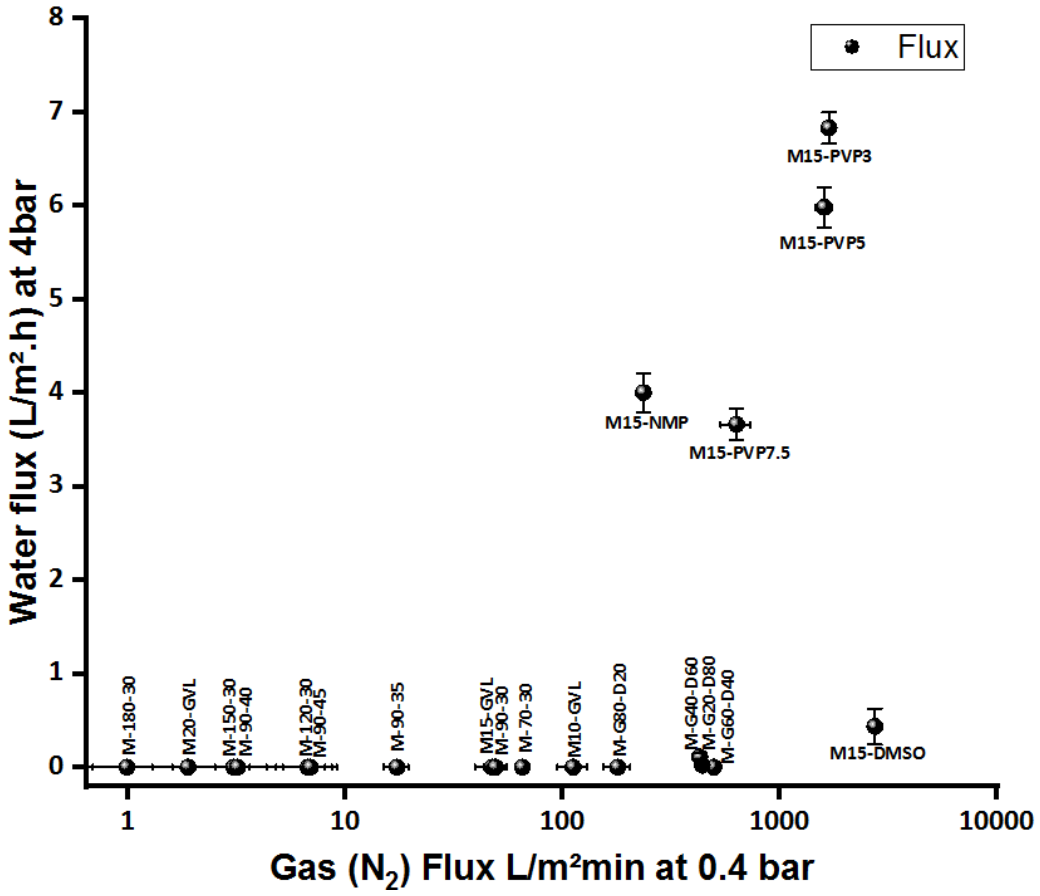

Figure 9.1: Evaluation of PVDF membrane performance due to the influence of various process parameters.

Despite GVL and NMP having similar physiochemical properties, PVDF membranes produced using these pure solvents showed different structural, textural, morphological and performance characteristics. The experimental lab scale study and knowledge gained from this work can be applied to the synthesisation of polymeric membranes on a pilot production scale to control the structure and performance of the resulting membrane for use in various membrane processes and applications.

9.2 RECOMMENDATIONS FOR FUTURE WORK

It has been demonstrated that the proposed PDV method can be used to examine the thermodynamic analysis of the PVDF/GVL/water system and determine the demixing boundaries and gelation data points. However, compositions of coexisting phases were not

identified from the PVDF samples prepared, which made it impossible to draw the tie-line. Hence, analytic techniques can be employed to correctly identify these compositions and improve understanding of the formation mechanism during the phase inversion process. Analytical tools include thermogravimetric analysis (TGA), centrifugation, size exclusion and gas chromatography. The approach is first to separate the demixed phase and immediately apply an appropriate analytical method to determine the exact compositions of each phase in a sample. The information obtained can be used to define the PVDF system's tie lines and phase equilibria.

Furthermore, another aspect that can provide further insight into the thermodynamics of the considered polymeric system process is comparing the demixing boundary data points for the PVDF ternary system to the theoretical modelling based on Flory Huggins's theory. Thermodynamics analyses can also be extended to obtaining phase diagrams for quaternary additive of PVP or cosolvent mixture, which were not presented in this thesis. The influence of the temperature by varying Tdissol and Tcast parameters to control the membrane formation process of PVDF membrane showed a significant difference in membrane performance which was reduced with increasing Tdissol and Tcast parameters. Further studies can be conducted to examine the rheological behaviour of the polymer dope prepared at different Tdissol or Tcast and to determine if the viscosity of the polymer dope is an important variable that strongly affects the behaviour of the final casting solution during the membrane formation process. In addition, the study can provide a good understanding of the phenomena that occur at the cast film's and nonsolvent interface during the membrane fabrication process. The resulting membranes show that using pore former as additives or solvent blends to synthesise PVDF membranes when using GVL as solvent exhibit increased gas and water performance that could apply to different membrane processes. However, controlling the fabrication process would be necessary to produce membranes for potential membrane processes such ultrafiltration and membrane distillation applications. The thermally induced phase separation approach could also be considered to develop PVDF membranes.

Further characterisation can be implemented to optimise the PVDF membrane properties by assessing the mechanical stability of cast film for considered process conditions and parameters investigated in the thesis. In addition, several other factors, such as the effect of nonsolvent activity, the thickness of membrane casting and the impact of humidity on the cast film, can be investigated to conduct a more detailed study to improve the resultant membrane structure and performance properties synthesised via the NIPS approach. Finally, the trade-offs of tailored PVDF membrane fabrication can be further investigated by

examining the selectivity and long term filtration (stable operation) without compromising on performance. In addition, a sustainable approach and use of materials have been developed in this study in fabricating PVDF membranes. Hence, further investigation could be conducted to examine the production process's life cycle assessment (LCA) and balance outcomes between sustainability, reliability and cost of the overall system.

APPENDICES

S.1 Conferences/ summer programs attended

Post presentation at Chemical and process Engineering Department Research celebration Event – University of Strathclyde (12th September 2018)

36th EMS Summer School –Membrane for a sustainable – University of Edinburgh, United Kingdom (23-28 June 2019)

Oral presentation International congress on membrane and membrane processes – United Kingdom (7-11 December 2020)

S.2 Table 1. Properties of problematic environmental solvents used to prepare membranes.

Solvent	CAS No.	Molecular formula	Density @25°C (g/ml)	MW (g/mol)	Bp (°C)	Hazard code/ Signal
***N,N*-dimethylacetamide** (DMAc)	127-19-5	C_4H_9NO	0.945	87.12	165	H312+H332 H319;H360D/ Danger
***N,N*-dimethylformamide** (DMF)	68-12-2	C_3H_7NO	0.948	73.10	152	H226 H312+H332 H319;H360D/ Danger
***N*-methyl-2-pyrrolidone** (NMP)	872-50-4	C_5H_9NO	1.028	99.13	202	H315;H319; H335;H360D/ Danger
Trimethyl phosphate (TMP)	512-56-1	$(CH_3O)_3PO$	1.197	140.08	197	H315; H302; H319; H340; H351 /Danger
1,3-Dimethyl-2-imidazolidinone (DMEU)	80-73-9	$C_5H_{10}N_2O$	1.056	114.15	225	H302; H318; H361; H373/ Danger
Tetrahydrofurfuryl alcohol (THF)	97-99-4	$C_5H_{10}O_2$	1.054	102.13	178	H319; H360Df/ Danger
Toluene	108-88-3	C_7H_8	0.865	92.14	111	H315; H304; H225; H336; H361d; H373 /Danger
Hexamethylphosphoramide (HMPA)	680-31-9	$C_6H_{18}N_3OP$	1.03	179.20	232	H340; H350/ Danger; carcinogen
Tetramethylurea (TMU)	632-22-4	$C_5H_{12}N_2O$	0.968	116.16	177	H302; H360D/ Danger

A: Hazard codes:

H226 Flammable liquid and vapour.

H302 Harmful if swallowed.

H312 + H332 Harmful in contact with skin or if inhaled.

H315 Causes skin irritation.

H318 Causes serious eye damage.

H319 Causes serious eye irritation.

H335 May cause respiratory irritation.

H336 May cause drowsiness or dizziness.

H340 May cause genetic defects.

H350 May cause cancer

H351 Suspected of causing cancer.

H360D May damage the unborn child.

H360Df May damage the unborn child. Suspected of damaging fertility

H361 Suspected of damaging fertility or the unborn child.

H373 May cause damage to organs (Testes) through prolonged or repeated

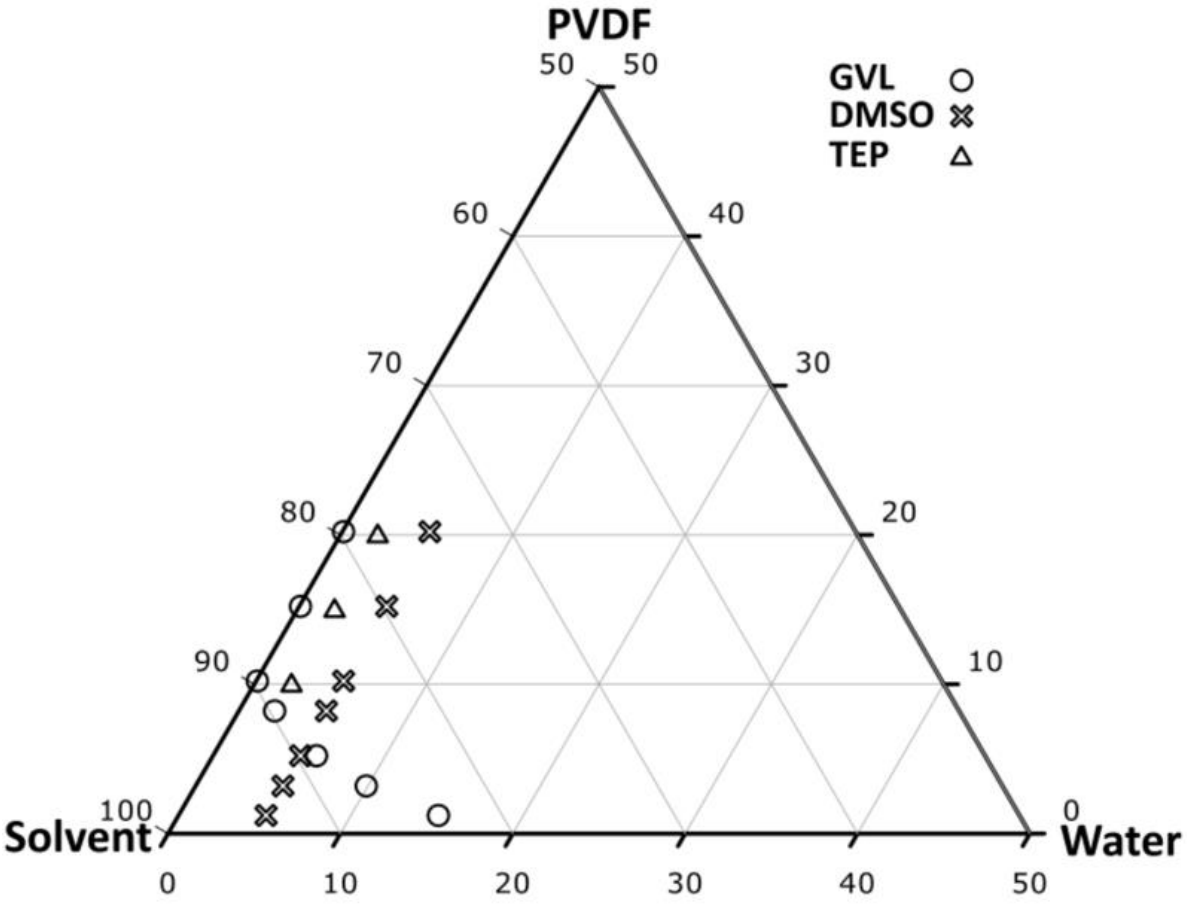

S.3 Figure 1: Cloud data points of PVDF/DMSO/water and PVDF/TEP/water systems using the PDV method.

S.4 Preparation of Dope solutions Setup

S.5 The casting machine setup for Flat sheet membranes preparation. 1. Casting machine 2. Glass plate 3. Casting knife

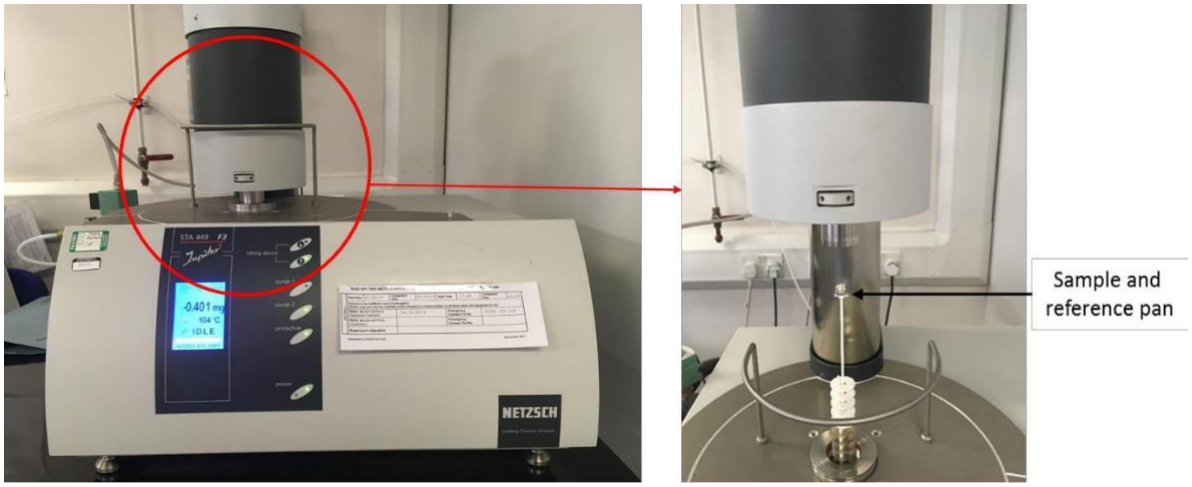

S.6 NTEZSCH 449 F3 Jupiter STA machine with view of sample and reference holder

S.7 FTIR spectrophotometer, QATR-S single-reflection ATR – Shimadzu's IRSpirit

S.8 Drop Shape Analyse DSA25 – KRÜSS

S.9 AFM5000 II model device – Hitachi

S.10 Gas and Pure water membrane test rig setup